Positional Behaviors and the Neck:

A Comparative Analysis of the Cervical Vertebrae of Living Primates and Fossil Hominoids

by

Thierra Kennéc Nalley

A Dissertation Presented in Partial Fulfillment
of the Requirements for the Degree
Doctor of Philosophy

Approved November 2013 by the
Graduate Supervisory Committee:

William Kimbel, Chair
Liza Shapiro
Kaye Reed

ARIZONA STATE UNIVERSITY

December 2013

ABSTRACT

Despite the critical role that the vertebral column plays in postural and locomotor behaviors, the functional morphology of the cervical region (i.e., the bony neck) remains poorly understood, particularly in comparison to that of the thoracic and lumbar sections. This dissertation tests the hypothesis that morphological variation in cervical vertebrae reflects differences in positional behavior (i.e., suspensory vs. nonsuspensory and orthograde vs. pronograde locomotion and postures). Specifically, this project addresses two broad research questions: (1) how does the morphology of cervical vertebrae vary with positional behavior and cranial morphology among primates and (2) where does fossil hominoid morphology fall within the context of the extant primates. Three biomechanical models were developed for the primate cervical spine and their predictions were tested by conducting a comparative analysis using a taxonomically and behaviorally diverse sample of primates. The results of these analyses were used to evaluate fossil hominoid morphology.

The two biomechanical models relating vertebral shape to positional behaviors are not supported. However, a number of features distinguish behavioral groups. For example, the angle of the transverse process in relation to the cranial surface of the vertebral body—a trait hypothesized to reflect the deep spinal muscles' ability to extend and stabilize the neck—tends to be greater in pronograde species; this difference is in the opposite of the direction predicted by the biomechanical models. Other traits distinguish behavioral groups (e.g., spinous process length and cross-sectional area), but only in certain parts of the cervical column. The correlation of several vertebral features, especially transverse process length and pedicle cross-sectional area, with anterior cranial

length supports the predictions made by the third model that links cervical morphology with head stabilization (i.e., head balancing).

Fossil hominoid cervical remains indicate that the morphological pattern that characterizes modern humans was not present in *Homo erectus* or earlier hominins. These hominins are generally similar to apes in having larger neural arch cross-sectional areas and longer spinous processes than modern humans, likely indicating the presence of comparatively large nuchal muscles. The functional significance of this morphology remains unclear.

To Keith and Kathyne Nalley

ACKNOWLEDGMENTS

First and foremost, I thank my committee members—William Kimbel, Kaye Reed, and Liza Shapiro— for their wisdom, patience, and support. I am grateful for the years they have dedicated to my education and the opportunity to be their student. I thank the School of Human Evolution and Social Change and the Institute of Human Origins for providing an extraordinary setting for training, research, and collaboration. I am the scholar I am today because of the faculty, graduate students, and staff in these institutions.

I thank Eileen Westwig at the American Museum of Natural History, Darrin Lunde at the National Museum of Natural History, Anna Goldman at the Field Museum, Arleyn Simon at Arizona State University, Christine Lefévre at the Muséum of National de'Histoire Naturelle, the staff of the National Museum of Ethiopia, Emma Mbua at the Nairobi National Museum, and Stephany Potze at the Ditsong National Museum of Natural History for permission to access fossil and skeletal specimens and for assistance during my visits.

Research funding came from a Dissertation Fieldwork Grant from the Wenner-Gren Foundation and a research grant from ASU's Graduate and Professional Students Association. I also gratefully acknowledge a SHESC dissertation fellowship for funding my final months of dissertation writing.

My fellow ASU graduate students provided unwavering intellectual, editorial, and moral support. They are too many to list, but I will try: Kristi Lewton, Terry Ritzman, Amy Rector-Verrelli, Laura Bidner, Stephanie Meredith, Teague O'Mara, Neysa Grider-Potter, Lynn Copes, Halszka Glowacka, Laura Stroik, and so many more.

My sister and brother (Shannon and Neil Nalley) have been a constant source of strength and love. They provided a foundation for me to stand on, and when I lost all others, a reason to finish. Finally, I thank my fellow traveler and husband Jeremiah Scott. His easy decency and humble brilliance are an inspiration. He is the partner I always wished for and so much more.

TABLE OF CONTENTS

LIST OF TABLES

Table Page

Table Page

Table Page

Table Page

LIST OF FIGURES

Figure Page

Figure Page

Chapter 1

INTRODUCTION

This dissertation addresses the functional morphology of the cervical vertebrae in primates with special reference to the biomechanics of positional behavior and head balance. Despite the critical role that the vertebral column plays in postural and locomotor behaviors, understanding of cervical vertebral form and function is limited in comparison to knowledge of thoracic and lumbar functional morphology (Schultz, 1942; Mercer, 1999; Manfreda et al., 2006; Ankel-Simons, 2007; Mitteroecker et al., 2007). The cervical spine acts as the bridge between the head and trunk, and provides a bony platform for the soft tissues of the pectoral girdle and upper limb (Shultz, 1942; Kapandji, 1974; Mercer and Bogduk, 2001). The pectoral girdle is composed of the scapula and clavicle, which are supported via musculature originating from the head and the cervical and upper thoracic vertebrae. Given that morphological variation in the scapula and clavicle has been linked to differences in positional behavior in extant primate species (Ashton and Oxnard, 1964; Rose, 1975; Fleagle, 1976, 1977; Larson, 1993, 1995; Voisin, 2006), it is reasonable to hypothesize that there are predictable patterns in the functional relationship between positional behaviors and the neck and head.

While many studies have focused on the thoracic and lumbar regions of the spine to investigate primate posture and locomotion and, in turn, infer behaviors in fossil taxa, the primate cervical spine has been largely ignored in functional analyses. Biomechanical and medical research concerning the human cervical vertebral column has demonstrated the functional significance of many features and provides experimental evidence linking function with form (Compere et al., 1958; Hall, 1965; Penning, 1968; Kapandji, 1974;

Yoganandan et al., 1988; White and Panjabi, 1990; Milne, 1991; Bogduk and Mercer, 2000; Mercer and Bogduk, 2001; Kurtz and Edidin, 2006). This previous research has primarily focused on the structural role certain vertebral features play in maintaining proper head and neck posture, specifically regarding injury and surgical implants (e.g., Holness et al., 1984; Yoshida et al., 1992; Whine et al., 1998: Panjabi et al., 2000). Researchers have also established normal ranges of motion for the human head and neck, including the proprioceptive role that the nuchal musculature plays during the maintenance of the visual field and natural head positions (e.g., Lind et al., 1989; Berthoz et al., 1992; Dvorak et al., 1992; Haymann and Donaldson, 1997; Feipel et al., 1999; Panjabi et al., 2001; Mercer and Bogduk, 2001; Takeuchi and Shono, 2007; Nagamoto et al., 2011). Limited investigations of nonhuman primate morphology have also reported functional patterns in a number of cervical features (Slijper, 1946; Schultz, 1961; Toerien, 1961; Ankel, 1972; Manfreda et al., 2006). This comparative work, however, has described vertebral shape in only a few primate taxa. Many of these studies did not document the full range of phylogenetic variation in primate cervical vertebral shape and lacked a biomechanical framework (Graf et al., 1995a; 1995b; Aiello and Dean, 1990; Dickman et al., 1994; Tominaga et al., 1995; Elias et al., 2006). Given that thoracic and lumbar vertebral correlates of posture and locomotion are often used to make inferences of positional behavior in fossil primates (e.g., lumbar vertebral wedging and lordosis in fossil hominins), it is puzzling that the adaptive significance and biomechanical context of the cervical spine has not been as thoroughly investigated.

Establishing the functional significance of cervical vertebral morphology has the potential to provide novel insights into primate postural and locomotor evolution. For

example, it is widely thought that arboreal suspensory behaviors were an important component of the locomotor repertoire of the last common ancestor of the *Pan-Homo* clade (Stern and Susman, 1983; Gebo, 1996; Richmond et al., 2001; Ward, 2002; Crompton et al., 2008). This inference finds support from several features of the upper limb of early hominins, including arms that are long relative to legs, long and curved phalanges, and a cranially oriented glenoid fossa (Stern and Susman, 1981, 1983, 1991; Stern, 2000; Larson et al., 2007). However, new fossil evidence calls this scenario into question. Lovejoy et al. (2009) argued that the postcranium of the fossil hominin *Ardipithecus ramidus*, dated to 4.4 Ma, indicates that the *Pan-Homo* last common ancestor was not a below-branch suspensory specialist while in the trees, but instead was an above-branch quadruped. The apparent lack of suspensory adaptations in the skeleton of *Ar. ramidus* led its describers to suggest that suspensory locomotion evolved in *Pan* subsequent to the *Pan-Homo* split and in parallel in *Gorilla*, *Pongo*, and hylobatids (Lovejoy et al., 2009). Lovejoy and colleagues (2009) hypothesized that bipedalism evolved from above-branch arboreal quadrupedalism and that any features originally interpreted as suspensory adaptations in early hominins were instead adaptations for increased shoulder mobility for bridging and climbing in the context of above-branch quadrupedalism. This scenario also implies that none of the great apes are good models for the anatomy or locomotor behavior of the last common ancestor. Further research is necessary to resolve the uncertainty regarding this issue. Arguments for a suspensory ancestor for the African ape and hominin clade rely on accurate interpretations of features as reflecting suspensory locomotion, and one of the primary goals of this project is to establish whether or not features of the cervical vertebrae can be used in this manner.

To achieve this objective, this dissertation tests the hypothesis that cervical vertebral morphological variation reflects differences in positional behavior. Specifically, this project addresses two broad research questions: (1) how does the bony morphology of cervical vertebrae vary with positional behavior and cranial morphology among primates and (2) where does fossil hominoid morphology fall within the context of the extant sample. Three biomechanical models were developed for the primate cervical spine and their predictions were tested by conducting a comparative analysis of cervical vertebrae using a taxonomically and behaviorally diverse sample of primates. The results of these analyses were used to evaluate fossil hominoid morphology.

It is useful to briefly discuss the differences between questions regarding adaptation and biomechanics. Specifically, adaptive questions are evolutionary in nature, while mechanical questions are functional. This project is concerned with both types of questions, and the methods to address these questions are further discussed below. Identifying adaptation requires a demonstrated causal link between trait and function (Kay and Cartmill, 1977). In the case of this project, the causal link will be demonstrated by the validation of models that relate variation in form to variation in function. Although accurately inferring function from morphology can be difficult (Lauder, 1995), the strength of inferences based on trait-function associations is increased when they can be demonstrated to occur repeatedly in a comparative sample. This is particularly true when the model (or models) holds for independent lineages of taxa with similar functional/behavioral requirements (Fleagle, 1976; Kay and Cartmill, 1977; Felsenstein, 1985; Harvey and Pagel, 1991; Ross et al., 2002; Spencer, 2003; Orr et al., 2007). Many existing hypotheses are based on trait-function correlation alone, and not on predictions

derived from the mechanical requirements of different positional behaviors (that is, traits hypothesized to be "adaptations" to posture or locomotion have not been shown to perform the specified function). One way to demonstrate that a trait performs a function is by using optimality criteria to formulate predictions of morphology based on the biomechanics of the system (Rudwick, 1964). In this way, the development of adaptive hypotheses relies on an understanding of a solid biomechanical foundation of the system. Biomechanical models of vertebral stress resistance in mammals have been proposed (Slijper, 1946, Badoux, 1965; 1968; Jenkins, 1971; 1974; Preuschoft, 1978; Preuschoft et al., 1988, Oxnard et al., 1990; Shapiro, 1995; Christian and Preuschoft, 1996; Bertram and Chang, 2001; Bertram, 2004). This project draws from this research to develop biomechanical models of the primate cervical spine and to test specific predictions of how cervical vertebrae resist stress related to either positional behavior or cranial morphology, or both.

In this dissertation, three theoretical models of spinal mechanics were refined and expanded from previous works (Slijper, 1946, Badoux, 1965; 1968; Jenkins, 1971; 1974; Preuschoft, 1978; Preuschoft et al., 1988, Oxnard et al., 1990; Shapiro, 1995; Christian and Preuschoft, 1996; Bertram and Chang, 2001; Bertram, 2004). Predictions derived from each model were tested using bony features of the cervical vertebrae and cranium previously found to be functionally relevant (Slijper, 1946; Swindler and Wood, 1982; Dean, 1982; Demes, 1985; Pal and Routal, 1986; Ward, 1991; 1993; Shapiro, 1995; Johnson and Shapiro, 1998; Mercer, 1999; Shapiro and Simons, 2002; Anderson et al., 2005; Shapiro et al., 2005; Shapiro, 2007; Russo, 2010). Biomechanically supported predictions between vertebral morphology and positional behavior and cranial

morphology were then tested using comparative morphometrics, specifically, targeted pairwise comparisons of closely related taxa, and taxonomically broader phylogenetic generalized least-squares analyses. The latter analyses were performed using a large sample of 51 extant primate taxa chosen to maximize representation of locomotor and postural categories. Fossil taxa were examined within the context of the extant comparative sample using box-and-whisker plots and discriminant function analysis. The fossil hominoid sample consisted of both complete and partial cervical vertebrae from 12 individuals representing five fossil hominoid taxa: *Nacholapithecus kerioi*, *Australopithecus afarensis*, *Australopithecus robustus*, *Homo* sp. indet., and *Homo erectus*. The utilization of comparative methods will provide a better understanding of primate cervical vertebrae variation and functional morphology, and the fossil taxa have the potential to inform on different aspects of hominoid evolution. These techniques are well suited for morphological reconstructions and behavioral inferences in fossil primates. For example, the Miocene ape provides a window into early hominoid cervical morphology and could comment on the evolution of suspensory locomotion. Furthermore, the early hominins could aid in the reconstruction of the locomotor repertoire of the *Pan-Homo* last common ancestor, and finally, the later hominins can help establish when fully modern cervical, and even pectoral girdle, morphology evolved.

Chapter 2

FUNCTIONAL MORPHOLOGY OF THE CERVICAL SPINE

The primary goal of this chapter is to provide a summary of previous research linking features of the primate vertebral column and pectoral girdle to positional behaviors, and specifically to suspensory postures and locomotion. The secondary goal is to demonstrate the gap in knowledge regarding an understudied, yet potentially informative region of the primate spinal column, the cervical vertebrae. Finally, three distinct biomechanical models of the cervical spine will be described and vertebral features that can be utilized for testing these models will be highlighted.

POSITIONAL BEHAVIOR CLASSIFICATION

Before morphology can be discussed, the positional behavioral classification used throughout this study must first be defined. This is required because it provides the discrete groupings necessary to compare morphological differences and test adaptive hypotheses.

Positional behavior includes both postural and locomotor behaviors. Postural behaviors do not imply movement and instead describe the positioning of the body or parts thereof (i.e., hands and/or feet) providing support to the overall body weight. Postural behaviors also explain the orientation of the torso relative to gravity (Hunt et al., 1996). For example, a *quadrupedal stand* is considered a postural behavior and is defined as "four-limbed standing on horizontal or subhorizontal supports; the elbow and knee are (relatively) extended and the trunk is near horizontal (Hunt et al., 1996, pg 371). In contrast, locomotor behaviors imply movement of the body and include limb movements and their relationship to the substrate. As with postural behaviors, locomotor behaviors

describe the orientation of the torso relative to gravity (Hunt et al., 1996). For example, *bipedal walking* is a locomotor behavior that is described when "the hindlimbs provide support and propulsion, with only insignificant contributions from other body parts. The hip and knee are relatively extended, in a manner similar to human walking. This mode is extremely rare in chimpanzees and probably even more in other nonhuman primates" (Hunt et al., 1996: pg 377). The torso would be considered parallel to the line of gravity during this locomotor behavior.

Two positional categories will be used in this study to test for adaptations to broad differences in posture: orthograde and pronograde. Positional behaviors characterized by habitually pronograde posture are characterized by the torso held oriented perpendicular to the line of gravity. Behaviors classified as pronograde include activities such as *quadrupedal walking* and *pronograde leaping* (Hunt et al., 1996). Orthograde behaviors are characterized by the torso held parallel to the line of gravity. Examples of orthograde behaviors include *flexed-elbow vertical climbing*, *brachiating*, and a *bipedal stand* (Hunt et al., 1996). Either of these positional classifications can be performed in arboreal and terrestrial settings and include both postural and locomotor behaviors.

When testing for adaptations to suspensory behaviors, taxa will be assigned to one of a different set of positional behavior categories: suspensory and nonsuspensory. Suspensory positional behaviors include both postural and locomotor behaviors and are defined as a slow- or moderate-paced brachiating locomotion that incorporates below-branch forelimb suspensory postural behaviors, where the arm is fully abducted, the torso rotates under the supporting arm and hand, and the elbow is fully extended (Fleagle, 1974; Jungers and Stern, 1984; Larson and Stern, 1986; Hunt et al., 1996). This

definition is distinct from "ricochetal" brachiation that includes an aerial phase and increased rates of speed (Tuttle, 1969). All extant hominoids and members of the subfamily Atelinae can perform these movements (Gebo, 1996). Following Gebo (1996), other forms of suspension characterized by flexed elbows, torsos that do not rotate, and brief sequences of movement are considered alternative forms of simple arm swinging and not true suspensory positional behaviors. Taxa that use such behaviors include indriids, colobines, and tarsiers (MacKinnnon and MacKinnon, 1980; Gebo, 1987; Bryon and Covert, 2004). Simple arm swinging, in addition to all other forms of positional behaviors, will fall into the nonsuspensory category.

COMPARATIVE PRIMATE MORPHOLOGY

Suspensory positional behaviors emphasize the use of the forelimbs, which are attached to the body via the pectoral girdle. The pectoral girdle has a close functional relationship with the cervical vertebral column because the girdle's components—the scapula and clavicle—are suspended via muscular attachments from the head and the cervical and upper thoracic vertebrae (Shultz, 1942; Kapandji, 1974; Mercer and Bogduk, 2001). In suspensory taxa, such as chimpanzees and orangutans, these muscular attachments include relatively powerful (i.e., greater physiological cross-sectional area) nuchal musculature with a greater number of muscle bellies, slips, and attachments among the complex's members when compared to humans, monkeys, and strepsirrhines (Ashton and Oxnard, 1964; Dean, 1982; Stern and Susman, 1983; Swindler and Wood, 1982; Larson, 1995). For example, in *Gorilla* and *Pan*, the occipital and cervical origins of trapezius are more extensive than in humans, and the muscle bellies are shortened and thickened (Ashton and Oxnard, 1964; Swindler and Wood, 1982; Dean, 1982; Jungers

and Stern, 1984; Larson et al., 1991). Jungers and Stern (1984) and Larson et al. (1991) suggested that the relatively large size of the cranial portion of trapezius in apes is associated with the muscular requirements of head turning and stabilization of the head on the trunk during suspensory locomotion. In contrast, the nuchal musculature is significantly reduced in nonsuspensory primates, including humans, and often exhibits fewer muscle attachments and less complexity between the forelimb and the body (Dean, 1982; Swindler and Wood, 1982). Morphological variation in the scapula and clavicle has also been linked to differences in positional behavior in extant species and will be summarized in the following section (Ashton and Oxnard, 1964; Rose, 1975; Fleagle, 1976, 1977; Larson, 1993, 1995; Voisin, 2006).

Comparative morphology of the scapula

Primate scapular position and form has been broadly correlated with differences in positional behavior (Stern and Susman, 1983; Larson and Stern, 1986; Larson, 1995; Young, 2008). First, the position of the scapula is functionally relevant. The scapula is located cranially and dorsally on the mediolaterally broad torsos of extant hominoids, including humans, whereas in most other primates the scapula rests along the lateral aspect of a mediolaterally narrow chest. Suspensory platyrrhines show an intermediate position (Chan, 2007). Differences in scapular position affect the range of the scapula-humeral articulation. The hominoid and suspensory playtrrhine morphologies result in greater range of movement than what is demonstrated in more quadrupedal primates (Larson, 1995, 1998; Ankel-Simons, 2007; Chan, 2007). The shape of the scapula can also broadly separate primates into positional groups. In general, suspensory apes are described as exhibiting broad (craniocaudally) and short (mediolaterally) scapulae,

whereas those of most other nonsuspensory anthropoids are narrow and long (Ashton and Oxnard, 1964; Young, 2008). These morphological differences broadly reflect the differences in the size of the supra- and infra- spinous fossae. For example, in suspensory primates, such as gorillas, the scapula demonstrates a well-developed and craniocaudally long supraspinous fossa, and in turn, supraspinatus muscle. The relatively large size of the spinatus muscles is functionally linked to the stabilization of a highly mobile glenohumeral joint, specifically resisting transarticular stresses during suspensory behaviors and providing a resistance to shear stress during knuckle-walking (Larson and Stern, 1986, 1987; Larson, 1993).

The glenoid fossa is the point of articulation of the humerus with the scapula and is informative about differences in primate positional behaviors. The glenoid fossa, relative to the ventral bar of the scapula, faces laterally in humans and ventrally in other nonsuspensory primates, while in apes and atelines it is oriented more cranially (Ashton and Oxnard, 1964). Overall, the lateral scapular position and ventral glenoid fossa orientation provide stability for the shoulder of quadrupedal primates and restricts the movement of the forelimb to a parasagittal plane. Lateral scapular position directs substrate reaction forces orthogonally to the shoulder joint surface, minimizing shear stress across the gleno-humeral joint (Latimer et al., 1989; Reynolds, 1985). In contrast, the ape condition is linked with increased forelimb mobility, which is required for overhead suspensory positional behaviors. The lateral orientation of the glenoid fossa in modern humans does not necessarily reduce the overall range of movement, but is argued to reflect a habitually lowered forelimb (Stern and Susman, 1983; Susman et al., 1984; Larson, 1995; Larson et al., 2007).

The morphological patterns of extant primates have been successfully applied to fossil hominins, specifically with regard to orientation of the glenoid fossa. For example, early fossil hominin scapulae such as Sts 7 (*A. africanus)*, A.L. 288-1 and Dik 1-1 (both representing *A. afarensis*) suggest affinities with ape morphology in their more cranially oriented glenoid fossa when compared to modern humans (Vrba 1979; Stern and Susman, 1983; Susman et al., 1984; Alemseged et al., 2006; Green and Alemseged, 2012). Not until *H. erectus* does the hominin fossil record exhibit a more laterally oriented glenoid fossa, similar to the human condition seen today (Larson et al., 2007).

Comparative morphology of the clavicle

The clavicle is an important member of the pectoral girdle because the clavicle is the only actual bony attachment of the upper limb to the torso. The clavicle attaches medioventrally at the manubrium and laterally with the acromion of the scapula. It not only holds the shoulder joint at the side of the torso, but also transmits forces from the arm to the sternum (Larson, 1998; Ankel-Simons, 2007). There are relatively few examples of comparative or functional studies focusing on the primate clavicle (Schultz, 1930; Fleagle, 1978; Jenkins et al., 1978; Harrington et al., 1993; Voisin, 2006; Voisin and Balzeau, 2004; Larson et al., 2007). However, variation in clavicular form has been found to separate primates into broad positional behavior categories (Voisin, 2006; Voisin and Balzeau, 2004).

Clavicular length has proven to be a reliable indicator of scapular position. Extant hominoids, including humans, have relatively elongated clavicles when compared to other primates and this morphology reflects the broad thorax and dorsal position of the scapula (Gregory, 1928; Schultz, 1937, 1968, 1969). A certain amount of variation within

Hominoidea does exist, and humans, with the exception of *Pongo*, have relatively longer clavicles than all other hominoids (Schultz, 1937; Gebo, 1996; Larson et al., 2007). Relatedly, the suspensory atelines possess longer clavicles when compared to other nonsuspensory platyrrhines (Erikson, 1963).

Clavicular curvature, specifically in dorsal view, also separates primate groups and is suggested to reflect the relative power and speed of arm elevation. The curvature has been modeled to act as a crankshaft during elevation of the upper limb, thereby translating linear movement of the shoulder joint into rotational movement and thus increasing the action of attaching muscles (Inman et al., 1944; Dvir and Berme, 1978). Voisin (2006) was able to use clavicular curvature to separate potential functional groups (Figure 2-1). A clavicle with either a single or double superior curvature, like that of the gibbons or chimpanzees, respectively, is associated with a relatively stable sternoclavicular joint because the length of costo-clavicular ligament is reduced (Figure 2-2). A clavicle without a superior curvature, as in baboons and colobines, is associated with a longer costo-clavicular ligament and thus, is suggested to exhibit a mobile sternoclavicular joint. Notably, humans do not have a superior curvature along the clavicle and are more similar to nonhominoids (Voisin, 2006).

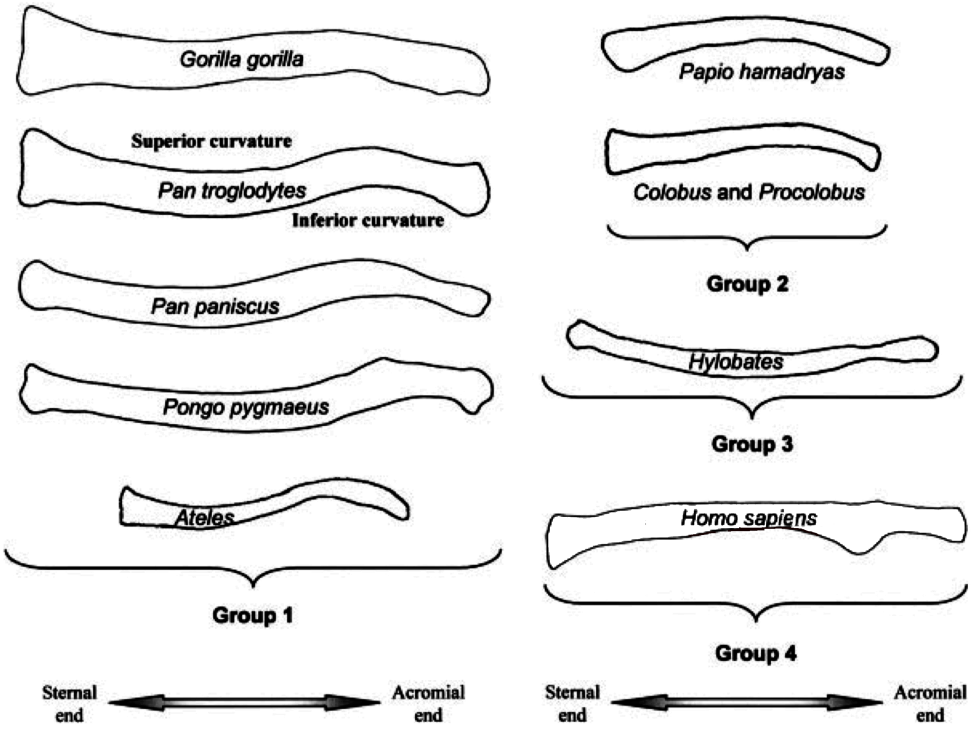

Figure 2-1. Adapted from Voisin (2006). Illustration of superior and inferior clavicular curvatures in dorsal view (not to scale). Groups 1 and 3 comprise the apes and *Ateles* and are distinguishable from Groups 2 and 4 by exhibiting a superior curve. Groups 2 and 4 include Old World Monkeys and *Homo sapiens* and demonstrate only an inferior curvature.

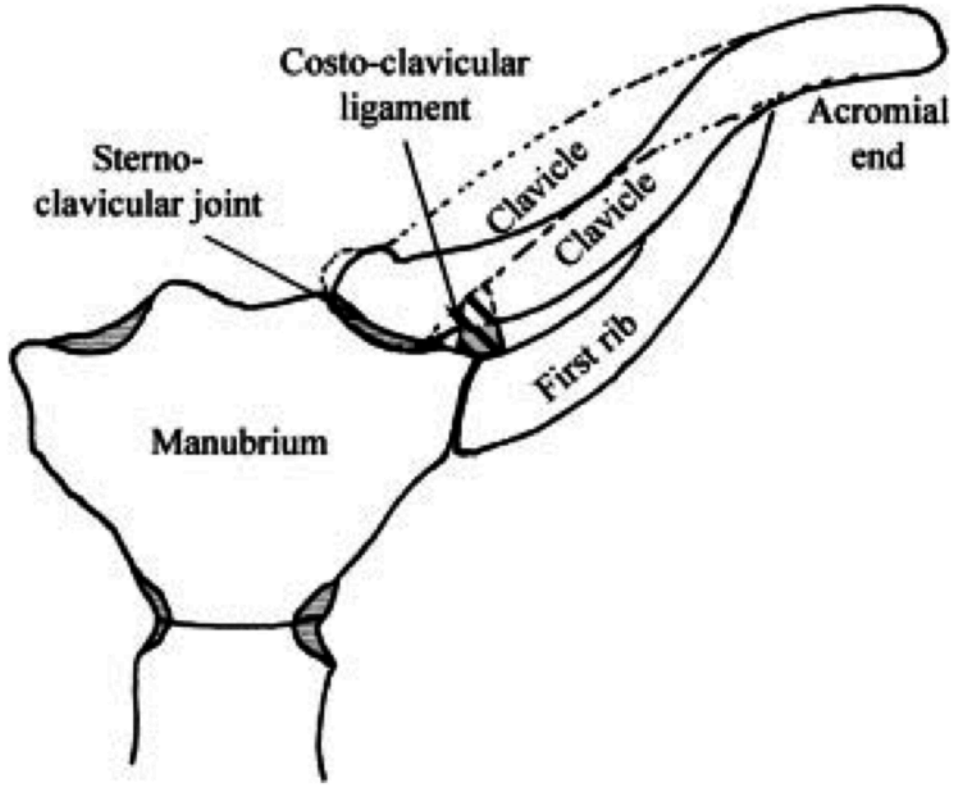

Figure 2-2. Adapted from Voisin (2006). Illustrates how the presence of a superior curvature (solid line), as seen in suspensory primates, reduces the length of the costo-clavicular ligament. The absence of a strong superior curvature (dotted line), as seen in humans and Old World Monkeys, increases costo-clavicular length.

Clavicular microanatomy also indicates differences between primate taxa. Voisin and Balzeau (2004) studied CT scans of modern *Homo*, *Pan*, and *Gorilla* clavicles and reported an increased proportion of dense cortical bone in the cross-sections of *Pan* clavicles in comparison to humans. The authors argued that these differences reflect increased forces transferred from the upper limb during knuckle-walking and suspensory positional behaviors.

Few clavicles are present in the fossil hominin record, but four nearly complete early hominin clavicles are known (OH 48, AL 333x-6/9, Dik 1-1, a juvenile) (Leakey, 1960; Lovejoy et al., 1982; Alemseged et al., 2006) and KNM-WT 15000 (and LB1,

representing *H. floresiensis*). Larson et al. (2007; 2009) found that earlier hominins (including *Homo erectus*) had shorter clavicles than modern humans, similar to chimpanzees and gorillas, while more recent *Homo* fossils (e.g., *H. neanderthalensis*) fall within modern human ranges of variation and exhibit relatively long clavicles. As mentioned earlier, *Homo erectus* exhibits a modern scapular morphology with a laterally directed glenoid fossae. However, because *Homo erectus* retains short clavicles, the entire pectoral girdle would have been positioned cranially on the torso, resulting in a ‘‘shrugged-shoulder’’ appearance. This configuration would have also reduced the amount of humeral torsion necessary to use the upper limb into the sagittal plane. This scenario is supported by the low humeral torsion found in KNM-WT 15000 (Larson, 2007; Larson et al., 2007).

Comparative morphology of the cervical vertebrae

The morphological variation observed in the bony components of the pectoral girdle has been correlated with differences in positional behavior and successfully applied to the hominin fossil record. The combination of bony and soft-tissue features described in the previous section are considered adaptations to suspensory positional behaviors because they are thought to allow the specialized movements of the shoulder and forelimb required for brachiation and suspended uni- and bimanual movements (i.e., abduction/adduction of the forelimb, circumduction at the shoulder joint, prolonged forearm extension, and the ability to control head movements during suspensory behaviors) (Ashton and Oxnard, 1964; Stern and Susman, 1983; Susman et al., 1984; Larson, 1995, Gebo, 1996; Larson, 2007). The cervical vertebral spine remains an

understudied component of this anatomical region and whether it provides the same functional signals has yet to be fully tested.

The spinal column as a whole has three fundamental biomechanical functions. First, it transfers the weight of the head, trunk, and any loads from the limbs. Second, it allows movement between these body parts, and third, it protects the spinal cord from being damaged by these forces and motions (Kapandji, 1974; White and Panjabi, 1990; Bogduk and Mercer, 2000). The cervical vertebral region, in particular, is the interface between the head and trunk and performs a diverse range of functions, including directing head movement and withstanding the forces of gravity and soft-tissue loading associated with the pectoral girdle (Schultz, 1942; Kapandji, 1974; Mercer and Bogduk, 2001). As with most mammals (with a few exceptions: e.g., manatees, sloths (Galis, 1999)), the primate cervical spine consists of seven vertebrae and is divided into two functionally distinct sections (White and Panjabi, 1990). The C0-C1-C2 (occipital-atlanto-axial) complex constitutes the upper cervical spine. The remainder (C3–C7) is typically referred to as the lower cervical spine. The upper cervical region regulates head movement, while the lower five vertebrae contribute to the role played by the entire vertebral column, as a robust, flexible axis of the body. More specifically, the lower cervical spine supports the head and neck, transmits the weight of the head and neck to the trunk, and absorbs and transmits forces from the upper extremity that travel to the cervical spine via muscular attachments (Kapandji, 1974; White and Panjabi, 1990; Bogduk and Mercer, 2000).

The cervical region of the spine is an understudied region in primates. This is perhaps partially due to fact that the human lumbar spine has a number of derived features that are clear indicators of obligate bipedalism (i.e., a distinct lumbar lordosis

and relatively large lumbar centra) (Schultz, 1961; Rose, 1975). Thus, combined with a relatively strong representation of lumbar vertebrae in the hominin fossil record, research efforts have focused on the primate thoracic and lumbar regions. Another reason little work has incorporated the cervical spine is because early descriptions concluded there was little variation and was therefore uninformative with regard to functional or phylogenetic questions (Schultz, 1961; Ankel, 1967, 1970, 1972). This idea has persisted in the literature without rigorous testing and results in a gap of understanding with regard to nonhuman primate cervical morphology. The few studies in the literature are primarily descriptive and tend not to address functional differences in shape (Schultz, 1960; Dickman et al., 1994; Tominaga et al., 1995). The following section summarizes the current state of knowledge of comparative morphology for both living primates and fossil hominins.

Typical cervical vertebrae

A typical lower cervical vertebra (C3–C7) can be divided into three functional components: the anterior component (vertebral body), the middle component (pedicles), and the posterior component (neural arch with its associated spinous, transverse, and articular processes). There is some research documenting differences between postural groups with regard to centrum morphology. Mercer (1999) conducted six intrageneric pairwise comparisons and found that more orthograde primate taxa had more circular surface areas. She argued that this morphology provided greater resistance to bending moments in all planes and was an adaptation to orthograde postural behaviors.

The spinous and transverse processes are sites of muscle attachment and their shape and size relative to the axis of motion are related to muscle function. These skeletal

features remain poorly studied in the cervical region of primates. Schultz (1960) observed that the lengths and projecting angle of the cervical transverse processes are highly variable across primates. So, for the most part, only very general descriptions of the processes prevail in the literature; for example, the term "monkey-like" is used to describe transverse processes that are "longer," and the term "human-like" is used to describe transverse processes that are "shorter" (Schultz, 1960; Tominaga et al., 1995). As mentioned earlier, no attempt has been made to support or refute these statements. Slijper (1946) and Toerien (1961) observed that quadrupedal monkeys generally have short spinous processes, while *Gorilla* and *Pan* exhibit long cervical spinous processes. These authors suggested that ape morphology was related to the size and balance of the head, but again, no quantitative data have been collected to verify what these qualitative terms actually mean.

Each transverse process has a foramen (*foramen transversarium*) through which the vertebral artery travels cranially to supply the brain. This foramen is unique to the cervical vertebrae. Notably, the *foramen transversarium* is commonly absent in the C7 of apes and humans and occasionally from C6 and/or C5 (Schultz, 1961). The absence of this feature is due to the underdevelopment of the anterior component of the transverse process (Ankel-Simons, 2007). When present, the foramen nearly divides the transverse process, so that two tubercles project from the process tips anteriorly and posteriorly. These anterior and posterior tubercles are the sites for muscle attachment. Mercer (1999) found that more orthograde species tend to have larger posterior tubercles on the transverse processes, which, she argued, increases the mechanical advantage of the attaching muscles in stabilizing bending movements on the coronal plane.

Atypical cervical vertebrae

Unlike the rest of the spine, in which the intervertebral discs and vertebral bodies resist axial compression, the atlas, C1 (which does not have a body), passes loads from the occipital condyles inferiorly through the articular facets to the axis, or C2 (Levangie and Norkin, 2001). The convex occipital condyles (C0) constitute the superior component of the atlanto-occipital joint, while the first cervical vertebra (C1) serves as the inferior component. The articulating surfaces of the joint vary greatly in *H. sapiens*, and the stereotypical elongated, oval, kidney-bean-shape morphology is actually uncommon. Most articular surfaces are irregular in shape, and the left and right condyles of the same individual may differ in size (Singh, 1965; Kapandji, 1974; Guidotti, 1984; Mercer and Bogduk, 2001; Billmann et al., 2007). The superior articular facet is generally considered a singular concavity, but variations in human form have been reported to include flat and split facets.

Documentation of nonhuman condylar morphology has been limited to the great apes, some fossil hominins, and *Papio anubis*. Descriptions are restricted to general morphology and in some cases degree of curvature is discussed (Graf et al., 1995a; 1995b; Aiello and Dean, 1990, p. 218; Dickman et al., 1994, p. 134; Tominaga et al., 1995; Elias et al., 2006; Nalley, 2008). Humans are commonly described as exhibiting flatter facets than other hominoids, but the little quantitative work reports conflicting results (Corner and Latimer, 1991; Nalley, 2008).

The atlanto-axial joint surfaces are flat and circular in shape and this geometric design allows considerable mobility. The axis is unique because of the dens, or odontoid process, a small peg of bone that protrudes upwards behind the anterior arch of the atlas.

The joint is positioned in a way that allows rotation of the atlas together with the head around the dens of the axis (White and Panjabi, 1990; Bogduk and Mercer, 2000). Axis morphology separates primates taxonomically and some of this variation has been linked to positional behavior (Ankel, 1972; Manfreda et al., 2006). For example, the angulations of the odontoid process and the superior articular facets of C2 are greatest in nonhominoids (odontoid process angled dorsally ~30 degrees and facets angled ~ 45 degrees); humans exhibit a relatively vertical odontoid process and horizontally flat facets, whereas Hylobatidae and great apes exhibit facets that are intermediate between those of humans and nonhominoids, though the odontoid processes in Hylobatidae and *Pan* tend to be straight, as in humans. *Pongo* and *Gorilla* have more inclined odontoid processes. Intraspecific variation in these features seems to be greater in nonhuman primates, perhaps reflecting more diverse positional repertoires or a weak association with positional behavior or both (Ankel, 1972).

Manfreda et al. (2006) and Mitteroecker et al. (2007) examined the relationship between locomotor pattern and the overall morphologies of C1 and C2. The researchers found that nonhuman primates differ in their atlas and axis morphologies along a locomotor gradient, ranging from pronograde to orthograde. The first cervical vertebra of more orthograde species exhibits relatively thinner anterior and posterior arches, more ventrally and caudally oriented transverse processes, and more inclined and laterally rounded superior articular facets. Notably however, human morphology in both vertebrae was distinctive and did not reflect an extrapolation from the more orthograde primate model. This could imply that the human cervical vertebral form reflects a unique adaptive history.

Examples from the primate fossil record demonstrate the inefficiency of the use of generalized terms (i.e., monkey-like or human-like) when describing fossil vertebrae and the need for more thorough morphological documentation. A.L. 333-106, representing *A. afarensis*, is one of the most complete and early vertebral specimens at ~3.2 Ma (Lovejoy et al., 1982). A.L. 333-106 (probably a C6) exhibits a long spinous process, which is not bifid, and has been noted for its relatively small vertebral body; it has thus been described as exhibiting a *Pan*-like morphology (Lovejoy et al., 1982). However, its actual degree of similarity to apes remains unexamined. In addition, the transverse and spinous processes of the KNM-WT 15000r *H. erectus* cervical vertebra seem to be intermediate between the short processes typical of modern humans and the long processes found in *Pan*. Previous studies of the early *Homo* cervical material have also noted that the size of the C7 vertebral canal relative to body weight for KNM-WT 15000r (*H. erectus*) and KNM-ER 164c (*Homo* sp. indet.) fall within the narrow range of extant hominoids (MacLarnon, 1993).

The superior articular facet of the *A. afarensis* atlas vertebra (A.L. 333-83), has been described as relatively concave and ape-like (Coroner and Latimer, 1991); however, a comparative study of primate atlanto-occipital joint shape found that the Hadar atlas cannot be distinguished from any extant hominids, including modern humans, with respect to facet curvature (Nalley, 2008). Hominin upper cervical specimens from the Plio-Pleistocene include a fragmentary atlas from Koobi Fora (KNM-ER 1825) and a more complete axis missing its spinous process from Swartkrans (SK 854) (Robinson, 1972; Leakey and Walker, 1985). Robinson (1972) described the SK 854 axis and attributed it to *Paranthropus*. The right superior facet was described as more curved than

in modern *Homo*. Robinson (1972) also noted that the preserved right inferior articular facet is more horizontal and seems to be set obliquely in the neural arch and not out on a clear bony projection as in modern human morphology. Once again, however, the significance of these features is unknown and the descriptions are qualitative; whether or not these features are truly more like one primate taxon or another remains to be determined.

Upper cervical vertebrae are well represented in more recent hominin fossil species. In addition to testing hypotheses regarding positional behavior, they may also shed light on the effects of differences in cranial shape, robusticity, and perhaps even phylogeny of cervical vertebral form. For example, middle Pleistocene Neandertal cervical vertebrae from Shanidar and *H. heidlebergensis* from Sima de los Huesos both show enlarged insertion areas for nuchal muscles and robust processes (Trinkhaus, 1983; Arsuaga et al., 1999; Carretero et al., 1999). One explanation for this increased robusticity is that these features indicate increased muscular forces acting at the atlanto-occipital joint to counter the greater degree of prognathism in comparison to modern humans described in these specimens (Gómez-Olivencia et al., 2013). An alternative (and more widely supported) scenario suggests that these enlarged muscular attachment areas simply reflect the overall robusticity of the skeleton and/or high activity levels, factors that could produce increased caudal projection of the C1 anterior tubercle, which would agree with the large body masses estimates for these hominins (Trinkhaus, 1983; Arsuaga et al., 1999; Carretero et al., 1999).

Though most research on cervical vertebrae has focused on modern humans, a limited number of investigations concerning nonhuman primate morphology have

reported biomechanical patterns in a variety of cervical features (Slijper, 1946; Schultz, 1961; Toerien, 1961; Ankel, 1972; Mercer, 1999; Manfreda et al., 2006; and Mitteroecker et al., 2007). The goal of the following section is to first discuss how the spine and cervical vertebrae can be biomechanically modeled and then secondly, highlight vertebral features found relevant in the medical and biomechanical literatures that can be used here to test predictions from the models in a comparative study of extant primate taxa.

THEORETICAL BIOMECHANICS

Support for a hypothesis of adaptation requires both a correlation between a trait and a function (i.e., locomotor behavior) and a demonstration that the trait performs the function (Kay and Cartmill, 1977). In this case, it is challenging to demonstrate that a trait performs a function because there is no straightforward way to directly observe whether a specific trait of the cervical spine functions to allow a particular positional behavior. Besides direct observation, another way to show that a trait performs a function is to build a biomechanical model of the system and to use optimality criteria (that are based on the expectations of optimal performance, however that may be defined for a given system) to generate predictions of adaptive morphology based on the mechanical requirements of the system (Rudwick, 1964). If mechanical predictions of morphology based on function are supported via hypothesis testing, then it can be concluded that the morphological trait performs the behavioral function.

The forces acting on the cervical spine are a result of the overall mechanics of an animal's movements, and so it is necessary to take positional behavior and the biomechanical forces it applies into account when generating and testing hypotheses of

vertebral adaptation to positional behaviors. Complex systems, such as a musculoskeletal system performing a postural or locomotor behavior, can be better understood by constructing and testing simplified models of those systems. Biomechanical models of different positional behaviors can describe the forces that act on the skeleton and in turn, how the skeleton reacts to the inferred modeled forces. The effect of stress resistance on skeletal morphology is likely to be particularly important because loading regimes characteristic of different positional groups will produce stereotypic stress patterns in bone, which is expected to produce adaptive variation in bony anatomy (Martin et al., 1998; Ruff, 2000).

Depending on the posture and distribution of body mass, the neck, torso, and tail of a resting animal experience forces and bending moments. Bending moments along the vertebral column act primarily in the sagittal plane (unless parts of the body, such as the tail, are accelerated quickly sideward) (Christian and Preuschoft, 1996). The pattern of bending moments along the vertebral column is different between pronograde and orthograde animals. These two models reflect fundamentally different loading regimes on the musculoskeletal systems and therefore are expected to be reflected in different morphological adaptations (Slijper, 1946; Christian and Preuschoft, 1996). Furthermore, the cervical spine is argued here to be under extraordinary bending forces during suspensory positional behaviors and support the development of an additional biomechanical model to account for this distinctive loading regime. The biomechanical differences among postural and locomotor groups are outlined below, and the differences in vertebral shape among groups are explored later in the chapter.

Pronograde model

The mammalian pronograde vertebral column has been previously modeled as a "bow-and-string" system in the sagittal plane (Figure 2-3) (Slijper, 1946; Badoux, 1965; 1967; Preuschoft, 1978; Preuschoft et al., 1988; Christian and Preuschoft, 1996). The elastic bow includes the precaudal vertebral column, pelvis, and epaxial musculature, and is flexed ventrally by a string, formed by the sternum and a number of ventrally located soft tissue structures such as the abdominal muscles and linea alba. This model includes the head and neck section of the vertebral column, though Badoux (1977) points out that the hard and soft tissues are inverted (see Figure 2.3). Regardless, similar biomechanical forces inferred from the string-and-bow model are expected.

The bow-and-string model predicts that the primary static function of the vertebral column will be to resist bending in the sagittal plane. In general, bending moments along the vertebral column are counteracted at the intervertebral junctions primarily by tension in epaxial muscles, tendons, and ligaments that are located dorsal to the vertebral centra (Preuschoft, 1976; Christian and Preuschoft, 1996; Christian and Henrich, 1998).

The vertebral column is critical for locomotion and must transmit loading from the hindlimbs to the forelimbs. Quadrupedal locomotion emphasizes flexion/extension movements in the sagittal plane (Jenkins, 1971; 1974); these movements are prominent in leaping and galloping because they increase stride length (English 1980; Zomlefer et al., 1984). A flexible spine accomplishes this and has been demonstrated in lumbar and thoracic vertebrae of pronograde primate taxa (Slijper, 1946; Ward, 1993; Shapiro, 1993, 1995, 2005; Johnson and Shapiro, 1998). The head and neck also move and translate

through space during locomotion. Experimental research demonstrates that, depending on the speed at which an animal moves, the neck also makes comparable, if not sometimes greater, movements in the sagittal plane when compared to other sections of the torso (Dunbar et al., 2004; 2008). Therefore, the cervical vertebrae can be expected to reflect the general patterns of movement found in the lower vertebral columns: providing flexibility for flexion/extension movements required for generalized pronograde positional behaviors.

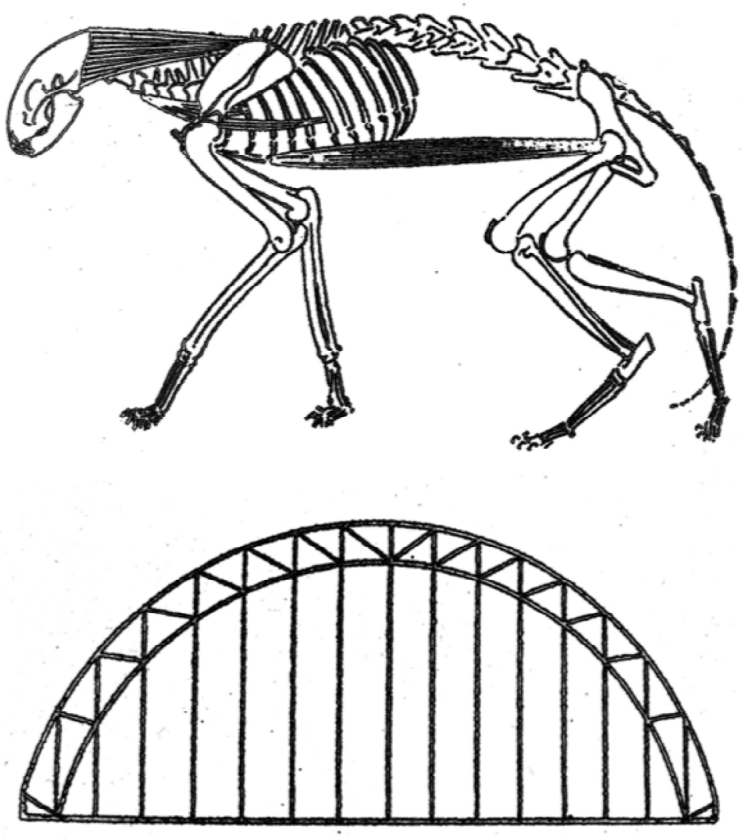

Figure 2-3. Adapted from Slijper (1946). The pronograde spinal column can be modeled as a bow-and-string construction where the vertebrae and associated soft tissues (i.e., expaxial muscles, tendons, and ligaments) act as the elastic bow and abdominal muscles and other tissues act as the string.

Orthograde model

In orthograde primates, the vertebral spine is habitually held perpendicular to the ground and has been modeled as a beam or column supported at single end (e.g., hips) (Slijper, 1946; Preuschoft, 1978; Preuschoft et al., 1988; Christian and Preuschoft, 1996) (Figure 2-4). The orthograde model also includes the head and neck, thus similar adaptations are expected across the vertebral column as a whole.

The orthograde model predicts a concentration on the maintenance of overall erect posture and thus a reduction in movement across most directional planes. For example, when the torso is erect, sufficient extensor leverage is required to prevent the vertebral column from falling forward, given that the center of mass is always ventral to spinal column. Furthermore, leverage for lateral flexion is also necessary in order to manage sway of the body in the coronal plane (Shapiro, 1995). Lateral flexion also can be a major movement during arm swinging or during flight phase of leaping in vertical clinging and leaping during which there is no support for the limbs and the back is held in a near vertical position (Oxnard et al., 1990). Therefore stability in both sagittal and coronal planes would be expected in more orthograde primates.

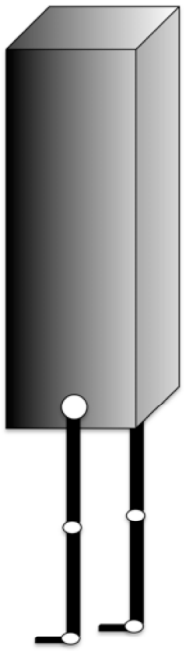

Figure 2-4. Schematic illustration of the orthograde model, which constructs the vertebral spine as a vertical column.

Suspensory model

Due to the fact that all suspensory primates are also orthograde, the vertebral column is vertically oriented to the ground and is again modeled as a beam supported at single end. However, due to increased bending moments placed on the cervical vertebrae via the pectoral girdle, the difference between the orthograde and suspensory models will be in the *degree* of stabilizing mechanisms and leverage for powerful extension. As previously mentioned, suspensory primates have highly mobile shoulder joints, which have the strength to support and move the entire body even uni-manually. A more stable cervical vertebral column must provide a rigid origin for the muscles acting on the shoulder and upper limb.

These powerful muscles primarily originate and insert dorsally and laterally, suggesting that this stability needs to occur during extension and movements on the coronal plane.

Head and axial body stabilization during brachiation and other suspensory movements are suggested to be important components of effective suspensory locomotor behavior. Suspensory locomotion (i.e., brachiation) can be modeled as a pendulum (when applied to continual contact brachiation) (Bertram and Chang, 2001; Bertram, 2004). When a brachiating primate's back arm releases its handhold, the torso makes two movements: a pendulum movement and a rotational movement under the supporting arm, which moves the torso in the direction of the pendulum movement. The torso is able to make this rotational movement under the supporting arm, because the scapula is kept in place by both the muscles attaching it to the torso and the clavicle, which keeps the acromio-manubrium length constant (Voisin, 2006). Research modeling suspensory locomotion indicates that a key factor for efficient movement is controlling the path of

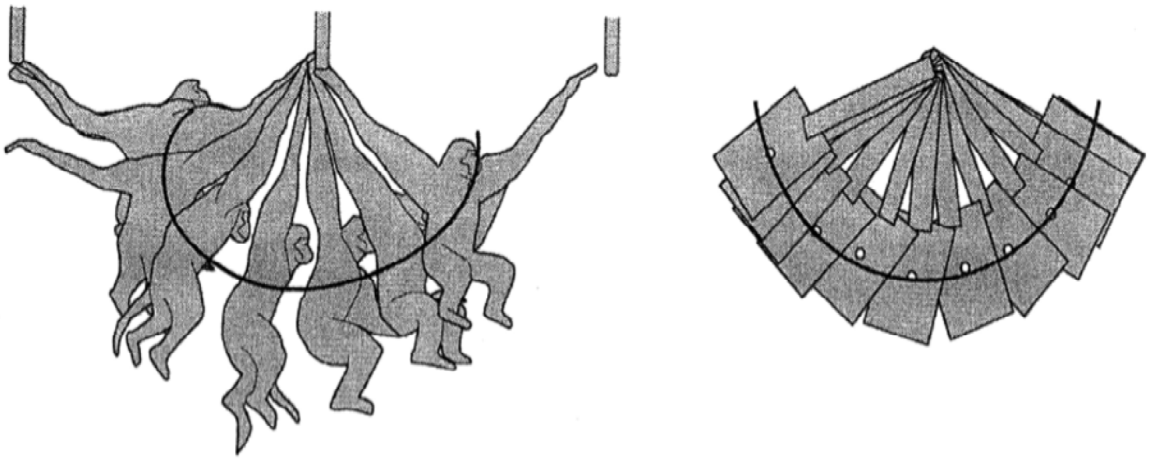

Figure 2-5. Suspensory model, adapted from Bertram and Chang (2001). Suspensory behavior can be modeled as a pendulum and the maintenance of path of the torso is critical to efficient movement.

the body's center of mass as it shifts from one arm to the next (Bertram and Chang, 2001; Bertram, 2004). The maintenance of the center of mass is critical to reduce collision-contact energy loss and thus maintain energetic efficiency (Figure 2-5). Muscles that attach the forelimb to the torso rather than the more distal muscles (i.e., those that control contact between the hand and substrate) are expected to better facilitate this control of motion (Bertram and Chang, 2001). This idea is supported by experimental work. Jungers and Stern (1984) and Larson et al. (1991) suggest that the relatively large size of the cranial portion of trapezius in apes is associated with the muscular requirements of head turning and stabilization during suspensory locomotion. Figure 2-6 demonstrates that the cranial trapezius is active during the entire sequence of suspensory behaviors, compared to the more caudal trapezius with is only active during arm raising.

Morphological features supporting this suspensory model have already been observed in the thoracic and lumbar regions of the spine (Keith 1923; Schultz, 1961; Cartmill and Milton, 1977; Ward, 1993; Johnson and Shapiro, 2002; Gebo, 1996) and thus it is reasonable to infer that the cervical region would be under similar

biomechanical requirements, particularly given the level of direct attachment between the neck and the pectoral girdle. Therefore, a further reduction in flexibility (in both sagittal and coronal planes) and emphasis on powerful extension are expected in suspensory primates — distinct from orthograde-nonsuspensory taxa.

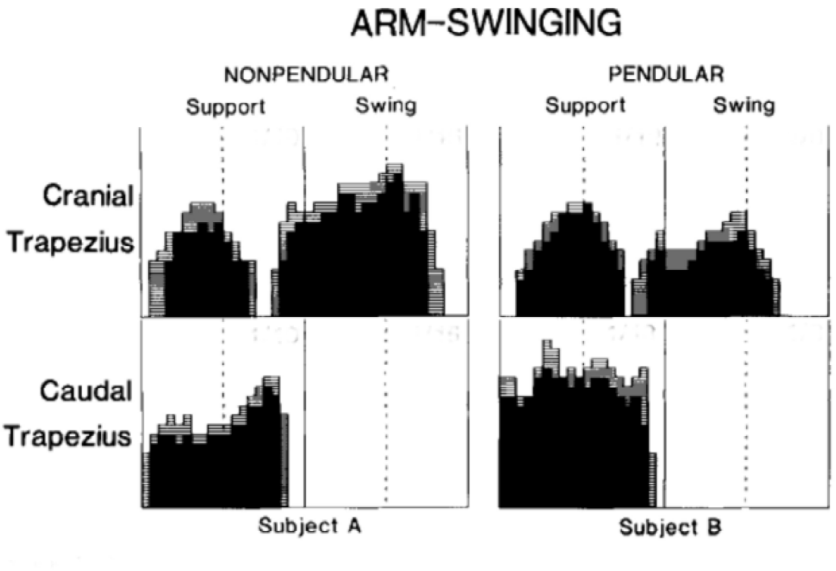

Figure 2-6. Electromygraphy output data taken from Larson et al., (1991). Data demonstrate that the cranial trapezius is active during the entire locomotor sequence.

Head-balancing model

If considered separately from the rest of the spinal column, the cervical region of the spine can also be modeled as a cantilevered flexible beam or rod (Slijper, 1946; Badoux, 1968, 1974; Demes, 1985), where the weight of the head and neck are supported by both the vertebral column and by the nuchal muscles and ligaments (i.e., nuchal and supraspinous ligaments) (Slijper, 1946; Preuschoft, 1978; Preuschoft et al., 1988). This would mean region-specific bending stresses should be considered instead. For example, if considered as a cantilevered beam supporting the weight of the head (essentially acting

as a class 1 lever system), stabilization of the head on the neck (particularly in long-faced taxa) might take precedence to overall positional behaviors. The cantilevered beam model (which will be referred to as the "head-balancing model") predicts a strong relationship between vertebral and cranial morphologies. Therefore, any relationships found between positional behavior and vertebral morphology may also need to account for differences in cranial morphology. Whether the positional behavior models (pronograde/orthograde or suspensory/nonsuspensory) better predict the bony morphological variation than the head-balancing model will be tested in Chapter 4.

BONY VERTEBRAL FEATURES

The spinal column can be considered a mechanical structure with components that articulate with each other through a series of levers (vertebrae), pivots (facets and discs), passive restraints (ligaments), and activations (muscles). This section discusses relevant skeletal features taken from the biomechanical research performed on the human spine (including the cervical region) and are thus appropriate for testing the biomechanical models described in the previous section (Compere et al., 1959; Penning, 1968; Kapandji, 1974; Hayashi and Yabuki, 1985; Penning and Wilmink, 1987; Yoganandan et al., 1988; White and Panjabi, 1990; Milne, 1991; Whyne et al., 1998; Bogduk and Mercer, 2000; Yoganandan et al., 2001; Takeshita et al., 2004; Kurtz and Edidin, 2006).

Centrum

The vertebral body or centrum is a roughly cylindrical mass of trabecular bone contained within a thin shell of cortical bone and is specialized for weight transmission (Kapandji, 1974; Yoganandan et al., 1988; Kurtz and Edidin, 2006). The shape of vertebral bodies is related to the stability and flexibility of the vertebral column.

The first trait to consider is craniocaudal length. In the lumbar region of the spine, craniocaudally long vertebrae reflect a more flexible vertebral column, while short vertebrae indicate a more stable or rigid vertebral column (Ward, 1993; Shapiro, 1995, 2007). This is because for a given angular excursion per vertebral pair, a shorter vertebral series result in smaller bending moments (Ward, 1991). Thus, for a given vertebral pair, reducing the length of the vertebrae (since reduction of the number of cervical vertebrae is under strict genetic constraint and thus less likely (Galis, 1999)) decreases the total amount of flexion at that spinal segment and of the column as a whole. This reduces the moment produced about the discs, and the stresses placed upon them (Figure 2-7) (Ward, 1993). When reaching for support in an arboreal setting, a suspensory animal with a large body mass would subject its spine to potentially large bending and torsional loads, all of which would be minimized by shortening the spinal column, increasing control over its movements. Therefore, it is expected that suspensory primates would have shorter cervical vertebral bodies, and thus less flexible cervical columns, compared to nonsuspensory primates in order to resist bending forces from the upper limb during suspensory locomotion.

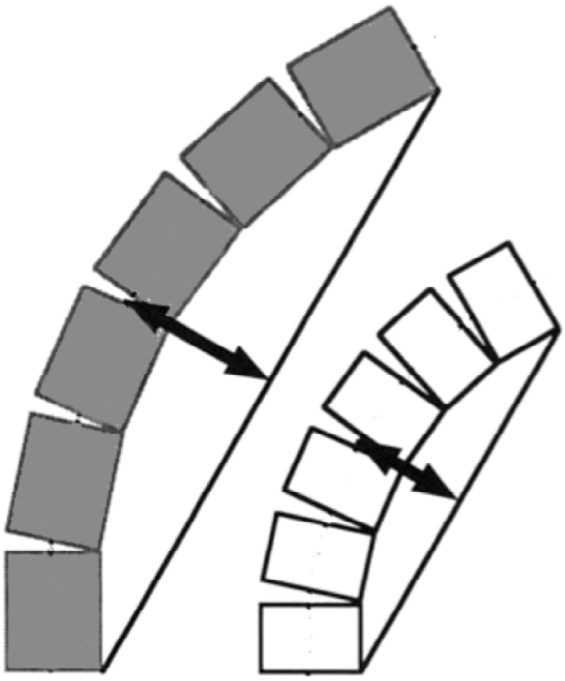

Figure 2-7. Schematic diagram of moments experienced in axial loading in long and short cervical columns, adapted from Ward (1993). The blocks represent vertebral centra and intervertebral discs would be located in between each block. The arrow indicates the maximum bending moment produced during axial loading. Longer vertebrae increase gross bending moments produced about the discs, where shorter vertebrae result in smaller bending moments.

Eccentricity of the vertebral body surface has also been suggested to affect spinal stability. Among primates, in general, the mediolateral width of the cervical centrum is greater than the dorsoventral dimension. This morphology is due in part to the presence of uncinate processes (further discussed below) on the lateral margins of the vertebral bodies (White and Panjabi, 1990; White, 1991). Mercer (1999) found that more orthograde primates have cervical vertebrae with increased ventrodorsal dimensions and thus a more circular shape (mediolateral width ≈ ventrodorsal height). Mercer argued that this morphology, which has also been documented in more stable lumbar vertebral columns (Slijper, 1946; Johnson and Shapiro, 1998), provides greater resistance to bending moments in the sagittal plane. However, this relationship in the cervical region

was documented in the context of positional behavior (i.e., more orthograde vs. more pronograde) in a relatively limited sample (six intrageneric pairwise comparisons). Since all extant hominoids are orthograde, testing for this pattern in the context of locomotor behavior (suspensory vs. nonsuspensory) and across a broader range of primate taxa would strengthen its applicability to the hominin fossil.

Unlike in thoracic or lumbar vertebrae, the articular surfaces of the lower five cervical vertebral bodies are not flat. Posterolaterally, the cranial margins curve upward as the uncus or uncinate processes. These processes stabilize movement between the vertebral bodies via the intervertebral disc—accommodating the coupling of lateral bending and axial rotation that is characteristic of this region of the spine (Compere et al.,

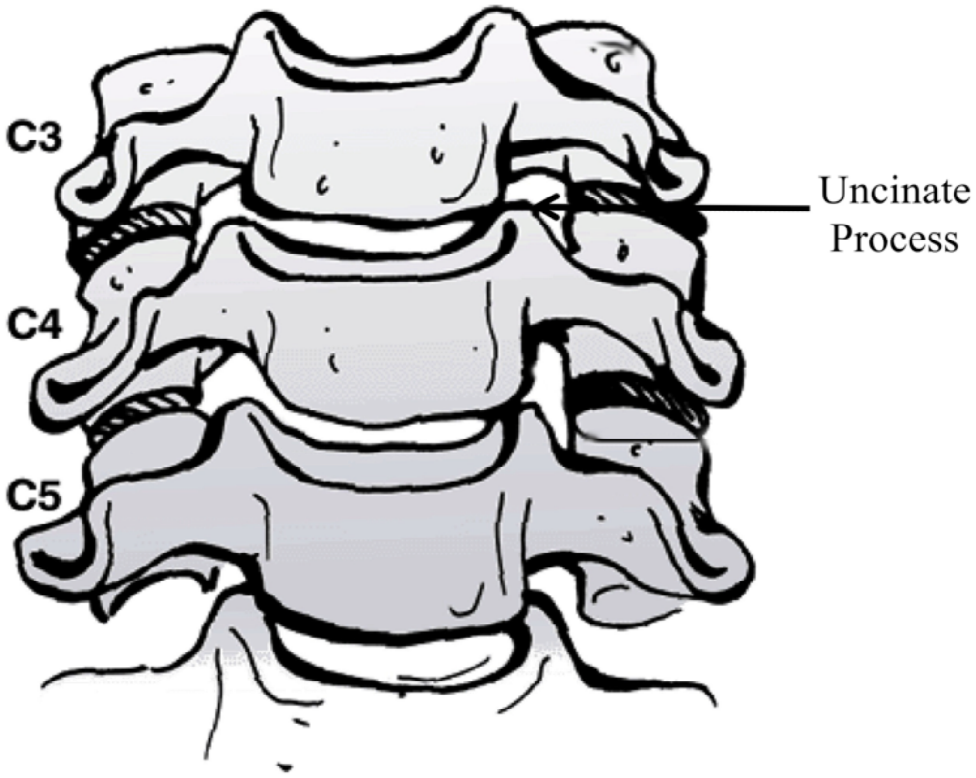

Figure 2-8. Adapted from Rockwood and Green (2006). Anterior view of human cervical spine: C3-C5. Uncinate process indicated by arrow.

1959; Penning, 1968; Hayashi and Yabuki, 1985; Penning and Wilmink, 1987; Yoganandan et al., 2001). Movement is permitted by the uncovertebral clefts formed by the uncinate processes and the vertebral body of the vertebra above, which specifically guide and limit anteroposterior translation during axial rotation in humans (Figure 2-8) (Milne, 1991).

Uncinate process features (e.g., height) are correlated with differences in cervical segmental movement. Milne (1991) found that the more horizontal the superior facets, the greater the uncinate process height. In humans, the processes with the greatest height are found in the upper cervical spine (C3-C4), where any axial rotation is coupled with lateral bending. These coupled movements result in greater shear forces at the intervertebral discs (Tondury, 1959). Milne (1991) argued that the link between facet angle and process height supports the hypothesis that uncinate processes guide and limit dorsoventral translation. If so, more pronograde taxa would be expected to exhibit taller uncinate processes due to increased dorsovental shearing forces inferred from a vertebral column (including the neck) that is more parallel to the substrate. This relationship has not been tested outside of modern human sample, but if this relationship were maintained in other primate taxa, the functional role suggested by Milne (1991) would be supported.

Neural Arch: Pedicles and Laminae

The pedicles provide the connection between the vertebral bodies and the posterior vertebral elements. This bony structure is of particular relevance because all of the mechanical forces received in the posterior components are directed to the pedicles, which then transmit these forces to the vertebral bodies. Pedicles have also been shown to play an important role as structural buttresses providing support to the posterior wall of

the vertebral body (Whyne et al., 1998). Differences in direction and degree of muscular forces transmitted from the posterior component would be expected to result in differences in morphology. According to generalized beam theory, increased bending forces require larger bony circumferences to maintain structural integrity. This has been demonstrated in other areas of the spine and skeleton (Martin et al., 1998; Ruff, 2000), and would provide the basis for testable differences in pedicle morphology.

The laminae are continuous with the pedicles dorsally via the articular pillars and, together with the spinous process, circumscribe the vertebral foramen. The laminae are positioned between the spinous process and articular pillars and any forces generated at these sites will be transmitted through the laminae. The laminae are functionally relevant because, with the exception of the prevertebral muscles (longus colli and longus capitis), all muscles acting on typical cervical vertebrae (C3–C7) take their attachment from the dorsal vertebral components (Kapandji, 1974; Dean, 1982; Swindler and Wood, 1982; White and Panjabi, 1990) and it can be assumed that any bending forces generated at these sites will be transmitted through the laminae. Therefore, pedicles and laminae with relatively greater cross-sectional areas are expected in suspensory taxa because they have relatively larger (i.e., greater physiological cross-sectional area) nuchal muscles (Swindler and Wood, 1982; Dean, 1982) to better resist increased bending loads.

Articular Processes

Each lower cervical vertebra (C3-C7) articulates with the vertebra above and below it via articular processes. Vertebral patterns of movement are heavily dependent on the shape and position of these processes, and predictions can be made regarding how taxa that differ in locomotor behavior should differ in morphology (Kapandji, 1974;

White and Panjabi, 1990). Coronal orientation of the facets allows lateral bending (i.e., movement in the coronal plane), but restricts translation and motion in the sagittal plane by providing greater resistance to the forward displacement of the cervical vertebrae; this condition is expected in more pronograde primates, where the neck is extended out from the torso more or less perpendicularly to the line of gravity (Figure 2-9) (Panjabi et al., 1993; Bogduk and Twomey, 2005; Russo, 2010).

In contrast, a more transverse orientation of the articular facets is thought to reflect an increased weight-bearing role in orthograde positional behaviors, because the facets are positioned perpendicular to the axial compressive forces acting on the joint from the head and neck (Mercer, 1999; Pal and Routal, 1986; 1999). Transverse orientation of the articular facets permits rotation and translation and this relationship has been documented in the cervical vertebrae of *Tarsius*, whose transversely oriented facets allow increased axial rotation (~180 degrees) when compared to most other primates (Ankel-Simons, 2007). A transverse orientation of the articular facets is expected in

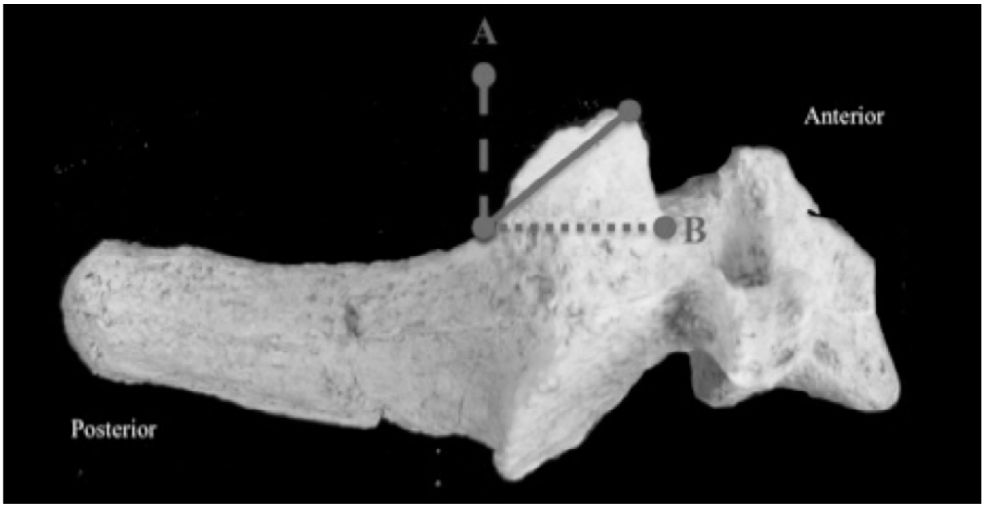

Figure 2-9. Lateral view. Solid line marks the orientation of the superior articular facets. The dashed line (A) demonstrates a more coronally oriented facet while the dotted line (B) illustrates a more transversely oriented facet.

orthograde and suspensory primates to help distribute increased compressive forces in more vertical positional behaviors.

Transverse and Spinous Processes

The spinous and transverse processes are sites of muscle attachment, and process length and orientation influence the moment arm and line of action of the nuchal muscles. Greater projection of the processes will increase the moment arm of the muscles, and hence their mechanical advantage (all other factors being equal), and reduced projection will decrease their mechanical advantage (Slijper, 1946; Shapiro, 1993; Cripton, 1999). In extant hominoids, the multifidus muscle attaches along the length of the cervical spinous processes and then spreads onto the laminae and articular pillars (Dean, 1982; Swindler and Wood, 1983; Anderson et al., 2005). This configuration is important for stability because greater dorsal projection of the spinous processes of C3–C6, as observed in *Gorilla* and *Pan*, increases the leverage of the multifidus muscles and the cervicis muscles of the *erector spinae* group. Experimental work has demonstrated that these muscles are key to spinal stability and maintenance of posture in humans (White and Panjabi, 1990; Anderson et al., 2005).

Size and orientation of the transverse processes will also affect muscular function. Reduced transverse processes decrease the moment arm (and thus mechanical advantage) of the more superficial muscles (e.g. *longissimus cervicis*) that laterally flex and rotate the cervical vertebrae. A more dorsal orientation of the processes increases the deep spinal muscles' ability for powerful extension and overall stability by increasing their moment arm, while ventral orientation will have the opposite effect (Ward, 1991, 1993; Shapiro, 1995; Shapiro et al., 2005). Suspensory primates are predicted to have more

dorsally oriented and reduced transverse processes, reflecting an overall greater need for stability, particularly in the coronal and sagittal planes (Ward, 1991; Shapiro, 1995, 2007).

Spinous processes of suspensory primates are predicted to be more projecting, indicating the presence of more powerful deep nuchal muscles and increased moment arms for extension (Shapiro and Simons, 2002). Greater spinous process cross-sectional areas are also predicted for more suspensory taxa, reflecting greater resistance to bending forces (Mercer, 1999; Anderson et al., 2005).

SUMMARY AND PROJECT OVERVIEW

This chapter outlined the incorporation of comparative vertebral research concerning the causes of variation in primate cervical and pectoral girdle morphology with biomechanical theory. Extant apes are characterized by a highly mobile shoulder joint that is positioned dorsally on the torso with a cranially oriented glenoid fossa. This bony morphology exists in concert with relatively powerful nuchal musculature (Ashton and Oxnard, 1964, Dean, 1982; Stern and Susman, 1983; Swindler and Wood, 1982; Larson, 1995). This combination of bony and soft-tissue features are considered adaptations to suspensory locomotion because they permit the specialized movements of required for brachiation and suspended postural behaviors (Ashton and Oxnard, 1964; Stern and Susman, 1983; Susman et al., 1984; Larson, 1995; Gebo, 1996; Larson, 2007). In contrast to the apes and atelines, most other primates use nonsuspensory positional behaviors. Quadrupedalism, either arboreal or terrestrial, is characterized by a more stable shoulder joint with scapulae that are located laterally on the torso and glenoid fossae that are oriented ventrally.

Vertical clingers and leapers also exhibit nonsuspensory scapular morphology (Stern and Susman, 1983; Larson, 2007). The modern human scapula is distinguishable from those of extant apes by its more caudally oriented glenoid fossa and more inferior location on the dorsal torso (Ankel-Simons, 2007; Larson et al., 2007).

This chapter has also established the importance of conducting a study of adaptation in the primate cervical spine. Previous research has identified skeletal correlates of positional behavior in both the pectoral girdle and the more caudal regions of the spinal column (Schultz, 1930; Slijper, 1946; Fleagle, 1978; Jenkins et al., 1978; Swindler and Wood, 1982; Dean, 1982; Stern and Susman, 1983; Larson and Stern, 1986; Pal and Routal, 1986; Ward, 1991; Harrington et al., 1993; Ward, 1993; Larson, 1995; Shapiro, 1995; Johnson and Shapiro, 1998; Mercer, 1999; Shapiro and Simons, 2002; Voisin and Balzeau, 2004; Anderson et al., 2005; Shapiro et al., 2005; Voisin, 2006; Larson et al., 2007; Shapiro, 2007; Young, 2008; Russo, 2010), but a gap in understanding still exists for primate cervical vertebrae shape. Furthermore, a primate-wide comparative study of cervical bony morphology has not been conducted. Accurately identifying which morphologies are adaptations to positional behavior requires a trait-function correlation (Kay and Cartmill, 1977). With this goal in mind, biomechanical models of the cervical spine were outlined in relationship to positional behavior (pronograde, orthograde, and suspensory models) and cranial morphology (head-balancing model). This study tests the predictions put forth by these difference scenarios using a comparative approach and a large, taxonomically diverse sample of primate species that exhibits variation in positional behaviors, cranial morphology, and body size. The results obtained from analyses will form the basis of a general model of cervical

stress resistance and to elucidate the form-function interface between cervical vertebral morphology, positional behavior, and cranial morphology.

Chapter 3

MATERIALS AND METHODS

Identification of adaptations in the cervical vertebrae requires a verified relationship between vertebral form and function. Preferably, this functional association should be demonstrated in a comparative context that accounts for sharing of traits among extant taxa due to common ancestry (homology). Therefore, a primary goal of this project is to determine if and how vertebral morphology is related to positional behavior and this concept represents the overarching adaptive hypothesis to be tested. The alternative cervical models proposed to test this hypothesis are described below and are followed by a rationale for the specific predictions for each model.

Once the patterns exhibited by extant species are established, fossil hominoid cervical vertebral morphology can be examined. Issues such as whether or not suspensory behaviors characterized the last common ancestor of chimpanzees and hominins has important implications with respect to the adaptive explanation for the origin of bipedality, a long-standing unresolved problem in paleoanthropology. Arguments for a suspensory ancestor for the African ape and hominin clade rely on accurate interpretations of features as reflective of suspensory positional behaviors.

CERVICAL VERTEBRAE MODELS

Suspensory model predictions

The first step in testing the hypothesis of adaptation was to test specific predictions regarding whether vertebral form followed biomechanical expectations of the suspensory model in pairs of anthropoid primate taxa that differ in locomotor behavior: (1) great apes (*Pan*, *Pongo*) versus *Homo*, (2) *Ateles* versus *Alouatta* and *Pithecia*, and

(3) hylobatids versus similar-sized cercopithecoids (*Papio* and *Nasalis*). These pairwise comparisons were chosen to minimize differences due to allometry (i.e., size-required changes in shape) and/or phylogenetic history (i.e., by comparing closely related, biologically similar species). The first two comparisons accomplish both of these goals: the comparisons include species that are broadly similar in body mass and are conducted within family-rank taxa. Phylogenetic distance may represent a confounding problem in the hylobatid-cercopithecoid comparison, as these taxa probably diverged at least 25 million years ago (Goodman et al., 1998; Glazko and Nei, 2003; Hasegawa et al., 2003). However, the highly suspensory hylobatids lack a closely related nonsuspensory relative of similar body size for comparison, and thus comparing them to cercopithecoids ensures that they are represented in the analysis. Comparisons of suspensory hominoids to nonsuspensory cercopithecoids have a long history in anthropology and have proved to be highly informative (Schultz, 1942, 1961; Ankel, 1972; Ward, 1991, 1993; Larson, 1995; Larson et al., 1991; Larson et al., 2007).

Specific Predictions. Relative to the nonsuspensory taxa, suspensory taxa in each comparison are predicted to show the following vertebral features (see summary in Table 3-1):

1. Centrum shape
    a. Suspensory taxa are expected to have relatively circular (an increase in dorsoventral height relative to mediolateral width) dimensions to withstand larger bending loads in both the sagittal and coronal planes, specifically during extension and/or lateral bending (Slijper, 1946; Shapiro, 1995; Johnson and Shapiro, 1998; Mercer, 1999).

b. Suspensory primates are also expected to demonstrate craniocaudally shorter bodies to resist increased bending forces in all planes from forelimb activity patterns during suspensory behaviors (e.g., forelimb abduction/adduction, head and torso rotation) (Ward, 1993; Shapiro, 1995, 2007).

2. Pedicle and Lamina shape
    a. Suspensory species will have greater pedicle and laminae cross-sectional areas than nonsuspensory species to better resist inferred increased bending loads during extension from more powerful nuchal musculature (Swindler and Wood, 1982; Dean, 1982)
3. Transverse process shape
    a. Transverse processes are predicted to be less projecting (i.e., shorter) to facilitate greater stability in the coronal plane by decreasing the mechanical efficiency of the superficial nuchal muscles during lateral bending and rotation.
    b. Transverse processes are also predicted to be more dorsally oriented, thereby increasing the deep nuchal muscles' ability to resist ventral flexion (and in turn perform more powerful extension) by increasing their moment arms (Ward, 1991; Shapiro, 1995; Shapiro et al., 2005).
4. Spinous process shape
    a. Spinous processes are predicted to be more projecting (i.e., longer), indicating the presence of larger (i.e., greater physiological cross-sectional

area) deep nuchal muscles and increased moment arms for extension (Shapiro and Simons, 2002).

b. Greater spinous process cross-sectional areas are also predicted for suspensory taxa, reflecting greater resistance to bending forces (Mercer, 1999; Anderson et al., 2005).

5. Articular process shape

a. Suspensory primates are predicted to have flatter articular processes oriented in the transverse plane, reflecting an increased weight-bearing role in response to more vertical compressive forces (Pal and Routal, 1986, 1999; Mercer, 1999).

TABLE 3-1. Predicted cervical vertebral morphology and inferred functional role for suspensory taxa

Vertebral feature	**Predicted suspensory morphology**	**Presence of large nuchal musculature**	**Stability in the sagittal plane**	**Stability in the coronal plane**	**Limited, powerful extension**	**Increased weight bearing**
Centrum	Craniocaudally short, more circular body		**X**			
Laminae/Pedicles	Greater cross-sectional areas	**X**			**X**	
Transverse process	Shorter length, dorsal orientation			**X**	**X**	
Spinous process	Greater length and cross-sectional area	**X**			**X**	
Articular facet orientation	Flat in transverse plane					**X**

Postural model predictions

As discussed in the previous chapter, another critical step in testing the hypothesis of vertebral adaptation to positional behaviors is to examine the role of posture. First, it is necessary to determine whether suspensory adaptations are distinct from orthograde adaptations (i.e., bipedalism and vertical clinging and leaping), as all suspensory taxa are also orthograde. On the other hand, the broader postural models described in Chapter 2 (orthograde vs. pronograde) may better explain primate cervical morphological variation than the suspensory/nonsuspensory dichotomy proposed by the suspensory model. To examine these issues, two comparisons were performed.

1. Suspensory taxa (apes and *Ateles*) were compared to orthograde-nonsuspensory taxa (*Homo*, *Hapalemur*, *Indri*, *Propithecus,* and *Tarsius*).
    a. *Specific predictions*: If a particular vertebral feature (and inferred function) constitutes an adaptation to suspensory positional behaviors, then orthograde-nonsuspensory taxa (*Homo*, *Hapalemur*, *Indri*, *Propithecus,* and *Tarsius*) will differ from apes and *Ateles* in the same manner as nonsuspensory taxa would differ in the suspensory model predictions.
2. All orthograde taxa, including suspensory and nonsuspensory primates (apes, *Ateles, Homo*, *Hapalemur*, *Indri*, *Propithecus,* and *Tarsius*), were compared to pronograde taxa (e.g. *Cercopithecus*, *Erythrocebus*, *Nasalis*, and *Theropithecus*). Many vertebral features are applicable to both positional behavioral models, specifically those related to stabilization in multiple planes of movement and

powerful extension. Some features however, are distinct to either model (e.g., those related to the presence of large nuchal muscles in the suspensory model). *Specific prediction*: If a particular vertebral feature (and inferred function) constitutes an adaptation to postural behavior, then orthograde taxa will differ from pronograde taxa in the following vertebral features (see Table 3-2 for summary):

b. Centrum shape
    i. Orthograde taxa are expected to demonstrate craniocaudally shorter bodies and have relatively circular (an increase in dorsoventral height relative to mediolateral width) dimensions to withstand larger bending loads in both the sagittal and coronal planes, specifically during extension and/or lateral bending (Slijper, 1946; Ward, 1993; Shapiro, 1995, 2007; Johnson and Shapiro, 1998; Mercer, 1999).
c. Uncinate process
    i. More orthograde primates are expected to have shorter uncinate processes, reflecting reduced dorsoventral shearing forces at the intervertebral joints (Milne, 1991).
d. Pedicle and Lamina shape
    i. Orthograde species will have greater pedicle and laminae cross-sectional areas than more pronograde species to better resist inferred increased bending loads during more powerful extension (Dean, 1982)

e. Transverse process shape

    i. Transverse processes are predicted to be less projecting (i.e., shorter) to facilitate greater stability in the coronal plane by decreasing the mechanical efficiency of the superficial nuchal muscles during lateral bending and rotation.

    ii. Transverse processes are also predicted to be more dorsally oriented, thereby increasing the deep nuchal muscles' ability to resist ventral flexion (and in turn perform more powerful extension) by increasing their moment arms (Ward, 1991; Shapiro, 1995; Shapiro et al., 2005).

f. Spinous process shape

    i. Spinous processes are predicted to be more projecting (i.e., longer), indicating the increased moment arms for extension (Shapiro and Simons, 2002).

    ii. Greater spinous process cross-sectional areas are also predicted for orthograde taxa, reflecting greater resistance to bending forces (Mercer, 1999; Anderson et al., 2005).

g. Articular process shape

    i. Orthograde primates are predicted to have flatter articular processes oriented in the transverse plane, reflecting an increased weight-bearing role in response to more vertical compressive forces (Pal and Routal, 1986, 1999; Mercer, 1999).

TABLE 3-2. Predicted cervical vertebral morphology and inferred functional role for orthograde taxa

Vertebral feature	Predicted orthograde morphology	Stability in the sagittal plane	Stability in the coronal plane	Limited, powerful extension	Reduced dorsoventral shearing	Increased weight bearing
Centrum	Craniocaudally short, more circular body	X				
Uncinate process	Shorter height				X	
Laminae/Pedicles	Greater cross-sectional areas			X		
Transverse process	Shorter length, dorsal orientation		X	X		
Spinous process	Greater length and cross-sectional area			X		
Articular facet orientation	Flat in transverse plane				X	X

Head-balancing model predictions

In addition to providing attachment for the pectoral girdle and upper extremity, nuchal musculature also assists with directing head movement and maintaining head position. An alternative spinal model suggests that the neck and head function as a distinct section of the vertebral column and may reflect the biomechanical requirements of head movement instead of the forces predicted from either positional behavioral model. The head-balancing model considered here describes the head and neck as a cantilevered rod, acting as class 1 level system (Figure 3-1), and suggests that the nuchal muscles in species with more projecting anterior sections of the cranium (i.e., anterior to the spinal column) would have to compensate for their reduced mechanical advantage by increasing force output (i.e., they should have greater physiological cross-sectional areas) (Slijper, 1946; Badoux, 1968, 1974; Demes, 1985). Increasing muscle force also increases the potential bending forces acting across the skeletal features that provide attachment. This scenario suggests a likely relationship between differences in cranial morphology and the cervical vertebral column. Thus, in an effort to more thoroughly investigate the two positional behavior models developed here, the influence of cranial morphology on the features of interest must also be examined.

In order to reach this goal, the length of the cranium anterior to the foramen magnum (anterior cranial length [ACL] is measured from basion to prosthion) will be incorporated into primate-wide comparisons. Three basic scenarios are possible. In the first, no significant relationship is found between ACL and the vertebral feature (e.g., pedicle cross-sectional area). This result would not support the head-balancing model and any correlation between positional behavior and the vertebral trait would be supported. In

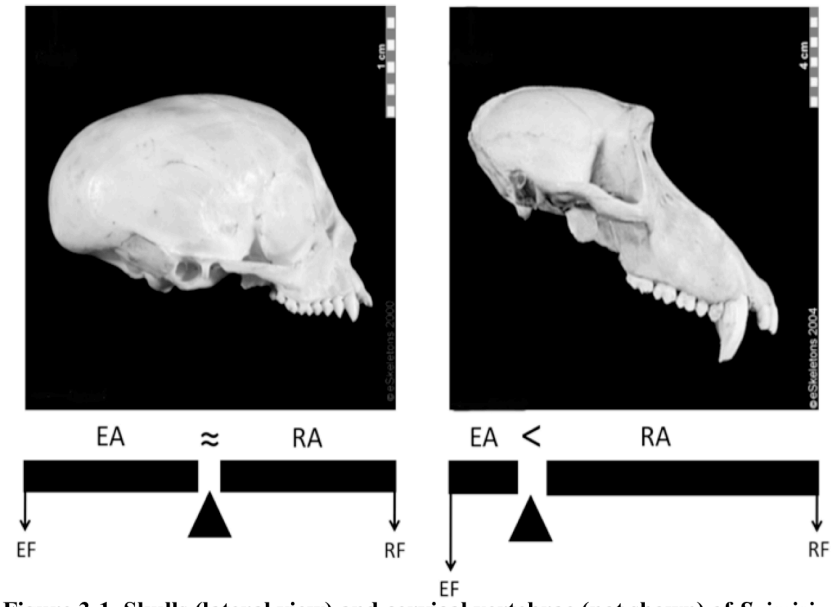

Figure 3-1. Skulls (lateral view) and cervical vertebrae (not shown) of *Saimiri* (left) and *Papio* (right) modeled as first class levers. Taxa with longer crania (with more projecting faces) would have to compensate for the reduced mechanical advantage of the nuchal musculature by increasing their force output or effort force. RA (resistance arm), EA (effort arm), RF (resistance force, EF (effort force). Images of skulls used with permission from eskeletons.org.

the second scenario, a significant relationship between a vertebral feature and ACL is found, and as a result of the addition of ACL to the PGLS analysis, removes any prior significant correlation between positional behavior and the feature. This outcome would strongly support the head-balancing model as a better biomechanical explanation for the bony variation in the primate cervical spine, at least in that particular feature. This result would reject the hypothesis that the vertebral feature is adapted to positional behavior. In the third scenario, a significant correlation is found between vertebral feature and ACL; however, the addition of ACL to a PGLS analysis does not remove the correlation between the vertebral feature and positional behavior. This result might be interpreted in two ways. First, there is a support for both models, indicating an interaction between the two biomechanical requirements of positional behavior and head-balancing. A second

interpretation is that instead of an interaction, positional behavior is influencing variation in some species (e.g., suspensory taxa), while anterior cranial length is the primary contributor to variation in other groups (e.g., those with the most projecting faces, such as baboons). The ability to distinguish between the two scenarios will depend on the pattern of results from the extant analyses.

MORPHOMETRIC SAMPLE

The extant comparative morphometric sample comprises over 2800 individual vertebrae (C1-C7) from 483 adult individuals representing 51 primate species derived from several osteological collections held at: American Museum of Natural History (New York, NY), National Museum of Natural History (Washington, DC), Field Museum (Chicago, IL), and the Muséum national de'Histoire naturelle (Paris, France) (the full list of taxa is in Appendix A, while Table 3-3, below provides a summary). Chosen taxa represent a broad cross-section of primate genera to facilitate comparisons between closely related and/or similar-sized species that differ in postural and locomotor behaviors.

TABLE 3-3. Extant comparative osteological sample

	Taxa	N
Suspensory		
	Ateles sp.	20
	Gorilla sp.	23
	Hylobates/*Nomacus*/*Symphalangus* sp.	28
	Pan troglodytes	21
	Pongo pygmaeus	22
Orthograde-nonsuspensory		
	Avahi laniger	8
	Hapalemur griseus	8
	Homo sapiens	20
	Indri indri	9
	Propithecus sp.	19
	Tarsius sp.	16
Pronograde		
	Alouatta sp.	21
	Cercopithecus mitis	21
	Cercocebus torquatus	7
	Cebus apella	19
	Chlorocebus aethiops	18
	Colobus guereza	21
	Erythrocebus patas	8
	Lemur catta	13
	Lepilemur mustelinus	18
	Macaca sp.	20
	Mandrillus sphinx	13
	Miopithecus talapoin	9
	Nasalis larvatus	19
	Papio anubis	21
	Pithecia sp.	20
	Pygathrix nemeaus	6
	Rhinopithecus roxellena	4
	Semopithecus entellus	6
	Theropithecus gelada	8
	Varecia varigata	13
Total sample size		480

Age determination

Adult age was determined based on fusion of vertebral epiphyseal caps because some of the landmarks investigated here were located on epiphyseal caps (e.g., transverse process length). While vertebral ossification patterns have not been widely studied in non-human primates, epiphyses of the cervical vertebrae are usually fused by the early 20s in humans; thus, adult status for specimens with fused epiphyses generally can be confidently assigned (Baker et al., 2005).

Sample size

Ideal sample size for those taxa that are included as species means is ten individuals of each sex per taxon. Constraints on sample size due to museum collection specimen availability resulted in less than ideal sample sizes for some taxa (see Table 3-1).

Rearing

While it is preferable to include only wild-shot specimens in morphometric studies due to possible differences in morphology caused by a captive environment, specimens obtained from zoos and other captive situations are included here to bolster sample sizes (72 captive specimens, see Appendix A). Nonparametric analyses of variance (Wilcoxon rank-sum tests) were conducted to test for differences due to rearing (captive vs. wild), and results indicate that differences between wild-shot and captive specimens are not statistically detectable at the 0.05 significance level. Thus, captive-bred and wild-caught specimens were combined to increase sample sizes. Appendix A lists the numbers of wild and captive specimens used for each taxon.

Fossil sample

The extinct hominoid morphometric sample consists of both complete and partial cervical vertebrae from 10 individuals representing five fossil taxa: *Nacholapithecus kerioi*, *Australopithecus afarensis*, *Australopithecus robustus*, *Homo* sp. indet., and *Homo ergaster* derived from several paleontological collections held at the National Museum of Natural History (Washington, DC), National Museum of Ethiopia (Addis Ababa, Ethiopia), Nairobi National Museum, (Nairobi, Kenya), and Ditsong National Museum of Natural History (Pretoria, South Africa) (the full list of specimens and assigned taxa are listed in Chapter 5, while Table 3-4 below provides a summary).

TABLE 3-4. Fossil comparative osteological sample

Taxon	C1	C2	C3-C7
Nacholapithecus kerioi	KMM-BG 40840n		KNM-BG 40793c, 40840o
Australopithecus afarensis	A.L. 333-83	A.L. 333-101	A.L. 333-106
Australopithecus robustus		SK 854	SKW 4776
Homo sp. indet.			KNM-ER 164c
Homo ergaster			KNM-WT 15000r

MEASUREMENTS

The data used for this project include linear and angular dimensions of both the cranium and cervical vertebrae.

Vertebral morphometrics

Vertebral data were collected using both three-dimensional landmark data collected using a Microscribe G2X digitizer (Immersion Corp.) and linear measurements acquired using a digital caliper (Mituotyo Corp.). In all, nineteen linear measurements and twelve landmarks were collected on a typical cervical vertebra (C3-C7). Due to the fact that C1 does not have a vertebral body and that the C2 body is unique in morphology (i.e., odontoid process), measurements were limited to those on the vertebral canal and bony processes (pedicles, laminae, and transverse/spinous processes) of the upper two cervical vertebrae. Table 3-5 describes the vertebral 3-D landmarks and they are illustrated in Figure 3-2.

TABLE 3-5. Three-dimensional vertebral landmarks

No.	Landmark	Definition
1	Ventral extent of vertebral body	The most ventral point on the cranial surface of the vertebral body in the midline.
2	Dorsal extent of vertebral body	The most dorsal point on the cranial surface of the vertebral body in the midline.
3	Lateral extent of the posterior tubercle of the transverse process	The most lateral point of the posterior tubercle of the transverse process
4	Lateral extent of the anterior tubercle of the transverse process	The most lateral point of the anterior tubercle of the transverse process
5	Ventral extent of the superior articular facet	The most ventral point of the superior articular facet
6	Dorsal extent of the superior articular facet	The most dorsal point of the superior articular facet
7	Medial extent of the superior articular facet	The most medial point of the superior articular facet
8	Lateral extent of the superior articular facet	The most lateral point of the superior articular facet
9	Dorsal extent of the inferior articular facet	The most dorsal point of the inferior articular facet, inferior to point 6.
10	Dorsal extent of vertebral canal	The most ventral point on the cranial surface of the vertebral canal in the midline.
11	Left lateral extent of vertebral canal	The most lateral point on the cranial surface of the left side of the vertebral canal in the midcoronal plane (not shown)
12	Right lateral extent of vertebral canal	The most lateral point on the cranial surface of the right side of the vertebral canal in the midcoronal plane

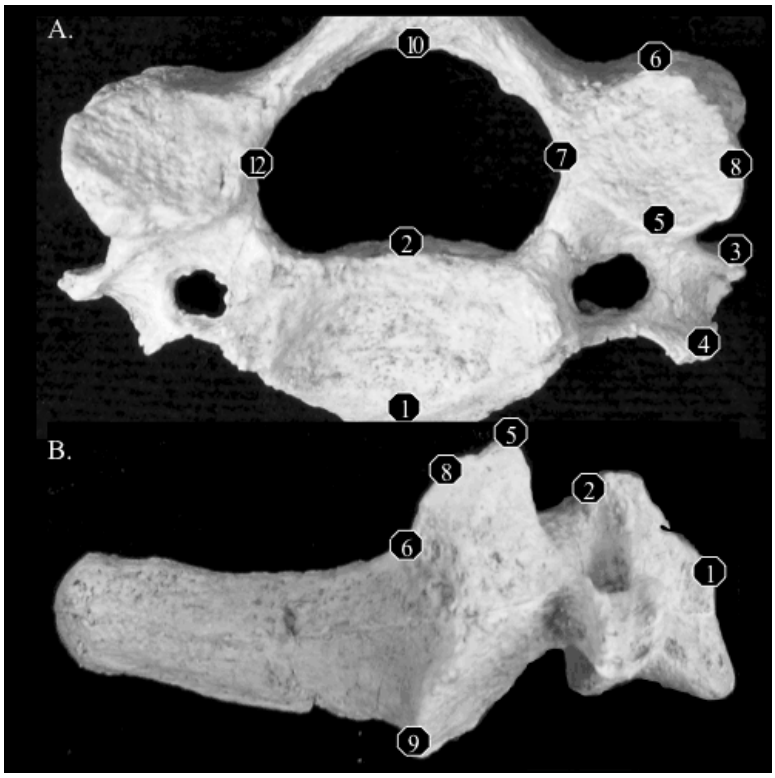

Figure 3-2. 3-D Landmarks captured on lower (3-7) cervical vertebrae. The upper image (A) shows a superior view. The lower image (B) shows a lateral view. See Table 3-3 for descriptions.

Table 3-6 describes the vertebral measures for comparison and their method of acquisition. These measures are illustrated in Figure 3-3.

TABLE 3-6. Linear and angular measurements of cervical vertebrae

Linear and Angular measures	Method	Definition
Vertebral body ventral length (VBVL)	Caliper	Maximum length along the ventral surface
Vertebral body dorsal length (VBDL)	Caliper	Maximum length along the dorsal surface
Vertebral body eccentricity (VB ECC)	Caliper	Ratio of maximum dorsoventral height along the cranial surface/ maximum mediolateral width along the cranial surface
Uncinate process height (UNC)	Caliper	Maximum length of the uncinate process (UNCL) – average of VBVL and VBDL
Spinous process length (SPL)	Caliper	Maximum length along the cranial surface
Anterior transverse process length (ATPL)	Caliper	Maximum length across anterior tubercles
Posterior transverse process length (PTPL)	Caliper	Maximum length across posterior tubercles
Pedicle cross-sectional area (PCSA)	Caliper	Craniocaudal length (not shown) X transverse width in the midline
Lamina cross-sectional area (LCSA)	Caliper	Craniocaudal length (not shown) X transverse width in the midline
Spinous process cross-sectional area (SCSA	Caliper	Craniocaudal length X transverse width in the midline
Transverse process angle – posterior tubercle (TPPA)	Landmark	Angle between line connecting landmarks 2, 10, and 3
Transverse process angle – anterior tubercle (TPAA)	Landmark	Angle between line connecting landmarks 2, 10, and 4
Articular facet angle (AFA)	Landmark	Angle between line connecting landmarks 6, 9 and the plane constructed from landmarks 5-8
Vertebral canal height (VCH)	Landmark	Length between landmarks 2 and 10
Vertebral canal width (VCW)	Landmark	Length between landmarks 11 and 12

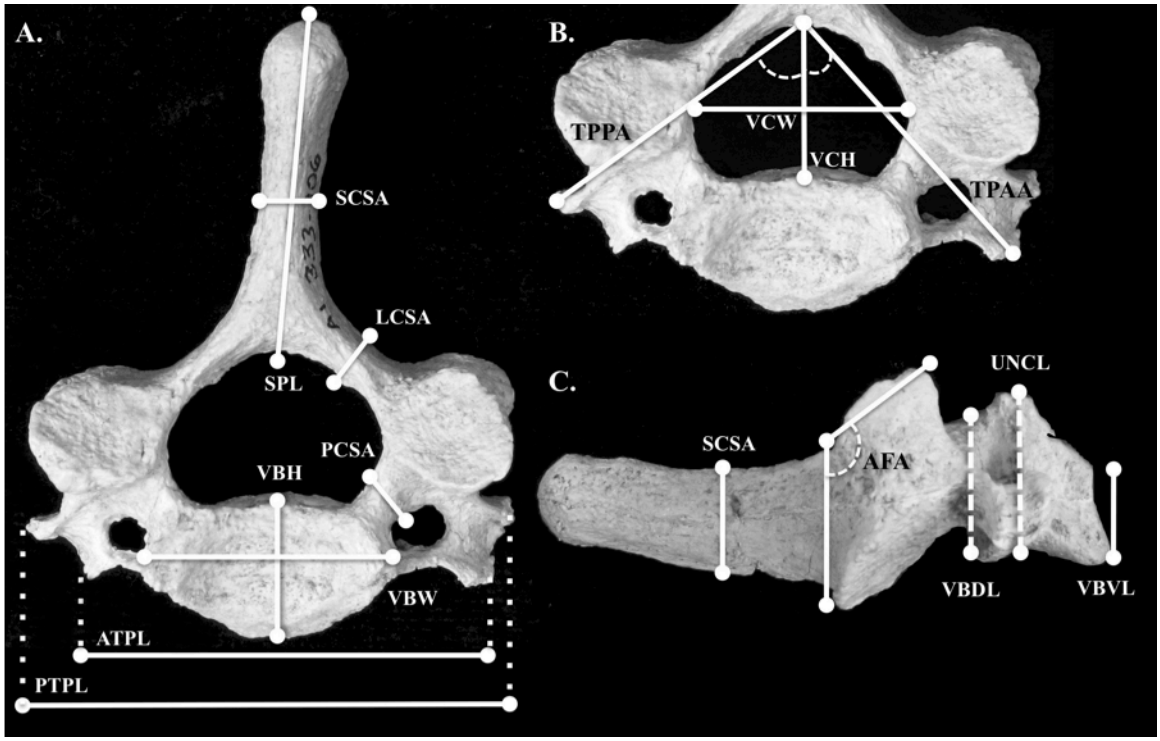

Figure 3-3. Linear and angular measurements taken on cervical vertebrae. (A) and (B) Superior view. (C) Lateral view. See Table 3-4 for measurement and variable descriptions.

The angle (θ) for measures TPPA and TPAA were calculated by determining the arccosine of the scalar (or dot) product of the two (normalized) vectors (*v* and *w*) composing each angle respectively:

$$\theta = \cos^{-1}\left[\frac{v \bullet w}{\|v\| \bullet \|w\|}\right]$$

$$= \cos^{-1}\left[\frac{\left(v_x w_x + v_y w_y + v_z w_z\right)}{\left(\sqrt{v_x{}^2 + v_y{}^2 + v_z{}^2}\right)\left(\sqrt{w_x{}^2 + w_y{}^2 + w_z{}^2}\right)}\right]$$

The angle (∝) for measure AFA was calculated by finding the complementary acute angle that forms between the vector of the line (a) determined by points 6,9 and the normal vector (b) of the plane formed by points 5-8. The first step was to find the normal

vector for the plane by calculating the cross product of any two vectors (*m* and *n*) from the plane:

$$m \times n = \det\begin{pmatrix} xyz \\ abc \\ def \end{pmatrix}$$
$$= \langle bf - ce, cd - af, bd - ae \rangle$$

Once coordinates for the normal vector were determined, the AFA angle was found by calculating the arcsine of the scalar product (similar to TPPA and TPAA equation above) of the vector of the line (*a*) and the normal vector of the plane (*b*) and then subtracting that angle from 180:

$$\alpha = \sin^{-1}\left[\frac{a \bullet b}{\|a\| \bullet \|b\|}\right]$$

$$= \sin^{-1}\left[\frac{\left(a_x b_x + a_y b_y + a_z b_z\right)}{\left(\sqrt{a_x{}^2 + a_y{}^2 + a_z{}^2}\right)\left(\sqrt{b_x{}^2 + b_y{}^2 + b_z{}^2}\right)}\right]$$

Calculations were completed in Excel, Version 12 (Microsoft Corp.).

Cranial morphometrics

A total of 12 three-dimensional landmarks were taken on the cranium and collected using an Immersion MicroScribe G2 three-dimensional digitizing system. The points are listed in Table 3-7 and illustrated in Figure 3-4.

TABLE 3-7. Cranial landmarks

Landmark[1]	Description[2]
1	*Staphylion* - midpoint of the posterior edge of the hard palate
2	*Prosthion* - anteroinferiormost midline point on the maxilla
3	*Nasion* – midline point at which the two nasal bones and the frontal bone meet
4	*Opisthocranion* - posteriormost point on the midline of the neurocranium
5	*Basion* – midpoint of the anterior edge of the foramen magnum
6 a, b	*Auriculare* – bilateral point on the suprameatal crest of the temporal bone directly above the center of the external auditory meatus
7a, b	*Ectoconchion*—bilateral point on the most lateral point on the orbital rim
8a, b	Maxillary M2 – bilateral point on the mesiobuccal cusps
9	*Bregma* – midline point where the coronal suture intersects with the sagittal suture

[1] Landmark numbers refer to Figure 3-4.
[2] Craniometric points (in italics) follow the definitions given in White (1991).

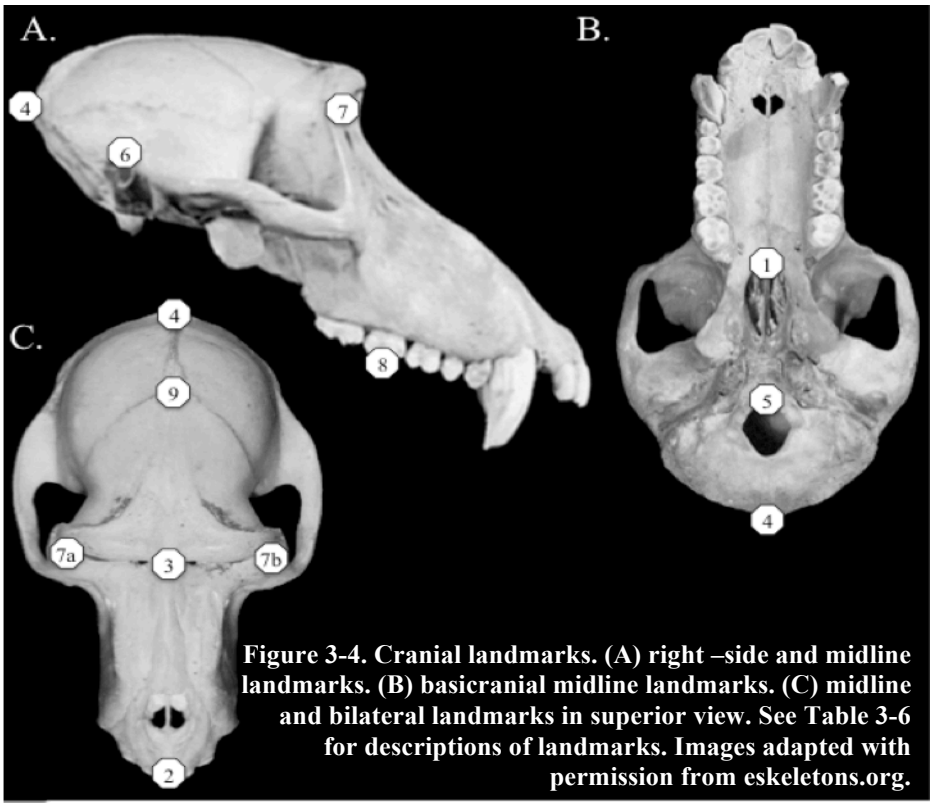

Figure 3-4. Cranial landmarks. (A) right –side and midline landmarks. (B) basicranial midline landmarks. (C) midline and bilateral landmarks in superior view. See Table 3-6 for descriptions of landmarks. Images adapted with permission from eskeletons.org.

These measurements can be divided into two sets: features related to anterior cranial length and linear measurements used to compute a geometric mean for size-adjustment.

Anterior cranial length

The first measurement is derived from landmark data and was used to calculate the relative length of the resistance arm (anterior cranial length) in the first class lever model of the head and neck. Anterior cranial length (ACL) is defined as the distance between basion and prosthion.

Size

The second set of measurements derived from landmark data consisted of five linear dimensions of the skull. These measurements were combined into a geometric

mean (GM) to represent size and was used to size-adjust variables for pairwise comparisons (discussed in greater detail below). The measurements are described in Table 3-8. Three of the skull measurements are from the face (biorbital width, posterior facial height, and snout width), and two are from the neurocranium (neurocranial width and height).

TABLE 3-8. Description of measurements used to compute the geometric mean

Landmarks	Descriptions	
8a, 8b	Snout width	Distance between left M2 and right M2
7a, 7b	Biorbital width	Distance from left ectoconchion to right ectoconchion
1, 3	Posterior facial height	Distance from staphylion to nasion
6a, 6b	Neurocranial width	Distance from left auriculare to right auriculare
5, 9	Neurocranial height	Distance from basion to bregma

ANALYTICAL METHODS

Statistical software

Analysis of variance (ANOVAs) tests (and their nonparametric equivalents when necessary), discriminant function analyses, and descriptive statistical analyses were performed using JMP Pro, Version 10 (SAS Institute, Inc.). Phylogenetic comparison analyses were performed in R (R Development Core Team, 2010); using the "APE" (Analysis of Phylogenetics and Evolution) and "GEIGER" packages (Paradis et al., 2005).

Statistical analysis

Raw data were first examined for violations of the assumptions of parametric statistics; normal probability plots indicated a violation of the assumption of normality, and this was corrected using a natural-logged transformation. Data were examined for outliers, which were determined as those individuals with extreme jackknife Mahalanobis distances, and when found, were removed from analyses. Error variances were examined for patterns that might signal inconstancy, and were found to be homoscedastic.

Pairwise comparisons and testing the suspensory model

Analyses were performed for sex-specific taxon means and were performed on each vertebral level (i.e., C1, C2, C3) separately. These comparisons test the specific predictions of the suspensory model outlined at the beginning of this chapter for each shape variable using a t-test with positional behavior as the categorical variable. Table 3-9 lists the taxa and sample sizes used in the pairwise comparisons.

TABLE 3-9. Taxa used in pairwise comparisons

Locomotion	Taxon	Male (n)	Female (n)	Combined (n)
Suspensory	*Pongo*	10	11	21
Suspensory	*Pan*	10	9	19
Nonsusp	*Homo*	10	10	20
Suspensory	*Ateles*	10	8	18
Nonsusp	*Alouatta*	11	8	19
Nonsusp	*Pithecia*	14	4	18
Suspensory	Hylobatids	9	16	25
Nonsusp	*Nasalis*	16	3	19
Nonsusp	*Papio*	9	7	16

Calculation of shape variables

Morphometric dimensions were adjusted to account for differences in size among taxa. The most common way of achieving a size-adjustment is to define a Mosimann shape variable (Mosimann, 1970; Darroch and Mosimann, 1985; Jungers et al., 1995), which is the variable of interest divided by a measure of size. While some have argued against the use of ratios as data because of their supposed tendency toward non-normality (Albrecht, 1978; Atchley, 1978; Atchley and Anderson, 1978; Albrecht et al., 1993, 1995), ratios retain important information about allometry and are readily interpretable (Jungers et al., 1995). In the pairwise comparison analyses, the size proxy was a geometric mean (GM) of cranial measures. A geometric mean is the *n*th root of the product of *n* variables. In this case, the geometric mean was chosen to represent overall skull size and is the fifth root of the product variables listed in Table 3-8. To ensure that the shape variables are dimensionless, the square-root of those vertebral traits that were measured in units of mm^2 (i.e., areal measures) was first taken before standardizing measures by the size proxy. Thus, shape variables for extant taxa pairwise comparisons were created by standardizing linear and areal measures by the geometric mean of overall cranial measures.

The use of the geometric mean as a size proxy was investigated by regressing the natural-logged average cranial geometric mean for taxa on the natural-logged species' body mass mean (raised to the one-third power, thus isometry would be indicated by a slope of 1) (body mass data are derived mostly from Smith and Jungers (1997) and Smith and Cheverud (2002) [see Appendix A for a complete list of body mass sources]). This regression yielded an R^2 of 0.95 and a slope of 1.15 with 95% confidence limits from

1.12 to 1.18. This analysis indicates a slight positive allometric relationship between the geometric mean and body mass. Thus, in large-bodied animals, the geometric mean will be relatively larger than in small-bodied animals. Because the geometric mean is the denominator of the shape variable, large-bodied animals will have relatively smaller values for shape variables than small-bodied taxa. Nonparametric analyses of variance (Wilcoxon rank-sum tests) were also conducted to test for sex differences (female vs. male), and, in general, the results indicate that differences are statistically significant at the 0.05 level, even after size standardization. Therefore, separate female and male taxon means were used as the unit of analysis.

Broad interspecific analyses and testing the postural and the head balancing models

To investigate the postural and head-balancing models, multiple regression analyses were conducted with phylogenetic generalized least squares (PGLS), which estimates the relationship between two variables while accounting for the degree of autocorrelation due to phylogenetic relatedness in the data set (Grafen, 1989; Freckleton, et al., 2002). A phylogenetic comparative approach is necessary because species may be similar to each other based on the fact that they share a common ancestor and thus do not represent independent observations, an important assumption of regression analyses (Felsenstein, 1985; Harvey and Pagel, 1991). A primate consensus phylogeny for the taxa studied here was obtained from the 10kTrees website (Arnold et al., 2010) (Figure 3-5). To test the postural model, natural-logged vertebral features were regressed on two independent variables (in addition to phylogeny): size and positional behavior. To test the head-balancing model, a third variable was added to the PGLS multiple regression — anterior cranial length (ACL).

Positional behavior was entered into the analyses as a set of binary dummy variables to allow categorical variables to be included in the regression analyses. Specifically, suspensory taxa were coded as 0, 0; pronograde as 0, 1; and orthograde-nonsuspensory as 1, 0 when testing the suspensory model (Garland et al., 1993). When investigating the postural model, orthograde taxa were coded as 0 and pronograde taxa were coded as 1. Size was measured as a species' average for body mass (BM). Body mass is used here instead of a cranial geometric mean for two reasons. First, PGLS analyses investigating the head-balancing model incorporate a measurement of cranial length into the model. Anterior cranial length and a cranial geometric mean are likely to be strongly correlated and the inclusion of both variables in a PGLS model may confound the interpretation of results. Second, body mass has a more direct influence on the positional behavior of an animal than the size of the skull and it is a more relevant feature to adjust for when testing hypotheses of postural and locomotor behavior (McMahon, 1975; Pedley, 1977; Heglund, 1984; Jungers and Susman, 1984).

To investigate allometric scaling, each vertebral measure (areal measures [mm^2] were raised to the one-half power) was regressed on the taxon-specific average of body mass (raised to the one-third power) using reduced major axis (RMA) regression. Reduced major axis was chosen over the ordinary least squares (OLS) regression model because it is a more appropriate method when the aim of the study is to address the scaling relationship between the Y- and X variables (Sokal and Rohlf, 1995; Warton et al., 2006; Smith, 2009). Significant departures from isometry were determined using the 95% confidence intervals for each slope. Following the recommendation of Sokal and

Rohlf (1995), 95% confidence intervals of the RMA slopes were calculated using standard errors from the OLS regressions.

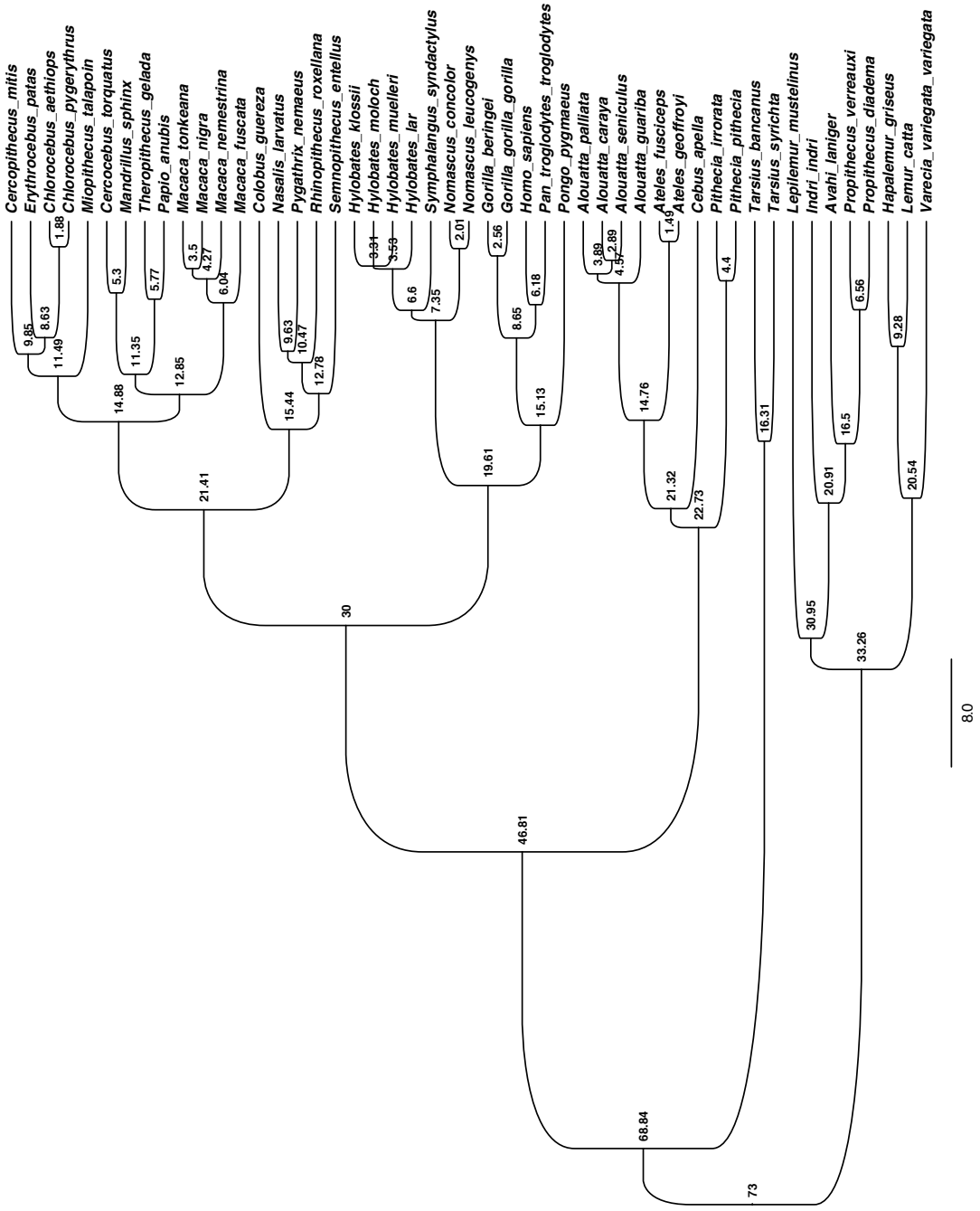

Figure 3-5. A consensus phylogeny of the taxa used in this study derived from GenBank data (from the 10kTrees website, Arnold et al., 2010).

Fossil analysis

Fossil specimens were compared to those extant taxa included in the pairwise comparisons (minus *Pithecia* due to the taxon's relatively small body size) and morphology was investigated in one of two ways: box-and-whisker plots or discriminant function analysis (DFA). Box-and-whisker plots of size-adjusted variables were used to describe relatively incomplete fossil specimens that preserved 3 or fewer vertebral features. More complete fossil taxa that preserved four or more vertebral features were analyzed using DFA. The 4-feature criterion was arbitrarily chosen, but preliminary analyses of extant taxa demonstrated that at least four features were necessary to keep the resulting DFA error rates low.

Discriminant function analyses were performed on size-adjusted variables from fossil taxa to test whether these species are more similar to (i.e., classify with) specific taxa chosen by summarizing previous descriptions and comparisons. This multivariate technique emphasizes the differences among previously determined groupings (i.e., extant taxon groups), providing Mahalanobis distances and classification functions to assist judgment of group distinctiveness (Groves, 1970; Howells, 1973; Albrecht, 1978b; Bilsborough and Wood, 1988; Shea et al., 1993). The effective discrimination of groupings can be influenced by inequalities of sample size. Thus, prior probabilities from the DFA are weighted by the number of specimens in each sample. The discriminant model includes each fossil as an "unknown" and interpolates them into the analysis after the fact. The pooled within-group dispersion matrix is therefore based on the extant sample.

While there are several varieties of discriminant analysis, the simplest case, linear discriminant analysis, was most appropriate and was implemented in this analysis (James and McCulloch, 1990). Classification results were then derived for which actual group membership was compared to predicted group membership. The separation of groups was then evaluated by the graphical ordination of discriminant function scores, followed by the analysis of standardized coefficients (i.e., the unique contribution of each variable to the discriminant function).

Once DFAs exploring taxonomic affinity were completed, a second series of DFA tests was used to identify likely positions within the vertebral column for isolated fossil vertebra. The DFAs included multiple possible levels (i.e., C3 and C4) of the most appropriate extant hominoid spinal column analog, determined by the affinity DFAs. Finally, it is important to note that DFA results used to evaluate fossil morphology should be taken as descriptive in the context of morphological similarity (Klecka, 1980; Tabachnick et al., 2001).

Calculation of shape variables

Associated fossil hominin crania and vertebrae often did not have all five dimensions used for the calculation of the cranial GM used in the analysis of extant taxa. Therefore, instead of a cranial GM, three possible vertebral canal dimensions were used, depending on trait preservation in the fossil specimen of interest: vertebral canal dorsoventral height (VCH), vertebral canal mediolateral width (VCW), or vertebral canal area (VCA) (see Table 3-4 for measurement descriptions). The use of vertebral canal dimensions as size proxies was evaluated by performing regression analyses on the natural-logged mean canal dimensions (VCA raised to the one-half power) and the

natural-logged mean body mass (raised to the one-third power; therefore isometry is equal to a slope of 1 in all cases) for each taxon.

Regression analyses of VCH, VCW, and VCA on body mass all demonstrate a high correlation with body mass with R2s above 0.9. Analyses indicate an overall slightly positively allometric relationship between the VCH and body mass with a slope of 1.07 and 95% confidence intervals (CIs) from 1.03 to 1.09. The VCW analyses indicate a slight negative allometric relationship between the vertebral canal width and body mass (slope of 0.92 with CIs from 0.89 to 0.95). Thus, in large-bodied animals, the VCW will be relatively smaller than in small-bodied animals. Because the VCW is the denominator of the shape variable, large-bodied animals will tend to have relatively larger values for shape variables than small-bodied taxa based solely on their larger body size. The VCA results also implies a slight negative allometric relationship with body mass, but the confidence interval overlaps with isometry (slope of 0.96 with CIs from 0.92 to 1). Similar to the relationship found for VCW, in large-bodied animals, the VCA will tend to be relatively smaller than in small-bodied primates; therefore large-bodied primates will have relatively larger values for shape variables than small-bodied taxa.

Measurement error

Measurements collected from three specimens from five taxa (*Ateles*, *Gorilla*, *Cercopithecus aethiops*, *Papio*, and *Tarsius*) were repeated on two different days. An estimate of measurement error (or deviation) was calculated as the percent error between all caliper measurements of repeated individuals following White (1991). The average percent error was 3% and is considered within accepted publishable rates.

Missing measurements and landmarks

As is often the case in osteological and paleontological collections, some specimens were damaged or not fully cleaned of soft tissue, so some measurements and/or landmarks were occasionally inaccessible. Thus, some specimens are missing landmarks and any measurements that are based on those missing landmarks. These specimens with missing data were removed from analyses of relevant individual variables.

Hypothesis rejection

Given the large number of statistical tests performed in this study, the possibility that some of the significant results ($p < 0.05$) are type I errors (i.e., false rejections of the null hypothesis) is a concern. The conventional way of dealing with this issue is to lower the level at which a test achieves statistical significance using Bonferroni adjustments so that the overall error rate for a study, or some component of the study, is maintained at $\alpha = 0.05$ (e.g., Holm, 1979; Rice, 1989; Sokal and Rohlf, 1995). This approach is not adopted here because, given the large number of statistical tests performed, it would reduce the power to detect significant differences to an unreasonably low level (Perneger, 1998; Moran, 2003; Nakagawa, 2004). As an alternative, following the arguments made by Perneger (1998) and Moran (2003), the overall pattern of significant differences is used to evaluate each model rather than the individual p-values for each statistical test. For example, a single significant result with p-value of, for example, $p = 0.03$ for one vertebral variable among many nonsignificant results for the same variable would be suspect and suggest an anomalous result. In contrast, several significant tests for a single variable that separate taxa in a biologically meaningful way, such as those with the most

dissimilar positional behaviors, would indicate a possible relationship. Therefore, statistical results will be interpreted within the context of the biological framework they are performed (i.e., phylogeny, size, behavior).

As described in the beginning of this chapter, the adaptive hypothesis of vertebral shape and its relationship to positional behavior is derived from expectations based on theoretical biomechanical models and previous experimental work on the kinematics of primate locomotor and postural behaviors (see Chapter 2). For this project, if a cervical feature is not consistently distinct between behavioral groups — that is, results do not produce a readily interpretable pattern — then the feature will not be supported as an adaptation to positional behaviors here.

Chapter 4

ANALYSIS OF CERVICAL MODELS USING EXTANT TAXA

INTRODUCTION

As stated in Chapters 2 and 3, the general hypothesis for this dissertation is that variation in cervical vertebral shape reflects differences associated with the various positional behaviors used by primates. The goal of this chapter is to apply comparative morphometric techniques to determine if vertebral differences in extant primates fit the patterns proposed by any of the three alternative biomechanical models outlined in Chapter 3.

To test the suspensory model, pairwise comparisons on a subset of the sample were performed for each shape variable using a nonparametric *t*-test (Wilcoxon-Mann-Whitney test) with positional behavior as the categorical variable. Taxa for the pairwise comparisons were chosen to minimize differences due to size and phylogeny. To investigate the postural and head-balancing models, multiple regression analyses were conducted on the entire extant sample using phylogenetic generalized least squares (PGLS), which accounts for similarities among taxa due to phylogenetic relatedness. When addressing the postural model, the PGLS analyses included two independent variables – a measure of organismal size and positional behavior. When investigating the head-balancing model, a third independent variable was added to the PGLS analyses – anterior cranial length (ACL).

PAIRWISE COMPARISONS

Pairwise comparisons of vertebral shape variables were performed between suspensory and nonsuspensory taxa. As explained in Chapter 3, vertebral dimensions

were size adjusted for the pairwise comparisons using a cranial geometric mean. Shape variables are dimensionless, meaning that the square-root of those vertebral traits that were measured in units of mm^2 (e.g., LCSA) was first taken before standardizing the measure by the geometric mean. Summary statistics for vertebral features, separated by sex and vertebral level, are presented in appendices B and C. Results of analyses; including directional outcomes at all vertebral levels for males are found in Tables 4-1-2, while female results are recorded in Tables 4-3-4- Results for each sex is reported separately because Chapter 3 analyses revealed statistically significant sex differences in many of the traits of interest.

***Pan troglodytes* and *Pongo pygmaeus* (suspensory) vs. *Homo sapiens* (nonsuspensory)**

Results of the Wilcoxon-Mann-Whitney tests are provided in Tables 4-1 - 4-4. The hypothesized relationship between the suspensory and nonsuspensory taxa is upheld in both sexes for several vertebral traits; however, few consistent patterns of significance are observed. Often, the suspensory model is supported in one comparison, but not in the other (the most common result being no significant difference). For example, the cross-sectional areas of the pedicles (PCSA) and laminae (LCSA) of male *Pongo* were larger than male *Homo* in 6 out of 7 comparisons, but only a single difference is found between male *Pan* and *Homo*. A similar scenario is found in females, though the LCSA comparisons resulted in fewer significant differences. Analyses of transverse process morphology produce similar results. *Pan* features shorter transverse process lengths than *Homo* (9 out of 10 comparisons for males and 7 out of 10 comparisons for females), but the *Pongo*/*Homo* comparisons only support the suspensory model in 2 out of 10 comparisons (for both sexes each). This being said, some analyses do produce a more

consistent morphological pattern. For example, at all lower cervical levels (C3-C7), a longer spinous process is found in the suspensory apes when compared to nonsuspensory humans, for both males and females (females also demonstrate a significant difference at the C2 level) (Tables 4-1, 4-3).

In summary, results from the first group of pairwise comparisons found more support for the suspensory model in male comparisons and at lower levels (C3-C7). The vertebral variable that produces the most support for the suspensory model was spinous process length (i.e., suspensory taxa had longer spinous processes than nonsuspensory taxa).

TABLE 4-1. Pairwise comparisons of relative linear and areal measures of cervical vertebrae in males

Comparison [1]	VBVL	VBDL	SPL	ATPL	PTPL	PCSA	LCSA	SCSA	# of features supporting suspensory model	# of features rejecting suspensory model
C1										
Pan, *Pongo* vs. *Homo*			<, =[2]		=	=	=, >		1	7
Hylobatids vs. *Nasalis*, *Papio*			>, <		=, <	<	=		2	6
Ateles vs. *Alouatta*, *Pithecia*			<, >		<, =	<, =	=		2	6
C2										
Pan, *Pongo* vs. *Homo*			=, >		<, >	=, >	=, >	<, =	4	6
Hylobatids vs. *Nasalis*, *Papio*			<		=, <	=, <	=, <	=	1	9
Ateles vs. *Alouatta*, *Pithecia*			<, >		<, =	=, >	<, >	<, =	4	6
C3										
Pan, *Pongo* vs. *Homo*	=, >	=, >	>		<, >	=, >	=, >	<, =	5	9
Hylobatids vs. *Nasalis*, *Papio*	=, <	<	=, <		=, <	=, <	<	>, =	5	9
Ateles vs. *Alouatta*, *Pithecia*	<, >	=, >	<, =		<, =	=, >	=, >	<, >	5	9
C4										
Pan, *Pongo* vs. *Homo*	=, >	=, >	>	<, =	<, =	=, >	=, >	<, =	6	10
Hylobatids vs. *Nasalis*, *Papio*	=	<	=, <	<	=, <	=, >	=, >	=, >	8	8
Ateles vs. *Alouatta*, *Pithecia*	=, >	<, >	<, =	<, =	<, =	=, >	<, >	=, >	6	10
C5										
Pan, *Pongo* vs. *Homo*	>	=, >	>	<, =	<, >	=, >	>	<, =	6	10
Hylobatids vs. *Nasalis*, *Papio*	=, <	<	=, <	<†	=, <	=, <†	<	>, =	7	9
Ateles vs. *Alouatta*, *Pithecia*	=, >	>	=	<, =	<, =	=, >	=, >	=, >	5	11
C6										
Pan, *Pongo* vs. *Homo*	=, >	=, >	>	<	<, =	=, >	=, >	>	9	7
Hylobatids vs. *Nasalis*, *Papio*	<	=, <†	=, <	<	<	<	=, <	=, <	7	9
Ateles vs. *Alouatta*, *Pithecia*	>	>	=, >	=	<, >	=, >	=, >	=, >	5	11
C7										
Pan, *Pongo* vs. *Homo*	<, =	=	>		<	=	=	=, >	6	8
Hylobatids vs. *Nasalis*, *Papio*	<	=	=†		<†	=†	<†	=†	4	10
Ateles vs. *Alouatta*, *Pithecia*	>	>	=, >		=, >	>	>	>	7	7

[1] For statistically significant comparisons, less-than and greater-than symbols indicate direction of difference (e.g., at the C3 level, the SPL is longer in both *Pan* and *Pongo* than in *Homo*; equality sign indicates that difference is not statistically significant).

[2] Two separate signs indicate that results of the multiple pairwise comparisons are different; the first sign represents the first comparison (e.g., *Pan* vs.

Homo) and the second sign represents the second comparison (e.g., *Pongo* vs. *Homo*).
† Results should be interpreted with caution because hylobatid n=3

TABLE 4-2. Pairwise comparisons of vertebral body ratio and angle measures of cervical vertebrae in males

Comparison [1]	VB ECC	TPAA	TPPA	AFA	# of comparisons supporting suspensory model	# of comparisons rejecting suspensory model
C1						
Pan, *Pongo* vs. *Homo*			>		2	0
Hylobatids vs. *Nasalis*, *Papio*			<		0	2
Ateles vs. *Alouatta*, *Pithecia*			<, =[2]		0	2
C2						
Pan, *Pongo* vs. *Homo*			<, =		0	2
Hylobatids vs. *Nasalis*, *Papio*			=		0	2
Ateles vs. *Alouatta*, *Pithecia*			=		0	2
C3						
Pan, *Pongo* vs. *Homo*	>		=	=	2	4
Hylobatids vs. *Nasalis*, *Papio*	=		<†	—[3]	0	4
Ateles vs. *Alouatta*, *Pithecia*	=		=	<, =	1	5
C4						
Pan, *Pongo* vs. *Homo*	>, =	=	=, >	<, =	3	5
Hylobatids vs. *Nasalis*, *Papio*	=, >	=, <	<	=	1	7
Ateles vs. *Alouatta*, *Pithecia*	<, =	<, =	<, =	=	0	8
C5						
Pan, *Pongo* vs. *Homo*	=	=	>	=	2	6
Hylobatids vs. *Nasalis*, *Papio*	<	<	=, <	>	0	8
Ateles vs. *Alouatta*, *Pithecia*	<, =	=	<, =	=	0	8
C6						
Pan, *Pongo* vs. *Homo*	=	=	=	=	0	8
Hylobatids vs. *Nasalis*, *Papio*	=	=†	=	=, >†	0	8
Ateles vs. *Alouatta*, *Pithecia*	<	=, <	=	=, >	0	8
C7						
Pan, *Pongo* vs. *Homo*	<, =		=, >	<	3	3
Hylobatids vs. *Nasalis*, *Papio*	<		=	=, >	0	6
Ateles vs. *Alouatta*, *Pithecia*	<		=	=, >	0	6

[1] For statistically significant comparisons, less-than and greater-than symbols indicate direction of difference (e.g., at the C1 level, TPPA is larger in both *Pan* and *Pongo* than in *Homo*; equality sign indicates that difference is not statistically significant).

[2] Two signs separate signs indicate that results of the multiple pairwise comparisons are different; the first sign represents the first comparison (e.g., *Ateles* vs. *Alouatta*) and the second sign represents the second comparison (e.g., *Ateles* vs. *Pithecia*).
[3] Dash (—) indicates that hylobatid group in the comparison had fewer than 3 individuals and the analysis was not conducted.
† Results should be interpreted with caution because hylobatid n=3.

TABLE 4-3. Pairwise comparisons of relative linear and areal measures of cervical vertebrae in females

Comparison [1]	VBVL	VBDL	SPL	ATPL	PTPL	PCSA	LCSA	SCSA	# of features supporting suspensory model	# of features rejecting suspensory model
C1										
Pan, *Pongo* vs. *Homo*			=, <[2]		=	=	=		0	8
Hylobatids vs. *Papio*			=		=	<	=		0	4
Ateles vs. *Alouatta*			=		=	<	=		0	4
C2										
Pan, *Pongo* vs. *Homo*			>		=	=, >	=	<	3	7
Hylobatids vs. *Papio*			<		=	=	=	=	0	5
Ateles vs. *Alouatta*			=		=	=	=	=	0	5
C3										
Pan, *Pongo* vs. *Homo*	=	=	>		<, =	=, >	=	<	4	10
Hylobatids vs. *Papio*	=	<	<		<	<	=	=	2	5
Ateles vs. *Alouatta*	>	>	=		<	=	=	=	1	6
C4										
Pan, *Pongo* vs. *Homo*	>, =	=	>	<, =	<, =	=, >	=, >	<	6	10
Hylobatids vs. *Papio*	=	<	<	—[3]	<	<	<	=	2	5
Ateles vs. *Alouatta*	>	>	=	<	<	=	>	=	3	5
C5										
Pan, *Pongo* vs. *Homo*	=	=	>	<, =	<, >	=, >	>	<, =	7	9
Hylobatids vs. *Papio*	=	=	=	<	<	<	<	=	2	6
Ateles vs. *Alouatta*	>	>	=	<	<	=	>	=	3	5
C6										
Pan, *Pongo* vs. *Homo*	=	=	>	<	<, =	>	>	=	9	7
Hylobatids vs. *Papio*	=	=	=	<	<	<	<	=	2	6
Ateles vs. *Alouatta*	>	>	=	>	=	=	>	=	1	7
C7										
Pan, *Pongo* vs. *Homo*	<, =	=	>		=, <	=	=	=, >	5	9
Hylobatids vs. *Papio*	=	=	=		<	=	=	=	1	6
Ateles vs. *Alouatta*	>	>	=		=	>	>	>	3	4

[1] For statistically significant comparisons, less-than and greater-than symbols indicate direction of difference (e.g., at the C2 level, the SPL is greater in both *Pan* and *Pongo* than in *Homo*; equality sign indicates that difference is not statistically significant).
[2] Two signs separate signs indicate that results of the multiple pairwise comparisons are different; the first sign represents the first comparison (e.g., *Pan* vs. *Homo*) and the second sign represents the second comparison (e.g., *Pongo* vs. *Homo*).
[3] Dash (—) indicates that hylobatid group had fewer than 3 individuals and the analysis was not conducted.

TABLE 4-4. Pairwise comparisons of vertebral body ratio and angle measures of cervical vertebrae in females

Comparison [1]	VB ECC	TPAA	TPPA	AFA	# of comparisons supporting suspensory model	# of comparisons rejecting suspensory model
C1						
Pan, *Pongo* vs. *Homo*			>		2	0
Hylobatids vs. *Papio*			=		0	1
Ateles vs. *Alouatta*			<		0	1
C2						
Pan, *Pongo* vs. *Homo*	=		=		0	4
Hylobatids vs. *Papio*	<		=		0	2
Ateles vs. *Alouatta*	=		=		0	2
C3						
Pan, *Pongo* vs. *Homo*	>		=	=	2	4
Hylobatids vs. *Papio*	=		<	=	0	3
Ateles vs. *Alouatta*	=		>	<	2	1
C4						
Pan, *Pongo* vs. *Homo*	=	<, =[2]	=, >	=	1	5
Hylobatids vs. *Papio*	=	<	<	=	0	4
Ateles vs. *Alouatta*	=	<	=	=	0	4
C5						
Pan, *Pongo* vs. *Homo*	=	=	>	>, =	2	6
Hylobatids vs. *Papio*	=	=	=	>	0	4
Ateles vs. *Alouatta*	=	=	=	=	0	4
C6						
Pan, *Pongo* vs. *Homo*	<, =	<	=	=	0	8
Hylobatids vs. *Papio*	=	=	=	=	0	4
Ateles vs. *Alouatta*	=	=	=	=	0	4
C7						
Pan, *Pongo* vs. *Homo*	<		=	=	0	6
Hylobatids vs. *Papio*	=		>	>	1	2
Ateles vs. *Alouatta*	=		>	=	1	2

[1] For statistically significant comparisons, less-than and greater-than symbols indicate direction of difference (e.g., at the C1 level, the TPPA is greater in

both *Pan* and *Pongo* than in *Homo*; equality sign indicates that difference is not statistically significant).

[2] Two signs separate signs indicate that results of the multiple pairwise comparisons are different; the first sign represents the first comparison (e.g., *Pan* vs. *Homo*) and the second sign represents the second comparison (e.g., *Pongo* vs. *Homo*).

Hylobatids (suspensory) v. *Nasalis larvatus* and *Papio anubis* (nonsuspensory)

Results of the Wilcoxon-Mann-Whitney tests are in Tables 4-1-4. There are too few female *Nasalis* specimens to include in the separate female analysis; so female hylobatids are compared only to *Papio* female individuals.

The comparison of hylobatids to cercopithecoids results in fewer significant differences than in the ape/human analysis. Furthermore, when differences are statistically significant, they are often in the opposite direction predicted by the suspensory model. This result is particularly common when comparing hylobatids to *Papio* (e.g., spinous process length [SPL], pedicle cross-sectional area [PCSA], and laminar cross-sectional area [LCSA]) (Table 4-1, 4-3). The exception to this pattern is transverse process length (both ATPL and PTPL). Analyses for both male and female hylobatid/*Papio* comparisons of PTPL produce significant differences in the majority of the cervical column (C1-C6), but results are not significant in the male hylobatid/*Nasalis* comparison (no female hylobatid/*Nasalis* comparison due to sample size). Notably, both male and female hylobatids demonstrate reduced ATPL at all applicable levels (C3-C5) in both *Nasalis* (males only) and *Papio* comparisons, thereby providing consistent support for the suspensory model in this single feature.

In some aspects, the hylobatid/cercopithecoid results mirror the ape/human comparisons, including more support for the suspensory model found in males and at lower cervical levels. In contrast to the ape comparison, however, a longer spinous process is not found at any vertebral level and in turn, weakens the form-function link suggested in the ape/human analyses. The feature producing the most support for the

suspensory model in the second set of pairwise comparisons is transverse process length measured at the anterior tubercle (ATPL).

***Ateles* sp. (suspensory) v. *Alouatta* sp. and *Pithecia* sp. (nonsuspensory)**

In the platyrrhine comparison, too few female *Pithecia* specimens are available to include in the separate female analysis, thus female *Ateles* are only compared to *Alouatta* female individuals. Results of the Wilcoxon-Mann-Whitney tests are in Tables 4-1-4.

The comparison of *Ateles* to *Alouatta* and *Pithecia* results in the fewest significant differences and again some contradictory results. For example, when *Ateles* is compared to *Alouatta*, transverse process length (measured at both anterior [ATPL] and posterior tubercles [PTPL]) follows the predicted pattern and is relatively shorter in suspensory taxa when compared to their nonsuspensory counterparts. This was true for 6 out of 7 vertebral levels in males and 3 out of 7 levels in females. However, this relationship is not found when comparing male *Ateles* to male *Pithecia* (no female *Ateles*/*Pithecia* comparison due to sample size) (Fig 4-1).

Clear support for the suspensory model is limited to the C7 level. The cross-sectional areas for the pedicle, laminae, and spinous process are larger in the both male and female suspensory taxa. This pattern is maintained for the pedicle and laminar cross-sectional areas throughout the cervical column when *Ateles* males are compared to *Pithecia* males. Female *Ateles* individuals also demonstrate significantly larger laminar cross-sectional areas in 4 out of 7 levels. The pattern does not precede the C7 level when *Ateles* males are compared to *Alouatta* males however, and reflects another example of conflicting results in this subset of comparisons.

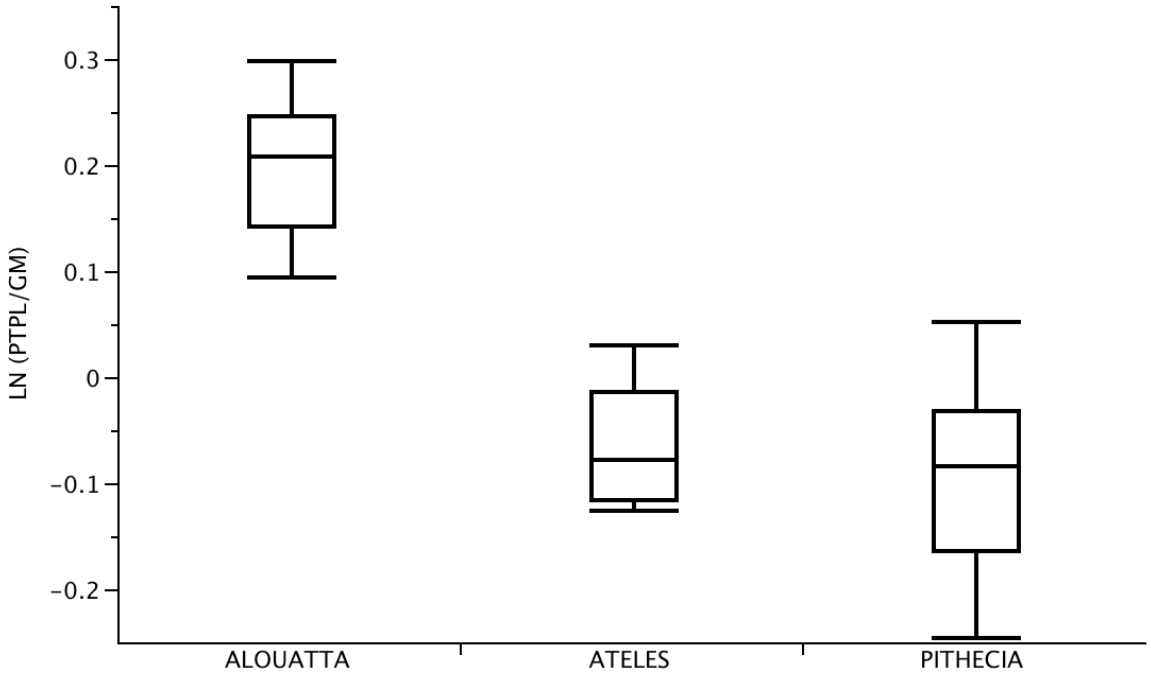

Figure 4-1. Box-and-whisker plot of relative transverse process length (posterior tubercle) *Ateles* vs. *Alouatta* and *Pithecia* at the C4 vertebral level in males. Graph highlights morphological pattern found throughout most of the cervical column; *Ateles*/*Alouatta* comparison supports the suspensory model: suspensory taxon (*Ateles*) has significantly shorter transverse processes when compared to nonsuspensory taxa (*Alouatta*), yet this pattern is not replicated in the *Ateles*/*Pithecia* comparisons.

pattern of the significant differences between the platyrrhine taxa does not provide support for the suspensory model in any one vertebral feature. Instead, support for the model seems to be found most often at a specific vertebral level (i.e., C7) instead.

Summary of pairwise comparisons

The goal of the targeted pairwise comparisons was to test the biomechanical predictions put forth by the suspensory model with an effort to minimize differences due to allometry and/or phylogenetic history. Broadly, results demonstrate that more significant differences are found in male comparisons and at the lower cervical spine (C3-C7) for both sexes. But few vertebral features consistently fit the pattern proposed by the suspensory model. Overall results of the pairwise analyses are equivocal.

The comparison of apes to humans yields the highest number of significant differences and best fit the proposed morphological patterns for suspensory and nonsuspensory taxa. Specifically, a longer spinous process is consistently found in the suspensory apes when compared to nonsuspensory humans (Tables 4-1, 4-3). The hylobatid/cercopithecoid comparison results in fewer significant differences than the ape/human comparison. When differences are significant, they are often not in the direction predicted by the suspensory model. For example, the model predicts that the suspensory hylobatid taxa will demonstrate longer spinous processes than either nonsuspensory taxa: *Nasalis* and *Papio*. The model is supported in the hylobatid/*Nasalis* comparison, and hylobatids had longer spinous processes. This relationship was not upheld, however, in the hylobatid/*Papio* comparison (Table 4-1, 4-3). Hylobatid transverse process lengths did support the suspensory model. In particular, the ATPL is consistently shorter (in the direction predicted by the suspensory model) when compared to similarly sized cercopithecoids for both males and females.

Finally, the comparison of *Ateles* to *Alouatta* and *Pithecia* resulted in the fewest significant differences and again some contradictory results. Clear support for the suspensory model is only found at the C7 level. The cross-sectional areas for the pedicle, laminae, and spinous process are larger in the suspensory taxa for both males and females. This pattern is also found throughout the cervical column, though not consistently (e.g., *Ateles* males vs. *Pithecia* males, but not in when comparing *Ateles* males to *Alouatta* males). Significant differences in the opposite direction predicted by the model are commonly found in *Ateles*/*Alouatta* comparisons (e.g., spinous process length). Therefore, the conflicting pattern of the significant differences between the

platyrrhine taxa does not provide support for the suspensory model in any single vertebral feature; however, support is found at a specific vertebral level, C7. This result corresponds with the fact that more significant differences are found at lower levels (C3-C7) and, in fact, the largest percentage of significant differences that supported the suspensory model is found at the C7 level for both males and females in all three comparisons. Nevertheless, not a single cervical feature successfully separated groups in the predicted direction for all three pairwise comparisons at any one level—C7 included.

Because the pairwise tests did not reliably support the morphological pattern in any single trait or at any one vertebral level predicted for the suspensory model, it must be rejected. No vertebral features were rejected in every instance—though a few rarely demonstrated the predicted morphology, such as vertebral eccentricity and articular facet angle. The vertebral traits that seem best correlated with suspensory behavior are spinous process length and transverse process morphology (ATPL more so than PTPL), though again, no feature was significant for all three comparisons. Therefore, according to the data presented here, these vertebral traits do not differ predictably according to ability to perform suspensory behaviors.

PRIMATE-WIDE ANALYSES

In this section, the biomechanical predictions of the postural and head-balancing models are examined using a broader sample of primates and incorporating additional categories of positional behavior (i.e., orthograde-nonsuspensory and pronograde). In contrast to the previous section, which was divided by taxonomic comparison, results are separated by vertebral feature (e.g., vertebral body ventral length [VBVL] and spinous process length [SPL]). In each section results of primate-wide scaling investigations are

discussed first, followed by the results of phylogenetic generalized least squares (PGLS) analyses. To ensure that a slope of 1 indicated isometry, nonangular variables were adjusted accordingly (i.e., square root of areal measurements [mm^2], cube root of body mass). For angular measurements, a slope of 0 indicates no change in shape with changes in size. As described in Chapter 3, species' means of body mass are used to adjust for size in PGLS analyses and sexes are separated.

Results of PGLS analyses are presented in two steps. First, results addressing the two positional models are discussed, stemming from PGLS analyses incorporating two independent variables: size and positional behavior. Second, results from analyses examining the head-balancing model are provided, reflecting the addition of a third variable to the PGLS model, anterior cranial length (ACL). Descriptors of the strength of support for a model or correlations between features are arbitrarily defined as follows: *very strong*, 100% to 90% of the cases or correlations were significant; *strong*, 89% to 70%; *moderate*, 69% to 50%; *weak*, 49% to 30%; and *very weak*, 29% to 1%.

TABLE 4-5. Scaling of ln vertebral variables against ln body mass

	Males				Females			
	RMA Slope[1]	**Lower CI**	**Upper CI**	**r^2**	**RMA Slope**	**Lower CI**	**Upper CI**	**r^2**
C1								
SPL	1.378***	1.157	1.599	0.716	1.416***	1.144	1.689	0.590
PTPL	0.783***	0.730	0.836	0.950	0.865***	0.779	0.952	0.887
PCSA	1.107***	0.945	1.268	0.771	1.136***	0.956	1.316	0.723
LCSA	1.026***	0.863	1.190	0.721	1.201***	0.948	1.454	0.491
TPPA	0.311	0.232	0.389	0.060	0.057	0.004	0.110	0.123
C2								
VB ECC	-1.363	-1.499	-1.227	0.003	0.158	-0.012	0.329	0.001
SPL	1.332***	1.155	1.510	0.804	1.207***	1.079	1.334	0.871
PTPL	0.969***	0.837	1.101	0.802	0.935***	0.835	1.035	0.870
PCSA	0.960***	0.864	1.055	0.901	1.003***	0.883	1.122	0.849
LCSA	1.075***	0.954	1.195	0.862	1.070***	0.957	1.184	0.873
SCSA	1.025***	0.843	1.208	0.649	1.019***	0.862	1.176	0.727
TPPA	0.307	0.211	0.403	0.010	-0.095	-0.195	0.005	0.001
C3								
VBVL	0.921***	0.760	1.081	0.688	1.073***	0.889	1.258	0.672
VBDL	0.958***	0.807	1.108	0.747	1.078***	0.931	1.225	0.801
VB ECC	2.152**	1.571	2.734	0.154	2.129***	1.616	2.642	0.355
UNC	0.261*	0.192	0.330	0.076	-0.290	-0.382	-0.198	0.001
SPL	2.351***	1.952	2.750	0.704	2.101***	1.838	2.363	0.828
PTPL	0.956***	0.803	1.108	0.745	1.018***	0.892	1.143	0.831
PCSA	1.045***	0.925	1.165	0.869	1.128***	1.003	1.254	0.870
LCSA	1.160***	1.013	1.307	0.835	1.104***	0.979	1.229	0.862
SCSA	1.217***	1.035	1.399	0.782	1.294***	1.107	1.481	0.776
TPPA	0.484	0.354	0.615	0.058	0.249	0.171	0.327	0.023
AFA	-0.232	-0.270	-0.195	0.009	0.225	0.167	0.283	0.067
C4								
VBVL	0.996***	0.840	1.151	0.744	1.092***	0.924	1.260	0.739
VBDL	0.970***	0.814	1.126	0.742	1.142***	0.983	1.300	0.787
VB ECC	1.392***	1.079	1.706	0.499	1.310***	1.062	1.558	0.612
UNC	-0.194*	-0.245	-0.143	0.079	-0.227	-0.282	-0.172	0.045
SPL	2.247***	1.865	2.629	0.696	2.126***	1.818	2.433	0.770
ATPL	1.013***	0.810	1.215	0.641	0.963***	0.817	1.110	0.830
PTPL	0.995***	0.858	1.132	0.807	1.058***	0.919	1.198	0.809
PCSA	1.053***	0.944	1.162	0.896	1.240***	1.094	1.387	0.850
LCSA	1.208***	1.059	1.358	0.839	1.240***	1.094	1.387	0.850
SCSA	1.349***	1.154	1.544	0.798	1.499***	1.237	1.761	0.670
TPAA	0.585	0.392	0.778	0.013	0.704	0.477	0.932	0.017
TPPA	0.409	0.313	0.505	0.033	0.362**	0.267	0.458	0.166
AFA	0.296	0.232	0.360	0.023	0.209*	-0.337	0.755	0.121
C5								
VBVL	1.019***	0.834	1.205	0.658	0.978***	0.822	1.135	0.725
VBDL	1.014***	0.854	1.174	0.757	1.055***	0.910	1.199	0.802
VB ECC	0.400	0.273	0.527	0.002	-0.491	-0.642	-0.339	0.014
UNC	1.877***	1.430	2.323	0.403	2.118***	1.586	2.651	0.306

SPL	2.140***	-1.235	5.515	0.843	2.012***	1.704	2.321	0.747
ATPL	1.005***	0.819	1.191	0.681	1.029***	0.886	1.172	0.808
PTPL	1.026***	0.855	1.197	0.723	1.033***	0.888	1.178	0.788
PCSA	1.040***	0.925	1.156	0.884	1.194***	1.065	1.323	0.881
LCSA	1.334***	1.151	1.518	0.806	1.255***	1.102	1.409	0.839
SCSA	1.328***	1.101	1.555	0.723	1.482***	1.199	1.765	0.615
TPAA	0.725	0.543	0.908	0.037	0.853	0.708	0.999	0.011
TPPA	0.344*	0.251	0.438	0.090	0.328**	0.242	0.414	0.178
AFA	0.286	0.195	0.378	0.017	0.384	0.306	0.462	0.020
C6								
VBVL	0.951***	0.809	1.094	0.752	1.009***	0.868	1.150	0.789
VBDL	1.012***	0.859	1.164	0.767	1.131***	0.975	1.287	0.807
VB ECC	-0.406	-0.530	-0.282	0.006	-0.454	-0.595	-0.314	0.004
UNC	1.906***	1.491	2.321	0.481	1.672***	1.329	2.015	0.558
SPL	2.112***	1.770	2.454	0.711	1.961***	1.653	2.269	0.732
ATPL	1.015***	0.902	1.128	0.861	1.027***	0.904	1.150	0.850
PTPL	1.037***	0.876	1.197	0.748	1.054***	0.901	1.206	0.779
PCSA	1.043***	0.946	1.140	0.912	1.182***	1.045	1.319	0.863
LCSA	1.289***	1.140	1.438	0.852	1.275***	1.117	1.434	0.834
SCSA	1.384***	1.149	1.620	0.703	1.464***	1.209	1.719	0.679
TPAA	0.378	0.285	0.471	0.044	0.190	0.053	0.327	0.318
TPPA	0.366	0.273	0.459	0.047	0.295**	0.218	0.373	0.183
AFA	0.308	0.229	0.386	0.058	0.266	0.200	0.333	0.055
C7								
VBVL	0.992***	0.814	1.170	0.669	1.003***	0.873	1.133	0.819
VBDL	1.018***	0.868	1.169	0.777	1.130***	0.988	1.273	0.834
VB ECC	0.584	0.399	0.769	0.009	-0.606	-0.793	-0.420	0.017
UNC	2.105***	1.574	2.637	0.316	2.256***	1.744	2.769	0.446
SPL	1.952***	1.580	2.324	0.633	1.721***	1.432	2.010	0.696
PTPL	0.921***	0.784	1.058	0.774	0.980***	0.848	1.113	0.805
PCSA	0.956***	0.853	1.059	0.886	1.149***	0.990	1.307	0.806
LCSA	1.371***	1.198	1.544	0.838	1.416***	1.234	1.597	0.824
SCSA	1.469***	1.203	1.736	0.671	1.425***	1.169	1.680	0.663
TPPA	0.813	0.727	0.899	0.003	0.376*	0.275	0.477	0.133
AFA	0.274	0.200	0.347	0.058	0.185***	0.140	0.229	0.362

[1] Isometry is indicated by a slope of 1 for nonangular variables. For variables measured degrees (e.g., TPPA and AFA) a slope of 0 indicates isometry.

Abbreviations are as follows: VBVL = vertebral body ventral length, VBDL = vertebral body dorsal length VB ECC = vertebral body eccentricity, UNC = uncinate process height, SPL = spinous process length, ATPL = transverse process length (anterior tubercle), PTPL = transverse process length (posterior tubercle), PCSA = pedicle cross-sectional area, LCSA = lamina cross-sectional area, SCSA = spinous process cross-sectional area, TPAA = transverse process angle (anterior tubercle), TPPA = transverse process angle (posterior tubercle), AFA = articular facet angle

Level of significance indicated as follows: * $p < 0.05$, ** $p < 0.01$, *** $p < 0.001$

TABLE 4-6. PGLS results of vertebral variable on ln body mass and positional behavior in females.

Variable	Suspensory vs. Orthograde, Nonsuspensory	Suspensory vs. Pronograde	Orthograde vs. Pronograde	Suspensory Model Supported?	Postural Model Supported?
C1					
LN SPL	=	>**[1]	>***	No	**Yes**
LN PTPL	=	>**	>**	No	No
LN PCSA	=	<**	<**	No	No
LN LCSA	=	=	=	No	No
LN TPPA	=	=	=	No	No
C2					
LN SPL	=	=	=	No	No
LN PTPL	=	=	=	No	No
LN PCSA	=	=	=	No	No
LN LCSA	=	=	=	No	No
LN SCSA	=	=	=	No	No
LN TPPA	=	=	=	No	No
LN VB ECC	=	=	=	No	No
C3					
LN VBVH	=	=	=	No	No
LN VBDH	=	=	=	No	No
LN SPL	>*	=	=	No	No
LN PTPL	=	=	=	No	No
LN PCSA	=	=	=	No	No
LN LCSA	=	=	=	No	No
LN SCSA	=	=	=	No	No
LN TPPA	=	=	=	No	No
LN VB ECC	=	=	<*	No	No
LN UNC	=	=	>**	na[2]	No
LN AFA	=	=	=	No	No
C4					
LN VBVH	=	=	=	No	No
LN VBDH	=	=	=	No	No
LN SPL	>**	=	=	No	No
LN ATPL	=	=	=	No	No
LN PTPL	=	=	=	No	No
LN PCSA	=	=	=	No	No
LN LCSA	=	=	=	No	No
LN SCSA	=	=	=	No	No
LN TPAA	=	=	=	No	No
LN TPPA	=	=	=	No	No
LN VB ECC	=	=	=	No	No
LN UNC	=	=	=	na	No
LN AFA	=	=	=	No	No
C5					
LN VBVH	=	=	=	No	No
LN VBDH	=	=	=	No	No
LN SPL	=	=	=	No	No
LN ATPL	=	<*	=	No	No
LN PTPL	=	=	=	No	No
LN PCSA	=	=	=	No	No
LN LCSA	=	=	=	No	No
LN SCSA	=	=	=	No	No

LN TPAA	=	=	<*	No	No
LN TPPA	=	=	=	No	No
LN VB ECC	=	=	=	No	No
LN UNC	=	=	=	na	No
LN AFA	=	=	=	No	No
C6					
LN VBVH	=	=	=	No	No
LN VBDH	=	=	=	No	No
LN SPL	=	>*	=	No	No
LN ATPL	=	=	=	No	No
LN PTPL	=	=	=	No	No
LN PCSA	=	=	=	No	No
LN LCSA	=	>*	=	No	No
LN SCSA	=	=	=	No	No
LN TPAA	=	=	=	No	No
LN TPPA	=	=	=	No	No
LN VB ECC	=	=	=	No	No
LN UNC	<*	=	=	na	No
LN AFA	=	=	=	No	No
C7					
LN VBVH	=	=	=	No	No
LN VBDH	=	=	=	No	No
LN SPL	=	=	=	No	No
LN PTPL	=	=	=	No	No
LN PCSA	=	=	=	No	No
LN LCSA	=	=	=	No	No
LN SCSA	=	>**	>*	No	**Yes**
LN TPPA	>***	>***	=	**Yes**	No
LN VB ECC	=	=	=	No	No
LN UNC	=	=	=	na	No
LN AFA	=	=	=	No	No

[1] For statistically significant comparisons, less-than and greater-than symbols indicate direction of difference (e.g., at the C1 level, the SPL (spinous process length) is greater in suspensory taxa than in pronograde taxa; equality sign indicates that difference is not statistically significant.

[2] Not applicable.

Abbreviations are as follows: VBVL = vertebral body ventral length, VBDL = vertebral body dorsal length VB ECC = vertebral body eccentricity, UNC = uncinate process height, SPL = spinous process length, ATPL = transverse process length (anterior tubercle), PTPL = transverse process length (posterior tubercle), PCSA = pedicle cross-sectional area, LCSA = lamina cross-sectional area, SCSA = spinous process cross-sectional area, TPAA = transverse process angle (anterior tubercle), TPPA = transverse process angle (posterior tubercle), AFA = articular facet angle.

Level of significance indicated as follows: * $p < 0.05$, ** $p < 0.01$, *** $p < 0.001$

TABLE 4-7. PGLS results of vertebral variable on ln body mass and positional behavior in males.

Variable	Suspensory vs. Orthograde, Nonsuspensory	Suspensory vs. Pronograde	Orthograde vs. Pronograde	Suspensory Model Supported?	Postural Model Supported?
C1					
LN SPL	=	=	=	No	No
LN PTPL	=	=	=	No	No
LN PCSA	=	<*[1]	<*	No	No
LN LCSA	=	=	=	No	No
LN TPPA	=	=	=	No	No
C2					
LN SPL	=	=	=	No	No
LN PTPL	<*	<**	=	**Yes**	No
LN PCSA	=	=	=	No	No
LN LCSA	=	=	=	No	No
LN SCSA	=	=	=	No	No
LN TPPA	=	<*	=	No	No
LN VB ECC	=	=	=	No	No
C3					
LN VBVL	=	=	=	No	No
LN VBDL	=	=	=	No	No
LN SPL	=	=	=	No	No
LN PTPL	=	=	=	No	No
LN PCSA	=	=	=	No	No
LN LCSA	=	<*	=	No	No
LN SCSA	=	=	=	No	No
LN TPPA	=	<**	<*	No	No
LN VB ECC	>**	=	=	No	No
LN UNC	<*	=	=	na[2]	No
LN AFA	=	=	=	No	No
C4					
LN VBVL	=	=	=	No	No
LN VBDL	=	=	=	No	No
LN SPL	>*	=	=	No	No
LN ATPL	<*	<*	=	**Yes**	No
LN PTPL	=	<*	=	No	No
LN PCSA	=	=	=	No	No
LN LCSA	=	=	=	No	No
LN SCSA	=	>**	>***	No	**Yes**
LN TPAA	=	<**	<**	No	No
LN TPPA	=	<*	<**	No	No
LN VB ECC	=	=	=	No	No
LN UNC	>*	=	=	na	No
LN AFA	>**	=	<**	No	**Yes**
C5					
LN VBVL	=	=	=	No	No
LN VBDL	=	=	=	No	No
LN SPL	>*	=	=	No	No
LN ATPL	<*	<*	<*	**Yes**	No
LN PTPL	=	<*	=	No	No

LN PCSA	=	=	=	No	No
LN LCSA	>**	=	=	No	No
LN SCSA	=	>***	>***	No	**Yes**
LN TPAA	=	<*	<**	No	No
LN TPPA	=	=	<*	No	No
LN VB ECC	=	=	=	No	No
LN UNC	=	=	=	na	No
LN AFA	=	=	=	No	No
C6					
LN VBVL	=	=	=	No	No
LN VBDL	=	=	=	No	No
LN SPL	=	=	=	No	No
LN ATPL	=	<*	<*	No	**Yes**
LN PTPL	<*	<*	=	**Yes**	No
LN PCSA	=	=	=	No	No
LN LCSA	=	=	=	No	No
LN SCSA	=	>**	>**	No	**Yes**
LN TPAA	=	<*	<**	No	No
LN TPPA	=	=	=	No	No
LN VB ECC	=	>*	=	No	No
LN UNC	=	=	=	na	No
LN AFA	>***	=	=	No	No
C7					
LN VBVL	=	=	=	No	No
LN VBDL	=	=	=	No	No
LN SPL	=	=	=	No	No
LN PTPL	=	<*	=	No	No
LN PCSA	=	=	=	No	No
LN LCSA	=	=	=	No	No
LN SCSA	=	>*	>**	No	**Yes**
LN TPPA	>*	>*	=	**Yes**	No
LN VB ECC	<*	=	=	No	No
LN UNC	=	=	=	na	No
LN AFA	>**	>**	=	No	No

[1] For statistically significant comparisons, less-than and greater-than symbols indicate direction of difference (e.g., at the C1 level, the PCSA (pedicle cross-sectional area) is smaller in suspensory taxa than in pronograde taxa; equality sign indicates that difference is not statistically significant.
[2] Not applicable.
Abbreviations are as follows: VBVL = vertebral body ventral length, VBDL = vertebral body dorsal length VB ECC = vertebral body eccentricity, UNC = uncinate process height, SPL = spinous process length, ATPL = transverse process length (anterior tubercle), PTPL = transverse process length (posterior tubercle), PCSA = pedicle cross-sectional area, LCSA = lamina cross-sectional area, SCSA = spinous process cross-sectional area, TPAA = transverse process angle (anterior tubercle), TPPA = transverse process angle (posterior tubercle), AFA = articular facet angle.
Level of significance indicated as follows: * $p < 0.05$, ** $p < 0.01$, *** $p < 0.001$

TABLE 4-8 PGLS results of vertebral variable on ln body mass, ln anterior cranial length (ACL), and positional behavior in females.

Variable	Suspensory vs. Orthograde, Nonsuspensory	Suspensory vs. Pronograde	Orthograde vs. Pronograde	Regression coefficient with ACL[†]	Suspensory Model Supported?	Postural Model Supported?	Head-Balancing Model Supported?
C1							
LN SPL	=	>**[1]	>***	1.85**	No	**Yes**	**Yes**
LN PTPL	=	>**	>***	0.71***	No	No	**Yes**
LN PCSA	=	<*	<*	0.93**	No	No	**Yes**
LN LCSA	=	=	=	1.46**	No	No	**Yes**
LN TPPA	=	=	=	ns[2]	No	No	No
C2							
LN SPL	=	=	=	1.08**	No	No	**Yes**
LN PTPL	=	=	=	0.92***	No	No	**Yes**
LN PCSA	=	=	=	0.98**	No	No	**Yes**
LN LCSA	=	=	=	1.06**	No	No	**Yes**
LN SCSA	=	=	=	1.11**	No	No	**Yes**
LN TPPA	=	=	=	ns	No	No	No
LN VB ECC	=	=	=	ns	No	No	No
C3							
LN VBVL	=	=	=	ns	No	No	No
LN VBDL	=	=	=	ns	No	No	No
LN SPL	=	=	=	ns	No	No	No
LN PTPL	=	=	=	0.98***	No	No	**Yes**
LN PCSA	=	=	=	1.48***	No	No	**Yes**
LN LCSA	=	=	=	1.07*	No	No	**Yes**
LN SCSA	=	=	=	1.29*	No	No	**Yes**
LN TPPA	=	=	=	0.44*	No	No	**Yes**
LN VB ECC	=	=	=	ns	No	No	No
LN UNC	=	=	>**	ns	na[3]	No	No
LN AFA	=	=	=	ns	No	No	No
C4							
LN VBVL	=	=	=	0.88**	No	No	**Yes**
LN VBDL	=	=	=	ns	No	No	No
LN SPL	>**	=	=	1.59*	No	No	**Yes**
LN ATPL	<*	=	=	0.91*	No	No	**Yes**
LN PTPL	=	=	=	0.86**	No	No	**Yes**
LN PCSA	=	=	=	1.35***	No	No	**Yes**
LN LCSA	=	=	=	ns	No	No	No
LN SCSA	=	>**	=	1.45*	No	No	**Yes**
LN TPAA	=	=	=	ns	No	No	No
LN TPPA	=	<*	<*	ns	No	No	No
LN VB ECC	=	=	=	ns	No	No	No
LN UNC	=	=	=	ns	na	No	No
LN AFA	=	=	=	ns	No	No	No
C5							
LN VBVL	=	=	=	0.90**	No	No	**Yes**
LN VBDL	=	=	=	ns	No	No	No
LN SPL	=	=	=	ns	No	No	No
LN ATPL	<*	=	=	0.73**	No	No	**Yes**
LN PTPL	=	=	=	0.64*	No	No	**Yes**

LN PCSA	=	=	=	1.37***	No	No	**Yes**
LN LCSA	=	=	=	0.87*	No	No	**Yes**
LN SCSA	=	>**	>**	ns	No	**Yes**	No
LN TPAA	=	<*	<*	ns	No	No	No
LN TPPA	=	=	=	ns	No	No	No
LN VB ECC	=	=	=	ns	No	No	No
LN UNC	=	=	=	ns	na	No	No
LN AFA	=	=	=	ns	No	No	No
C6							
LN VBVL	=	=	=	ns	No	No	No
LN VBDL	=	=	=	ns	No	No	No
LN SPL	=	=	=	ns	No	No	No
LN ATPL	=	=	=	0.83**	No	No	**Yes**
LN PTPL	=	=	=	0.59*	No	No	**Yes**
LN PCSA	=	=	=	1.22**	No	No	**Yes**
LN LCSA	=	=	=	ns	No	No	No
LN SCSA	=	>*	>*	ns	No	**Yes**	No
LN TPAA	=	=	=	ns	No	No	No
LN TPPA	=	=	=	0.46*	No	No	**Yes**
LN VB ECC	=	=	=	ns	No	No	No
LN UNC	>*	=	=	3.24***	na	No	**Yes**
LN AFA	=	=	=	ns	No	No	No
C7							
LN VBVL	=	=	=	0.76*	No	No	**Yes**
LN VBDL	=	=	=	0.89**	No	No	**Yes**
LN SPL	=	=	=	ns	No	No	No
LN PTPL	=	=	=	0.76*	No	No	**Yes**
LN PCSA	=	=	=	1.31***	No	No	**Yes**
LN LCSA	=	=	=	ns	No	No	No
LN SCSA	=	>*	>***	ns	No	**Yes**	No
LN TPPA	>**	>***	=	0.60**	**Yes**	No	**Yes**
LN VB ECC	=	=	=	ns	No	No	No
LN UNC	=	=	=	ns	na	No	No
LN AFA	=	=	=	ns	No	No	No

† Since body mass is included in the PGLS analyses, the regression coefficient refers to the relationship between *relative* ACL and the *relative* vertebral feature (e.g. SPL).

[1] For statistically significant comparisons, less-than and greater-than symbols indicate direction of difference (e.g., at the C1 level, the SPL (spinous process length) is greater in suspensory taxa than in pronograde taxa; equality sign indicates that difference is not statistically significant.

Abbreviations are as follows: VBVL = vertebral body ventral length, VBDL = vertebral body dorsal length VB ECC = vertebral body eccentricity, UNC = uncinate process height, SPL = spinous process length, ATPL = transverse process length (anterior tubercle), PTPL = transverse process length (posterior tubercle), PCSA = pedicle cross-sectional area, LCSA = lamina cross-sectional area, SCSA = spinous process cross-sectional area, TPAA = transverse process angle (anterior tubercle), TPPA = transverse process angle (posterior tubercle), AFA = articular facet angle.

[2] regression correlation was not significant.

[3] Not applicable.

Level of significance indicated as follows: * $p < 0.05$, ** $p < 0.01$, *** $p < 0.001$

TABLE 4-9 PGLS results of vertebral variable on ln body mass, ln anterior cranial length (ACL), and positional behavior in males.

Variable	Suspensory vs. Orthograde, Nonsuspensory	Suspensory vs. Pronograde	Orthograde vs. Pronograde	Correlation coefficient with ACL[†]	Suspensory Model Supported?	Postural Model Supported?	Head-Balancing Model Supported?
C1							
LN SPL	=	>*[1]	>**	0.80*	No	**Yes**	**Yes**
LN PTPL	=	=	=	0.39**	No	No	**Yes**
LN PCSA	=	<*	<*	ns[2]	No	No	No
LN LCSA	=	=	=	ns	No	No	No
LN TPPA	=	=	=	ns	No	No	No
C2							
LN SPL	=	=	=	ns	No	No	No
LN PTPL	=	=	=	0.50*	No	No	**Yes**
LN PCSA	=	=	=	ns	No	No	No
LN LCSA	=	=	=	0.87***	No	No	**Yes**
LN SCSA	=	=	=	ns	No	No	No
LN TPPA	=	=	=	ns	No	No	No
LN VB ECC	=	=	=	ns	No	No	No
C3							
LN VBVL	=	=	=	0.44*	No	No	**Yes**
LN VBDL	=	=	=	0.41*	No	No	**Yes**
LN SPL	=	=	=	1.01**	No	No	**Yes**
LN PTPL	=	=	=	0.61***	No	No	**Yes**
LN PCSA	=	=	=	0.57**	No	No	**Yes**
LN LCSA	=	=	=	0.46**	No	No	**Yes**
LN SCSA	=	=	=	0.77**	No	No	**Yes**
LN TPPA	=	<*	<*	ns	No	No	No
LN VB ECC	>**	=	=	ns	No	No	No
LN UNC	>*	=	=	ns	na[3]	No	No
LN AFA	=	=	=	0.22*	No	No	**Yes**
C4							
LN VBVL	=	=	=	0.65*	No	No	**Yes**
LN VBDL	=	=	=	ns	No	No	No
LN SPL	>*	=	=	1.39*	No	No	**Yes**
LN ATPL	<*	<*	=	ns	**Yes**	No	No
LN PTPL	=	=	=	0.61*	No	No	**Yes**
LN PCSA	=	=	=	ns	No	No	No
LN LCSA	=	=	=	0.63*	No	No	**Yes**
LN SCSA	=	>**	>***	ns	No	**Yes**	No
LN TPAA	=	<**	<**	ns	No	No	No
LN TPPA	=	<*	<**	ns	No	No	No
LN VB ECC	=	=	=	ns	No	No	No
LN UNC	>*	=	=	ns	na	No	No
LN AFA	>*	=	<**	ns	No	**Yes**	No
C5							
LN VBVL	=	=	=	0.73*	No	No	**Yes**
LN VBDL	=	=	=	0.66*	No	No	**Yes**
LN SPL	>*	=	=	1.23*	No	No	**Yes**
LN ATPL	=	<*	=	ns	No	No	No
LN PTPL	=	=	=	ns	No	No	No
LN PCSA	=	=	=	0.77**	No	No	**Yes**

LN LCSA	=	=	=	0.79*	No	No	**Yes**
LN SCSA	=	>***	>***	ns	No	**Yes**	No
LN TPAA	=	<*	<*	ns	No	No	No
LN TPPA	=	=	<*	ns	No	No	No
LN VB ECC	=	=	=	ns	No	No	No
LN UNC	=	=	=	ns	na	No	No
LN AFA	=	=	=	ns	No	No	No
C6							
LN VBVL	=	=	=	ns	No	No	No
LN VBDL	=	=	=	ns	No	No	No
LN SPL	=	=	=	ns	No	No	No
LN ATPL	=	<*	=	ns	No	No	No
LN PTPL	=	<*	=	ns	No	No	No
LN PCSA	=	=	=	0.65**	No	No	**Yes**
LN LCSA	=	=	=	ns	No	No	No
LN SCSA	=	>**	>**	ns	No	**Yes**	No
LN TPAA	=	<*	<*	ns	No	No	No
LN TPPA	=	=	=	ns	No	No	No
LN VB ECC	=	=	=	ns	No	No	No
LN UNC	=	=	=	ns	na	No	No
LN AFA	>**	=	=	ns	No	No	No
C7							
LN VBVL	=	=	=	ns	No	No	No
LN VBDL	=	=	=	0.54*	No	No	**Yes**
LN SPL	=	=	=	ns	No	No	No
LN PTPL	=	=	=	ns	No	No	No
LN PCSA	=	=	=	0.72**	No	No	**Yes**
LN LCSA	=	=	=	0.58*	No	No	**Yes**
LN SCSA	=	=	>*	ns	No	**Yes**	No
LN TPPA	>*	>*	=	ns	**Yes**	No	No
LN VB ECC	<*	=	=	ns	No	No	No
LN UNC	=	=	=	ns	na	No	No
LN AFA	>**	>**	=	ns	No	No	No

† Since body mass is included in the PGLS analyses, the regression coefficient refers to the relationship between *relative* ACL and the *relative* vertebral feature (e.g. SPL).

[1] For statistically significant comparisons, less-than and greater-than symbols indicate direction of difference (e.g., at the C1 level, the SPL (spinous process length) is greater in suspensory taxa than in pronograde taxa; equality sign indicates that difference is not statistically significant.

Abbreviations are as follows: VBVL = vertebral body ventral length, VBDL = vertebral body dorsal length VB ECC = vertebral body eccentricity, UNC = uncinate process height, SPL = spinous process length, ATPL = transverse process length (anterior tubercle), PTPL = transverse process length (posterior tubercle), PCSA = pedicle cross-sectional area, LCSA = lamina cross-sectional area, SCSA = spinous process cross-sectional area, TPAA = transverse process angle (anterior tubercle), TPPA = transverse process angle (posterior tubercle), AFA = articular facet angle.

[2] regression correlation was not significant

[3] Not applicable.

Level of significance indicated as follows: * $p < 0.05$, ** $p < 0.01$, *** $p < 0.001$

Ventral and Dorsal Vertebral Body Lengths (VBVL and VBDL)

Suspensory Model Predictions: Suspensory (Sus) < Orthograde-nonsuspensory (On) & Pronograde (P)

Postural Model Predictions: Orthograde (O) < Pronograde (P)

The ventral and dorsal vertebral body lengths are very strongly correlated with body mass (BM) in both males and females (Table 4-5). The slope indicates a negative allometric relationship, averaging around 0.98, but the slopes' confidence intervals do overlap with isometry (isometry indicated by slope of 1 [VBVL/cube root of BM]) (Table 4-5). PGLS results controlling for body mass and positional behavior do not indicate a significant effect of positional behavior on vertebral body length (ventral or dorsal) for either males or females (Tables 4-6, 4-7).

The addition of anterior cranial length (ACL) into PGLS analyses to test the head-balancing model does not change results and comparisons do not exhibit any significant differences between positional groups. A significant correlation with ACL is found in the lower cervical spine for males (C3-C5, C7) and females (C4-C5, C7) (Tables 4-8, 4-9). The positive sign of the regression coefficient suggests that if holding body size (and positional behavior) constant, as relative ACL increases, so does the relative height of the vertebral body.

The PGLS results do not follow the predictions of the suspensory model, nor the broader postural model, and thus do not support the hypothesis that either ventral or dorsal vertebral body length is related to positional behaviors. Results of the PGLS analyses including ACL do support the head-balancing model in the lower cervical spine for both males and females.

Vertebral Body Eccentricity (VB ECC)

Suspensory Model Predictions: Sus (less than, but closer to 1) > On & P (closer to 0)

Postural Model Predictions: O (less than, but closer to 1) > P (closer to 0)

Results of primate-wide scaling analyses demonstrate little correlation between the eccentricity of the vertebral body and body mass. The only vertebral level that does indicate a relationship was at C4 for both males and females (r^2 = 0.499 and 0.612, respectively) (isometry indicated by slope of 0 [(VBH/VBW)/cube root of BM]) (Table 4-5).

PGLS results incorporating body mass and posture indicate that there is little significant effect of positional behavior on vertebral body eccentricity for either males or females (Tables 4-6, 4-7). Significant differences are found among postural groups in both females and males at the C3 level and in males only at C6 and C7 (Table. 4-7). However a morphological pattern is not apparent as results change direction and groupings. For example, at the C3 level, orthograde-nonsuspensory taxa have a smaller ratio, closer to 0 (i.e., indicating a shorter dorsoventral dimensions and thus a less circular vertebral body), than suspensory and pronograde taxa (e.g., female C3 VB ECC values: On = 0.74 vs. Sus = 0.88 and P = 0.77; male C3 VB ECC values: On = 0.77 vs. Sus = 0.92 and P = 0.83). In contrast, at the C7 level, this relationship flips, where orthograde-nonsuspensory taxa are now more circular (indicated by a higher ratio, closer to 1) than the other two behavioral groups.

Results from PGLS analyses testing the head-balancing model remove the significant difference found at the C6 level in males and the C3 level in females in the

first PGLS model, but the differences in males at C3 and C7 remain. No significant correlation with ACL is found in this second set of PGLS analyses.

In sum, these results do not reflect expectations set by the suspensory or broader postural models. A link between eccentricity of the cervical centra and body size or anterior cranial length is not supported either.

Uncinate Process Height (UNC)

Postural Model Predictions: O < P

The influence of body mass on uncinate process height increases at lower cervical levels (isometry indicated by slope of 1 [UNC/cube root of BM]) (Table 4-5). Negligible r^2s are reported until the lower cervical levels (i.e., C5-C7) for both males and females (r^2 = 0.403, 0.481, 0.316 and 0.306, 0.558, 0.446 respectively). Reduced major axis slopes for levels C5-C7 indicate a positive allometric relationship between uncinate process height and body mass for both sexes (Table 4-5).

PGLS results testing controlling for body mass and behavior indicate that there is little significant or predictable effect of positional behavior on uncinate process height for either males or females. The few significant correlations suggest that orthograde taxa have higher uncinate processes when compared to pronograde taxa: C3 in females (Tables 4-6).

The second series of PGLS analyses incorporating ACL, in addition to body mass and positional behavior, report the same pattern found in the first PGLS (Table 4-8). Uncinate process height is not significantly correlated with ACL in females at the C3 level.

These results do not support any of the three models proposed in this study. Evidence for the hypothesis that uncinate process height is correlated with postural behaviors or anterior cranial length in primates remains very weak.

Spinous Process Length (SPL)

Suspensory Model Predictions: Sus > On & P

Postural Model Predictions: O > P

There is a very strong influence of body mass on spinous process length and a positively allometric relationship is indicated for both males and females at all vertebral levels (isometry indicated by slope of 1 [SPL/cube root of BM]) (Table 4-5).

PGLS results including body mass and all positional categories indicate that there is a weak effect of positional behavior on spinous process length in females (i.e., 4 out of 7 vertebral level comparisons) (Tables 4-6). Only a single difference is in the predicted direction of the postural model: C1 in females. Two of the differences separate orthograde-nonsuspensory taxa from the other two postural categories (suspensory and pronograde), while the third only distinguishes suspensory females from pronograde females. Males produce a similar signal, exhibiting significant differences at only two vertebral levels (C4 and C5) and separating orthograde-nonsuspensory taxa from suspensory and pronograde taxa (Tables 4-7). Overall, a relatively weak correlation between positional behavior and spinous process length is found in both males and females (i.e., 6 out of 14 comparisons were significant) (Tables 4-6, 4-7).

PGLS analyses that incorporated body mass, positional behavior, and anterior cranial length produce slightly different results with regard to the separation of positional groups. In females, positional groups are separated at the C1 and C4 levels, but

differences at C3 and C6 are no longer significant. In males, significant differences are found at the C1 level, in addition to C4 and C5 (Tables 4-8, 4-9). The significant results at the first cervical level support the postural model for both males and females. Significant regression coefficients with ACL are found at the C1, C2, and C4 levels in females, and C1 and C3-C5 levels in males. All are positive correlations, suggesting that as relative ACL increases, so does relative SPL. Notably, the significant results from the PGLS analyses including ACL are limited to the upper and midsection of the cervical column. In other words, results for the PGLS analyses that include ACL are distinct from the relationship between spinous process length and positional behavior indicated by the pairwise comparison results, which found the majority of differences in lower vertebral levels.

These results provide support for the broader postural model, but only in the first cervical vertebrae. Otherwise, results demonstrate a general lack of evidence for the hypothesis that spinous process length reflects postural or locomotor behaviors in primates. Support for the head-balancing model is limited to the upper section of the spine (C1-C5). The significant results at C1 in both males and females provide the support for *both* postural and head-balancing models.

Transverse Process Length: Anterior and Posterior Tubercle (ATPL and PTPL)

Suspensory Model Predictions: Sus < On & P

Postural Model Predictions: O < P

There is a very strong correlation between body mass and transverse process length (for both anterior and posterior tubercles) at all levels for both males and females (Table 4-5). Regression results indicate that the relationship is slightly negatively

allometric in the first cervical level, but in all other cases an isometric relationship between body size and process length is found (isometry indicated by slope of 1 [ATPL/cube root of BM]).

PGLS results controlling for body mass and behavioral categories indicate a possible effect of positional behavior on transverse process length (both anterior and posterior tubercles) with a stronger signal found in males (Table 4-7). Suspensory males have shorter lengths at the anterior tubercle at C4 and C5 than their nonsuspensory counterparts. Suspensory males also demonstrate shorter lengths at the posterior tubercles at levels C2 and C6. These results are in the predicted direction and provide weak support for the suspensory model in these particular features.

Orthograde males (both suspensory and nonsuspensory) have shorter lengths at the anterior tubercle at C6 than their pronograde counterparts. This result provides very weak support for the broader postural model (i.e., orthograde vs. pronograde).

PGLS analyses that included ACL, in addition to size and behavior, to test the head-balancing model reduced the number of significant comparisons from 10 to 7 out of 20 (Table 4-9). Only the anterior tubercle length at the C4 level in males demonstrates a difference in the predicted direction of the suspensory model (i.e., suspensory taxa have shorter transverse processes). Significant differences for females at levels C1, C4, and C5 and males at C5 and C6 do not support either suspensory or postural model. The head-balancing model is supported in male PTPL comparisons in the upper section of the cervical spine (C1-C4). Female comparisons indicated a correlation between ATPL and PTPL with anterior cranial length in all seven vertebral levels. The regression coefficients

are positive, indicating that, as relative ACL gets bigger (holding body mass and positional behavior constant), so do relative ATPL and PTPL lengths.

The PGLS analyses reveal that the correlation between behavior and transverse process length is not consistent across vertebral levels or sexes. Results from the second set of PGLS analyses suggest that transverse process length is very weakly correlated with differences in suspensory positional behavior (the only instance of support found at the C4 level in males). Very strong support for the head-balancing model is found in the upper cervical spine for both males and females (C1-C4).

Pedicle Cross-sectional area (PCSA)

Suspensory Model Predictions: Sus > On & P

Postural Model Predictions: O > P

Regression results indicate a very strong, mostly isometric relationship between body mass and pedicle cross-sectional area at all levels for both males and females (isometry indicated by slope of 1 [square root of PCSA/cube root of BM]) (Table 4-5). After the C5 level, the relationship transitions to become positively allometric for both males and females.

PGLS results incorporating body mass and positional behavior groups indicate little significant correlation between behavior and pedicle cross-sectional area for either males or females (Tables 4-6, 4-7). Both males and females demonstrate significant differences between orthograde and pronograde groups at the first cervical level, but in the opposite direction predicted by the postural model. In this comparison, pronograde taxa have larger cross-sectional areas.

Results from PGLS analyses controlling for ACL did not differ from the first PGLS analysis with regards to separating positional behavior groups. The first cervical level again marks significant differences between orthograde and pronograde taxa, where pronograde species demonstrate larger cross-sectional areas for both males and females. This second set of PGLS analyses does demonstrate a significant correlation between PCSA and ACL for all cervical levels for females and level C3 and levels C5-C7 in males. Regression coefficients are positive, indicating an increase in relative PCSA when there is an increase in relative ACL.

In general, these results do not follow the predictions put forth by the suspensory or broader postural models. With C1 being the exception, the hypothesis that pedicle cross-sectional area is related to postural or locomotor behaviors is not supported. Instead, pedicle morphology tracks strongly with body size and ACL. These results provide strong support for the head-balancing model.

Lamina Cross-Sectional Area (LCSA)

Suspensory Model Predictions: Sus > On & P

Postural Model Predictions: O > P

Similar to the pedicle scaling results, PGLS regressions indicate a very strong correlation between body mass and laminar cross-sectional area at all levels for both males and females (Table 4-5). The relationship between body size and laminar cross-sectional area transitions from isometry in upper levels (C1 to C4) to slight positive allometry in lower levels (C5 to C7). This trend is more dramatic in males, but females follow the same pattern.

PGLS results, incorporating both body size and behavioral categories as independent variables, do not indicate a significant effect of positional behavior on lamina cross-sectional area for either males or females (Tables 4-6, 4-7).

PGLS analyses incorporating all three independent variables: body size, ACL, and positional behavior demonstrate no significant differences between behavioral groups (Tables 4-8, 4-9). Laminar cross-sectional area is significantly correlated with ACL, but with contrasting results for males and females. Specifically, significant correlations are found in the upper and middle cervical spine for females (C1-C3, C5), while in males, significant correlations between LCSA and ACL are found across most of the cervical column (C2-C5 and C7). Regression coefficients are positive, indicating a positive correlation between relative ACL and relative LCSA.

Broadly, these results do not follow the expectations described in the suspensory or postural models and thus do not support the hypothesis that lamina cross-sectional area reflects postural or locomotor behaviors. The head-balancing model is more often supported, but patterns of correlation are not consistent between males and females.

Spinous Process Cross-sectional Area (SCSA)

Suspensory Model Predictions: Sus > On & P

Postural Model Predictions: O > P

There is a very strong correlation between body mass and spinous process cross-sectional area at all levels for both males and females (isometry indicated by slope of 1 [square root of SCSA/cube root of BM]) (Table 4-5). Similar to LCSA morphology, the slope of the SCSA correlation transitions from isometry at C2 to a positively allometric relationship at subsequent levels (C3 - C7) for both males and females.

PGLS results incorporating positional groups and body mass indicate behavior may have a possible effect on spinous process cross-sectional area for males and females (Tables 4-6, 4-7). Males mark a difference between orthograde and pronograde groups at lower cervical levels (C4-C7), while females only present this signal at C7, all of which follow predictions proposed by the postural model.

PGLS results including ACL provide a more consistent pattern of correlation between behavior and SCSA. An increased number of significant differences between broad postural groups (orthograde vs. pronograde) are found once anterior skull length is added to the PGLS model—from C4-C7 for both males and females. Spinous process cross-sectional area is significantly correlated with ACL in females in the upper cervical spine (C2-C4), while males demonstrate only a single occurrence of correlation at the C3 level. The positive sign of the regression coefficient indicate that when holding body size and positional behavior constant, as relative ACL increases, so does relative SCSA.

Results from the lower levels of the cervical column (C4-C6) provide moderate support for the broad postural model, specifically when controlling for both body mass and anterior cranial length. Correlations between SCSA and ACL are limited to the upper cervical spine and are found more often in females than males, which provides weak support for the head-balancing model.

Anterior and Posterior Tubercle Angles (TPAA and TPPA)

Suspensory Model Predictions: Sus > On & P

Postural Model Predictions: O > P

For both males and females, there is no relationship between body mass and transverse process angle at the anterior tubercle for all levels (isometry indicated by slope

of 0 [TPAA/cube root of BM]) (Table 4-5). There is a positive relationship between body mass and transverse process angle at the posterior tubercle in females in the lower cervical region (C4-C7) and confidence intervals do not overlap with isometry (isometry indicated by slope of 0 [TPPA/cube root of BM]) (Table 4-5). A significant relationship is only found in males at the C5 level (Table 4-5).

PGLS results testing differences between broad behavioral categories indicate a possible correlation between positional behavior and transverse process angle (both anterior and posterior tubercles) in females at C5 and in males for most of the lower cervical spine (C3-C6) (Tables 4-6, 4-7). Notably however, the differences are in the opposite direction predicted by the models outlined in Chapter 3, such that pronograde taxa have larger angles, indicating more dorsally oriented tubercles. These results also mimic the pattern found in the pairwise comparisons. This morphological relationship flips at the last cervical vertebrae. In both males and females, the C7 transverse process morphology in suspensory taxa now exhibits significantly larger angles than either orthograde-nonsuspensory or pronograde groups, and in turn, supports the suspensory model.

These patterns are also found in the second set of PGLS analyses that control for anterior cranial length (Tables 4-8, 4-9). Male results mark significant differences between positional groups in 5 of 7 vertebral levels. Again, the differences from levels C3 to C6 are in the opposite direction predicted. This is also found in the female C4 level. This pattern, as seen in the first PGLS analysis, switches at C7 (in both males and females). Now, suspensory taxa display larger angles than other behavioral groups. The C7 level results support the suspensory model. Correlations between transverse process

angle and ACL are all positive, but are limited to 3 cases—females at the C3, C6 and C7 levels and only for the posterior tubercle (TPPA). These results offer very weak support for the head-balancing model.

Broadly results provide weak support for the hypothesis that the angle of the transverse process tubercles is related to positional behaviors, but not the models presented in Chapter 2 and 3. Unexpectedly, the manner of the relationship is opposite to the predicted direction, where pronograde taxa have larger angles, and thus more dorsally positional processes. The exception at C7 corresponds with other results that highlight the stronger behavioral signals produced by the lower cervical spine. The C7 results, in conjunction with the SCSA C7 regression results and the platyrrhine pairwise comparison C7 results (i.e., PCSA, LCSA, and SCSA), support a possible morphological shift at the last cervical level. Finally, these results found very weak support for the head-balancing model.

Superior Articular Facet Angle (AFA)

Suspensory Model Predictions: Sus < On & P

Postural Model Predictions: O < P

Similar to the relationship indicated by the transverse process angles, there is little, if any, correlation between body mass and superior facet angle (isometry indicated by slope of 0 [AFA/cube root of BM])(Table 4-5). Regression results demonstrate this for both males and females and at all vertebral levels.

PGLS analyses of the primate-wide sample suggest that there is no significant relationship between positional behavior and articular facet angle for females (Tables 4-6, 4-8). Males, however, demonstrate differences in the lower cervical column, in both

PGLS analyses (with and without controlling for anterior cranial length) (Tables 4-7, 4-9). In the both PGLS models, orthograde males separate out with smaller AFAs than pronograde taxa at C4. This relationship supports the postural model. Suspensory males are larger than orthograde-nonsuspensory males, but this is in the opposite direction predicted by the suspensory model. In contrast, at the C7 level, suspensory males separate from the other two positional groups, demonstrating larger AFAs. These results do not support the predictions put for by either suspensory or broader postural models. There is only a single instance of significant correlation between AFA and ACL, which is positive and at the C3 level in males.

The PGLS results here provide very weak support for the broader postural and head-balancing models, but otherwise results do not follow the expectations set by any the models proposed here.

Analyses using neck inclination data

One critique of this project is the assignment of an entire species to a discrete postural or locomotor category. This method potentially discards real variation that does not fit within the defined behavioral categories and thereby oversimplifies species-typical behavioral repertoires and their biomechanical requirements. This issue of unclear boundaries between categories may result in "noise" in the data that can obscure functional signals in vertebral variation. A solution to this problem is to quantify relevant aspects of behavior instead of assigning postural and locomotor categories, which would provide a more fine-grained approach to describing behavior. To conduct a preliminary test of whether higher-resolution behavioral data might produce a clearer pattern of significant correlation, neck inclination data were taken from Strait and Ross's study

(1999) and used in place of positional behavior dummy variables in a final series of PGLS analyses. Strait and Ross (1999) measured the inclination of the neck as the angle of the dorsal surface of the neck relative to the line of gravity taken from videos of locomoting primates. The PGLS analysis includes: phylogeny, body mass, anterior cranial length (ACL), and neck inclination angle. The analyses were performed on each vertebral trait for the 14 primate species that overlapped between Strait and Ross's (1999) sample and the one for this project. *Pan* and *Gorilla* were excluded from this comparison because neck inclination data were collected during bouts of knuckle-walking, not suspensory or orthograde locomotor behaviors. The complete sample used in this analysis is reported in Table 4-10. Male and female results are presented separately in Tables 4-11 and 4-12.

TABLE 4-10. Taxa used in PGLS comparisons including Strait and Ross (1999) neck inclination data

Taxon	Male (n)	Female (n)	Combined (n)
Alouatta seniculus	1		1
Ateles fusciceps	9	4	13
Ateles geoffroyi	1	4	5
Cebus apella	12	7	19
Cholorcebus aethiops	8	6	14
Colobus guereza	12	7	19
Erythrocebus patas	5	3	8
Homo sapiens	10	10	20
Hylobates lar	1	1	2
Lemur catta	7	4	12
Macaca fuscata	3	2	5
Pongo pygmaeus	10	11	22
Symphalangus syndactylus	1	5	6
Varecia variegata	3	7	10

TABLE 4-11. PGLS results of vertebral variable on ln body mass, ln anterior cranial length (ACL), and ln neck posture angle in females

	Variable	Regression Coefficient	SE
C1			
	LN SPL	-0.41	0.32
	LN PTPL	-0.00	0.10
	LN PCSA	-0.03	0.12
	LN LCSA	0.15	0.22
	LN TPPA	0.18**	0.05
C2			
	LN SPL	0.43*	0.14
	LN PTPL	-0.06	0.09
	LN PCSA	0.17	0.15
	LN LCSA	0.02	0.07
	LN SCSA	-0.33*	0.14
	LN TPPA	0.02	0.07
	LN VB ECC	-0.00	0.16
C3			
	LN VBVH	0.05	0.11
	LN VBDH	0.06	0.12
	LN SPL	0.68*	0.26
	LN PTPL	-0.01	0.07
	LN PCSA	0.11	0.17
	LN LCSA	0.15	0.16
	LN SCSA	-0.30	0.24
	LN TPPA	0.05	0.05
	LN VB ECC	0.30	0.29
	LN UNC	0.05	0.10
	LN AFA		
C4			
	LN VBVH	0.06	0.12
	LN VBDH	0.11	0.11
	LN SPL	0.58	0.30
	LN ATPL	0.04	0.09
	LN PTPL	0.06	0.07
	LN PCSA	0.27	0.15
	LN LCSA	0.36*	0.14
	LN SCSA	-0.20	0.22
	LN TPAA	-0.07	0.48
	LN TPPA	-0.08	0.32
	LN VB ECC	-0.05	0.09
	LN UNC	-0.06	0.06
	LN AFA	0.08	0.05
C5			
	LN VBVH	0.01	0.08
	LN VBDH	0.10	0.11
	LN SPL	0.49	0.34
	LN ATPL	0.10	0.08
	LN PTPL	0.08	0.09
	LN PCSA	0.18	0.17
	LN LCSA	0.39**	0.10
	LN SCSA	-0.15	0.26
	LN TPAA	0.10	0.12

LN TPPA	0.16	0.07
LN VB ECC	-0.25	0.16
LN UNC	0.10	0.29
LN AFA	0.01	0.05
C6		
LN VBVH	0.09	0.15
LN VBDH	0.11	0.12
LN SPL	0.25	0.35
LN ATPL	-0.08	0.08
LN PTPL	0.04	0.12
LN PCSA	0.26	0.14
LN LCSA	0.27	0.14
LN SCSA	0.07	0.28
LN TPAA	0.03	0.16
LN TPPA	0.05	0.09
LN VB ECC	-0.29	0.18
LN UNC	0.05	0.22
LN AFA	-0.02	0.05
C7		
LN VBVH	-0.03	0.11
LN VBDH	0.04	0.11
LN SPL	0.17	0.18
LN PTPL	-0.06	0.08
LN PCSA	0.21	0.11
LN LCSA	0.12	0.18
LN SCSA	-0.05	0.27
LN TPPA	-0.03	0.08
LN VB ECC	-0.15	0.15
LN UNC	0.37	0.25
LN AFA	0.01	0.05

Abbreviations are as follows: VBVL = vertebral body ventral length, VBDL = vertebral body dorsal length, SPL = spinous process length, ATPL = transverse process length (anterior tubercle), PTPL = transverse process length (posterior tubercle), PCSA = pedicle cross-sectional area, LCSA = lamina cross-sectional area, SCSA = spinous process cross-sectional area, TPAA = transverse process angle (anterior tubercle), TPPA = transverse process angle (posterior tubercle), VB ECC = vertebral body eccentricity, UNC = uncinate process height, AFA = articular facet angle.
Level of significance indicated as follows: * $p < 0.05$, ** $p < 0.01$, *** $p < 0.001$

TABLE 4-12. PGLS results of vertebral variable on ln body mass, ln anterior cranial length (ACL), and ln neck posture in males

Variable	Regression Coefficient	SE
C1		
LN SPL	-0.10	0.16
LN PTPL	-0.07	0.08
LN PCSA	-0.01	0.17
LN LCSA	0.13	0.15
LN TPPA	0.19**	0.05
C2		
LN SPL	0.61**	0.16
LN PTPL	0.05	0.06
LN PCSA	0.03	0.12
LN LCSA	0.11	0.14
LN SCSA	-0.20	0.17
LN TPPA	0.06	0.12
LN VB ECC	0.10	0.14
C3		
LN VBVH	0.17	0.14
LN VBDH	0.12	0.12
LN SPL	0.85*	0.29
LN PTPL	0.10	0.08
LN PCSA	0.24	0.16
LN LCSA	0.26*	0.09
LN SCSA	-0.15	0.12
LN TPPA	0.15	0.09
LN VB ECC	0.43*	0.18
LN UNC	0.09	0.10
LN AFA	0.07	0.04
C4		
LN VBVH	0.15	0.15
LN VBDH	0.15	0.13
LN SPL	0.82*	0.28
LN ATPL	0.20	0.16
LN PTPL	0.08	0.07
LN PCSA	0.17	0.14
LN LCSA	0.27*	0.09
LN SCSA	-0.26	0.20
LN TPAA	0.22	0.11
LN TPPA	0.19**	0.05
LN VB ECC	0.27	0.14
LN UNC	0.08*	0.04
LN AFA	0.09	0.04
C5		
LN VBVH	0.12	0.14
LN VBDH	0.15	0.10
LN SPL	0.74*	0.26
LN ATPL	0.12	0.10
LN PTPL	0.11	0.12
LN PCSA	0.25*	0.11
LN LCSA	0.38*	0.14
LN SCSA	-0.15	0.17
LN TPAA	0.17	0.08

LN TPPA	0.18**	0.05
LN VB ECC	-0.11	0.11
LN UNC	0.13	0.22
LN AFA	0.01	0.04
C6		
LN VBVH	0.07	0.10
LN VBDH	0.18	0.11
LN SPL	0.11	0.06
LN ATPL	-0.06	0.06
LN PTPL	0.04	0.08
LN PCSA	0.20	0.11
LN LCSA	0.18	0.15
LN SCSA	0.10	0.21
LN TPAA	0.05	0.12
LN TPPA	0.11	0.06
LN VB ECC	-0.16	0.09
LN UNC	-0.17	0.34
LN AFA	0.11	0.06
C7		
LN VBVH	0.06	0.12
LN VBDH	0.09	0.08
LN SPL	0.29	0.16
LN PTPL	-0.01	0.09
LN PCSA	0.14	0.09
LN LCSA	0.08	0.15
LN SCSA	0.04	0.29
LN TPPA	0.12	0.07
LN VB ECC	-0.10	0.18
LN UNC	0.17	0.22
LN AFA	0.23***	0.05

Abbreviations are as follows: VBVL = vertebral body ventral length, VBDL = vertebral body dorsal length, SPL = spinous process length, ATPL = transverse process length (anterior tubercle), PTPL = transverse process length (posterior tubercle), PCSA = pedicle cross-sectional area, LCSA = lamina cross-sectional area, SCSA = spinous process cross-sectional area, TPAA = transverse process angle (anterior tubercle), TPPA = transverse process angle (posterior tubercle), VB ECC = vertebral body eccentricity, UNC = uncinate process height, AFA = articular facet angle.
Level of significance indicated as follows: * $p < 0.05$, ** $p < 0.01$, *** $p < 0.001$

The PGLS results suggest a correlation between neck inclination angle and the following traits (in both males and females): TPPA (C1), SPL (C2-C3), and LCSA (C4-C5). These results do not provide a more obvious pattern of significant correlations that link positional behavior with vertebral morphology than those patterns of differences found in the primate-wide comparisons using broad postural categories.

Summary of primate-wide analyses

The goal of the primate-wide investigation of vertebral shape was to examine vertebral variation from the same perspective as the pairwise comparisons, but within a taxonomically broad sample of primate species. Among the three models, significant differences in the predicted direction were found for 5 of the 13 vertebral variables after controlling for phylogeny, body mass, and anterior cranial length. The suspensory model received few instances of support; specifically the transverse process length at the anterior tubercle (ATPL) at the C4 level in males and transverse process angle at the anterior tubercle (TPPA) at the C7 level for both males and females. The transverse process angles (TPPA) of suspensory taxa tend to be larger when compared to other positional groups. This feature provides the most consistent support for the suspensory model because it was found in both males and females at the same vertebral level. Otherwise, specific predictions for the suspensory model are not supported. The broader postural model was corroborated in a larger number of analyses, specifically those including spinous process length (SPL), transverse process length at the anterior tubercle (ATPL), and spinous process cross-sectional area (SCSA). Two features produced consistent support for the postural model in both males and females in the same vertebral levels. The first is spinous process length (SPL) at the C1 level, with orthograde taxa

exhibiting relatively longer processes than pronograde taxa. The second feature is spinous process cross-sectional area (SCSA) at levels C4 to C6, which, following predictions set by the postural model, are relatively greater in orthograde taxa.

The head-balancing model was tested by incorporating anterior cranial length into the primate-wide PGLS analyses. Results support the head-balancing model alone in several features for both males and females: VBVH (C4, C5), VBDH (C7), PTPL (C1-C4), PCSA (C3, C5-C7), LCSA (C2, C3), and SCSA (C3). These features, at these particular levels, are significantly correlated with ACL while controlling for body mass, phylogeny, and positional behavior. A few features seem to support both the head-balancing model and indicate a relationship with positional behavior. These variables demonstrate a significant correlation with ACL, but also successfully separate behavioral groups, but not necessarily in the direction predicted by the suspensory or postural models: for both males and females — SPL (C1); for males only —AFA (C4); and for females only — ATPL (C4) PTPL (C1), PCSA (C1), SCSA (C4), and TPPA (C7).

A final investigation into the relationship between positional behavior and vertebral morphology was conducted by replacing discrete behavioral categories with a variable that quantified neck posture during locomotion in a subset of the extant sample. Results of these additional primate-wide PGLS analyses do not indicate a more consistent pattern of correlation between any vertebral variable and neck posture than the three cervical models developed and tested here.

Chapter 5

FOSSIL HOMINIOD ANALYSIS

INTRODUCTION

In this chapter I investigate the vertebral morphology of fossil hominoids within the comparative framework of the extant sample with two goals in mind. The first goal is to be able to discuss any functional or behavioral implications of fossil morphology in the context of the extant analysis results from Chapter 4. The second is to test the accuracy of descriptive terms such apelike, *Pan*-like, and *Homo*-like, which are often used to describe fossil vertebrae in the paleoanthropological literature. To reach these goals, this chapter focuses on the quantification and comparison of individual fossils to the subset of the extant primate species used in the pairwise comparisons minus *Pithecia* (i.e., hominoids, *Ateles*, *Alouatta*, *Papio* and *Nasalis*). These taxa were chosen because they are the most similar in body size to the fossil sample and have sufficient sample sizes for discriminant function analysis. I examine each fossil taxon separately and first discuss general preservation, context, any functional or taxonomic hypotheses proposed by previous work, and end the section by offering a prediction for morphological affinity.

These predictions represent the current consensus for each fossil specimen or specimens, and act to guide the investigation into fossil cervical morphology. Following the description sections, results of analyses performed to quantify morphology are reported (a summary table of fossil vertebral metrics is presented in Table 5-1). Discriminant function analysis plots and results tables specific to a fossil specimen are incorporated into the chapter text. Tables provide summaries of the predictive power of each discriminant function (i.e., how well the function predicts group membership of

cases) and show the number of known cases that were correctly and incorrectly classified. Discriminant functions of variables included in analyses are also reported to indicate which variables are driving differences between groups. Box-and-whisker plots illustrating the distribution of trait variation are reported for fossil specimens too incomplete for discriminant function analysis (see Chapter 3 for details). Due to the uncertain spinal level assignment of some of the fossil specimens, several of the vertebrae were included in analyses at multiple spinal levels (i.e., C4 and C5) and discussion of vertebral position is included where applicable. Finally, support for predictions of morphological similarity is briefly discussed.

TABLE 5-1. Vertebral metrics of hominoid fossils

C1	VCH	VCW	VBVL	VBDL	VB ECC	UNC	SPL	ATPL	PTPL	PCSA	LCSA	SCSA	TPAA	TPPA	AFA
N. kerioi KNM-BG 40840n	18.39										28.96			78.24	
A. afarensis A.L. 333-83	26.13										6.63				
C2															
A. afarensis A.L. 333-101	21.43	18.95					12.60				38.94	120.68			
A. robustus SK 854	16.84	19.24			0.91					50.56	48.12			40.35	
C3															
***A.** robustus* SKW 4776*		15.43	10.25		0.99						39.20				
C4															
N. kerioi KNM-BG 40793c*	7.81		7.53							20.55	12.32			47.54	129.86
A. robustus SKW 4776*		15.43	10.25		0.99						39.20				
C5															
N. kerioi KNM-BG 40793c*	7.81		7.53							20.55	12.32			47.54	129.86
A. afarensis A.L. 333-106*	14.72	17.76	10.47	12.02	0.74	8.18	28.46	37.13	44.39	19.01	26.20	46.65	36.67	51.32	139.25
A. robustus SKW 4776*		15.43	10.25		0.99						39.20				
C6															
N. kerioi KNM-BG 40840o*	11.84	16.15	9.04	10.11	0.57	3.97				23.56	26.38	19.98			150.42

A. afarensis A.L. 333-106*	14.72	17.76	10.47	12.02	0.74	8.18	28.46	37.13	44.39	19.01	26.20	46.65	36.67	51.32	139.25
C7	VCH	VCW	VBVL	VBDL	VB ECC	UNC	SPL	ATPL	PTPL	PCSA	LCSA	SCSA	TPAA	TPPA	AFA
N. kerioi KNM-BG 40840o*	11.84	16.15	9.04	10.11	0.57	3.97				23.56	26.38	19.98			150.42
A. afarensis A.L. 333-106*	14.72	17.76	10.47	12.02	0.74	8.18	28.46		44.39	19.01	26.20	46.65		51.32	139.25
Homo sp. KNM-ER 164c	15.34	18.58	12.77		0.52					52.23	56.69				157.41
H. ergaster KNM-WT 15000r	11.23	20.65	8.32	9.15	0.59	1.71	30.17		60.05	34.51	54.67	34.48		80.50	149.14

Abbreviations are as follows: VCH = vertebral canal height, VCW = vertebral canal width, VBVL = vertebral body ventral length, VBDL = vertebral body dorsal length VB ECC = vertebral body eccentricity, UNC = uncinate process height, SPL = spinous process length, ATPL = transverse process length (anterior tubercle), PTPL = transverse process length (posterior tubercle), PCSA = pedicle cross-sectional area, LCSA = lamina cross-sectional area, SCSA = spinous process cross-sectional area, TPAA = transverse process angle (anterior tubercle), TPPA = transverse process angle (posterior tubercle), AFA = articular facet angle

* indicates specimen that was included in more than one vertebral level analysis

FOSSIL TAXA DESCRIPTIONS AND RESULTS

Nacholapithecus kerioi

Nacholapithecus kerioi is a mid- to large-sized primate fossil species excavated from Nachola, Kenya and dates to ~ 15 Ma (millions of years ago) (Nakatsukasa et al., 2000). Previous descriptions have suggested that the *Nacholapithecus* postcrania, including the axial skeleton, displays intermediate morphologies between extant great apes and other more pronograde primate species (Nakatsukasa et al., 2003; Senut et al., 2004; Kikuchi et al., 2012). This has led to functional interpretations suggesting that *Nacholapithecus* was not an exclusively pronograde animal, but occasionally incorporated orthograde climbing behaviors seen in extant apes (Kikuchi et al., 2012). Thirteen individual cervical elements represent this fossil species and are relatively well-described compared to other fossil hominoid cervical specimens (Kikuchi et al., 2012). Kikuchi and colleagues (2012) compared the *N. kerioi* cervical vertebrae elements to 13 extant primate species. In contrast to the comparative study here, however, extant species were often represented by only a single sex and an alternative size proxy was used (i.e., the cranial surface area of the first lumbar vertebrae). Furthermore, though several indices of size and shape were compared among taxa (e.g., C1 anterior tubercle height/ anterior arch length), many of the vertebral variables considered in this study (e.g. pedicle cross-sectional area and transverse process angle) were not investigated. The inclusion of the *Nacholapithecus* specimens into this study not only provides an opportunity to further investigate *Nacholapithecus* cervical vertebral morphology, but also provides the opportunity test the Kikuchi et al (2012) conclusions with an extant sample including both sexes and an increased number of vertebral features. Only those specimens (n=3)

that present the features of interest (including vertebral canal measurements necessary for size adjustment) for this study will be discussed: KNM-BG 40840n, 40793c, and 40840o.

Affinity prediction: Nacholapithecus specimens are expected to group with taxa that are intermediate in positional behavior between suspensory apes and more terrestrial pronograde monkeys (i.e., *Papio*), specifically a taxon that represents an above-branch arboreal quadruped, but that can incorporate orthograde postural behaviors into its repertoire (Nakatsukasa et al., 2003; Senut et al., 2004; Kikuchi et al., 2012). Based on the extant sample here, *N. kerioi* is expected to group with *Nasalis*, because not only it is a relativity large-bodied arboreal quadruped, *Nasalis* also occasionally performs more orthograde postures (Yeager, 1990; Gorzitze, 1996).

KNM-BG 40840n is a partial adult atlas, retaining the majority of the right side, but the tip of the transverse process is broken. The posterior arch continues until just before the left lateral mass and the anterior arch is broken midway, ending at the anterior tubercle. Vertebral canal height is preserved in this specimen and was used to adjust for size. The two features present for comparison are the cross-section of the posterior arch (or lamina) and the angle of the transverse process at the posterior tubercle (Table 5-1). Box-and-whisker plots demonstrate that the KNM-BG 40840n posterior arch cross-sectional area (LCSA) is relatively large compared to the sample and falls within the distribution of hylobatids and *Ateles* (Figure 5-1).

The KNM-BG 40840n transverse process angle at the posterior tubercle (TPPA) is large compared to the sample's distribution and falls within the ranges of those taxa with the largest angles, and thus, the most dorsally oriented transverse processes (i.e., *Alouatta*, *Pongo*, *Nasalis*, and *Gorilla*) (Figure 5-2).

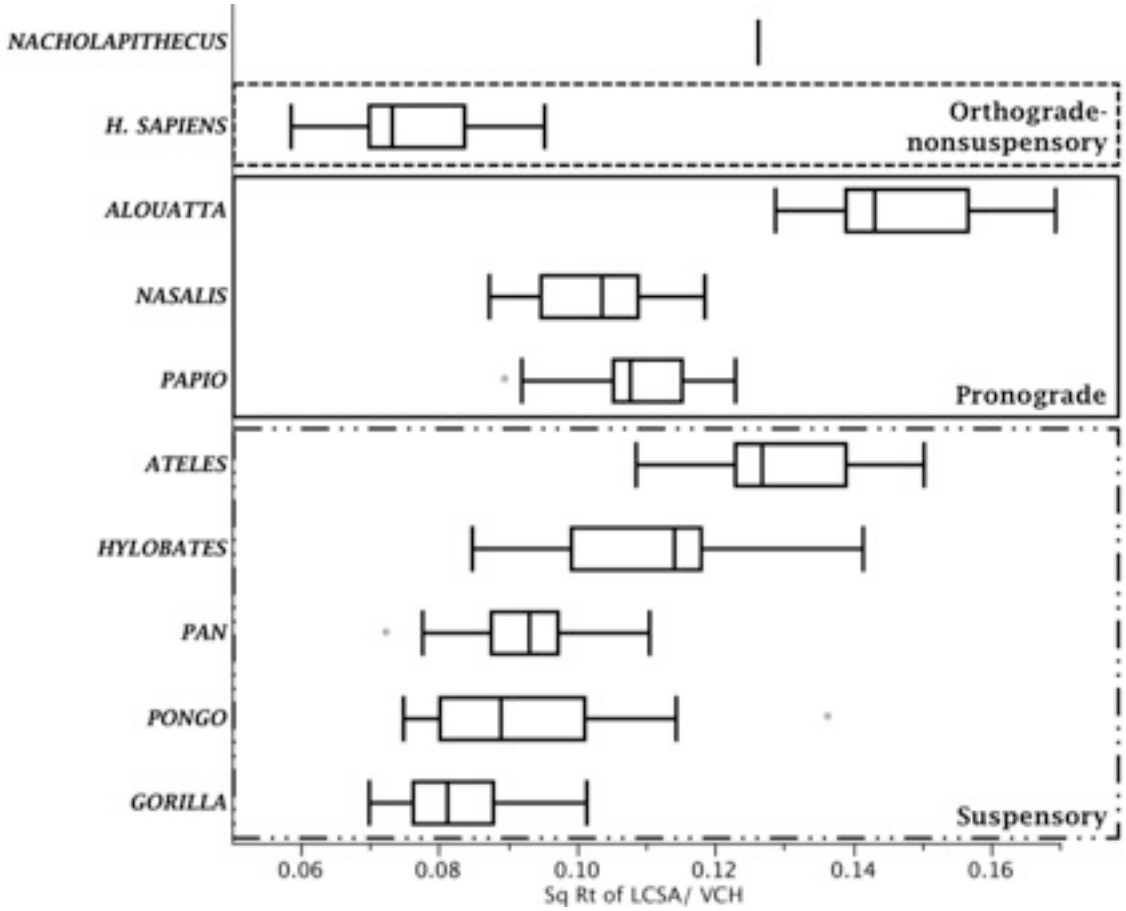

Figure 5-1. Box-and-whisker plots illustrate the distribution of the ratio of the square root of the lamina (posterior arch) cross-sectional area (LCSA) divided by vertebral canal height (VCH) at the first cervical level (C1) for each taxon and positional behavior group. The line within each box represents the median value and the ends of the box represent the 1st and 3rd quartiles. The whiskers extend to the outermost data points within another ±1.5 quartiles.

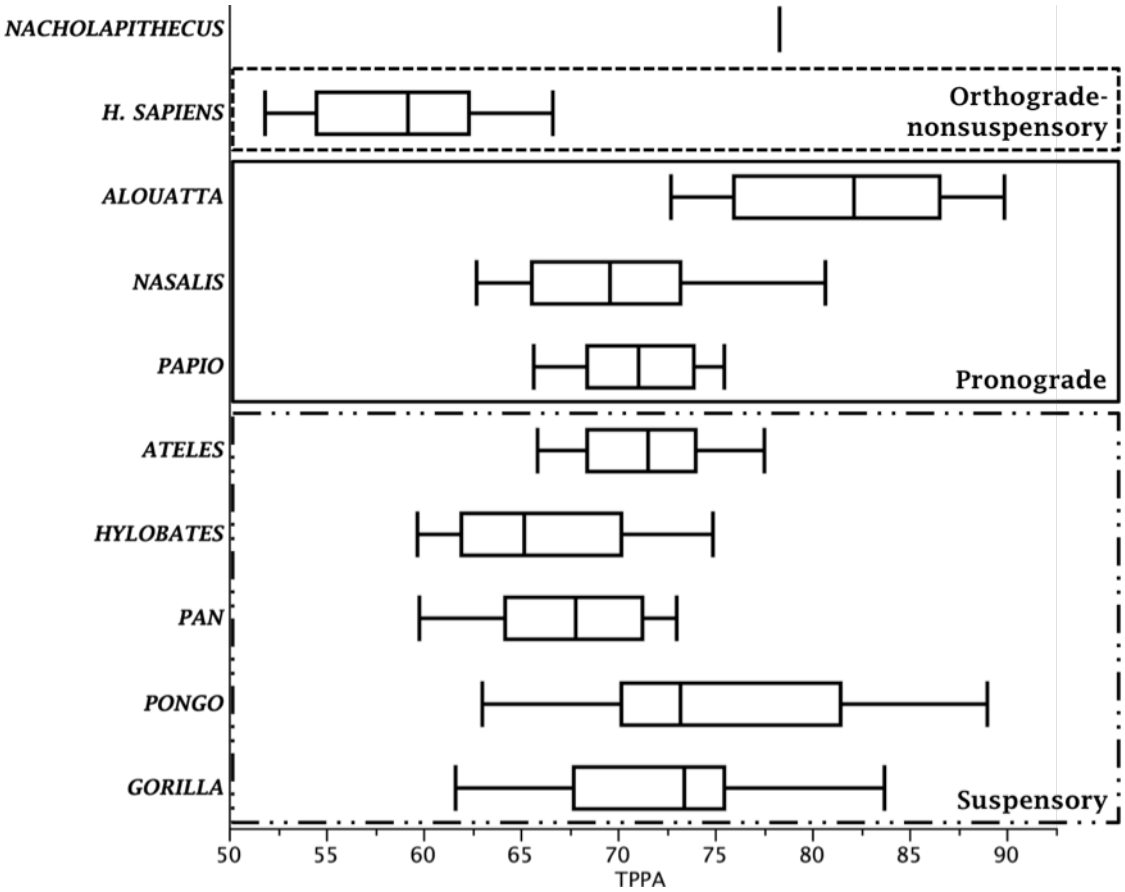

Figure 5-2. Box-and-whisker plots illustrate the distribution of the transverse process angle at the posterior tubercle (TPPA) at the first cervical level (C1) for each taxon and positional behavior group. The line within each box represents the median value and the ends of the box represent the 1st and 3rd quartiles. The whiskers extend to the outermost data points within another ±1.5 quartiles.

KNM-BG 40793c is a midlevel adult vertebra identified as either a C4 or C5 based on the angle of the superior articular facets (Nakatsukasa et al., 2007). The specimen preserves the right side of the centrum, right pedicle, and base of the right transverse process, right lamina, and right articular pillar with both superior and inferior articular facets. Though the specimen appears to display adult morphology (i.e., fused annular rings), it is relatively small and is suggested to be female (Kikuchi et al., 2012). Vertebral canal height (VCH) is preserved in this specimen and was used to adjust for size when appropriate. The natural log of the five preserved features were included in the

DFA: relative ventral vertebral body length (LN (VBVL/VCH)), relative pedicle cross-sectional area (LN ((sqrt of PCSA)/VCH)), relative lamina cross-sectional area (LN (sqrt of LCSA)/VCH)), transverse process angle at the posterior tubercle (LN TPPA) and superior articular facet angle (LN AFA) (Table 5-1). Analyses were performed at C4 and C5 levels separately.

Results of the DFA at the C4 level are presented in Table 5-2, with their corresponding standardized coefficients presented in Table 5-3, and classification results in Table 5-4. Graphical ordination of the first two discriminant function scores (accounting for 95.21% of the variation among the groups) is displayed in Figure 5-3. The DFA resulted with significant Wilk's Lambda for four of the five functions (p<0.05) (Table 5-3). The first two discriminant functions accounted for 86.09% and 9.12% of the between group variation, respectively (Table 5-3). As for KNM-BG 40793c, the fossil hominoid morphologically resembles the hylobatids with a posterior probability of 0.99 and does not group with *Nasalis*, as predicted.

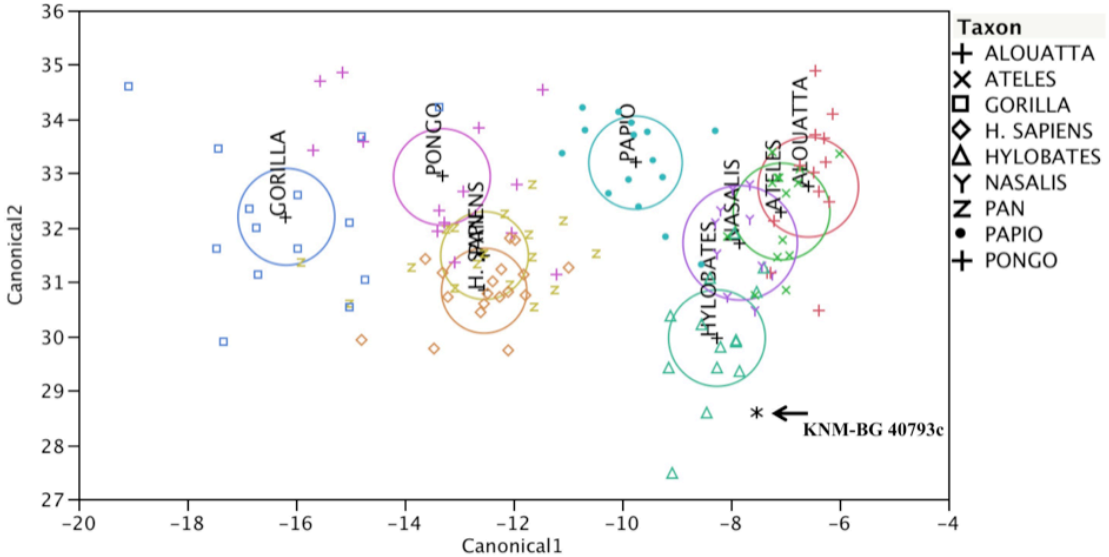

Figure 5-3. Discriminant function plot for the analysis of the extant sample and KNM-BG 40793c at the C4 level. Discriminant scores from function 1 are plotted against those from function 2. Asterisk represents KNM-BG 40793c. Group mean 95% confidence interval contours shown. DFA results are presented in Tables 5-2. The standardized coefficients are shown in Table 5-3.

TABLE 5-2. Results of discriminant function analyses for KNM-BG 40793c at the C4 level

Function	Eigenvalue	% of Variance	Cumulative %	Canonical Correlation	*p*-value
1	10.16	86.09	86.09	0.95	<.0001
2	1.08	9.12	95.21	0.72	<.0001
3	0.36	3.07	98.28	0.52	<.0001
4	0.14	1.22	99.50	0.36	0.01
5	0.06	0.50	100.00	0.24	0.14

TABLE 5-3. Standardized coefficients of discriminant function analyses for KNM-BG 40793c at the C4 level

Function	VBVL	TPPA	AFA	PCSA	LCSA
1	-0.318	0.252	-0.193	-0.144	1.236
2	0.004	0.921	-0.196	-1.611	1.367
3	0.958	-0.522	-0.168	-4.028	3.832
4	-0.412	-0.029	0.698	-4.368	4.456
5	0.543	0.157	0.678	4.306	-4.431

TABLE 5-4. Classification results of discriminant function analyses for KNM-BG 40793c at the C4 level

	Alouatta	*Ateles*	*Gorilla*	*H. sapiens*	Hylobatids	*Nasalis*	*Pan*	*Papio*	*Pongo*
Alouatta	9	1	0	0	2	1	0	0	0
Ateles	3	11	0	0	0	0	0	0	0
Gorilla	0	0	12	0	0	0	0	0	2
H. sapiens	0	0	0	13	0	0	5	0	0
Hylobatids	0	1	0	0	11	2	0	0	0
Nasalis	2	0	0	0	1	7	0	0	0
Pan	0	0	1	7	0	0	8	1	0
Papio	0	0	0	0	1	1	0	13	0
Pongo	0	0	0	1	0	0	6	1	6
# misclassified		39							
% misclassified		30.23							

The standardized coefficients of the predictor variables suggest that the separation along the first function is caused by an increase in relative lamina cross-sectional area (Table 5-3). Hominids have relatively small cross-sectional areas, while hylobatids, the platyrrhines, *Nasalis*, and the *N. kerioi* specimen have relatively large cross-sectional areas (LCSA). The separation along the second function is caused by a few variables, chiefly by a decrease in relative pedicle cross-sectional area (PCSA). The hylobatids and fossil specimen group together with relatively large PCSAs. Overall, 69.8% of the cases were correctly classified, with the majority of the misclassifications being among *Pongo* and *Pan* individuals.

Results of the DFA at the C5 level are presented in Table 5-5, with their corresponding standardized coefficients presented in Table 5-6, and classification results in Table 5-7. A bivariate plot of the first two discriminant function scores (accounting for 81.03% of the variation among the groups) is displayed in Figure 5-4. The DFA resulted with significant Wilk's Lambda for four of the five functions ($p<0.05$) (Table 5-5). The first two discriminant functions accounted for 56.43% and 24.60% of the between group variation, respectively (Table 5-5). The first discriminant function separates *Homo* from the left side of the sample and the platyrrhines from the right side of the sample. The second discriminant function separates *Pongo* and *Gorilla* from the rest of the group (Figure 5-4).

Contrary to the C4 results, the fossil hominoid most closely resembles *Homo*, but with a relatively low posterior probability of 0.456. The standardized coefficients of the predictor variables suggest that the separation along the first function is caused by increases in relative lamina cross-sectional area (LCSA) and decreases in pedicle cross-

sectional area (PCSA). Modern humans and the *N. kerioi* specimen have relatively small LCSAs and large PCSAs, while the remainder of the extant sample has relatively large LCSAs and small PCSAs.

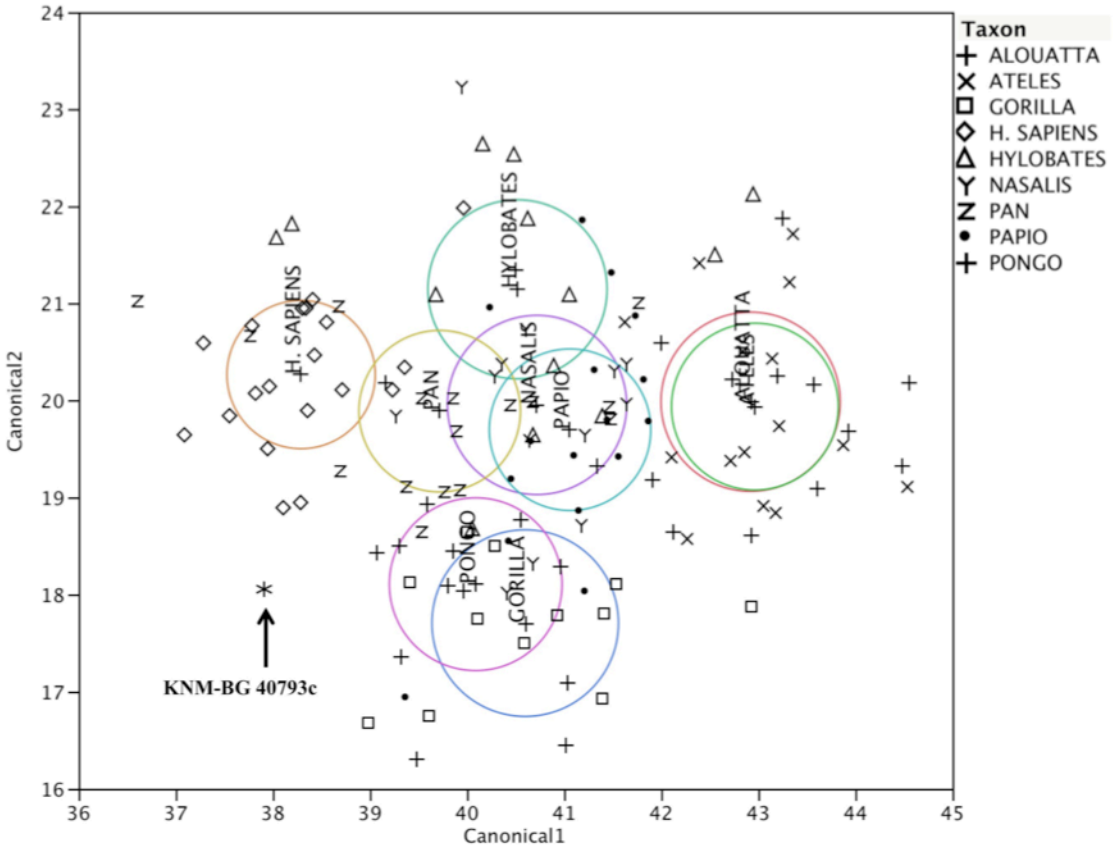

Figure 5-4. Discriminant function plot for the analysis of extant sample and KNM-BG 40793c at the C5 level. Discriminant scores from function 1 are plotted against those from function 2. Functions 3-5 are not shown. Asterisk represents KNM-BG 40793c. Group mean 95% confidence interval contours shown. DFA results are presented in Tables 5-5. The standardized coefficients are shown in Table 5-6. 63.4% of all cases were classified correctly (Table 5-7).

TABLE 5-5. Results of discriminant function analyses for KNM-BG 40793c at the C5 vertebral level

Function	Eigenvalue	% of Variance	Cumulative %	Canonical Correlation	*p*-value
1	2.25	56.43	56.43	0.83	<.0001
2	0.98	24.60	81.03	0.70	<.0001
3	0.53	13.26	94.29	0.59	<.0001
4	0.16	3.93	98.22	0.37	0.00
5	0.07	1.78	100.00	0.26	0.08

TABLE 5-6. Standardized coefficients of discriminant function analyses for KNM-BG 40793c at the C5 vertebral level

Function	VBVL	TPPA	AFA	PCSA	LCSA
1	0.394	0.561	0.177	-0.798	0.733
2	1.061	0.032	0.134	-0.637	-0.721
3	-0.082	-0.782	0.457	-0.475	0.754
4	-0.021	0.174	0.807	0.674	-0.415
5	0.613	-0.420	-0.304	0.426	0.079

TABLE 5-7. Classification results of discriminant function analyses for KNM-BG 40793c at the C5 vertebral level

	Alouatta	*Ateles*	*Gorilla*	*H. sapiens*	Hylobatids	*Nasalis*	*Pan*	*Papio*	*Pongo*
Alouatta	8	2	1	0	1	0	0	1	0
Ateles	2	12	0	0	0	0	0	1	0
Gorilla	0	0	12	0	0	0	0	0	0
H. sapiens	0	0	0	17	1	0	1	0	0
Hylobatids	0	1	0	1	7	1	3	0	0
Nasalis	0	0	0	1	2	8	1	1	0
Pan	0	1	0	1	2	0	11	0	1
Papio	0	0	0	0	2	0	0	12	2
Pongo	0	1	2	0	0	0	2	2	7
# misclassified		48							
% misclassified		36.6							

The separation along the second function is mainly caused by an increase in relative ventral vertebral body length. *Pongo*, *Gorilla*, and the fossil specimen group together with relatively short centra lengths. Overall, 63.4% of the cases were correctly classified, with the majority of the misclassifications being among *Pongo* and hylobatid individuals.

Because results from the two DFAs do not produce similar signals, a third DFA investigating vertebral position was not conducted. The discriminant function results from the C4 and C5 levels more strongly support a C4 position and a hylobatid affinity for the *Nacholapithecus* vertebra. This assessment is based on the higher posterior probability produced by the C4 analysis (hylobatid 0.99). However, this conclusion must be viewed with caution because the posterior probability directly reflects the increased success of the C4 analysis to correctly classify taxa.

KNM-BG 40840o is a lower adult cervical vertebra with a complete vertebral centrum, pedicles, laminae, articular pillars, and partial spinous process. The uncinate processes are more dorsally located on vertebral body, suggesting a lower vertebra (C6-C7). This assessment is supported by superior articular facet orientation (Kikuchi et al., 2012). The vertebral canal is preserved, thus VCA (VCW*VCH) was used to adjust for size in certain features. The logged vertebral features of interest entered into the DFAs include: relative ventral vertebral body length (LN (VBVL/(sqrt of VCA)), relative dorsal vertebral body length (LN (VBDL/(sqrt of VCA)), vertebral body eccentricity (LN VB ECC), uncinate process height (LN UNC), relative pedicle cross-sectional area (LN PCSA/VCA), relative lamina cross-sectional area (LN LCSA/VCA), relative spinous process cross-sectional area (LN SCSA/VCA), superior articular facet angle (LN AFA) (Table 5-1). Analyses were performed at C6 and C7 levels separately.

Results of the DFA at the C6 level is presented in Table 5-8, with their corresponding standardized coefficients presented in Table 5-9, and classification results in Table 5-10. A bivariate plot of the first two discriminant function scores (accounting for 84.70% of the variation among the groups) is displayed in Figure 5-5. The DFA resulted with significant Wilk's Lambda for the first five of eight functions ($p<0.05$) (Table 5-8). The first two discriminant functions accounted for 58.36% and 26.33% of the between group variation, respectively (Table 5-8).

As for the *Nacholapithecus* specimen, the fossil hominoid morphologically resembles *Pan*, hylobatids, and *Pongo* with similar posterior probabilities (0.40, 0.30, 0.28, respectively). This result does not support the prediction of affinity with *Nasalis*. The standardized coefficients of the predictor variables for the discriminant functions suggest that the separation along the first function is caused by differences in relative lamina cross-sectional areas. Modern humans have relatively small cross-sectional areas and the platyrrhines have relatively large cross-sectional areas, while the remainder of the extant sample and the *N. kerioi* specimen fall between the two groups. The separation along the second function is caused by a decrease in relative spinous process cross-sectional area and an increase in pedicle cross-sectional area. *Papio* and *Nasalis* separate from the rest of the group with relatively small SCSAs and large PCSAs. Overall, 72.9% of the cases were correctly classified, with the majority of the misclassifications being among *Pongo* and hylobatid individuals.

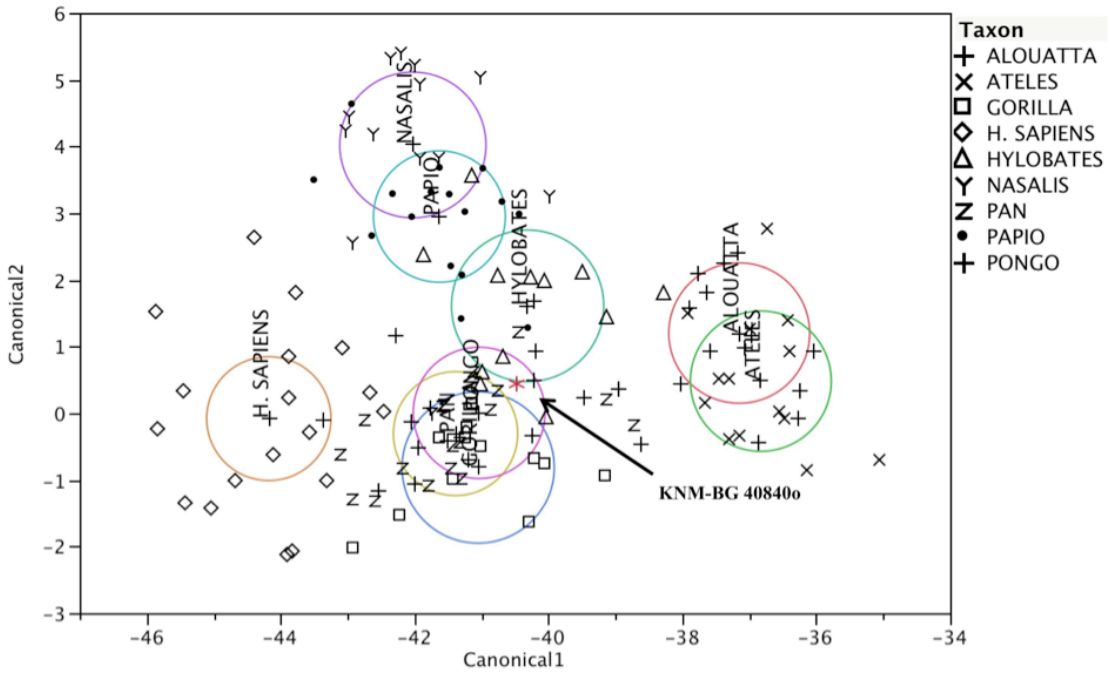

Figure 5-5. Discriminant function plot for the analysis of extant sample and KNM-BG 40840o at the C6 level. Discriminant scores from function 1 are plotted against those from function 2. Functions 3-8 are not shown. Asterisk represents KNM-BG 40840o. Group mean 95% confidence interval contours shown. DFA results are presented in Tables 5-8. The structure coefficients are shown in Table 5-9. 72.9% of all cases were classified correctly (Table 5-10).

TABLE 5-8. Results of discriminant function analyses for KNM-BG 40840o at the C6 level

Function	Eigenvalue	% of Variance	Cumulative %	Canonical Correlation	*p*-value
1	5.27	58.36	58.36	0.92	<.0001
2	2.38	26.33	84.70	0.84	<.0001
3	0.62	6.82	91.52	0.62	<.0001
4	0.38	4.25	95.77	0.53	<.0001
5	0.25	2.79	98.56	0.45	0.00
6	0.08	0.90	99.47	0.27	0.08
7	0.05	0.52	99.99	0.21	0.21
8	0.00	0.01	100.00	0.03	0.71

TABLE 5-9. Standardized coefficients of discriminant function analyses for KNM-BG 40840o at the C6 level

Function	VB ECC	AFA	VBVL	VBDL	UNC	PCSA	LCSA	SCSA
1	-0.295	-0.210	0.247	-0.431	-0.033	0.055	0.902	0.253
2	0.276	0.046	-0.217	0.266	0.059	0.806	0.444	-1.180
3	0.190	0.364	-0.387	-0.623	0.512	0.915	-0.698	0.504
4	0.767	0.185	0.503	-0.226	-0.531	-0.443	0.454	0.021
5	0.160	-0.500	-0.499	-0.621	1.168	-0.182	0.392	0.075
6	0.188	0.305	-1.372	1.283	0.451	-0.155	-0.224	0.319
7	-0.205	0.724	0.297	-0.523	0.469	-0.277	0.485	-0.422
8	0.449	-0.029	0.779	0.247	0.060	0.087	-0.621	0.285

TABLE 5-10. Classification results of discriminant function analyses for KNM-BG 40840o at the C6 level

	Alouatta	*Ateles*	*Gorilla*	*H. sapiens*	Hylobatids	*Nasalis*	*Pan*	*Papio*	*Pongo*
Alouatta	12	2	0	0	0	0	0	0	0
Ateles	0	14	0	0	0	0	0	0	0
Gorilla	0	0	9	0	0	0	1	0	2
H. sapiens	0	0	0	16	0	0	2	0	0
Hylobatids	1	1	0	0	5	2	2	1	0
Nasalis	0	0	0	0	1	9	1	2	0
Pan	0	0	2	0	2	0	12	0	2
Papio	0	0	0	0	2	1	0	13	0
Pongo	0	1	1	2	1	0	4	0	7
# misclassified		36							
% misclassified		27.07							

Results of the DFA at the C7 level is presented in Table 5-11, with their corresponding standardized coefficients presented in Table 5-12, and classification results in Table 5-13. Graphical ordination of the first two discriminant function scores (accounting for 84.62% of the variation among the groups) is displayed in Figure 5-6. The DFA resulted with significant Wilk's Lambda for first six of eight functions ($p<0.05$) (Table 5-11). The first two discriminant functions accounted for 59.53% and 25.09% of the between group variation, respectively (Table 5-11).

The KNM-BG 40840o specimen morphologically resembles both *Pongo* with a posterior probability of 0.42 and *Homo* with a probability of 0.30. This result does not support the predicted affinities to more intermediate taxa such as *Nasalis*. The standardized coefficients of the predictor variables for the discriminant functions suggest that the separation along the first function is caused by a few variables, specifically differences in relative dorsal vertebral body length and relative pedicle and lamina cross-sectional areas. The platyrrhines have relatively large cross-sectional areas and short dorsal vertebral body lengths, while the remainder of the extant sample and the *N. kerioi* specimen demonstrate smaller cross-sectional areas and longer centra lengths. The separation along the second function is caused by an increase in relative uncinate process height and an increase in pedicle cross-sectional area. *Papio* and *Nasalis* separate from the rest of the group with relatively large PCSAs and tall UNCs. Overall, 73.2% of the cases were correctly classified, with the majority of the misclassifications among *Pongo* individuals.

Results from both DFAs indicate that the KNM-BG 40840o vertebra most closely resembles those of *Pongo*, thus a final DFA investigating vertebral position was

conducted. Vertebral metrics from *Pongo* C6 (n=16) and C7 (n=16) were included in the DFA. Results of the DFA are presented in Table 5-14. Graphical ordination of the single discriminant function scores is displayed in Figure 5-7. The DFA resulted with a significant Wilk's Lambda (p<0.05) (Table 5-14). The discriminant function successfully separates the two vertebral levels in *Pongo* (Figure 5-7). The fossil hominoid morphologically resembles a *Pongo* C6. The standardized coefficients of the predictor variables suggest that the separation along the discriminant function is primarily caused by an increase in lamina cross-sectional area (LCSA) and decrease in pedicle cross-sectional area (PCSA) (Table 5-14). The *N. kerioi* specimen has a relatively small LCSA and large PCSA.

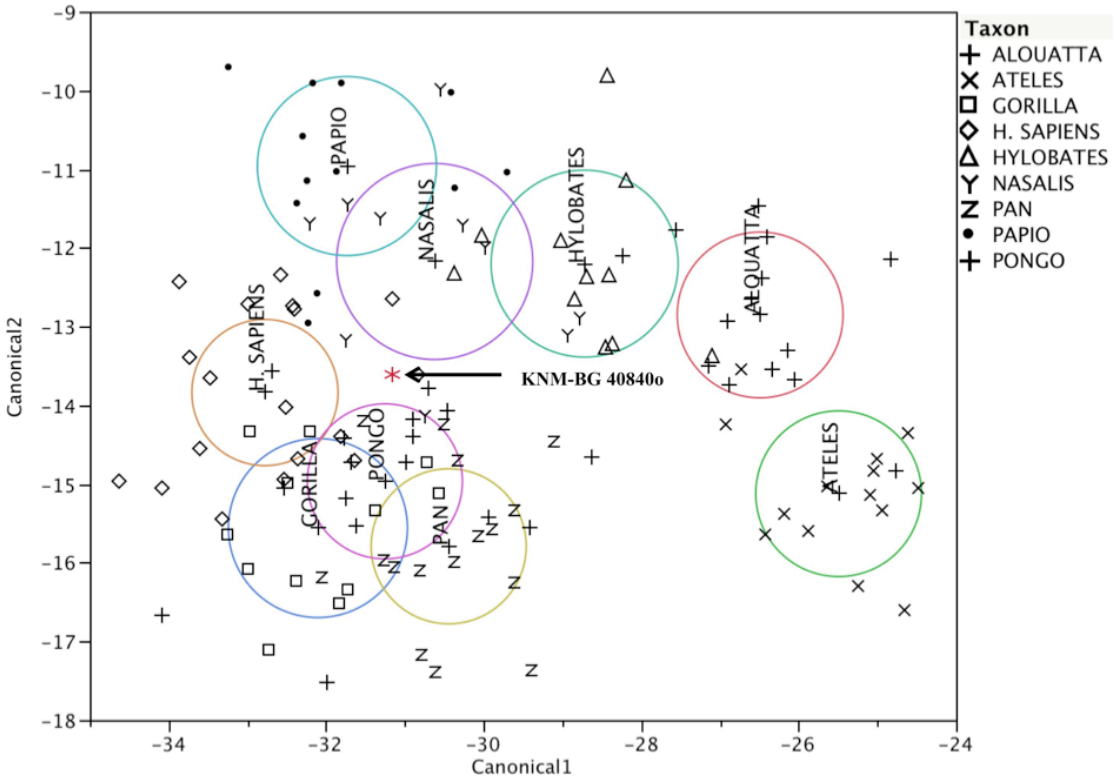

Figure 5-6. Discriminant function plot for the analysis of extant sample and KNM-BG 40840o at the C7 level. Discriminant scores from function 1 are plotted against those from function 2. Functions 3-8 are not shown. Asterisk represents KNM-BG 40840o. Group mean 95% confidence interval contours shown. DFA results are presented in Tables 5-11. The structure coefficients are shown in Table 5-12. 84.6% of all cases were classified correctly (Table 5-12).

TABLE 5-11. Results of discriminant function analyses for KNM-BG 40840o at the C7 vertebral level

Function	Eigenvalue	% of Variance	Cumulative %	Canonical Correlation	*p*-value
1	6.45	59.53	59.53	0.93	<.0001
2	2.72	25.09	84.62	0.86	<.0001
3	0.64	5.94	90.56	0.63	<.0001
4	0.52	4.80	95.36	0.58	<.0001
5	0.27	2.53	97.89	0.46	<.0001
6	0.22	2.00	99.90	0.42	0.01
7	0.01	0.08	99.98	0.09	0.87
8	0.00	0.02	100.00	0.04	0.64

TABLE 5-12. Standardized coefficients of discriminant function analyses for KNM-BG 40840o at the C7 vertebral level

Function	VB ECC	AFA	VBVL	VBDL	UNC	PCSA	LCSA	SCSA
1	-0.427	-0.133	0.009	-0.467	0.131	0.599	0.443	0.213
2	0.457	-0.043	-0.588	-0.444	0.835	1.143	0.041	-0.682
3	0.298	0.775	-0.116	-0.279	0.596	0.079	-0.504	0.694
4	0.448	0.055	-0.366	0.080	-0.524	0.238	-0.489	0.738
5	-0.069	0.456	-1.197	1.467	0.223	0.230	-0.372	-0.030
6	0.429	-0.192	-0.456	0.352	0.415	-0.802	1.131	-0.079
7	0.433	-0.015	1.129	0.204	-0.539	0.146	-0.507	0.084
8	-0.076	-0.508	-0.718	0.284	0.701	0.045	-0.791	0.857

TABLE 5-13. Classification results of discriminant function analyses for KNM-BG 40840o at the C7 vertebral level

	Alouatta	*Ateles*	*Gorilla*	*H. sapiens*	Hylobatids	*Nasalis*	*Pan*	*Papio*	*Pongo*
Alouatta	12	2	0	0	0	0	0	0	0
Ateles	1	13	0	0	0	0	0	0	0
Gorilla	0	0	8	2	0	0	0	0	2
H. sapiens	0	0	0	16	0	1	0	1	0
Hylobatids	2	1	0	0	6	1	0	1	0
Nasalis	0	0	0	0	2	6	0	1	1
Pan	0	0	0	0	0	0	13	0	3
Papio	0	0	0	0	1	0	0	11	0
Pongo	0	0	4	3	0	0	4	0	5
# misclassified		33							
% misclassified		26.83							

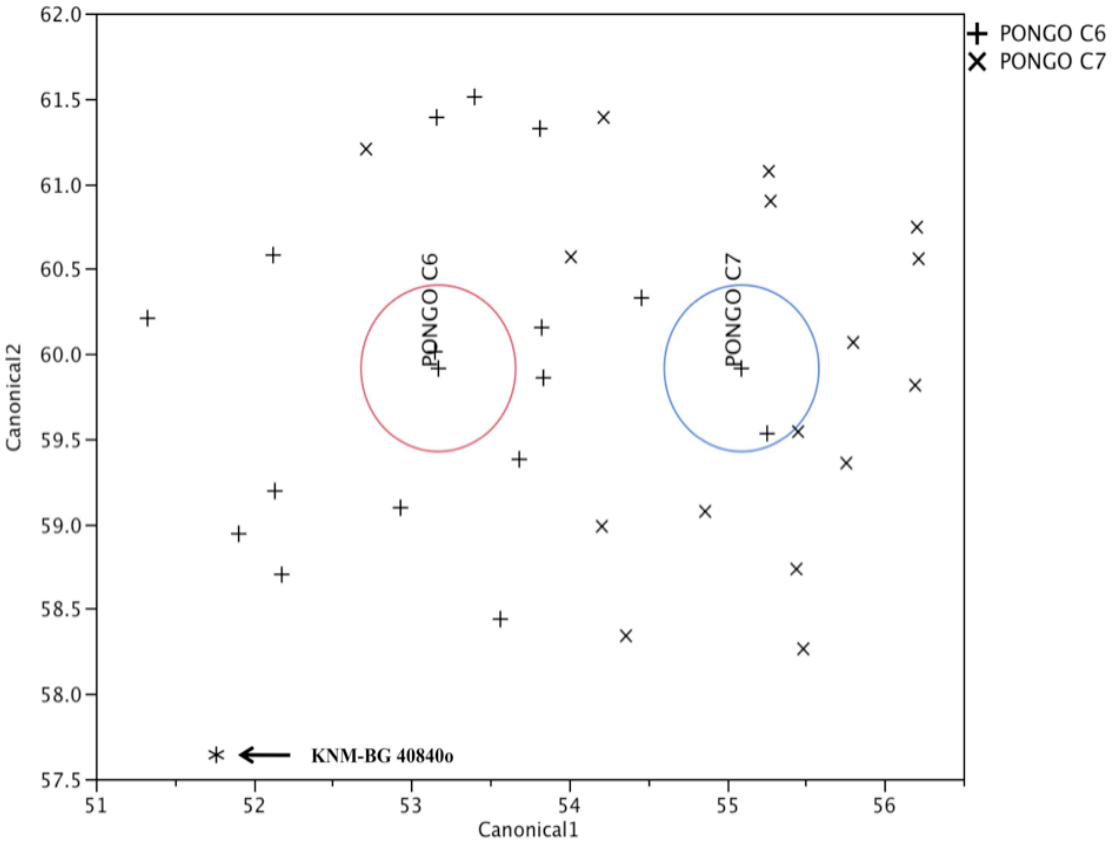

Figure 5-7. Discriminant function plot for the analysis of vertebral position for *Pongo* and KNM-BG 40840o at the C6 and C7 levels. Discriminant scores from function 1. Asterisk represents KNM-BG 40840o. Group mean 95% confidence interval contours shown. DFA results are presented in Tables 5-15.

TABLE 5-14. Results of discriminant function analyses for KNM-BG 40840o at the C6 and C7 vertebral levels

Function	Eigenvalue	% of Variance	Cumulative %	Canonical Correlation	*p*-value
1	0.99	100.00	100.00	0.70	0.02

Function	VBVL*	VBDL	VB ECC	PCSA	LCSA	SCSA	UNC	AFA
1	-0.061	0.598	-0.292	-1.164	1.234	-0.340	-0.480	0.647

# misclassified	4
% misclassified	12.5

*DFA standardized coefficients for each variable

Summary of **Nacholapithecus kerioi** *results*

The univariate analyses of the *N. kerioi* first cervical vertebra did not support the affinity prediction. Though the two features preserved fell within the distributions of taxa that are intermediate in positional behavior to suspensory apes and pronograde monkeys—*Nasalis*—the C1 morphology also overlapped with hylobatids, *Pongo*, *Gorilla*, and *Alouatta* (Figures 5-1, 5-2). The analysis reveals that relative to the extant sample here, the Miocene hominoid demonstrates large pedicle cross-sectional areas and more dorsally oriented transverse processes.

Results from the multivariate analyses indicate that the mid- and lower-level *Nacholapithecus* vertebral elements are both morphologically similar to hominoids, specifically hylobatids and *Pongo*. Neither discriminant function analysis supported the prediction affinity. KNM-BG 40793c reveals relatively large pedicle large cross-sectional areas and short vertebral bodies when compared to the sample. The DFA results more strongly support a C4 position for this specimen. KNM-BG 40840o analyses indicate that the great apes and *N. kerioi* cross-sectional areas fall between the extremes of the relatively large platyrrhines and the relatively small *Homo* values. The positional DFA for KNM-BG 40840o supports a C6 position.

Australopithecus afarensis

The A.L. 333 locality at Hadar, Ethiopia, has yielded three cervical elements included in this study: an atlas (A.L. 333-83), an axis (A.L. 333-101), and a lower cervical vertebra (A.L. 333-106.) The fossils are dated to ~3.2 Ma and have been described as representing the hominin species *A. afarensis* (Lovejoy et al., 1982; Walter 1994). The dense fossil record for this species has produced a relatively complete

reconstruction of one of the earliest obligate bipeds, but little comparative work has been conducted to characterize the *A. afarensis* cervical morphology (Ward, 2002; Kimbel and Delezene, 2011). This study provides an opportunity to aid in that reconstruction by analyzing previously understudied elements of the *A. afarensis* skeleton.

Previous work on the *A. afarensis* cervicals has suggested both ape- and humanlike affinities. The superior articular facet of the *A. afarensis* atlas vertebra (A.L. 333-83) has been described as relatively concave and apelike (Coroner and Latimer, 1991); however, a comparative study of primate atlanto-occipital joint shape found that the Hadar atlas cannot be distinguished from extant hominids, including modern humans, with respect to facet curvature (Nalley, 2008).

The morphology of the A.L. 333-101 vertebral body and superior articular facets has been described as humanlike, specifically the flat, shelflike superior articular facets in relationship to a vertical odontoid process. This has been argued to correspond to compressive forces typical of upright posture and obligate bipedality (Ankel, 1972; Gommery, 2006).

A.L. 333-106 exhibits a long straight spinous process, which is not bifid or inferiorly angled as is typical of human morphology. This vertebral element has also been noted for its relatively small centrum. The combination of these features has lead researchers to suggest a more *Pan*-like morphology (Lovejoy et al., 1982). Others, however, have suggested that the vertebral body is more humanlike, specifically citing a wide centrum compared to its height and a relatively low angle between the vertebral body and superior articular facet. These features are argued to indicate the mechanical requirements of holding the head upright during a bipedal gait (Gommery, 2006).

However, for the majority of these features, the quantification and investigation into the actual degree of similarity to apes or humans remains unexamined.

Affinity prediction: Though debate exists in the literature, the broader consensus suggests that *Australopithecus afarensis* cervical specimens are expected to group with *Pan* (Lovejoy et al., 1982; Coroner and Latimer, 1991).

Four individual cervical specimens represent this fossil species in total, but only those specimens (n=3) that present the features of interest (including vertebral canal measurements necessary for size adjustment) for this study will be discussed: A.L. 333-83, A.L. 333-101, and A.L. 333-106. The neural arch fragment, A.L. 444-9, is too fragmentary to include in analyses here.

A.L. 333-83 is a partial adult first cervical vertebra. The specimen includes the left lateral mass, both superior and inferior articular facets, plus a portion of the posterior arch. Vertebral canal height (VCH) is preserved and is used for size adjustment. The only relevant feature preserved in A.L. 333-83 is the posterior arch cross-sectional area (LCSA). Box-and-whisker plots demonstrate that the size of the A.L. 333-83 posterior arch cross-sectional area (LCSA) is not distinctive and falls within the distribution of most extant taxa sampled (Figure 5-8). The three groups that do not include the Hadar specimen are *Ateles* and *Alouatta*, which represent the largest relative LCSAs of the sample, and *Homo*, which represents the smallest relative LCSA.

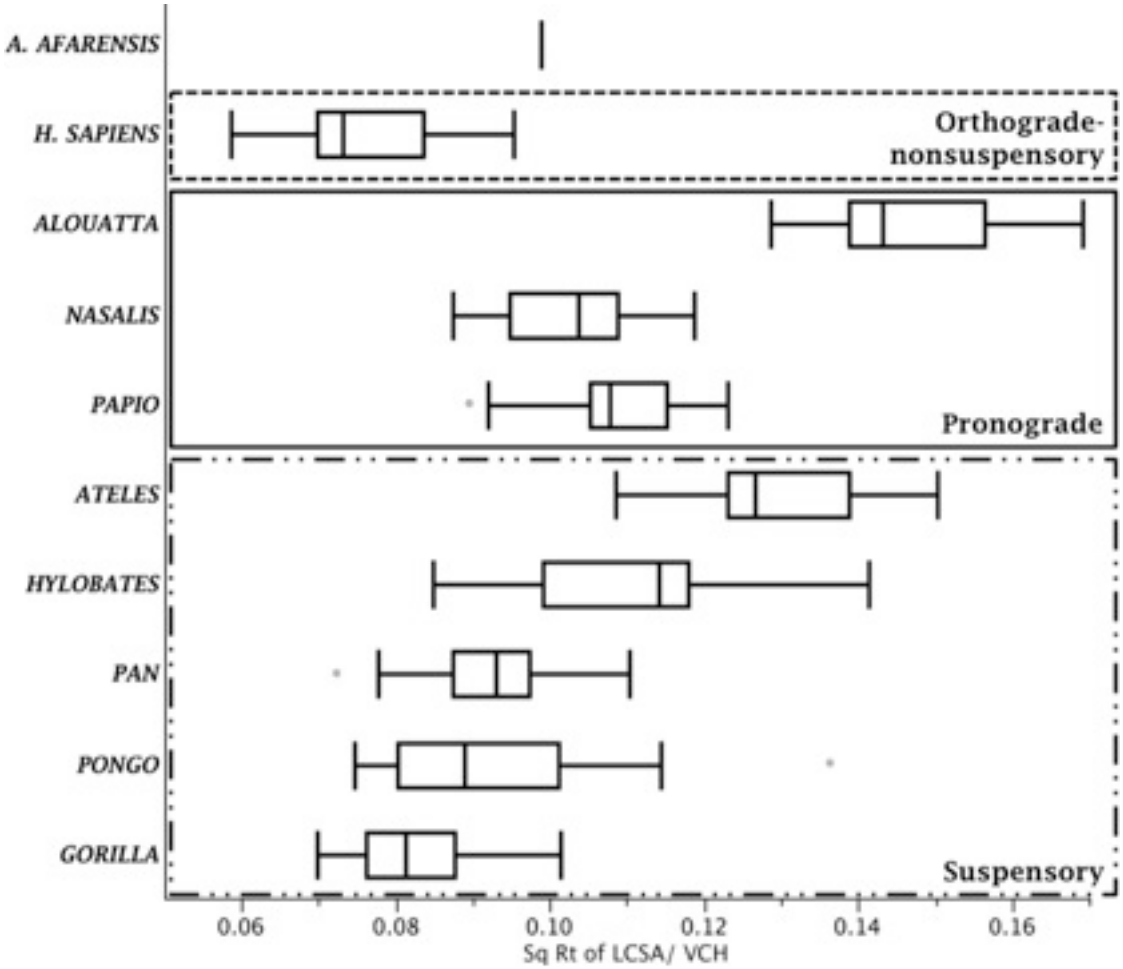

Figure 5-8. Box-and-whisker plots illustrate the distribution of the ratio of the square root of lamina (posterior arch) cross-sectional area (LCSA) divided by vertebral canal length (VCH) at the first cervical level (C1) for each taxon and positional behavior group. The line within each box represents the median value and the ends of the box represent the 1st and 3rd quartiles. The whiskers extend to the outermost data points within another ±1.5 quartiles.

A.L. 333-101 is a complete, but heavily abraded, adult second cervical vertebra. The specimen retains most bony elements, though the caudal body, pedicles, and transverse processes are damaged. The dorsal components are better preserved and include the laminae, spinous process, and postzygapophyses. Both canal height and width are preserved, thus vertebral features are size-adjusted by the vertebral canal area (VCA). Three vertebral metrics were collected and analyzed: spinous process length (SPL),

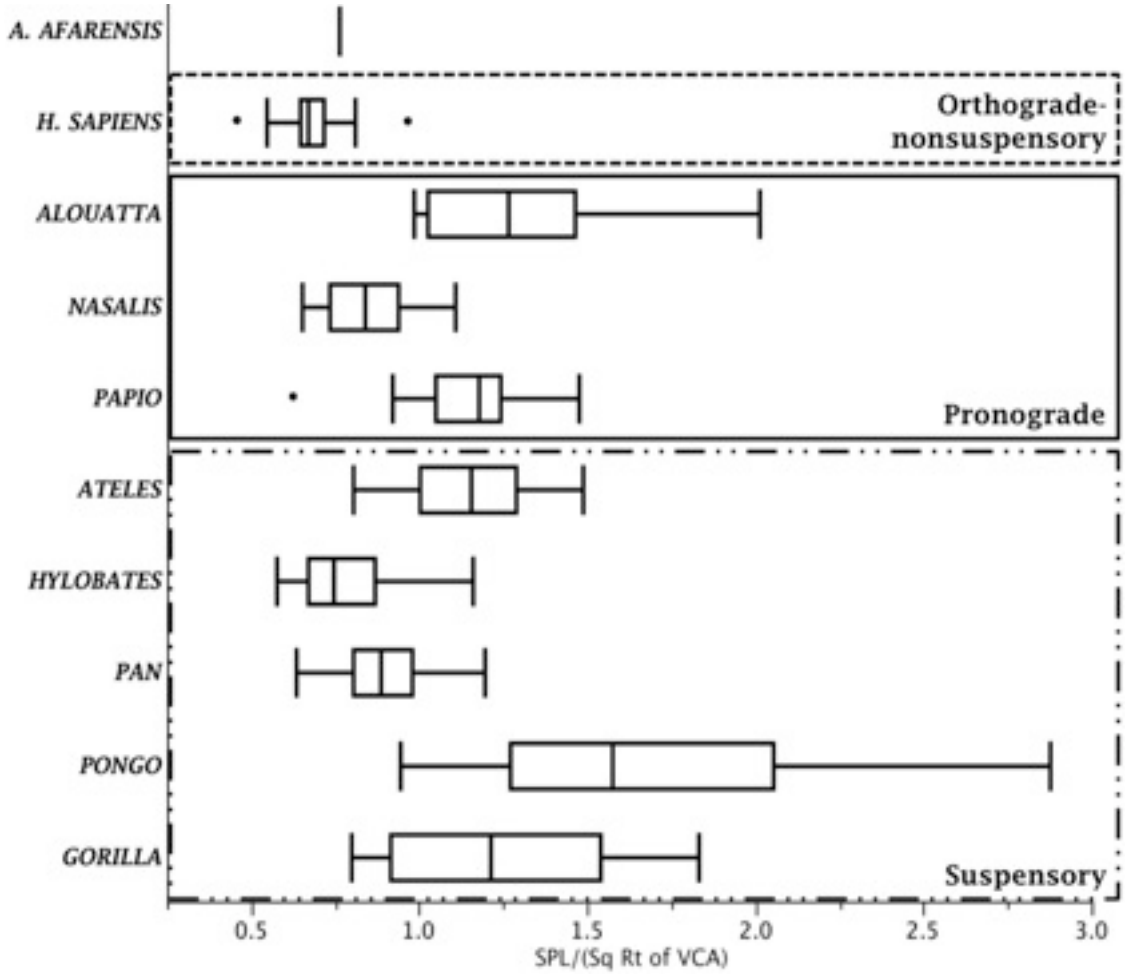

Figure 5-9. Box-and-whisker plots illustrate the distribution of spinous process length (SPL) divided by the square root of vertebral canal area (VCA) at the second cervical level (C2) for each taxon and positional behavior group. The line within each box represents the median value and the ends of the box represent the 1st and 3rd quartiles. The whiskers extend to the outermost data points within another ±1.5 quartiles.

laminar cross-sectional area (LCSA), and spinous process cross-sectional area (SCSA). The box-and-whisker plot of relative spinous process length of A.L. 333-101 illustrates that the Ethiopian specimen resides within the lower half of the sample and overlaps with *Homo*, hylobatids, *Nasalis*, and *Pan* groups (Figure 5-9). These taxa demonstrate relatively shorter spinous processes than the platyrrhines, *Gorilla*, *Papio*, and *Pongo*. The box-and-whisker plot of relative lamina cross-sectional area demonstrates that distributions of all sampled taxa overlap (Figure 5-10 – upper graph). The fossil specimen

is not distinct and falls midrange within the plot, indicating a similar morphology found for all groups, including modern humans. The final comparison investigates relative spinous process cross-sectional area (SCSA). A.L. 333-101 has a relatively large SCSA and groups with the upper half of the sample (Figure 5-10 – lower graph). The fossil specimen falls within the distributions of platyrrhine taxa, *Gorilla*, *Homo*, and *Pongo*.

AL 333-106 is a mostly complete adult lower cervical element (C5-C7) with excellent preservation. Both vertebral canal height and width are preserved; so appropriate features are size-adjusted using vertebral canal area (VCA). All relevant features are present in this specimen, however DFAs of only six features are discussed due to sample size. A general rule of thumb for the ratio of variables to individuals in discriminant function analyses is that the number of variables be fewer than the sample size of the smallest group and that the overall number of cases be about 10 times larger than the number of variables (Diekhoff, 1992). The smallest group sizes for the A.L. 333-106 DFAs are seven hylobatids and seven *Nasalis* at C5 and C7 levels, respectively. A forward stepwise discriminant functional analysis was conducted to determine which features best explain the variation of the sample. The six logged variables included in the C5 DFA are as follows: spinous process length (LN (SPL/(sqrt of VCA))), transverse process at the anterior tubercle (LN (ATPL/(sqrt of VCA))), transverse process at the posterior tubercle (LN (PTPL/(sqrt of VCA))), dorsal vertebral body length (LN (VBDL/(sqrt of VCA))), lamina cross-sectional area (LN (LCSA/VCA)), and spinous process cross-sectional area (LN (SCSA/VCA)).

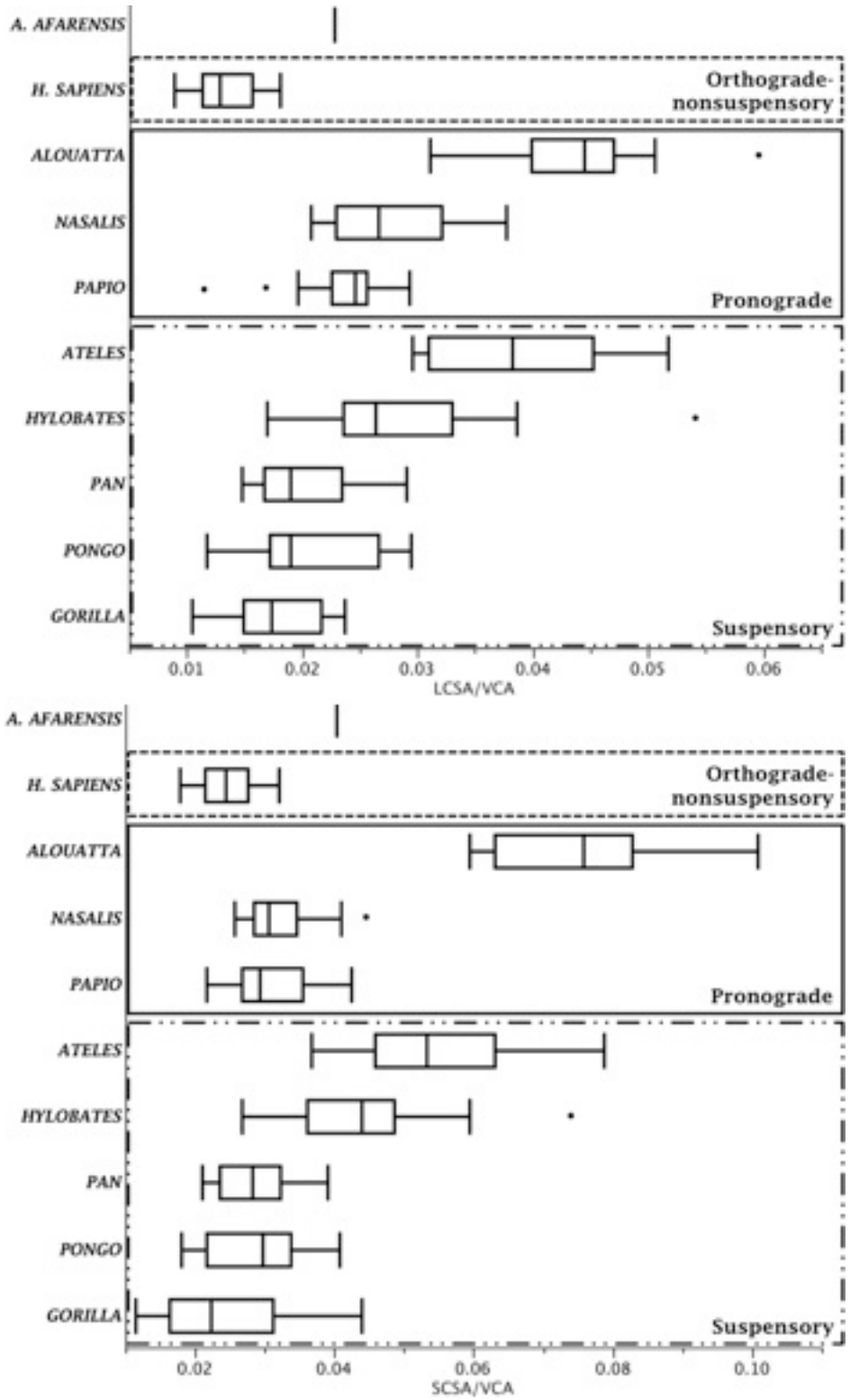

Figure 5-10. Box-and-whisker plots illustrate the distribution of the ratios of spinous process cross-sectional area (SCSA)/vertebral canal area (VCA) in the lower graph and lamina cross-sectional area (LCSA)/VCA in the upper graph, at the C2 level for each taxon and positional behavior group. The line within each box represents the median value and the ends represent the 1st and 3rd quartiles. The whiskers extend to the outermost data points within another ±1.5 quartiles.

Results of the DFA at the C5 level are presented in Table 5-15, with their corresponding standardized coefficients presented in Table 5-16, and classification results in Table 5-17. Graphical ordination of the first two discriminant function scores (accounting for 72.92% of the variation among the groups) is displayed in Figure 5-11. The DFA resulted with significant Wilk's Lambda for all six functions ($p<0.05$) (Table 5-15). The first two discriminant functions accounted for 40.67% and 32.25% of the between group variation, respectively (Table 5-15).

The A.L. 333-106 specimen morphologically resembles *Pan* with a posterior probability of 0.68 and *Pongo* to a lesser degree at 0.32. This result supports the affinity prediction. The standardized coefficients of the predictor variables for the discriminant functions suggest that the separation along the first function is caused by a few variables; the two with the greatest influence are relative lamina cross-sectional area and relative spinous process length (Table 5-16). *Gorilla* and *Pongo* have relatively small cross-sectional areas and long spinous process lengths. In contrast, *Nasalis* demonstrates smaller cross-sectional areas and shorter process lengths, while the remainder of the extant sample, including *A. afarensis*, is intermediate in shape. The separation along the second function is predominately caused by an increase in lamina cross-sectional area (Table 5-16). *Homo* separates from the rest of the group with relatively small cross-sectional areas. Overall, 98.3% of the cases were correctly classified.

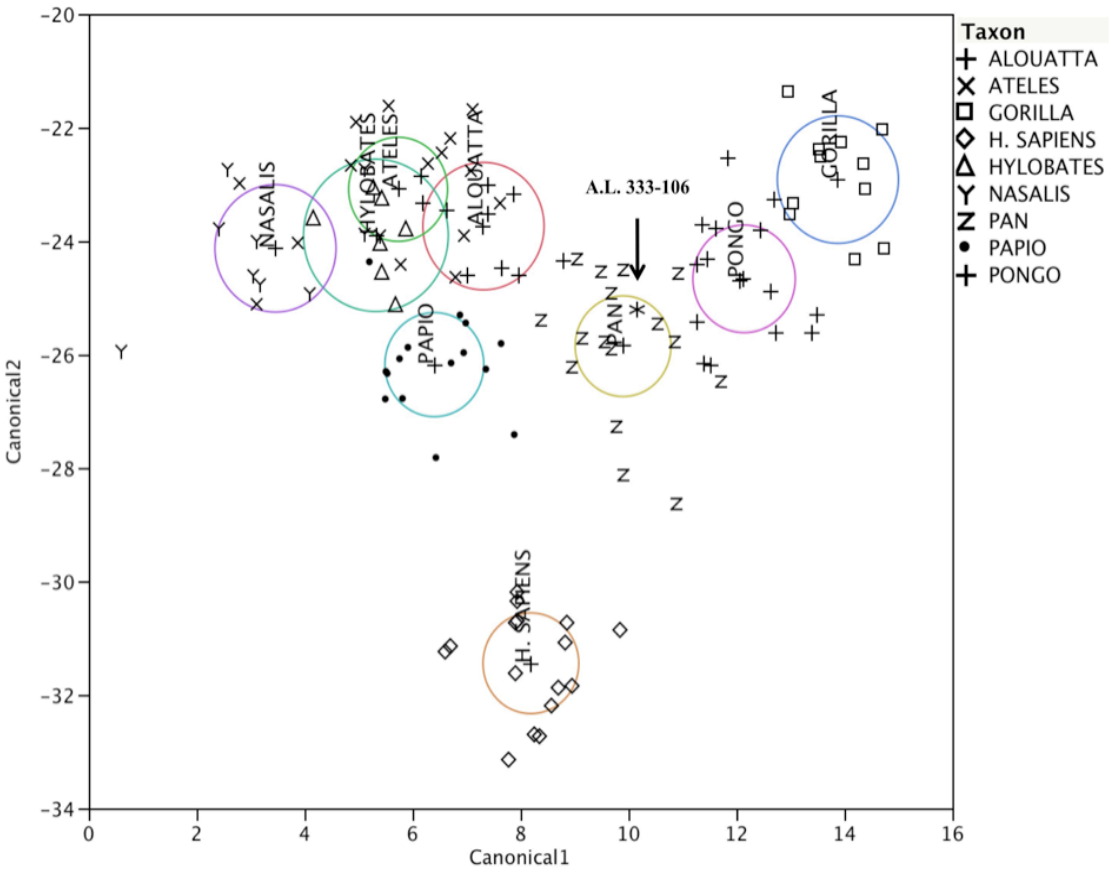

Figure 5-11. Discriminant function plot for the analysis of extant sample and A.L. 33-106 at the C5 level. Discriminant scores from function 1 are plotted against those from function 2. Functions 3-8 are not shown. Asterisk represents A.L. 333-106. Group mean 95% confidence interval contours shown. DFA results are presented in Tables 5-15. The structure coefficients are shown in Table 5-16. 98.3% of all cases were classified correctly (Table 5-17).

TABLE 5-15. Results of discriminant function analyses for A.L. 333-106 at C5 vertebral level

Function	Eigenvalue	% of Variance	Cumulative %	Canonical Correlation	*p*-value
1	9.77	40.67	40.67	0.95	<.0001
2	7.75	32.25	72.92	0.94	<.0001
3	4.18	17.38	90.29	0.90	<.0001
4	1.80	7.48	97.77	0.80	<.0001
5	0.35	1.47	99.25	0.51	<.0001
6	0.18	0.75	100.00	0.39	0.00

TABLE 5-16. Standardized coefficients of discriminant function analyses for A.L. 333-106 at C5 vertebral level

Function	VBDL	LCSA	SCSA	SPL	PTPL	ATPL
1	-0.460	-0.659	0.474	0.979	0.337	-0.244
2	-0.151	1.128	-0.146	0.578	-0.390	-0.315
3	-0.945	0.199	0.252	-0.152	0.719	0.659
4	-0.007	-0.313	0.834	0.061	-1.002	0.612
5	0.141	-0.109	0.730	-0.272	0.737	-0.962
6	1.132	-0.511	0.087	0.023	-0.199	0.308

TABLE 5-17. Classification results of discriminant function analyses for A.L. 333-106 at C5 vertebral level

	Alouatta	*Ateles*	*Gorilla*	*H. sapiens*	Hylobatids	*Nasalis*	*Pan*	*Papio*	*Pongo*
Alouatta	10	0	0	0	0	0	0	0	0
Ateles	0	15	0	0	0	0	0	0	0
Gorilla	0	0	11	0	0	0	0	0	0
H. sapiens	0	0	0	16	0	0	0	0	0
Hylobatids	0	0	0	0	6	1	0	0	0
Nasalis	0	0	0	0	0	10	0	0	0
Pan	0	0	0	0	0	0	16	0	0
Papio	0	0	0	0	0	0	0	15	0
Pongo	0	0	0	0	0	0	1	0	14
# misclassified	2								
% misclassified	1.7								

The six logged variables for the C6 level DFA include: vertebral eccentricity (LN VB ECC), spinous process length (LN (SPL/(sqrt of VCA))), transverse process length at the posterior tubercle (LN (PTPL/(sqrt of VCA))), pedicle cross-sectional area (LN (PCSA/VCA)), lamina cross-sectional area (LN (LCSA/VCA)), and spinous process cross-sectional area (LN (SCSA/VCA)).

Results of the DFA at the C6 level are presented in Table 5-18, with their corresponding standardized coefficients presented in Table 5-19, and classification results in Table 5-20. A bivariate plot of the first two discriminant function scores (accounting for 71.76% of the variation among the groups) is displayed in Figure 5-12. The DFA resulted with significant Wilk's Lambda for all six functions ($p<0.05$) (Table 5-18). The first two discriminant functions accounted for 43.28% and 28.49% of the between group variation, respectively (Table 5-18). The first discriminant function separates the hylobatids, *Nasalis*, and *Papio* from the left side of the sample. The second discriminant function separates *Homo* from the rest of the taxonomic groups (Figure 5-12).

The Hadar specimen morphologically resembles *Pan* with a posterior probability of 0.97. This result supports the predicted affinities to *Pan*. The standardized coefficients of the predictor variables for the discriminant functions suggest that the separation along the first function is caused by an increase in spinous process length and spinous process cross-sectional area (Table 5-19). The nonhuman hominids, including *A. afarensis*, have relatively large cross-sectional areas and spinous process lengths. *Nasalis*, *Papio*, and the hylobatids have relatively short spinous processes and small cross-sectional areas. The remainder of the extant sample falls intermediate to the two groups. The separation along the second function is largely caused by an increase in relative lamina cross-sectional

area (LCSA) (Table 5-19). *Homo* separates from the rest of the group with relatively small LCSAs. Overall, 89.51% of the cases were correctly classified.

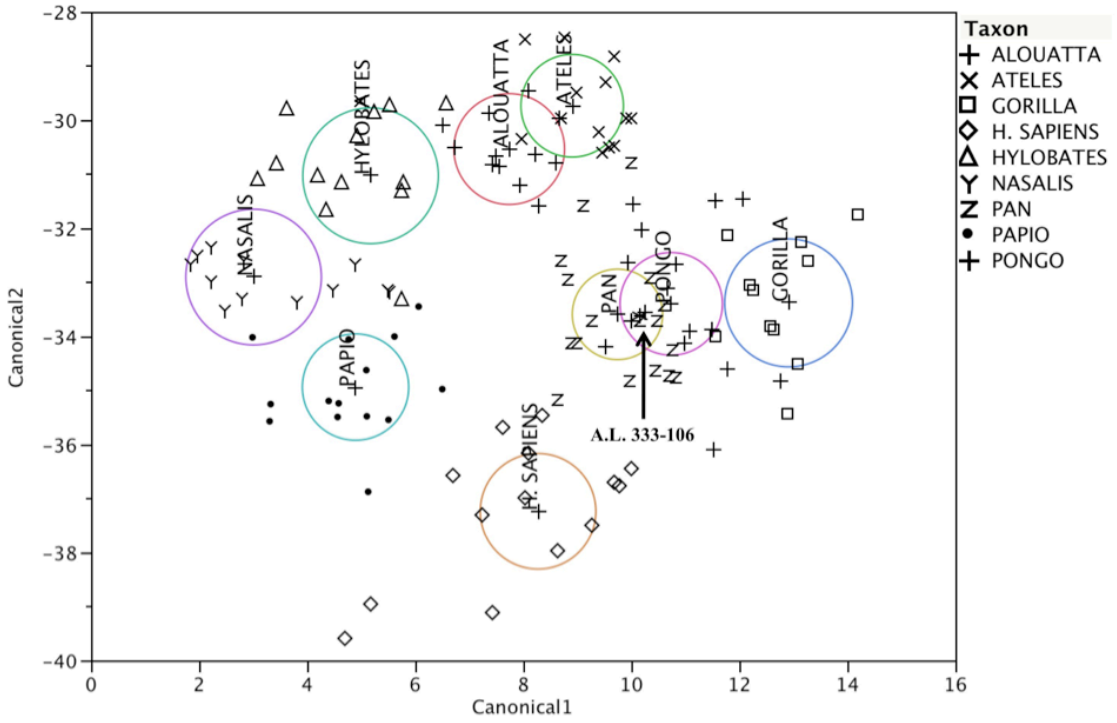

Figure 5-12. Discriminant function plot for the analysis of extant sample and A.L. 333-106 at the C6 level. Discriminant scores from function 1 are plotted against those from function 2. Functions 3-6 are not shown. Asterisk represents A.L. 333-106. Group mean 95% confidence interval contours shown. DFA results are presented in Tables 5-18. The structure coefficients are shown in Table 5-19. 89.5% of all cases were classified correctly (Table 5-20).

TABLE 5-18. Results of discriminant function analyses for A.L. 333-106 at the C6 vertebral level

Function	Eigenvalue	% of Variance	Cumulative %	Canonical Correlation	*p*-value
1	7.89	43.28	43.28	0.94	<.0001
2	5.19	28.49	71.76	0.92	<.0001
3	2.91	15.93	87.69	0.86	<.0001
4	1.53	8.39	96.08	0.78	<.0001
5	0.42	2.28	98.36	0.54	<.0001
6	0.30	1.64	100.00	0.48	<.0001

TABLE 5-19. Standardized coefficients of discriminant function analyses for A.L. 333-106 at the C6 vertebral level

Function	VB ECC	SPL	PTPL	PCSA	LCSA	SCSA
1	-0.242	0.802	-0.018	-0.641	-0.520	0.856
2	-0.150	0.081	-0.569	0.323	0.832	0.112
3	-0.014	-0.255	1.136	-0.400	0.143	0.110
4	0.423	0.722	-0.119	0.401	0.638	-1.241
5	0.896	-0.044	0.010	0.139	-0.417	0.582
6	0.069	-0.143	-0.074	-1.140	1.029	-0.115
7	-0.242	0.802	-0.018	-0.641	-0.520	0.856
8	-0.150	0.081	-0.569	0.323	0.832	0.112

TABLE 5-20. Classification results of discriminant function analyses for A.L. 333-106 at the C6 vertebral level

	Alouatta	*Ateles*	*Gorilla*	*H. sapiens*	Hylobatids	*Nasalis*	*Pan*	*Papio*	*Pongo*
Alouatta	12	0	0	0	0	0	0	0	0
Ateles	1	13	0	0	0	0	0	0	0
Gorilla	0	0	11	0	0	0	0	0	0
H. sapiens	0	0	0	14	0	0	0	0	0
Hylobatids	0	1	0	0	12	0	0	0	0
Nasalis	0	0	0	0	2	10	0	0	0
Pan	0	1	0	0	0	0	16	0	1
Papio	0	0	0	0	0	0	0	14	0
Pongo	0	0	2	0	0	0	5	0	9
# misclassified		13							
% misclassified		10.48							

The six logged variables for the C7 level DFA include: vertebral eccentricity (LN VB ECC), spinous process length (LN (SPL/(sqrt of VCA))), transverse process length at the posterior tubercle (LN (PTPL/(sqrt of VCA))), transverse process angle at the posterior tubercle (LN TPPA), pedicle cross-sectional area (LN (PCSA/VCA)), and spinous process cross-sectional area (LN (SCSA/VCA)).

Results of the DFA at the C7 level is presented in Table 5-21, with their corresponding standardized coefficients presented in Table 5-22, and classification results in Table 5-23. Graphical ordination of the first two discriminant function scores (accounting for 83.43% of the variation among the groups) is displayed in Figure 5-13. The DFA resulted with significant Wilk's Lambda for all six functions ($p<0.05$) (Table 5-21). The first two discriminant functions accounted for 43.25% and 40.19% of the between group variation, respectively (Table 5-21).

As for A.L. 333-106, the Ethiopian vertebra morphologically resembles *Nasalis*, with a posterior probability of 0.998. This result does not support the predicted affinities to *Pan*. The standardized coefficients of the predictor variables for the discriminant functions suggest that the separation along the first function is caused primarily by an increase in relative spinous process length (Table 5-22). *Pongo* and *Gorilla* have the longest relative spinous process lengths, while *Papio* have the shortest spinous process lengths. The remainder of the extant sample, including the *A. afarensis* specimen, demonstrates an intermediate morphology. The separation along the second function is caused by an increase in relative spinous process cross-sectional area (SCSA) (Table 5-22). The hylobatids and the platyrrhines separate from the rest of the group with relatively small SCSAs. Overall, 90% of the cases were correctly classified.

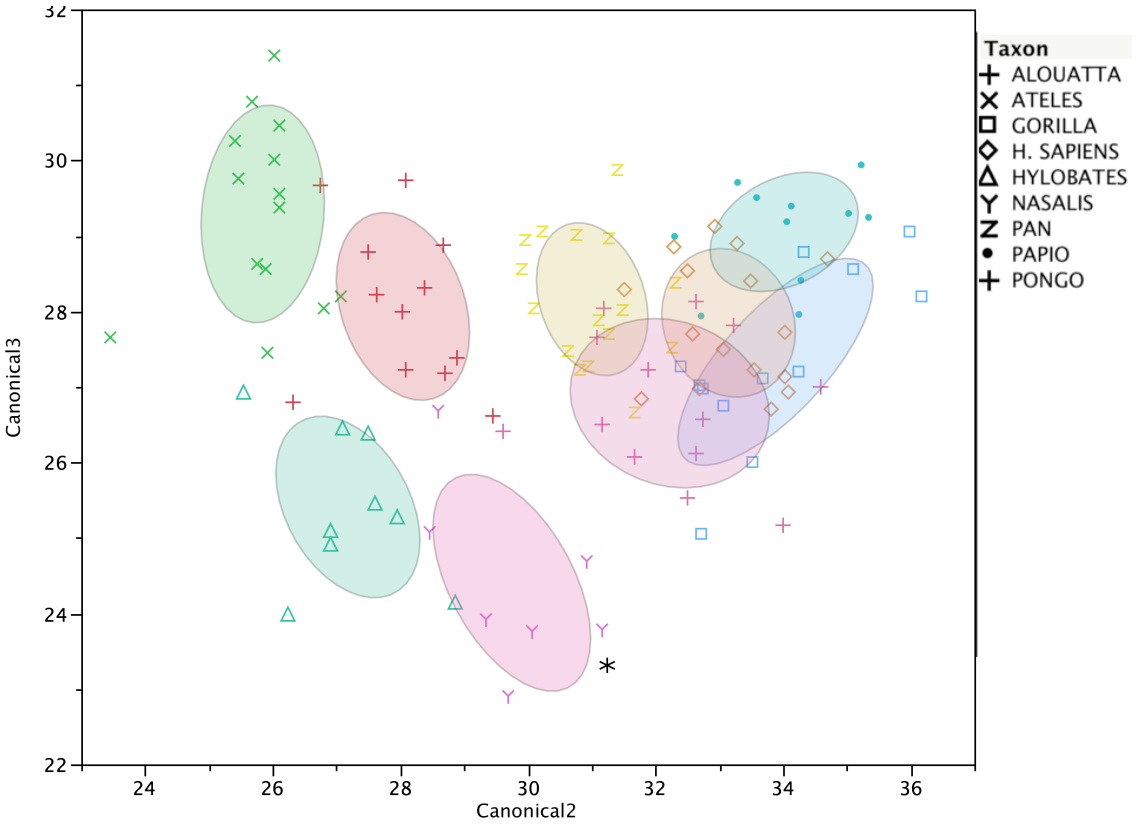

Figure 5-13. Discriminant function plot for the analysis of the extant sample and A.L. 333-106 at the C7 level. Discriminant scores from function 2 are plotted against those from function 3. Functions 1, 4-6 are not shown. Asterisk represents A.L. 333-106. Group 50% coverage ellipse contours shown. DFA results are presented in Tables 5-21. The structure coefficients are shown in Table 5-22. 90% of all cases were classified correctly (Table 5-23).

TABLE 5-21. Results of discriminant function analyses for A.L. 333-106 at the C7 vertebral level

Function	Eigenvalue	% of Variance	Cumulative %	Canonical Correlation	*p*-value
1	9.47	43.25	43.25	0.95	<.0001
2	8.80	40.19	83.43	0.95	<.0001
3	1.88	8.59	92.02	0.81	<.0001
4	1.19	5.45	97.48	0.74	<.0001
5	0.36	1.64	99.12	0.51	<.0001
6	0.19	0.88	100.00	0.40	0.00

TABLE 5-22. Standardized coefficients of discriminant function analyses for A.L. 333-106 at the C7 vertebral level

Function	VB ECC	TPPA	PTPL	SPL	PCSA	SCSA
1	-0.255	0.486	-0.707	0.957	-0.410	0.480
2	0.315	-0.014	0.446	0.468	-0.542	-0.817
3	-0.621	0.075	1.022	-0.065	-0.020	-0.422
4	0.201	-0.494	-0.048	0.666	0.768	-0.616
5	0.083	0.752	-0.259	0.052	0.956	-0.795
6	0.646	0.167	0.499	-0.139	-0.360	0.592

TABLE 5-23. Classification results of discriminant function analyses for A.L. 333-106 at the C7 vertebral level

	Alouatta	*Ateles*	*Gorilla*	*H. sapiens*	Hylobatids	*Nasalis*	*Pan*	*Papio*	*Pongo*
Alouatta	12	0	0	0	0	0	0	0	0
Ateles	2	12	0	0	0	0	0	0	0
Gorilla	0	0	9	0	0	0	0	0	3
H. sapiens	0	0	0	16	0	0	0	0	0
Hylobatids	0	0	0	0	9	0	0	0	0
Nasalis	0	0	0	0	0	7	0	0	0
Pan	0	0	0	1	0	0	15	0	0
Papio	0	0	0	0	0	0	0	11	0
Pongo	0	0	3	0	0	0	2	0	8
# misclassified		11							
% misclassified		10							

Results from the three DFAs produce conflicting results. Analyses at C5 and C6 levels support a *Pan*-like morphology, while the C7 analysis suggests a *Nasalis* affinity. This is unexpected because no previous descriptions have linked *A. afarensis* morphology with this particular arboreal monkey and furthermore, *Nasalis* specimens are not misclassified for *Pan* individuals or vice versa. These results, along with the presence of an anterior tubercle on the transverse process, which is rare for any primate C7 vertebrae, suggest the A.L. 333-106 is not a C7. Therefore the affinity DFA will only include C5 and C6 individuals from *Pan*. To remain comparable to the previous analyses, a forward stepwise DFA was again used to determine those variables that best explained the variation in the data. The following six vertebral metrics from *Pan* C5 (n=17) and C6 (n=18) were included in the DFA: vertebral eccentricity (LN VB ECC), relative ventral vertebral body length (LN (VBVL/(sqrt of VCA)), and relative dorsal vertebral body length (LN (VBDL/(sqrt of VCA)) pedicle cross-sectional area (LN (PCSA/VCA)), and spinous process cross-sectional area (LN (SCSA/VCA)), and transverse process length at the posterior tubercle (LN (PTPL/(sqrt of VCA))). Results of the DFA are presented in Table 5-24. A bivariate plot of the single discriminant function scores is displayed in Figure 5-14. The DFA resulted with a significant Wilk's Lambda ($p<0.05$) (Table 5-24). The discriminant function successfully separates the two vertebral levels in *Pan* (Figure 5-14). The fossil hominin morphologically resembles *Pan* C6. The standardized coefficients of the predictor variables suggest that the separation along the discriminant function is chiefly caused by a decrease in vertebral body eccentricity, or the ratio of vertebral height divided by vertebral width (Table 5-24). Upper cervical vertebrae have relatively tall cervical centra compared to their mediolateral width. As the cervical

transition to from the C2 to the C7, that relationship transitions and the vertebral width increases relative to the height of the centrum (Mercer and Bogduk, 2001; Ankel-Simons, 2007). The A.L. 333-106 specimen has a dorsoventrally short vertebral centrum relative to its width and thus suggests a lower vertebral position.

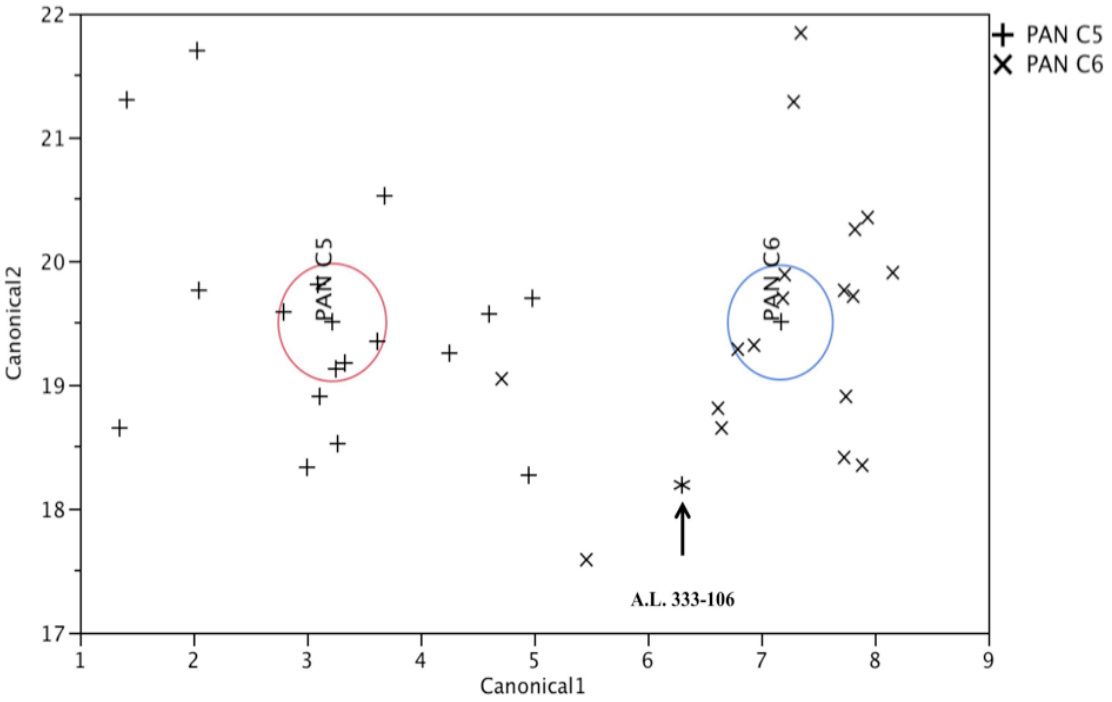

Figure 5-14. Discriminant function plot for the analysis of vertebral position for *Pan* and A.L. 333-106 at the C5 and C6 levels. Discriminant scores from function 1. Asterisk represents A.L. 333-106. Group mean 95% confidence interval contours shown. DFA results are presented in Tables 5-24.

TABLE 5-24. Results of discriminant function analyses for A.L. 333-106 at the C5 and C6 vertebral levels

Function	Eigenvalue	% of Variance	Cumulative %	Canonical Correlation	*p*-value
1	4.12	100.00	100.00	0.90	<.0001

Function	VB ECC	VBVL	VBDL	PCSA	SCSA	PTPL
1	-0.929	-0.445	-0.721	0.591	0.750	0.366

# misclassified	1
% misclassified	2.86

*DFA standardized coefficients for each variable

Summary of **Australopithecus afarensis** *analyses*

The univariate analysis of the A.L. 333 first cervical did not support the affinity prediction. The single preserved feature (lamina cross-sectional area (LCSA)) did fall within the *Pan* distribution, but it also overlapped with most other taxa, except the platyrrhines and modern humans (Figures 5-9). The C2 analyses provided a similar results regarding comparative LCSA morphology. The length of the C2 spinous process was relatively short and fell within both *Homo* and *Pan* distributions, as well as hylobatids and *Nasalis*. The spinous process cross-sectional area is relatively thick and overlapped with the largest taxa in the sample: *Gorilla*, *Homo*, *Pongo*, and the platyrrhines.

Results from the multivariate analyses indicate that the lower-level vertebral element A.L. 333-106 is morphologically most similar to *Pan*. Two of three discriminant function analyses supported the prediction of an affinity with chimpanzees. A.L. 333-106 reveals relatively large spinous process cross-sectional areas and long spinous process lengths when compared to the hylobatids, humans, and other monkeys. The LCSA for the Hadar specimen is not small and *Homo*-like. The positional DFA suggest a likely C6 position due to the decrease in vertebral body height relative to its width.

Australopithecus robustus

SK 854 and SKW 4776 represent some of the oldest hominin vertebral specimens from South Africa. SK 854 is an adult second cervical (axis) vertebra and SKW 4776 is an adult midlevel (C3 or C4) vertebra. Both were recovered at Swartkrans, South Africa, and date to ~1.8-1.5 Ma (Robinson, 1972; Brain, 1993). Robinson (1972) first described the Swartkrans axis and attributed it to *Paranthropus robustus*. SK 854's morphology is

described as more *Pan*-like, exhibiting features such as superior facets set at an angle relative to the odontoid process. This relationship is unlike the shelflike morphology of modern humans (Robinson, 1972; Gommery, 2006). In addition, the SK 854 axis has also been described as relatively robust with a well-developed ventral keel, traits argued to be more primitive (Robinson, 1972). SKW 4776 is described as smaller than the C3 or C4 of modern humans, but larger than *Pan paniscus* (Susman, 1993). SKW 4776 is assigned to *A. robustus*, but is otherwise little described (Susman et al., 2001). These fossils provide an opportunity to compare morphologies between southern and eastern hominin lineages.

Affinity prediction: SK 854 and SKW 4776 have been described as more apelike and are expected to group with *Pan* (Robinson, 1972; Gommery, 2006)

The SK 854 dens is present, but damaged. The centrum, pedicles, laminae, and base of the spinous process are well preserved. The right superior and inferior articular facets, as well as the right transverse process, are also intact. Both vertebral canal height and width are preserved in the SK 854 specimen; therefore relevant features are size-adjusted using vertebral canal area (VCA). An initial DFA analysis of the preserved logged variables included: vertebral eccentricity (LN VB ECC), pedicle cross-sectional area (LN (PCSA/VCA)), lamina cross-sectional area (LN (LCSA/VCA)), and transverse process angle at the posterior tubercle (LN TPPA). However, the variables poorly predicted group affinity with an error of 40.6%. Therefore, the four vertebral features present in this specimen were examined via box-and-whisker plots.

The box-and-whisker plot of vertebral eccentricity for SK 854 illustrates that the South African specimen resides within the distribution of the majority of the sample, the exceptions being *Papio* and *Nasalis* (Figure 5-15). Compared to the catarrhine monkey

species, the rest of the sample, including the fossil hominin, demonstrate relatively wide vertebral bodies compared to their vertebral body height.

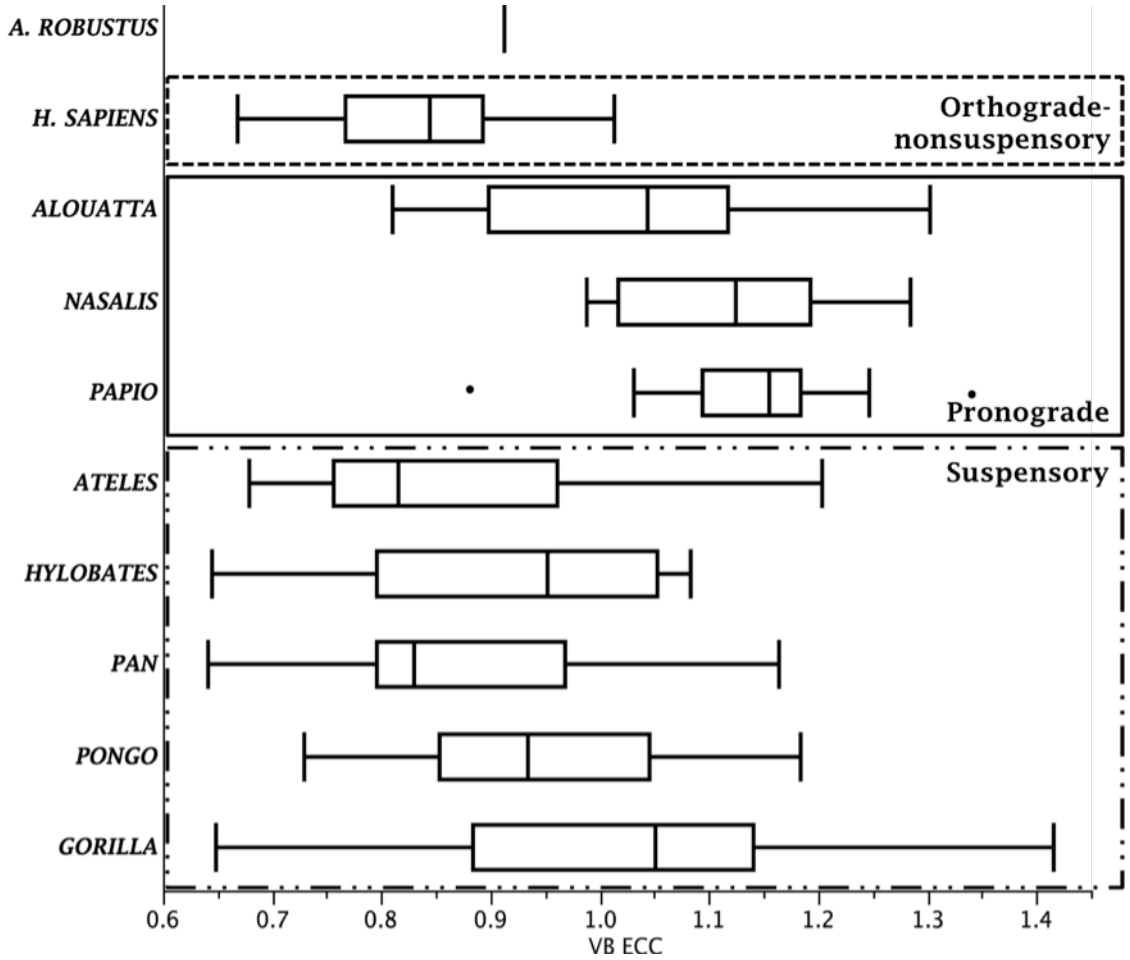

Figure 5-15. Box-and-whisker plots illustrate the distribution of vertebral body eccentricity (VB ECC) at the second cervical level (C2) for each taxon and positional behavior group. The line within each box represents the median value and the ends of the box represent the 1st and 3rd quartiles. The whiskers extend to the outermost data points within another ±1.5 quartiles.

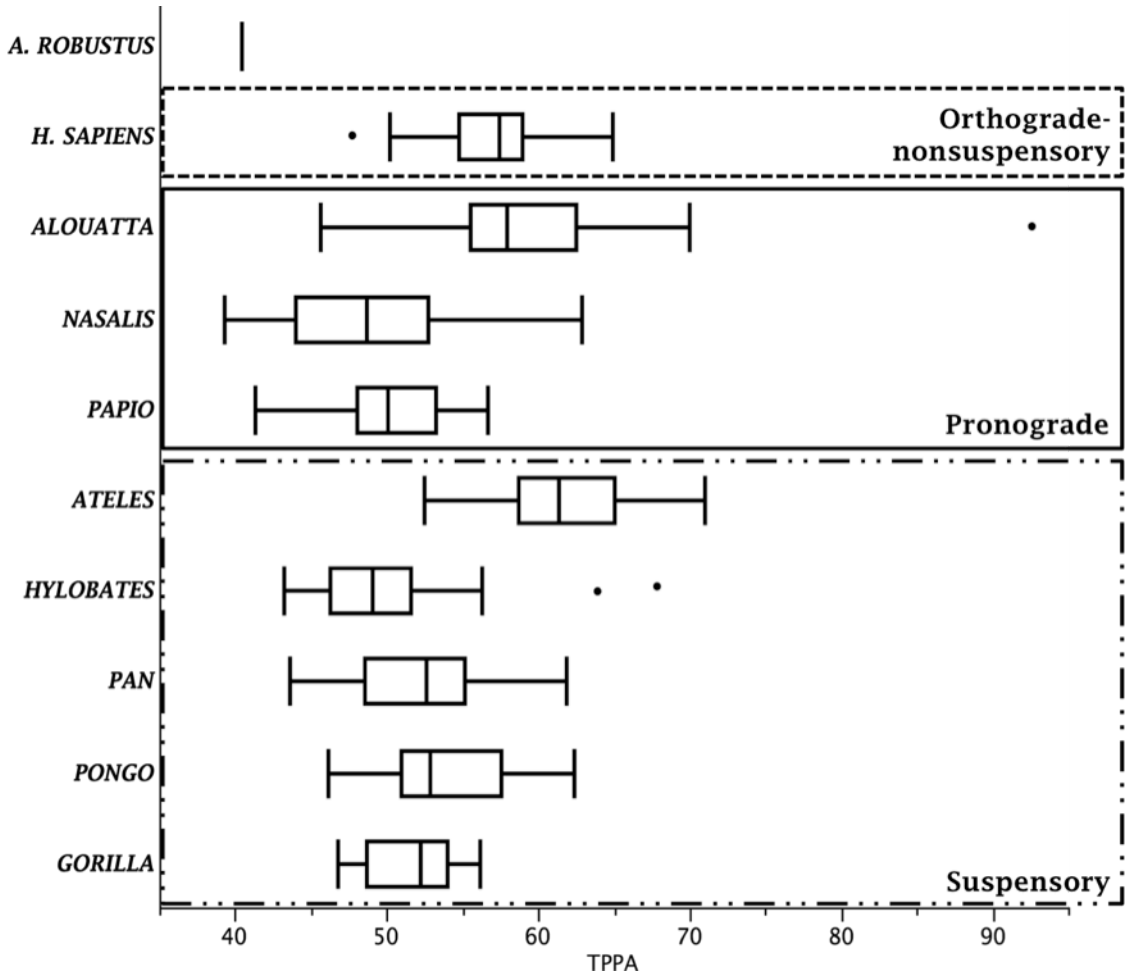

Figure 5-16. Box-and-whisker plots illustrate the distribution of transverse process angle at the posterior tubercle (TPPA) at the second cervical level (C2) for each taxon and positional behavior group. The line within each box represents the median value and the ends of the box represent the 1st and 3rd quartiles. The whiskers extend to the outermost data points within another ±1.5 quartiles.

The box-and-whisker plot of transverse process angle at the posterior tubercle (TPPA) illustrates that SK 854 sits at the very bottom of the distribution and only overlaps with the *Nasalis* group (Figure 5-16). Compared to the rest of extant sample, the fossil hominin demonstrates a relatively small process angle indicating a ventrally oriented transverse process.

The box-and-whisker plots of both the pedicle and lamina cross-sectional areas provide similar morphological signals for SK 854. The Swartkrans fossil resides in the

lower section of the extant distribution and overlaps with several taxa (Figure 5-17). The LCSA plot illustrates SK 854 falling within *Gorilla*, *Pan*, *Papio*, and *Pongo*. The PCSA plot shows that the fossil specimen overlaps with the previous four taxa plus *Nasalis* and hylobatids as well. The platyrrhine groups indicate relatively large cross-sectional areas, while *Homo* demonstrates very small cross-sectional areas. *Australopithecus robustus* falls just outside the modern human distribution in both plots.

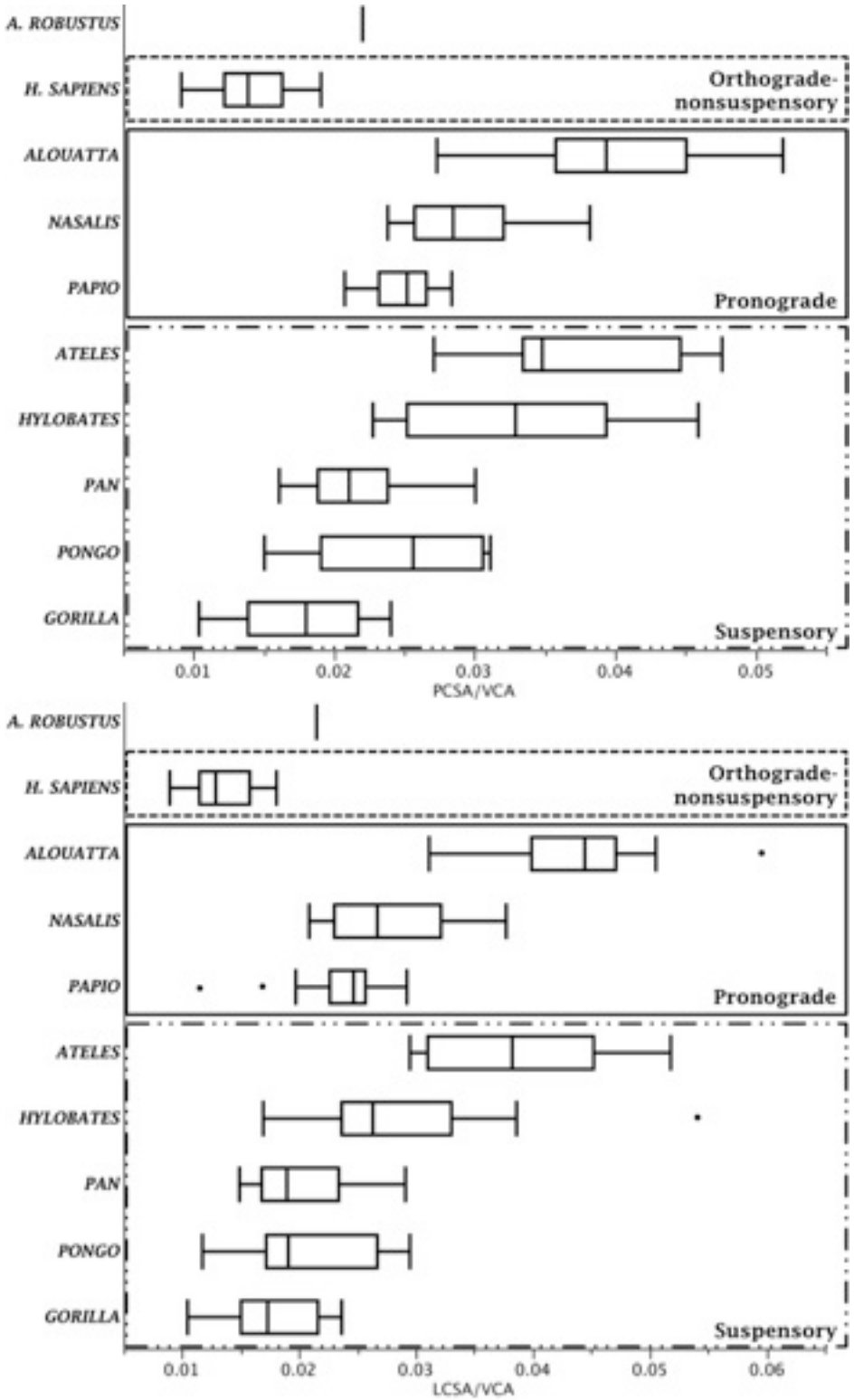

Figure 5-17. Box-and-whisker plots illustrate the distribution of the ratios of laminar cross-sectional area (LCSA)/vertebral canal area (VCA) in lower graph and the pedicle cross-sectional area (PCSA)/VCA in the upper graph, at the C2 level for each taxon and positional behavior group. The line within each box represents the median value and the ends represent the 1st and 3rd quartiles. The whiskers extend to the outermost data points within another ±1.5 quartiles.

SKW 4776 is an adult midlevel cervical vertebra (C3-C5) and preserves most of the body, with a complete left pedicle, articular pillar with both superior and inferior facets, and left lamina. Portions of the left transverse and spinous processes also remain. The vertebral canal width (VCW) is present and is used to size adjust relevant vertebral measures. Only three vertebral variables of interest are preserved: ventral vertebral body length (VBVL), vertebral body eccentricity (VB ECC) and laminar cross-sectional area (LCSA). Due to the unknown position of the vertebral element, comparisons were simultaneously conducted for C3, C4, and C5 levels.

The box-and-whisker plots of VB ECC produce a different morphological signal than what is observed for SK 854. The SKW 4776 fossil resides in the upper section of the extant distribution and overlaps with most taxa at most levels (Figure 5-18). Exceptions are the platyrrhines at all levels, *Homo* at all levels, and the lower levels of *Pan*, *Papio*, and *Pongo.* The LCSA plot illustrates SKW 4776 again falling in the upper half of the distribution and the fossil specimen overlaps with most extant taxa but *Homo* and *Pan* (Figure 5-19). The relative LCSA morphology of *Nasalis* and hylobatids at the C5 are also smaller than SKW 4776. The VBVL plot shows that the fossil specimen overlaps with most of the extant sample, however the modern human distributions are well below the *A. robustus* vertebra (Figure 5-20).

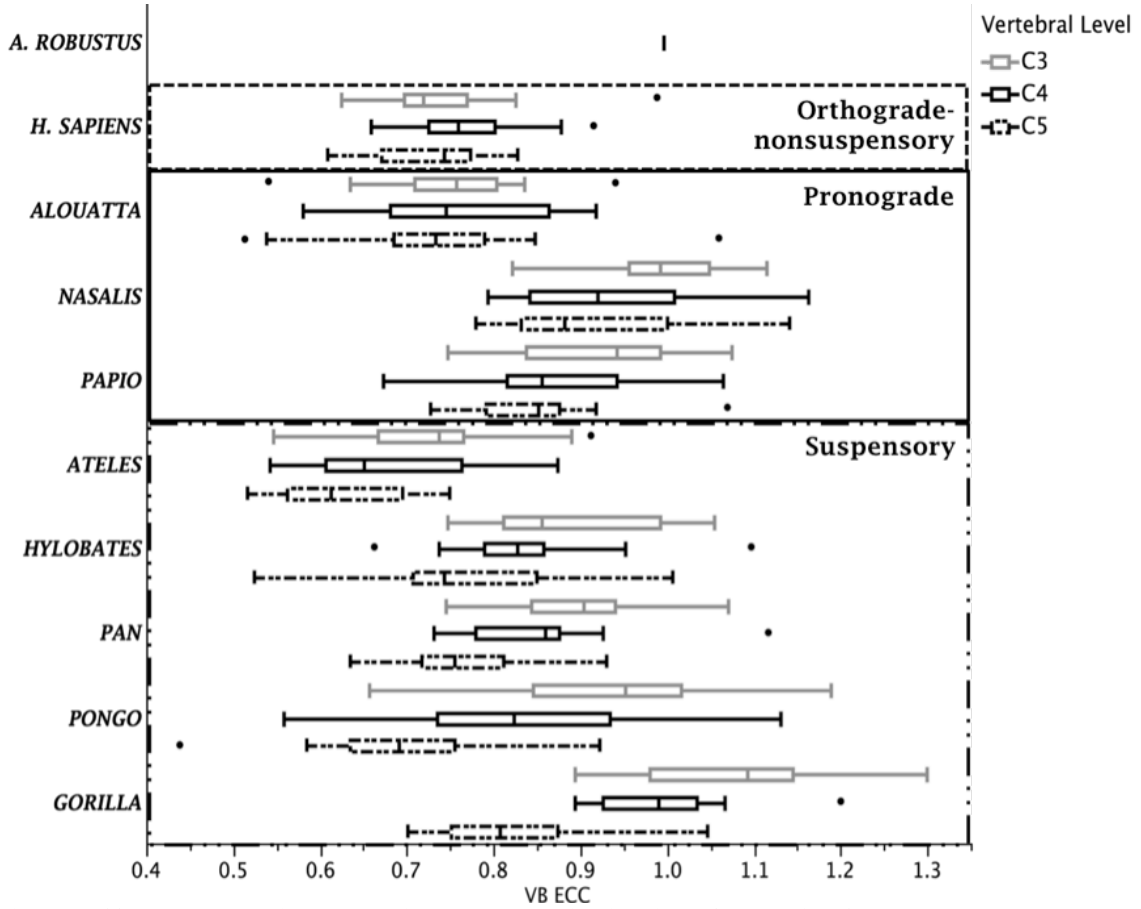

Figure 5-18. Box-and-whisker plots illustrate the distribution of the ratio of the vertebral body eccentricity (VB ECC) at cervical levels C3 (gray), C4 (black), C5 (dotted) for each taxon and postional behavior group. The line within each box represents the median value and the ends of the box represent the 1st and 3rd quartiles. The whiskers extend to the outermost data points within another ±1.5.

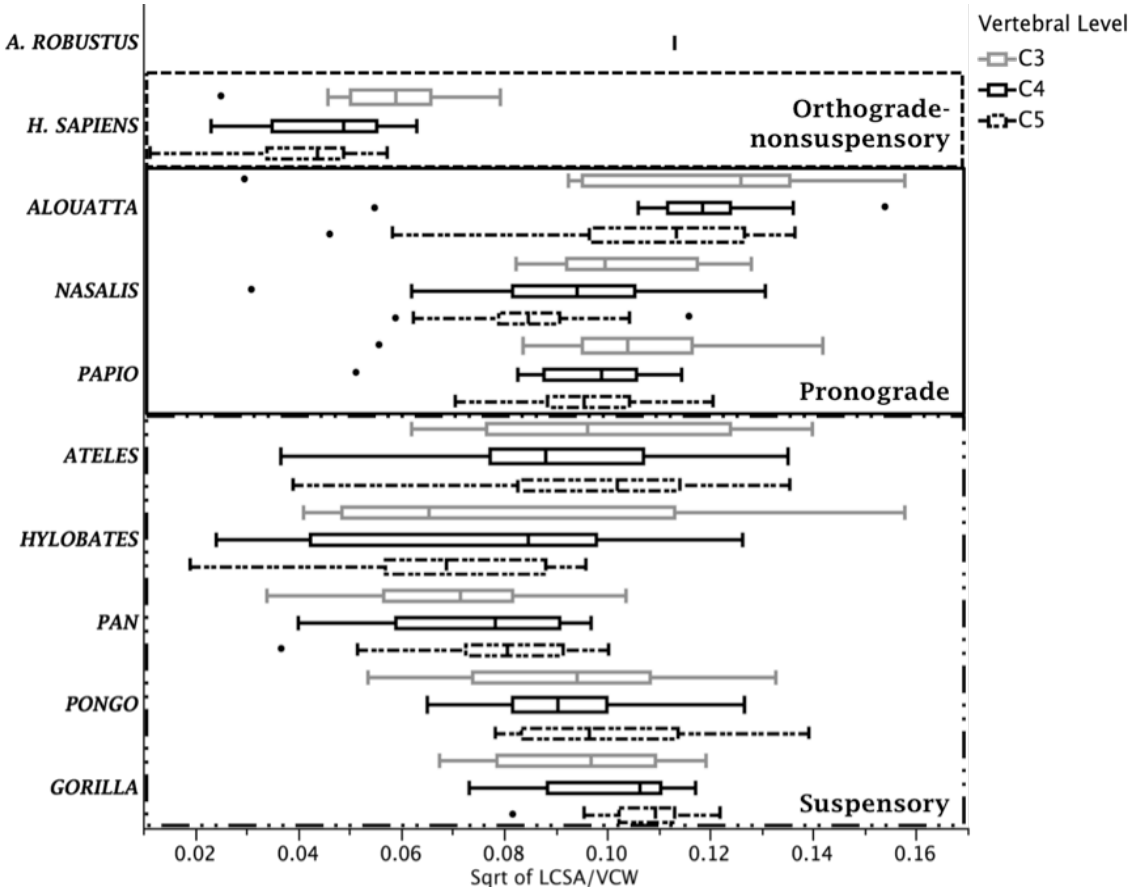

Figure 5-19. Box-and-whisker plots illustrate the distribution of the ratio of the sqrt of lamina cross-sectional area (LCSA) divided by vertebral body width (VBW) at cervical levels C3 (gray), C4 (black), and C5 (dotted) for each taxon and positional behavior group. The line within each box represents the median value and the ends of the box represent the 1st and 3rd quartiles. The whiskers extend to the outermost data points within another ±1.5.

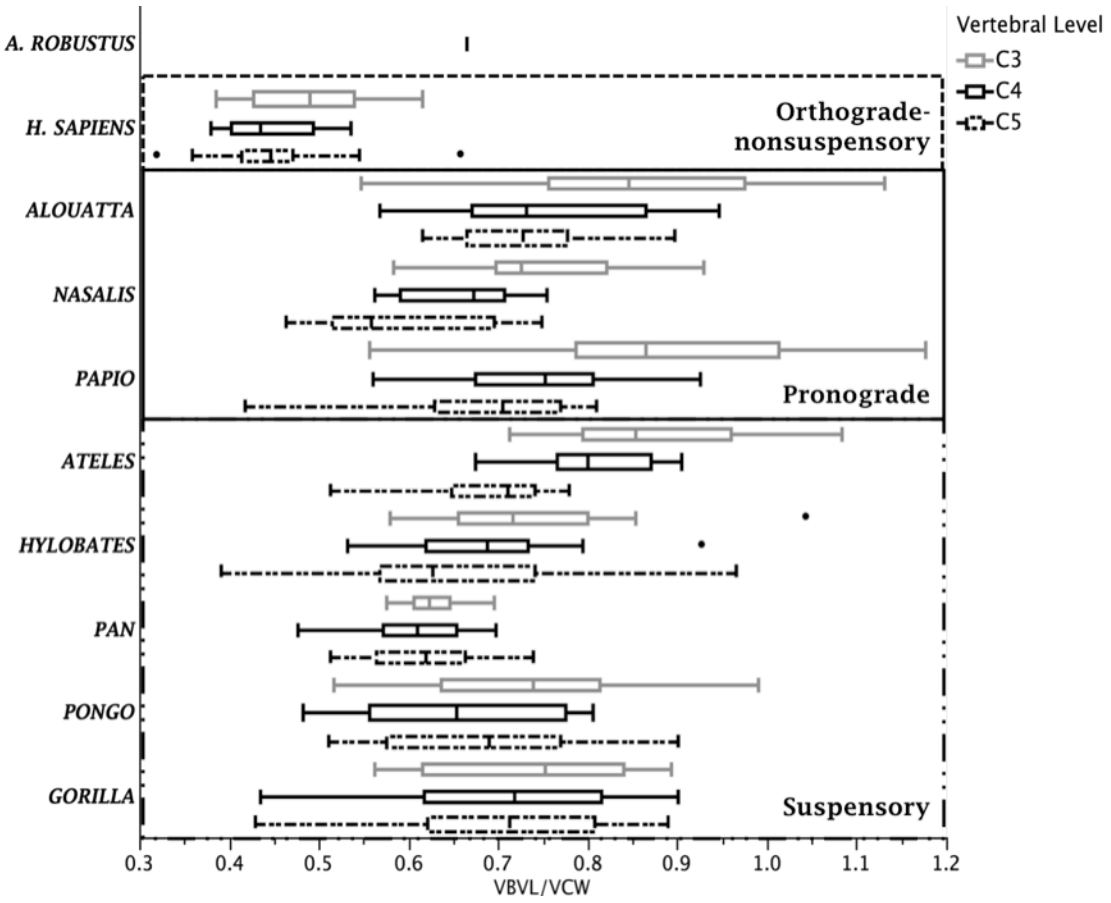

Figure 5-20. Box-and-whisker plots illustrate the distribution of the ratio of ventral vertebral body length (VBVL) divided by vertebral body width (VBW) at cervical levels C3 (gray), C4 (black), and C5 (dotted) for each taxon and positional behavior group. The line within each box represents the median value and the ends of the box represent the 1st and 3rd quartiles. The whiskers extend to the outermost data points within another ±1.5.

Summary of *Australopithecus robustus* analyses

The comparative analyses of the SK 854 second cervical vertebra did not support the affinity prediction. The preserved features (VB ECC, TPPA, PCSA, and LCSA) did sometimes fall within the *Pan* distribution, but they also overlapped with most other taxa as well (Figures 5-15, 5-16, and 5-17). The VB ECC ratio for SK 854 overlaps the ranges for all taxa, except *Nasalis* and *Papio*. The angle of the C2 transverse process is relatively small and falls within just a single group's distribution—*Nasalis*. The cross-sectional areas are intermediate and fall between the largest taxa (e.g., *Gorilla* and the platyrrhines) and the smallest (e.g., *Homo*).

The univariate analyses of SKW 4776 also did not support the affinity prediction. Based on these comparisons, the SKW vertebra does not resemble *Pan* morphology and never overlaps with modern humans. The fossil specimen has relatively a high VB ECC ratio and this suggests a higher vertebral position—C3—instead of C4 or C5. The LCSA of SKW 4776 is relatively large compared to *Homo* and *Pan*, and the vertebral body length is generally not distinctive, but is longer than modern humans.

Homo sp. indet

KNM-ER 164c is an adult seventh cervical vertebra articulated with a first thoracic vertebra (Day and Leakey, 1973). It was recovered at Koobi Fora, Kenya, and dates to ~1.8 Ma (Brown and McDougall, 1993). The vertebrae were found with a left parietal fragment, two proximal phalanges, the base of a third phalanx, and the head of a metacarpal. The fossil is attributed to the genus *Homo*, but is not assigned to any specific species (Day and Leakey, 1973). Wood (1991) confirmed the *Homo* designation for the skull fragment. The phalanges are also described as derived, with *Homo*-like morphology

based on the lack of strong curvature and flexor sheath markings that characterize *A. afarensis* (McHenry and Coffing, 2000). The vertebrae have been described as displaying humanlike morphology, but are otherwise unexamined (Walker and Leakey, 1993). KNM-ER 164c currently represents one of the earliest adult vertebral specimens of the genus *Homo*.

Affinity prediction: Based primarily on previous descriptions and the taxonomic assignments for better-studied associated skeletal elements, KNM-ER 164c is predicted to resemble *Homo* (Day and Leakey, 1973; Wood, 1991; Walker and Leakey, 1993).

The cervical vertebra is incomplete with a loss of both transverse and spinous processes. The right superior articular facet is also missing. The position of the vertebra is confidently assigned due to (among other features) the presence of a *foramen transversarium*, thus indicating its cervical status. The presence of a costal facet on the articulated inferior vertebra indicates its thoracic membership and reaffirms the designation of the cervical vertebra as the seventh in its region and the thoracic vertebra as the first in its section of the spine. The vertebral canal is preserved thus VCA (VCW*VCH) was used to adjust for size in relevant features. The five logged vertebral features for the DFAs include: relative ventral vertebral body length (LN (VBVL/(sqrt of VCA)), vertebral body eccentricity (LN VB ECC), relative pedicle cross-sectional area (LN PCSA/VCA), relative lamina cross-sectional area (LN LCSA/VCA), superior articular facet angle (LN AFA). Analyses were performed at the C7 level.

Results of the DFA at the C7 level are presented in Table 5-25, with their corresponding standardized coefficients presented in Table 5-26, and classification results in Table 5-27. A bivariate plot of the first and second discriminant function scores

(accounting for 91.1% of the variation among the groups) is displayed in Figure 5-21. The DFA resulted with significant Wilk's Lambda for all five functions (p<0.05) (Table 5-25).

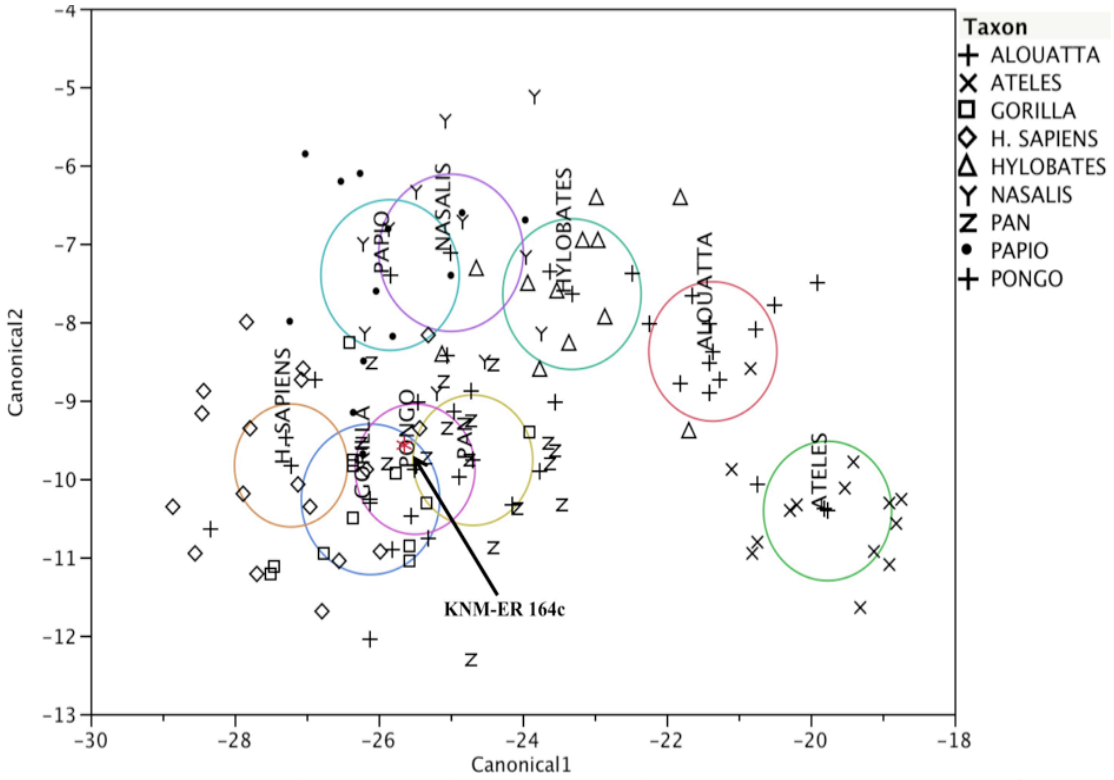

Figure 5-21. Discriminant function plot for the analysis of extant sample and KNM-ER 164c at the C7 level. Discriminant scores from function 1 are plotted against those from function 2. Functions 3-5 are not shown. Asterisk represents KNM-ER 164c. Group mean 95% confidence interval contours shown. DFA results are presented in Tables 5-25. The structure coefficients are shown in Table 5-26. 68.8% of all cases were classified correctly (Table 5-27).

TABLE 5-25. Results of discriminant function analyses for KNM-ER 164c at the C7 vertebral level

Function	Eigenvalue	% of Variance	Cumulative %	Canonical Correlation	*p*-value
1	5.79	72.09	72.09	0.92	<.0001
2	1.53	19.01	91.10	0.78	<.0001
3	0.39	4.88	95.97	0.53	<.0001
4	0.23	2.89	98.87	0.43	0.00
5	0.09	1.14	100.00	0.29	0.04

TABLE 5-26. Standardized coefficients of discriminant function analyses for KNM-ER 164c at the C7 vertebral level

Function	VB ECC	AFA	VBVL	PCSA	LCSA
1	-0.471	-0.111	-0.126	0.495	0.534
2	0.591	0.014	-0.452	1.125	-0.617
3	0.139	0.979	0.344	0.392	-0.487
4	0.548	0.191	-0.185	-0.638	1.044
5	0.396	-0.274	0.966	-0.130	-0.079

TABLE 5-27. Classification results of discriminant function analyses for KNM-ER 164c at the C7 vertebral level

	Alouatta	*Ateles*	*Gorilla*	*H. sapiens*	Hylobatids	*Nasalis*	*Pan*	*Papio*	*Pongo*
Alouatta	11	1	0	0	1	1	0	0	0
Ateles	2	12	0	0	0	0	0	0	0
Gorilla	0	0	6	3	0	0	1	0	2
H. sapiens	0	0	0	16	0	1	0	1	0
Hylobatids	2	0	0	0	8	2	0	0	0
Nasalis	0	0	0	0	2	8	0	0	1
Pan	0	0	0	1	0	0	10	0	5
Papio	0	0	0	0	1	0	1	9	1
Pongo	0	0	2	3	0	0	4	1	6
# misclassified		39							
% misclassified		31.2							

The first and second discriminant functions accounted for 72.09% and 19.01% of the between group variation, respectively (Table 5-25).

As for the fossil specimen, the Kenyan vertebra most closely resembles *Pongo* with a posterior probability of 0.42 and *H. sapiens* with a posterior probability of 0.30. This does not strongly support the prediction that the C7 vertebra would group with *Homo*. The standardized coefficients of the predictor variables for the discriminant functions suggest that the separation along the first function is principally caused by an increase in lamina cross-sectional area (LCSA) (Table 5-26). As demonstrated throughout this chapter, modern humans have relatively small cross-sectional areas. In contrast, the platyrrhines have relatively large cross-sectional areas, while the remainder of the extant sample and the Kenyan specimen fall between the two groups. The separation along the second function is strongly driven by an increase in pedicle cross-sectional area (PCSA). The KNM-ER 164c vertebra is most similar to hominids and *Ateles* with relatively smaller PCSAs. Overall, 68.8% of the cases were correctly classified, with the majority of the misclassifications being among *Pongo* and *Gorilla* individuals (Table 5-27).

Homo ergaster

KNM-WT 15000r is a relatively complete seventh cervical vertebra uncovered in West Turkana, Kenya and dates to ~1.53 Ma (Brown and McDougall, 1993; Walker and Leakey, 1993). It is attributed to an adolescent male of *Homo ergaster* (Brown et al., 1985). This specimen is confidently assigned to the seventh cervical level because: 1) it exhibits definitive features of the cervical region (i.e., *foramen transversarium*) and 2) it articulates with the first vertebra of a complete thoracic region associated with the KNM-

WT 15000 skeleton. Though certain features of the vertebra are suggested to have reached adult size (i.e., vertebral canal dimensions) (MacLarnon, 1993), other features do not exhibit adult morphology. For example, the epiphyseal cap of the spinous process is unfused and this is consistent with an adolescent developmental stage, as the union of the secondary centers of ossification is completed between 17-25 years of age in humans (O'Rahilly et al., 1980). Morphological comparisons must therefore take the skeletal age of the specimen into account. Even with a subadult status, the inclusion of this fossil specimen is reasonable because it represents one of the earliest vertebral elements for the genus *Homo*.

The transverse and spinous processes of the KNM-WT 15000 *H. erectus* cervical vertebra have been described as short and gracile, revealing a more humanlike morphology. Previous studies of the KNM-WT 15000 cervical material have noted that the relative dorsoventral diameter (or height) of the KNM-WT 15000 vertebral canal falls at the low end of hominid range, while canal width sits in the middle of both great ape and human ranges of variation (Day and Leakey, 1973; MacLarnon, 1993). These results do not produce an obvious taxon for the affinity prediction and considering other elements of the KNM-WT 15000 skeleton does not produce a clearer picture either. Several features of the KNM-WT 15000 skeleton resemble geologically younger and more apomorphic members of genus *Homo* while differing from older, more plesiomorphic australopiths (i.e., sacrum, femur) (MacLarnon, 2003; Ruff and Walker, 1993; Anton, 2003). This supports an affinity prediction for *Homo*. However, other features of the KNM-WT 15000 skeleton are apelike, such as the clavicle, proximal humerus, and proposed scapular position (Larson et al., 2007). Given that the KNM-WT

15000 C7 is a member of a more plesiomorphic pectoral girdle supports an affinity with *Pan*.

Affinity prediction: In view of the fact that that both *Homo* and *Pan* predictions receive support, both predictions will be tested: (A) Based on previous descriptions of the KNM-WT 15000r vertebra and other derived morphologies of the skeleton, the C7 vertebra is expected to be most morphologically similar to modern humans (Day and Leakey, 1973; Ruff and Walker, 1993; Walker and Leakey, 1993), (B) Due to the primitive features of associated pectoral girdle elements, the C7 is expected resemble *Pan* (Larson et al., 2007).

Both vertebral canal height and width are preserved; so appropriate features are size-adjusted using vertebral canal area (VCA). All relevant features are present in this specimen, however a DFA of only six features is discussed here due to sample size (*Nasalis* n=7). A forward stepwise DFA was utilized to determine those variables that best explained the variation in the data. The six logged variables in the DFA include: vertebral eccentricity (LN VB ECC), spinous process length (LN (SPL/(sqrt of VCA))), transverse process length at the posterior tubercle (LN (PTPL/(sqrt of VCA))), transverse process angle at the posterior tubercle (LN TPPA), pedicle cross-sectional area (LN (PCSA/VCA), and spinous process cross-sectional area (LN (SCSA/VCA)).

Results of the DFA at the C5 level is presented in Table 5-28, with their corresponding standardized coefficients presented in Table 5-29, and classification results in Table 5-30. Graphical ordination of the first two discriminant function scores (accounting for 83.43% of the variation among the groups) is displayed in Figure 5-22. The DFA resulted with significant Wilk's Lambda for all six functions ($p<0.05$) (Table 5-

28). The first two discriminant functions accounted for 43.25% and 40.19% of the between group variation, respectively (Table 5-28).

The KNM-WT 15000 specimen morphologically resembles *Pan* with a posterior probability of 0.53 and *Homo* with a posterior probability of 0.45. This result does not strongly support the predicted affinities to *Homo* alone. The standardized coefficients of the predictor variables for the discriminant functions suggest that the separation along the first function is principally caused by a two variables: an increase relative spinous process length and a decrease in relative transverse process length at the posterior tubercle (Table 5-29). *Gorilla* and *Pongo* have relatively long spinous processes lengths (SPL) and short transverse process lengths (PTPL). *Papio*, in contrast, has the shortest relative SPL and the longest relative PTPL, while the majority of taxa, include *H. ergaster*, fall in between. The separation along the second function is caused by an increase in relative spinous process cross-sectional area (SCSA). KNM-WT 15000r, the hominids, and *Papio* separate from the rest of the taxa groups with relatively large SCSAs. Overall, 90% of the cases were correctly classified (Table 5-30).

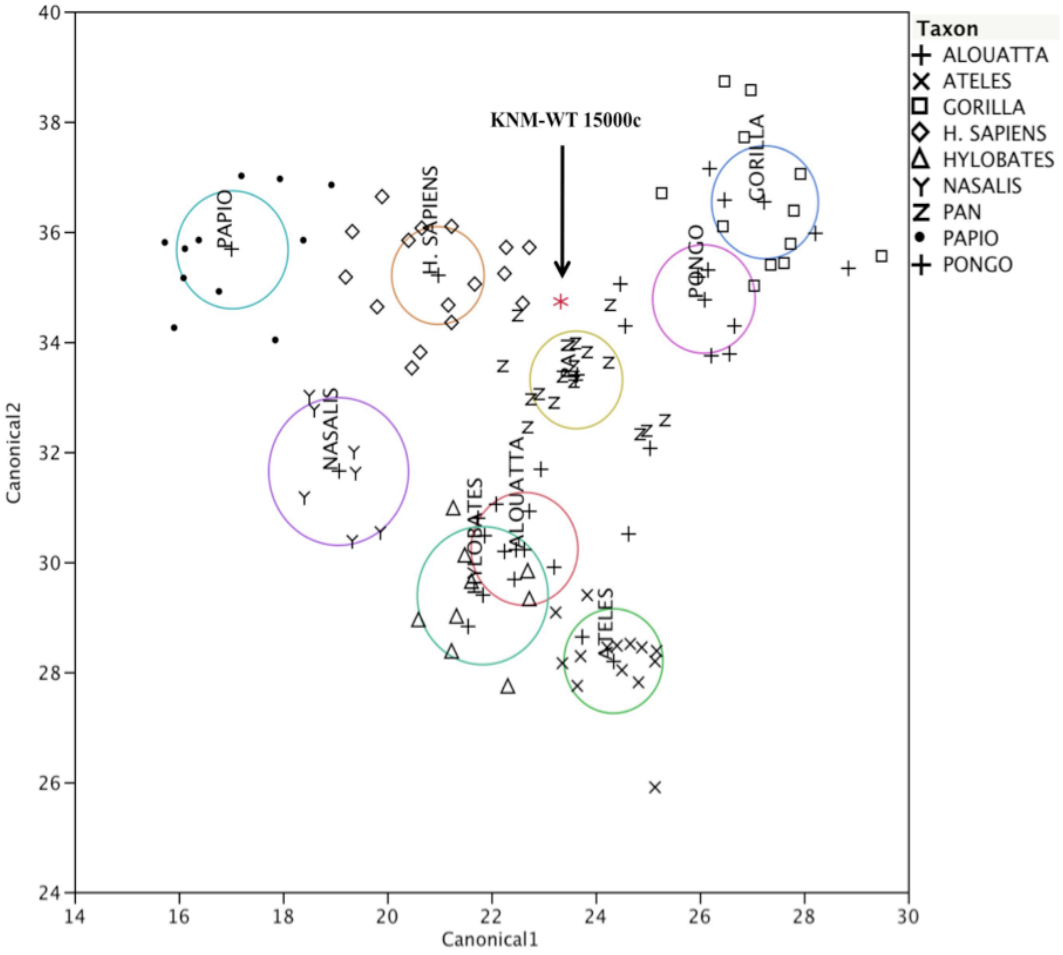

Figure 5-22. Discriminant function plot for the analysis of extant sample and KNM-WT 15000 at C7 level. Discriminant scores from function 1 are plotted against those from function 2. Functions 3-7 are not shown. Asterisk represents KNM-WT 15000r. Group mean 95% confidence interval contours shown. DFA results are presented in Tables 5-28. The structure coefficients are shown in Table 5-29. 90% of all cases were classified correctly (Table 5-30).

TABLE 5-28. Results of discriminant function analyses for KNM-WT 15000 at the C7 vertebral level

Function	Eigenvalue	% of Variance	Cumulative %	Canonical Correlation	*p*-value
1	9.47	43.25	43.25	0.95	<.0001
2	8.80	40.19	83.43	0.95	<.0001
3	1.88	8.59	92.02	0.81	<.0001
4	1.19	5.45	97.48	0.74	<.0001
5	0.36	1.64	99.12	0.51	<.0001
6	0.19	0.88	100.00	0.40	0.00

TABLE 5-29. Standardized coefficients of discriminant function analyses for KNM-WT 15000 at the C7 vertebral level

Function	VB ECC	SPL	PTPL	PCSA	SCSA	TPPA
1	-0.255	0.957	-0.707	-0.410	0.480	0.486
2	0.315	0.468	0.446	-0.542	-0.817	-0.014
3	-0.621	-0.065	1.022	-0.020	-0.422	0.075
4	0.201	0.666	-0.048	0.768	-0.616	-0.494
5	0.083	0.052	-0.259	0.956	-0.795	0.752
6	0.646	-0.139	0.499	-0.360	0.592	0.167

TABLE 5-30. Classification results of discriminant function analyses for KNM-WT 15000 at the C7 vertebral level

	Alouatta	*Ateles*	*Gorilla*	*H. sapiens*	Hylobatids	*Nasalis*	*Pan*	*Papio*	*Pongo*
Alouatta	12	0	0	0	0	0	0	0	0
Ateles	2	12	0	0	0	0	0	0	0
Gorilla	0	0	9	0	0	0	0	0	3
H. sapiens	0	0	0	16	0	0	0	0	0
Hylobatids	0	0	0	0	9	0	0	0	0
Nasalis	0	0	0	0	0	7	0	0	0
Pan	0	0	0	1	0	0	15	0	0
Papio	0	0	0	0	0	0	0	11	0
Pongo	0	0	3	0	0	0	2	0	8
# misclassified		11							
% misclassified		10							

SUMMARY AND CONCLUSION

The goals of the Chapter 5 analyses were to examine fossil hominoid cervical morphology within the context of extant variation and to test predictions of similarity to specific primate taxa based on previous description and research.

The Miocene hominoid *Nacholapithecus kerioi* was predicted to resemble taxa such as *Nasalis,* arboreal pronograde taxa that also incorporate orthograde positional behaviors into their repertoires. The prediction was not supported. Though several traits in the C1 specimen overlapped with the predicted taxa, it was fell within the distributions of several other primates as well, including *Pongo*, hylobatids, and *Alouatta*. Results from the DFA analyses of the mid- and lower-level cervical elements suggested a morphological affinity with hylobatids and *Pongo*. The *N. kerioi* cervical vertebrae can be characterized broadly as intermediate in pedicle and lamina cross-sectional areas; specifically, larger than modern humans, but generally smaller than platyrrhine taxa. The vertebral body lengths are relatively short and the transverse process is more dorsally oriented, both traits shared with *Pongo* and *Gorilla.* Results for the positional DFAs for KNM-BG 40793c and KNM-BG 40840o supported C4 and C6, respectively.

Australopithecus afarensis vertebrae were predicted to group with *Pan* exclusively and analyses produced some support for this. The A.L. 333-83 C1 LCSA analysis did overlap with *Pan* distributions, but not to the exclusion of most other taxa. Modern humans, however, did not coincide with the Hadar specimen. The A.L. 333-101 C2 analyses revealed a generalized hominid morphology, including *Homo*. The DFA analyses of the lower vertebral specimen A.L. 333-106 supports the affinity prediction and results indicate the *A. afarensis* lower cervical as exhibiting a relatively long spinous

process with a large spinous process cross-sectional area when compared to humans, but not as large as found in *Gorilla* or *Pongo*. The LCSA is similar to most nonhuman hominoids, but larger than modern humans and smaller than platyrrhines. The positional DFAs support a C6 position.

Based on their initial descriptions, both South African specimens, SK 854 and SKW 4776, were predicted to resemble *Pan*. This prediction is not supported; their cervical features were similar to several taxa in addition to chimpanzees, including *Gorilla*, the platyrrhines, and modern humans. The transverse process angle was distinctive small and only fell within one taxon's range of variation — *Nasalis*. Notably, SKW 4776 morphology did not overlap with modern humans. The *A. robustus* vertebrae can be broadly characterized as displaying an increased robusticity of LCSA, relatively larger than either the very small LCSAs of modern humans or the more intermediate *Pan* morphology. SKW 4776 vertebral body is also relatively longer than the short centra of modern *Homo*. The positional DFA results suggest a C3 level position.

The fossil hominin KNM-ER 164c was predicted to most closely resemble our own genus based on previous qualitative work; however, contradictory descriptions of KNM-WT 15000r did not produce a clear taxon for the affinity prediction. Therefore two predictions were tested, one for *Homo* and one for *Pan*. The predictions for a *Homo* affinity receive little support from the comparative analyses. The adult Kenyan specimen, KNM-ER 164c, has a relatively large LCSA when compared to modern humans and overall was like a generalized nonhuman hominid, most similar to *Pongo*. The analyses of subadult fossil, KNM-WT 15000r, produced a similar result and is most similar to *Pan*, though it was also linked with *Homo*. However, due to the subadult status of this

specimen, some of the shape ratios calculated here might be an underestimate of the adult morphology. The features used to adjust for size had reached adult status (MacLarnon, 1993), but other features had not (spinous process). Larger relative cross-sectional areas and longer relative spinous processes remove affinity with modern humans.

The results from this chapter will used in discussion of the functional or behavioral implications of morphological similarity between fossil and extant taxa in Chapter 6. Results from the extant analyses imply a complex relationship between function and cervical vertebral morphology. No single cervical model proposed was clearly supported. However, a number of vertebral features did provide support for one or more of the cervical models. Keeping this in mind, fossil morphology can be interpreted functionally, both within the context of the extant results and biomechanical theory. Finally, the goal to examine the accuracy of qualitative terms such as apelike, *Pan*-like, or *Homo*-like when describing fossil cervical vertebrae will also be further discussed. Few affinity predictions were supported to the exclusion of other taxa. This result highlights the danger of using such terms when describing fossil cervical vertebral morphology.

Chapter 6

DISCUSSION AND CONCLUSIONS

INTRODUCTION

The aim of this dissertation research was twofold. The first goal was to test the hypothesis of adaptation in the primate cervical spine to positional behavior using a comparative framework. The second goal was to use the morphological context established by analyses of extant taxa to describe and interpret fossil hominoid cervical vertebrae. The analysis sections of this study (Chapters 4 and 5) are summarized and discussed here; and the results of the extant and fossil components of the project are unified to produce a current state of understanding of primate cervical functional morphology. Future avenues of research will also be discussed, including addressing the issue of behavioral positional categories and how research outside of primates may aid in the understanding of the functional morphology of the mammalian cervical spine.

Three specific biomechanical models guided the extant component of this study: the suspensory model, the postural model, and the head-balancing model. Results of the pairwise comparisons and primate-wide analyses used to test these models were equivocal; no specific predictions were supported across all vertebral levels in both sexes. However, some patterns did emerge from the results. Specifically, both pairwise comparisons and primate-wide analyses demonstrated more support for the suspensory and postural models in male comparisons and in the lower half of the cervical spine (C4-C7) for both sexes. Results also supported the head-balancing model in contrast to the suspensory or postural models; this evidence was concentrated in the upper half of the

cervical spine (C1-C3). One feature provided support for two models (i.e., spinous process length at the C1 level). Implications of this result will be discussed below.

Fossil analyses revealed that extinct hominoids were often distinct from modern human variation. Univariate analyses found that fossil morphology could generally not be distinguished from that of other anthropoid taxa, but rarely overlapped modern human morphology. This result in particular highlights the error of applying undefined terms such as apelike, monkeylike, and humanlike to individual fossil features. Multivariate analyses of overall cervical vertebral shape were able to differentiate fossil specimens from other nonhominoid anthropoids, but also separated fossil hominoids from modern humans. This is true for fossils assigned to our own genus. Fossil hominoids overall displayed greater robusticity (i.e., larger cross-sectional areas), longer spinous processes, and more dorsally oriented transverse processes. Overall, these results suggest that modern human cervical morphology did not appear in the hominin fossil record until later into the Pleistocene, at least after the appearance of *Homo erectus*.

EXTANT ANALYSES

The overall goal of the extant analyses was to identify vertebral adaptations to positional behavior in living primates. Evidence for adaptation requires a predictable association between the trait and function. In Chapter 4, models relating vertebral anatomy to the mechanical requirements of differing positional behaviors were tested to demonstrate a correlation between vertebral traits and their postural and locomotor functions. Pairwise comparisons and primate-wide PGLS analyses were conducted in tandem to achieve the goals of this chapter.

The extant results were too inconsistent to conclude with a finding of unequivocal support for any of the cervical models proposed here, but certain vertebral features provide some evidence for a correlation with either positional behavior or balancing the head (or both). These deserve further investigation. The vertebral traits that are most likely related to positional behavior are spinous process length (SPL), spinous process cross-sectional area (SCSA), and transverse process orientation (TPPA). A long cervical spinous process is suggested to indicate increased moment arms for extension (Shapiro and Simons, 2002). These features were expected to separate suspensory from nonsuspensory taxa or orthograde from pronograde taxa based on the suspensory and postural models, respectively. Support for this functional link was found in both pairwise and primate-wide comparisons. Suspensory apes had longer spinous processes than nonsuspensory humans, but significant differences were found only in the lower cervical spine, and no other pairwise contrasts showed significant differences. The primate-wide PGLS analyses found that orthograde taxa had longer spinous processes than pronograde taxa (no differences between suspensory and nonsuspensory taxa were found), but unlike the ape/human pairwise comparison results, this relationship was significant only at the C1 level.

Greater spinous process cross-sectional area (SCSA) was predicted to reflect greater resistance to bending forces (Mercer, 1999; Anderson et al., 2005) and expected to differentiate suspensory from nonsuspensory taxa or orthograde from pronograde taxa based on their respective positional behaviors. Support for a link with positional behavior was found in both pairwise comparisons and primate-wide PGLS analyses. In the pairwise comparisons, suspensory platyrrhines had greater SCSA in comparison to their

nonsuspensory counterparts, though only at the C7 level. In the primate-wide tests, SCSA separated orthograde taxa from pronograde taxa, this time at multiple levels in the cervical spine (C4-C6).

The transverse processes were expected to be more dorsally oriented in suspensory or orthograde taxa in order to increase the deep spinal muscles ability for powerful extension and to assist in overall stability (Ward, 1991, 1993; Shapiro, 1995; Shapiro et al., 2005). The primate-wide analyses supported this prediction in the suspensory model, but only at the last cervical level (C7). Surprisingly, the relationship was opposite to that predicted at all other levels where significant differences were found (C3-C6). Contrary to suspensory and postural model predictions, the transverse process angles (for both the anterior and posterior tubercles) were smaller in orthograde taxa when compared to pronograde taxa. These results provide potential support for the hypothesis that the orientation of the transverse processes are related to positional behaviors, but just not the models presented in Chapters 2 and 3.

The head-balancing model sought correlations between anterior cranial length and vertebral morphology. The head-balancing model received the most widespread support from the primate-wide analyses, though a clear pattern of influence on vertebral morphology was not readily apparent. Some trends do present and in fact differ with the general pattern of results for the two positional behavior models; specifically more significant differences were found in female comparisons and in the upper levels of the spine (C1-C3). The vertebral traits that are mostly likely related to cranial morphology are vertebral body length (VBVL), transverse process length at the posterior tubercle (PTPL), and pedicle and laminar cross-sectional areas (PCSA and LCSA, respectively).

A positive correlation was found between each of these vertebral traits and anterior cranial length (ACL) for both males and females at the indicated vertebral levels: VBVL at the C4 and C5 levels, PTPL from C1-C4, PCSA at levels C3 and C5-C7, and finally LCSA at levels C2 and C3.

Why there are a greater number of significant differences in the female analyses testing the head-balancing model is not immediately evident; however, the concentration of these differences in the upper section of the cervical column is likely linked to the role of region's soft tissue anatomy. The deep nuchal musculature in this area is responsible for stabilizing the head on the neck, moving and maintaining the integrity of the atlanto-occipital and atlanto-axial joints, and relaying important proprioceptive information about head movement to the brain. The suboccipital muscle group includes the *rectus capitis* muscles and the superior and inferior obliques. Corneil et al. (2001) suggests that the increased relative size of some *Macaca* suboccipital muscles, when compared to modern humans, is linked to maintaining head position when the animal adopts a quadrupedal posture (Corneil et al., 2001). This proposed relationship supports the head-balancing model, such that taxa with larger ACLs require a greater effort force (i.e., more powerful muscles) to counterbalance the larger resistance force caused by a longer ACL. This relationship is reflected in the increased robusticity of the suboccipital muscles' areas of attachment (i.e., longer transverse processes and larger cross-sectional areas (PTPL, PCSA, and LCSA) in the upper cervical spine.

Primate-wide analyses also demonstrated that spinous process length (SPL) at the C1 level was significantly different among postural groups, but was also correlated with ACL. This result marks an example of when both postural and head-balancing models

were supported. Unfortunately, the existing pattern of significant results for SPL at other vertebral levels does not provide a consistent signal to aid in the further interpretation of this result. These results do not support one model over the other in explaining variation in C1 spinous process length. Future efforts to further address this issue are discussed below.

Considering these results together, it is apparent further work is required for the development of more accurate cervical models. Many predictions of vertebral morphology received only partial support, and this may indicate that biomechanical assumptions upon which these cervical models rely are incorrect, or that there is no functional relationship between these measures and positional behavior. Further development and validation of biomechanical models of the cervical spine may be able to help distinguish between these two possibilities. There are a few avenues of research that would aid in the development of more accurate cervical models.

First, it would be useful to consider the categorization of positional behavior. The process of assigning taxa to behavioral groups forces categorization of what is essentially a continuous trait. The broad spectrum of positional behaviors that individuals and species use cannot fully be described by discrete categories. The use of categorical behavior groups runs the risk of masking functional signals in skeletal variation. A preliminary analysis of whether higher-resolution behavioral data (i.e., angle of neck inclination relative to the substrate) is more appropriate for testing hypotheses of adaptation to positional behavior in cervical morphology was conducted in Chapter 4. Results did not reveal a greater incidence of significant correlations or produce a clearer pattern of association between behavior and cervical anatomy. Although these results do

not support the function-form link for the primate cervical column proposed in this dissertation, many related avenues of research remain unexplored. Future efforts should focus on expanding the sample used here to include more orthograde and antipronograde taxa (e.g., strepsirrhines). Furthermore, due to increased access and advances in technology, anthropological research has begun to develop better methodologies for recording and quantifying primate locomotion and posture (e.g., Demes et al., 1996; Strait and Ross, 1999; Isler and Thorpe, 2003; Dunbar et al., 2004; Franz et al., 2005; Togasaki et al., 2005; Schoonaert et al., 2006; Larson and Stern, 2007; Dunbar et al., 2008; DeSilva, 2009; Carlson and Demes, 2010; Patel and Wunderlich, 2010; Schmitt, 2011; Duarte et al., 2012). This area of research will help determine whether other measurements of positional behavior would better explain cervical morphological variation than the broad categories defined here.

A second issue to consider is one of phylogeny. The objective of this study was to determine whether specific morphologies are behavioral adaptations, but this task is not easily achieved within the primates sampled here, because there is a strong correlation between positional behaviors and phylogeny (i.e., most suspensory primates are hominoids, most terrestrial pronogrades are catarrhines). To further address this question, it may be more helpful to investigate adaptation to positional behaviors across a broader mammalian context. One cervical feature in particular provides an interesting case study for further investigation. The transverse process angle at the posterior tubercle (TPPA) significantly separates postural groups in 6 out of 7 vertebral levels in male and 3 out of 7 levels in females. This correlation between TPPA and posture is supported in both the pairwise comparisons and the primate-wide analyses. Nonetheless, the direction of

differences between groups only supports the broader postural model at the C7 level (i.e., where orthograde taxa were expected to exhibit larger angles and thus more dorsally oriented transverse processes). Results in the upper vertebral levels (C1-C6) were also significant, but in the opposite direction predicted by the model (i.e., pronograde taxa displayed larger TPPAs). A comparison of multiple clades of mammals may be able to identify whether this morphology is a common adaptation due to posture that is not a consequence of phylogenetic inertia or constraint.

Another important issue is the incorporation of soft tissues mechanics into cervical models. One structure in particular, the nuchal ligament, has been considered an important, yet enigmatic, feature of the primate cervical vertebral region. A wide range of functional roles for this structure has been hypothesized in the human medical literature; it has been described as (1) a supportive structure for the head, (2) an attachment site for muscles, (3) a ligament to limit and control flexion, (4) a loading dampener, and (5) a major proprioceptive structure for the head (Fielding 1976; White and Panjabi, 1990; Mitchell et al., 1998; Johnson et al., 2000; Mercer and Bogduk, 2003; Kadri and Al-Mefty; 2007). Although the nuchal ligament has received little attention outside of medical research, its presence/absence has been incorporated into functional hypotheses regarding bipedal locomotion in fossil hominins. The nuchal ligament is surprisingly absent in the great apes (Swindler and Wood, 1973). This fact has been used to argue that the nuchal ligament is functionally related to bipedality (Bramble and Lieberman, 2004). However, further research is required to understand the role of the nuchal ligament: it is commonly found in many nonprimate mammals and has been documented in *Papio* and *Macaca* (Swindler and Wood, 1973; Fielding, 1976; Dean, 1982; Bianchi, 1989).

FOSSIL ANALYSES

The goal of the fossil analyses in Chapter 5 was to examine cervical variation within the context of the extant morphological framework and test the accuracy of descriptive terms prevalent in the literature such “apelike,” “*Pan*-like,” and “*Homo*-like.” To achieve these goals, the morphologies of individual fossil specimens were quantified and compared to a subset of the primate sample. Box-and-whisker plots and discriminant function analyses were performed. Univariate results demonstrated a great deal of overlap among taxa, indicating that single features can rarely be described appropriately with qualitative terms such as "monkeylike" or "apelike." Notably, measurements for the Miocene ape *Nacholapithecus* and the Plio-Pleistocene hominins mostly fell outside of the modern human ranges of variation. In the multivariate analyses, fossil cervical morphology was distinct from both extant New and Old World monkeys and modern humans. Fossil hominins were most similar to *Pongo* and *Pan*, though posterior probabilities were not always particularly high. *Nacholapithecus* tended to group with hylobatids. The following section discusses these results in greater detail, including the functional and behavioral implications of the morphological similarity between fossil and extant taxa.

Nacholapithecus kerioi

Previous research suggested that the postcranium of the Miocene hominoid Nacholapithecus kerioi was an arboreal pronograde quadruped that included orthograde behaviors in its positional repertoire (Nakatsukasa et al., 2003; Senut et al., 2004; Kikuchi et al., 2012). Therefore, the three cervical vertebrae examined here were predicted to most closely resemble *Nasalis*. Neither the univariate nor the discriminant

function analyses supported this prediction. Furthermore, multivariate analyses suggested that *Nacholapithecus* was most similar to apes, specifically hylobatids and *Pongo*. The vertebral features found to be the most informative for separating taxa in the *Nacholapithecus* DFAs are not among those suggested by the extant analyses in Chapter 4 to support one of the behavioral models.

Australopithecus afarensis

The majority of researchers have described the *A. afarensis* vertebrae as more *Pan*-like than *Homo*-like (Lovejoy et al., 1982; Coroner and Latimer, 1991). It was therefore predicted that the three cervical elements from the A.L. 333 locality would most closely resemble those of chimpanzees. Multivariate analyses support this prediction for A.L. 333-106 (most likely a C6), the only specimen whose preservation permits inclusion in a DFA. Specimen A.L. 333-106 has a relatively large spinous process cross-sectional area and a long spinous process when compared to the hylobatids, humans, and other monkeys; these structures are relatively smaller than those of *Gorilla* or *Pongo*. The LCSA is apelike, being intermediate between the smaller values for modern humans and the larger values for *Ateles* and *Alouatta*.

In contrast to the multivariate results for A.L. 333-106, univariate analyses of the more fragmentary specimens A.L. 333-83 (C1) and 333-101 (C2) present a more complex picture. As noted, univariate results indicate that features examined individually can only rarely distinguish hominoid taxa from each other. For example, LCSA of A.L. 333-83 falls within the *Pan* distribution, but it also falls with other taxa, the exceptions being platyrrhines and modern humans. The analyses of A.L. 333-101 provided a similar result regarding LCSA morphology. Notably, the A.L. 333-101 spinous process is

relatively short and falls within the *Homo* and *Pan* distributions, as well as with the hylobatids and *Nasalis*. This comparison marks one of the few instances where a fossil hominin falls within the modern human distribution. Similarly, the spinous process cross-sectional area (SCSA) of A.L. 333-101 is relatively thick, similar to that of *Homo*, but it also resembles those of *Gorilla*, *Pongo*, and the platyrrhines and is distinct from those of *Pan*, hylobatids, and cercopithecoids.

Spinous process cross-sectional area was one of the few features in the extant sample that consistently supported the broader postural model, specifically in the lower region of the cervical column (C4-C6). Orthograde taxa have larger SCSAs than pronograde taxa, suggesting the presence of powerful (i.e., greater physiological cross-sectional area) deep nuchal muscles (Shapiro and Simons, 2002). The postural signal indicated by the relatively large SCSA in A.L. 333-106 accords well with many previous interpretations of orthograde positional behaviors for *A. afarensis* (e.g., Stern and Susman, 1983; Aiello and Dean, 1990; Ward, 2002). In addition, two features that did not separate positional groups in the comparative analyses, spinous process length and LCSA, distinguish A.L. 333-106 from modern humans: in comparison to modern humans, this fossil has a relatively long spinous process and a relatively large LCSA. These differences suggest that the mechanical environment of A.L. 333-106 was distinct from that of the modern human lower cervical column, with larger nuchal musculature and greater resistance to bending forces.

Australopithecus robustus

The *A. robustus* specimens, particularly SK 854, have been described as displaying primitive traits and being more *Pan*-like in morphology (Robinson, 1972;

Susman, 1993; Gommery, 2006). Thus, the comparative analyses of SK 854 (C2) and SKW 4776 (likely C3) were conducted with the expectation that it would be most similar to *Pan*. The preservation of these specimens did not permit inclusion in DFAs. Univariate analyses show that these fossils did not always fall within the *Pan* distribution, being in some cases more similar to other taxa. The cross-sectional areas of the *A. robustus* specimens are intermediate in relative size, falling between *Gorilla* and the platyrrhines (relatively large) and *Homo* (relatively small). Similar to the Hadar material, the Swartkrans vertebrae differ from those of modern human in having relatively large LCSA and PCSA, again suggesting a distinct functional environment.

Homo ergaster **and** ***Homo*** **sp. indet.**

The early *Homo* vertebral element KNM-ER 164c was predicted to most closely resemble our own genus based on previous qualitative work (Day and Leakey, 1973; Wood, 1991; Walker and Leakey, 1993). However, contradictory descriptions of the *Homo ergaster* specimen KNM-WT 15000r did not produce a clear taxon for the affinity prediction (MacLarnon, 2003; Ruff and Walker, 1993; Anton, 2003; Larson et al., 2007). Therefore two predictions were tested, one for *Homo* and one for *Pan*. The predictions for a *Homo* affinity receive little support from either set of comparative analyses. The less complete KNM-ER 164c vertebra falls with apes in the DFA and, like *Australopithecus* vertebrae, has a relatively large LCSA in comparison to humans. The KNM-WT 15000c vertebra is the more complete early *Homo* specimen. The DFA identifies it as differing from modern humans and resembling living apes in having a relatively longer spinous process and shorter transverse processes. The plesiomorphic morphologies of the KNM-ER 164 and KNM-WT 15000 C7s combine with previously

available evidence suggesting an overall more plesiomorphic pectoral girdle in early *Homo* (Larson et al., 2007).

Future Work

Across the cervical spine fossil hominoids displayed intermediate cross-sectional areas, between the small morphology of modern humans and the large values of the platyrrhines. This morphology implies greater bending forces acting across the bone (Martin et al., 1998; Ruff, 2000), but whether this morphology is due to an overall increased robusticity of the hominoid skeleton or indicative of a mechanical environment distinct from modern humans requires further examination. Results from the extant analyses here do not suggest that differences in positional behavior are driving the morphological variation among taxa, though differences in head-balancing mechanics are a potential avenue of investigation.

Future work should also include later Pleistocene specimens to document when in the fossil record modern human morphology develops and to aid in polarity determination of cervical traits. There is a relatively abundant fossil record for Neanderthals across Europe and eastern Asia, in addition to a number of even older hominin Pleistocene sites such as Atapuerca, Spain and Dmanisi, Georgia. Though only a small number of the features investigated here have been reported for these more recent hominin specimens, researchers commonly observe morphology outside of modern human variation. For example, the Dmanisi C2 and C3 specimens, representing *H. erectus*, exhibit a relatively long C2 spinous process and relatively large pedicle and laminar cross-sectional areas at both C2 and C3 levels (Meyer, 2005). Descriptions of Neanderthal vertebrae have also noted significant differences from modern humans

(Trinkaus, 1983; Gómez-Olivencia et al., 2007; 2013). For example, a recent analysis of eight Neanderthal specimens, found significant differences at all levels of the cervical region of the spine (Gómez-Olivencia et al., 2013). Among other features, Neanderthal vertebrae exhibit longer spinous processes and shorter vertebral body lengths when compared to modern humans. Since modern human morphology seems to appear quite late in hominin evolutionary history, cervical morphology could aid in phylogenetic studies of late Pleistocene specimens, particularly those entirely lacking, or with incomplete, cranial elements.

CONCLUSIONS

While is it necessary to remain aware of the effects of body size and phylogeny on these results, there are several conclusions that can be drawn from the study of comparative morphometrics of the primate cervical spine. In general, the biomechanical predictions of the adaptive hypothesis relating vertebral shape to positional behaviors are rejected. Though the results of this study were not exactly as expected based on biomechanical predictions, a number of features do seem to be biomechanically relevant. The finding of sexual size dimorphism in vertebral traits that are hypothesized to be related to stress resistance bolsters the hypothesis that these traits function to resist increased stress associated with larger bending forces. Furthermore, features such as transverse process angle, a trait hypothesized to reflect the deep spinal muscles ability for powerful extension and stability, does appear to be an adaptation to positional behavior, though variation was not always in the direction predicted by the biomechanical models outlined here. Other traits may be positional behavior adaptations—spinous process length and cross-sectional area—but their specific biomechanical functions are uncertain

because some tests rejected the hypothesis of adaptation. The correlation of several vertebral features, especially transverse process length (i.e., PTPL) and pedicle cross-sectional area, with anterior cranial length supports the predictions set by the head-balancing model. These results support further investigation into the functional relationship between the head and neck and argue that the cervical spine should potentially be modeled as a separate and distinct section of the vertebrate spinal column. All other vertebral traits do not differentiate taxa based on the alternate cervical models, and the results of this study contradict the hypothesis that they constitute adaptations to differences in positional behavior.

Ultimately, this study sought to shed light on primate evolution by providing a functional basis for answering questions regarding how primate cervical morphology evolved and to use information derived from data on extant primate cervical vertebrae to infer positional behavior in fossil taxa. Discrete vertebral traits that were analyzed separately did not vary as predicted according to positional behavior. Hominoid fossil taxa indicated that modern human morphology did not appear until the later in the Pleistocene, after *Homo erectus*. Fossil morphology demonstrated larger cross-sectional areas and longer spinous processes, which indicates the presence of larger nuchal musculature, more similar to extant apes than modern humans. Future work incorporating soft tissue mechanics, broader measures of shape, and the inclusion of non-primates in analyses may assist in the development and validation of more accurate biomechanical models of the primate cervical spine. Furthermore, investigating the extent of functional relationship between the cervical spine and basicranium is another avenue to

understanding their constraints and the selective pressure that shaped them both through hominoid evolutionary history.

REFERENCES

Aiello, Leslie and Christopher Dean. 1990. *An Introduction to Human Evolutionary Anatomy.* Access Online via Elsevier.

Albrecht, Gene H. 1978a. Some comments on the use of ratios. *Systematic Zoology* 27 (1): 67-71.

———. 1978b. The craniofacial morphology of the sulawesi macaques: Multivariate approaches to biological problems. *Contributions to Primatology* 13: I.

Albrecht, Gene H, Bruce R Gelvin, and S E Hartman. 1993. Ratios as a size adjustment in morphometrics. *American Journal of Physical Anthropology* 91 (4): 441-468.

———. 1995. Ratio adjustments in morphometrics: A reply to dr. Corruccini. *American Journal of Physical Anthropology* 96 (2): 193-197.

Alemseged, Zeresenay, Fred Spoor, William H Kimbel, René Bobe, Denis Geraads, Denné Reed, and Jonathan G Wynn. 2006. A juvenile early hominin skeleton from dikika, ethiopia. *Nature* 443 (7109): 296-301.

Anderson, J S, A W Hsu, and A N Vasavanda. 2005. Morphology, architecture, and biomechanics of human cervical multifudus. *Spine* 30: 86-91.

Ankel, F. 1967. *Morphologie Von Wirbelsäule Und Brustkorb.* Karger.

———. 1970. Einführung in die Primatendkunde. *Gustav Fischer Verlag*. Stuttgart.

———. 1972. Vertebral morphology of fossil and extant primates. *The Functional and Evolutionary Biology of Primates.* Chicago: Aldine. 223-240.

Ankel-Simons, Friderun. 2007. *Postcranial Skeleton, Primate Anatomy An Introduction, 3rd Edi*., Durham, North Carolina. Elsevier.

Antón, Susan C. 2003. Natural history of Homo erectus. *American journal of physical anthropology* 122 (S37): 126-170.

Arnold, Christian, Luke J Matthews, and Charles L Nunn. 2010. The 10ktrees website: A new online resource for primate phylogeny. *Evolutionary Anthropology: Issues, News, and Reviews* 19 (3): 114-118.

Arsuaga, Juan-Luis, Ignacio Martinez, Carlos Lorenzo, Ana Gracia, Alberto Muñoz, Oscar Alonso, and Jesús Gallego. 1999. The human cranial remains from gran dolina lower pleistocene site (sierra de atapuerca, spain). *Journal of Human Evolution* 37 (3): 431-457.

Ashton, E H and C E Oxnard. 1964. Functional adaptations in the primate shoulder girdle. In *Proceedings of the Zoological Society of London* 142 (1): 49-66. Blackwell Publishing Ltd.

Atchley, William R. 1978. Ratios, regression intercepts, and the scaling of data. *Systematic Zoology* 27 (1): 78-83.

Atchley, William R and Dwane Anderson. 1978. Ratios and the statistical analysis of biological data. *Systematic Zoology* 27 (1): 71-78.

Badoux, D M. 1965. A contribution to the study of the body axis in mammals with special reference% o domesticated dogs. *Prec. Ken. Ned. Akad. V. Wetenschappen, C* 68 (5): 374-390.

———. 1967. Some notes on the curvature of the vertebral column in vertebrates with special reference to mammals. *Acta Morphologica Neerlando-Scandinavica* 7 (1): 29-40.

———. 1974. An introduction to biomechanical principles in primate locomotion and structure. *Primate Locomotion* 1-44.

———. 1977. Advances in veterinary biomechanics. *Veterinary Science Communications* 1 (1): 7-15.

Bertram, John E A. 2004. New perspectives on brachiation mechanics. *American Journal of Physical Anthropology* 125 (S39): 100-117.

Bertram, John E A and Young-Hui Chang. 2001. Mechanical energy oscillations of two brachiation gaits: Measurement and simulation. *American Journal of Physical Anthropology* 115 (4): 319-326.

Bianchi, M. 1989. The thickness, shape and arrangement of elastic fibres within the nuchal ligament from various animal species. *Anatomischer Anzeiger* 169: 53-66.

Billmann, Franck, Jean-Marie Le Minor, and Matthias Steinwachs. 2007. Bipartition of the superior articular facets of the first cervical vertebra (atlas or C1): A human variant probably specific among primates. *Annals of Anatomy-Anatomischer Anzeiger* 189 (1): 79-85.

Bilsborough, Alan and Bernard A Wood. 1988. Cranial morphometry of early hominids: Facial region. *American Journal of Physical Anthropology* 76 (1): 61-86.

Bogduk, Nikolai and Susan Mercer. 2000. Biomechanics of the cervical spine. I: Normal kinematics. *Clinical Biomechanics* 15 (9): 633-648.

Bogduk N and L Twomey. 2005. *Clinical anatomy of the lumbar spine and sacrum*. Livingstone: Churchill.

Brain, Charles Kimberlin. 1993. *Swartkrans: A Cave's Chronicle of Early Man.* Transvaal Museum.

Brown, Frank, John Harris, Richard Leakey, and Alan Walker. 1985. Early homo erectus skeleton from west lake turkana, kenya. *Nature* 316 (6031): 788-792.

Brown, Francis H and Ian McDougall. 1993. Geologic setting and age. *The Nariokotome Homo erectus Skeleton*. Harvard University Press, Cambridge: 9-20.

Brown, Peter, Thomas Sutikna, Michael J Morwood, and Raden P Soejono. 2004. A new small-bodied hominin from the late pleistocene of flores, indonesia. *Nature* 431 (7012): 1055-1061.

Byron, Craig D and Herbert H Covert. 2004. Unexpected locomotor behaviour: brachiation by an Old World monkey (Pygathrix nemaeus) from Vietnam. *Journal of Zoology* 263 (1): 101-106.

Carlson, Kristian J and Brigitte Demes. 2010. Gait dynamics of Cebus apella during quadrupedalism on different substrates. *American journal of physical anthropology* 142 (2): 273-286.

Carretero, José Miguel, Carlos Lorenzo, and Juan Luis Arsuaga. 1999. Axial and appendicular skeleton of homo antecessor. *Journal of Human Evolution* 37 (3): 459-499.

Cartmill, Matt and Katharine Milton. 1977. The lorisiform wrist joint and the evolution of "brachiating" adaptations in the hominoidea. *American Journal of Physical Anthropology* 47 (2): 249-272.

Chan, Lap Ki. 2006. Scapular position in primates. *Folia Primatologica* 78 (1): 19-35.

Christian, Andreas and Holger Preuschoft. 1996. Deducing the body posture of extinct large vertebrates from the shape of the vertebral column. *Palaeontology* 39 (4): 801-812.

Christian, Andreas and Wolf-Dieter Heinrich. 1998. The neck posture of brachiosaurus brancai. *Fossil Record* 1 (1): 73-80.

Compere, E L, M O Tachdjian, and W T Kernahan. 1959. The luschka joints: their anatomy, physiology and pathology, *Orthopaedics* 1: 159-168.

Corneil, Brian D, Etienne Olivier, Frances JR Richmond, Gerald E Loeb, and Douglas P Munoz. 2001. Neck muscles in the rhesus monkey. II. Electromyographic patterns of activation underlying postures and movements. *Journal of Neurophysiology* 86 (4): 1729-1749.

Coroner, B D and B Latimer. 1991. Functional analysis of the atlanto-occipital joint in extant African hominoids and early hominids. *Am J Phys Anthropol Supplement* 12: 61.

Cripton, P A. 1999. *Load-sharing in the human cervical spine*. PhD Thesis, Queen's University, Kingston, Ontario, Canada.

Darroch, John N and James E Mosimann. 1985. Canonical and principal components of shape. *Biometrika* 72 (2): 241-252.

Day, M H and R E F Leakey. 1973. New evidence of the genus homo from east rudolf, kenya. I. *American Journal of Physical Anthropology* 39 (3): 341-354.

DeSilva, Jeremy M. 2009. Functional morphology of the ankle and the likelihood of climbing in early hominins. Proceedings of the National Academy of Sciences 106 (16): 6567-6572.

Dean, M C and B A Wood. 1981. Metrical analysis of the basicranium of extant hominoids and Australopithecus. *Am J Phys Anthrop* 54: 63-71.

———. 1982. Basicranial anatomy of Plio-Pleistocene hominids from East and South Africa. *Am J Phys Anthrop* 59: 157-174.

Dean, Christopher, Meave G Leakey, Donald Reid, Friedemann Schrenk, Gary T Schwartz, Christopher Stringer, and Alan Walker. 2001. Growth processes in teeth distinguish modern humans from homo erectus and earlier hominins. *Nature* 414 (6864): 628-631.

Demes B. 1985. Biomechanics of the primate skull base. *Advances in Anatomy, Embryology and Cell Biology* 94: 1-57.

Demes, B, W L Jungers, J G Fleagle, R E Wunderlich, B G. Richmond, and P Lemelin. 1996. Body size and leaping kinematics in Malagasy vertical clingers and leapers. *Journal of Human Evolution* 31 (4): 367-388.

Dickman, Curtis A, Neil R Crawford, Teiji Tominaga, Anna GU Brantley, Stephen Coons, and Volker KH Sonntag. 1994. Morphology and kinematics of the baboon upper cervical spine: A model of the atlantoaxial complex. *Spine* 19 (22): 2518-2523.

Diekhoff, George. 1992. *Statistics for the social and behavioral sciences: Univariate, bivariate, multivariate. Dubuque*, IA: Wm. C. Brown Publishers.

Duarte, Marcos, Jandy Hanna, Evandro Sanches, Qing Liu, and Dorothy Fragaszy. 2012. Kinematics of bipedal locomotion while carrying a load in the arms in bearded capuchin monkeys (Sapajus libidinosus). *Journal of human evolution* 63 (6): 851-858.

Dunbar, Donald C., Gyani L. Badam, Benedikt Hallgrímsson, and Stéphane Vieilledent. 2004. Stabilization and mobility of the head and trunk in wild monkeys during terrestrial and flat-surface walks and gallops. *Journal of experimental biology* 207 (6): 1027-1042.

Dunbar, Donald C, Jane M Macpherson, Roger W Simmons, and Athina Zarcades. 2008. Stabilization and mobility of the head, neck and trunk in horses during overground locomotion: comparisons with humans and other primates. *Journal of Experimental Biology* 211 (24): 3889-3907.

Dvir, Z and N Berme. 1978. The shoulder complex in elevation of the arm: A mechanism approach. *Journal of Biomechanics* 11 (5): 219-225.

Elias, P Z, D Nuckley, and R P Ching. 2006. Effect of loading rate on the compressive mechanics of the immature baboon cervical spine. *Journal of Biomechanical Engineering* 128: 18-24.

English, Arthur W. 1980. The functions of the lumbar spine during stepping in the cat. *Journal of Morphology* 165 (1): 55-66.

Erikson, G E. 1963. Brachiation in new world monkeys and in anthropoid apes. *Symp. Zool. Soc. Lond* 10: 135-164.

Felsenstein, Joseph. 1985. Phylogenies and the comparative method. *American Naturalist* 1-15.

Fielding, J W, A H Burstein, and V H Frankel. 1976. The nuchal ligament. *Spine* 1:3-15.

Fleagle, John. 1974. Dynamics of a brachiating siamang [hylobates (symphalangus) syndactylus. *Nature* 248: 259-260

Fleagle, John G. 1976. Locomotion and posture of the malayan siamang and implications for hominoid evolution. *Folia Primatologica* 26 (4): 245-269.

Fleagle, J G. 1978. Mechanical function of primate clavicles. *Am J Phys Anthrop* 48: 394.

Franz, Theresa M., Brigitte Demes, and Kristian J Carlson. 2005. Gait mechanics of lemurid primates on terrestrial and arboreal substrates. *Journal of human evolution* 48 (2): 199-217.

Freckleton, R P, P H Harvey, and M Pagel. 2002. Phylogenetic analysis and comparative data: A test and review of evidence. *The American Naturalist* 160 (6): 712-726.

Galis, Frietson. 1999. Why do almost all mammals have seven cervical vertebrae? Developmental constraints, hox genes, and cancer. *Journal of Experimental Zoology* 285 (1): 19-26.

Garland, Theodore, Allan Dickerman, Christine Janis, and Jason Jones. 1993. Phylogenetic analysis of covariance by computer simulation. *Systematic Biology* 42: 265-292.

Gebo, Daniel L. 1987. Locomotor diversity in prosimian primates. *American Journal of Primatology* 13: 271-281.

Gebo, Daniel L. 1996. Climbing, brachiation, and terrestrial quadrupedalism: Historical precursors of hominid bipedalism. *American Journal of Physical Anthropology* 101 (1): 55-92.

Glazko, Galina V and Masatoshi Nei. 2003. Estimation of divergence times for major lineages of primate species. *Molecular Biology and Evolution* 20 (3): 424-434.

Gómez-Olivencia, Asier, Ella Been, Juan Luis Arsuaga, and Jay T Stock. 2013. The neandertal vertebral column 1: The cervical spine. *Journal of Human Evolution*. In press.

Gómez-Olivencia, Asier, José Miguel Carretero, Juan Luis Arsuaga, Laura Rodríguez-García, Rebeca García-González, and Ignacio Martínez. 2007. Metric and morphological study of the upper cervical spine from the sima de los huesos site (sierra de atapuerca, burgos, spain). *Journal of Human Evolution* 53 (1): 6-25.

Gommery, Dominique. 2006. Evolution of the vertebral column in Miocene hominoids and Plio-Pleistocene hominids." In *Human Origins and Environmental Backgrounds* 31-43. Springer US.

Goodman, Morris, Calvin A Porter, John Czelusniak, Scott L Page, Horacio Schneider, Jeheskel Shoshani, Gregg Gunnell, and Colin P Groves. 1998. Toward a phylogenetic classification of primates based on DNA evidence complemented by fossil evidence. *Molecular Phylogenetics and Evolution* 9 (3): 585-598.

Gorzitze, A. 1996. Birth-related behaviors in wild proboscis monkeys (*Nasalis larvatus*). *Primates* 37: 75-78.

Graf, W, C De Waele, and P P Vidal. 1995a. Functional anatomy of the head-neck movement system of quadrupedal and bipedal mammals. *Journal of Anatomy* 186 (1): 55.

Graf, W, C De Waele, P P Vidal, D H Wang, and C Evinger. 1995b. The orientation of the cervical vertebral column in unrestrained awake animals (part 1 of 2). *Brain, Behavior and Evolution* 45 (4): 209-220.

Grafen, Alan. 1989. The phylogenetic regression. *Philosophical Transactions of the Royal Society of London. Series B, Biological Sciences* 326 (1233): 119-157.

Green, David J and Zeresenay Alemseged. 2012. Australopithecus afarensis scapular ontogeny, function, and the role of climbing in human evolution. *Science* 338 (6106): 514-517.

Gregory, William K. 1928. Were the ancestors of man primitive brachiators? *Proceedings of the American Philosophical Society* 67 (2): 129-150.

Groves, Clin P. 1970. Population systematics of the gorilla. *Journal of Zoology* 161 (3): 287-300.

Guidotti, Assunta. 1984. Morphometrical considerations on occipital condyles. *Anthropologischer Anzeiger* 117-119.

Harrington Jr, M A, T S Keller, J G Seiler III, D R Weikert, E Moeljanto, and H S Schwartz. 1993. Geometric properties and the predicted mechanical behavior of adult human clavicles. *Journal of Biomechanics* 26 (4): 417-426.

Harvey, Paul H and Mark Pagel. 1991. *Comparative method in evolutionary biology*. Oxford University Press, Oxford, England.

Hasegawa, Masami, Jeffrey L Thorne, and Hirohisa Kishino. 2003. Time scale of eutherian evolution estimated without assuming a constant rate of molecular evolution. *Genes & Genetic Systems* 78 (4): 267-283.

Hayashi, K and T Yabuki. 1985. Origin of the uncus and of luschka's joint in the cervical spine. *The Journal of Bone and Joint Surgery. American Volume* 67 (5): 788.

Heglund, N C. 1984. Comparative energetics and mechanics of locomotion: How do primates fit in? *Size and Scaling in Primate Biology*. Plenum Press, New York. 319–335.

Holm, Sture. 1979. A simple sequentially rejective multiple test procedure. *Scandinavian Journal of Statistics* 65-70.

Howells, William W. 1973. Cranial variation in man. Papers of the Peabody Museum of Archaeology and Ethnology. *Cranial variation in man: Papers from the Peabody Museum of Archaeology and Ethnology* 67.

Hunt, Kevin D, John GH Cant, Daniel L Gebo, Michael D Rose, Suzanne E Walker, and Dionisios Youlatos. 1996. Standardized descriptions of primate locomotor and postural modes. *Primates* 37 (4): 363-387.

Inman, Verne T and LeRoy C Abbott. 1944. Observations on the function of the shoulder joint. *The Journal of Bone & Joint Surgery* 26 (1): 1-30.

Isler, Karin, and Susannah KS Thorpe. 2003. Gait parameters in vertical climbing of captive, rehabilitant and wild Sumatran orang-utans (Pongo pygmaeus abelii). *Journal of experimental biology* 206 (22): 4081-4096.

James, Frances C and Charles E McCulloch. 1990. Multivariate analysis in ecology and systematics: Panacea or pandora's box? *Annual Review of Ecology and Systematics* 21: 129-166.

Jenkins, Farish A. 1971. Limb posture and locomotion in the virginia opossum (didelphis marsupialis) and in other non-cursorial mammals. *Journal of Zoology* 165 (3): 303-315.

Jenkins, Farish A, Philip J Dombrowski, and E P Gordon. 1978. Analysis of the shoulder in brachiating spider monkeys. *American Journal of Physical Anthropology* 48 (1): 65-76.

Johnson, Steig E and Liza J Shapiro. 1998. Positional behavior and vertebral morphology in atelines and cebines. *American Journal of Physical Anthropology* 105 (3): 333-354.

Johnson, G M, M Zhang, and D G Jones. 2000. The fine connective tissue architecture of the human ligamentum nuchae. *Spine* 25 (1): 5-9.

Jungers, William L and J T Stern. 1984. Kinesiological aspects of brachiation in lar gibbons. *The Lesser Apes: Evolutionary and Behavioral Biology* 119-134.

Jungers, William L and Randall L Susman. 1984. Body size and skeletal allometry in african apes. *The Pygmy Chimpanzee.* Springer.

Jungers, William L, Anthony B Falsetti, and Christine E Wall. 1995. Shape, relative size, and size-adjustments in morphometrics. *American Journal of Physical Anthropology* 38 (S21): 137-161.

Jungers, William L, W E H Harcourt-Smith, R E Wunderlich, Matthew W Tocheri, Susan G Larson, Thomas Sutikna, Rhokus Awe Due, and M J Morwood. 2009. The foot of homo floresiensis. *Nature* 459 (7243): 81-84.

Kadri, P A and O Al-Mefty. 2007. Anatomy of the nuchal ligament and its surgical applications. *Neurosurgery* 615: 301-4.

Kapandji, I A. 1974. *The Physiology of the Joints, 2nd edn, vol III: The Trunk and the Vertebral Column*. Churchill Livingstone, Edinburgh London New York.

Kay, Richard F and Matt Cartmill. 1977. Cranial morphology and adaptations of palaechthon nacimienti and other paromomyidae (plesiadapoidea,? Primates), with a description of a new genus and species. *Journal of Human Evolution* 6 (1): 19-53.

Keith, Arthur. 1923. Hunterian lectures on man's posture: Its evolution and disorders: Given at the royal college of surgeons of england. *British Medical Journal* 1 (3251): 669.

Kikuchi, Yasuhiro, Yoshihiko Nakano, Masato Nakatsukasa, Yutaka Kunimatsu, Daisuke Shimizu, Naomichi Ogihara, Hiroshi Tsujikawa, Tomo Takano, and Hidemi Ishida. 2012. Functional morphology and anatomy of cervical vertebrae in nacholapithecus kerioi, a middle miocene hominoid from kenya. *Journal of Human Evolution* 62 (6): 677-695.

Kimbel, William H., and Lucas K. Delezene. 2011. “Lucy” redux: A review of research on Australopithecus afarensis. *American journal of physical anthropology* 140 (49): 2-48.

Klecka, William R. 1980. *Discriminant Analysis.* Sage.

Kurtz, Steven M and Avram Edidin. 2006. *Spine Technology Handbook.* Access Online via Elsevier.

Larson, S G. 1993. Functional morphology of the shoulder in primates. *Postcranial Adaptation in Nonhuman Primates*. 45-69.

———. 1995. New characters for the functional interpretation of primate scapulae and proximal humeri. *American Journal of Physical Anthropology* 98 (1): 13-35.

———. 1998. Parallel evolution in the hominoid trunk and forelimb. *Evolutionary Anthropology: Issues, News, and Reviews* 6 (3): 87-99.

———. 2007. Evolutionary transformation of the hominin shoulder. *Evolutionary Anthropology: Issues, News, and Reviews* 16 (5): 172-187.

Larson, Susan G and Jack T Stern. 1986. EMG of scapulohumeral muscles in the chimpanzee during reaching and "arboreal" locomotion. *American Journal of Anatomy* 176 (2): 171-190.

———. 1987. EMG of chimpanzee shoulder muscles during knuckle-walking: Problems of terrestrial locomotion in a suspensory adapted primate. *Journal of Zoology* 212 (4): 629-655.

Larson, Susan G., and Jack T. Stern. 2007. Humeral retractor EMG during quadrupedal walking in primates. *Journal of Experimental Biology* 210 (7): 1204-1215.

Larson, Susan G, Jack T Stern, and William L Jungers. 1991. EMG of serratus anterior and trapezius in the chimpanzee: Scapular rotators revisited. *American Journal of Physical Anthropology* 85 (1): 71-84.

Larson, Susan G, William L Jungers, Michael J Morwood, Thomas Sutikna, E Wahyu Saptomo, Rokus Awe Due, and Tony Djubiantono. 2007. Homo floresiensis and the evolution of the hominin shoulder. *Journal of Human Evolution* 53 (6): 718-731.

Larson, Susan G, William L Jungers, Matthew W Tocheri, Caley M Orr, Michael J Morwood, Thomas Sutikna, Rokhus Due Awe, and Tony Djubiantono. 2009. Descriptions of the upper limb skeleton of (homo floresiensis). *Journal of Human Evolution* 57 (5): 555-570.

Leakey, L S B. 1960. Recent discoveries at olduvai gorge. *Nature* 188: 1050-1052.

Leakey, R E F and A C Walker. 1985. Further hominids from the plio-pleistocene of koobi fora, kenya. *American Journal of Physical Anthropology* 67 (2): 135-163.

MacKinnon J, and K MacKinnon. 1980. The behavior of wild spectral tarsiers. *Int. J. Primatol* 1: 361-379.

MacLarnon, Ann. 1993. The vertebral canal. *The Nariokotome Homo Erectus Skeleton* 359-390.

Manfreda, Evelyn, Philipp Mitteroecker, Fred L Bookstein, and Katrin Schaefer. 2006. Functional morphology of the first cervical vertebra in humans and nonhuman primates. *The Anatomical Record Part B: The New Anatomist* 289 (5): 184-194.

Martin, R Bruce, David B Burr, and Neil A Sharkey. 1998. *Skeletal Tissue Mechanics*. Springer.

McHenry, Henry M, and Katherine Coffing. 2000. Australopithecus to Homo: transformations in body and mind. *Annual review of Anthropology* 2000: 125-146.

McMahon, Thomas A. 1975. Using body size to understand the structural design of animals: Quadrupedal locomotion. *Journal of Applied Physiology* 39 (4): 619-627.

Mercer, S. 1999. Functional morphology of the lower cervical spine in nonhuman primates. PhD Dissertation. University of Pittsburgh, Pittsburgh.

Mercer, S R and N Bogduk. 2001. Joints of the cervical vertebral column. *The Journal of Orthopaedic and Sports Physical Therapy* 31 (4): 174.

Meyer, Marc R. 2005. *Functional biology of the homo erectus axial skeleton from dmanisi, georgia*. PhD Dissertation, University of Pennsylvania.

Milne, N. 1991. The role of zygapophysial joint orientation and uncinate processes in controlling motion in the cervical spine. *Journal of Anatomy* 178: 189.

Mitchell, B S, B K Humphreys, and E O'Sullivan. 1998. Attachments of the ligamentum nuchae to cervical posterior spinal dura and the lateral part of the occipital bone. *J Manipulative Physiol Ther* 213: 145-148.

Mitteroecker, P, E Manfreda, F L Bookstein, and K Schaefer. 2007. Does the morphology of the human atlas and axis reflect bipedality? A multivariate approach to functional morphology. *American Journal of Physical Anthropology* 172-173.

Moran, Matthew D. 2003. Arguments for rejecting the sequential bonferroni in ecological studies. *Oikos* 100 (2): 403-405.

Mosimann, James E. 1970. Size allometry: Size and shape variables with characterizations of the lognormal and generalized gamma distributions. *Journal of the American Statistical Association* 65 (330): 930-945.

Nagamoto, Yukitaka, Takahiro Ishii, Hironobu Sakaura, Motoki Iwasaki, Hisao Moritomo, Masafumi Kashii, Takako Hattori, Hideki Yoshikawa, and Kazuomi Sugamoto. 2011. In vivo three-dimensional kinematics of the cervical spine during head rotation in patients with cervical spondylosis. *Spine* 36 (10): 778-783.

Nakagawa, Shinichi. 2004. A farewell to bonferroni: The problems of low statistical power and publication bias. *Behavioral Ecology* 15 (6): 1044-1045.

Nakatsukasa, M, Y Kunimatsu, Y Nakano, and H Ishida. 2000. A new skeleton of the large hominoid from Nachola, northern Kenya. *American Journal of Physical Anthropology* 235-235.

Nakatsukasa, Masato, Yutaka Kunimatsu, Yoshihiko Nakano, Tomo Takano, and Hidemi Ishida. 2003. Comparative and functional anatomy of phalanges in Nacholapithecus kerioi, a Middle Miocene hominoid from northern Kenya. *Primates* 44 (4): 371-412.

Nakatsukasa, Masato, Yutaka Kunimatsu, Yoshihiko Nakano, and Hidemi Ishida. 2007. Vertebral morphology of nacholapithecus kerioi based on KNM-BG 35250. *Journal of Human Evolution* 52 (4): 347-369.

Nalley, T K. 2008. *A comparative analysis of the relationship between neck position and atlanto-occipital joint morphology in anthropoids*. Master's thesis. Arizona State University.

O'Rahilly, R, F Müller, and D B Meyer. 1983. The human vertebral column at the end of the embryonic period proper. 2. The occipitocervical region. *Journal of Anatomy* 136 (1): 181.

Oxnard C E, C K Hoylandwilks, and C K Runnion. 1990. Cancellous patterns in human vertebrae – implications for function and disease. *American Journal of Physical Anthropology* 81: 277–277.

Pal, G P and R V Routal. 1986. A study of weight transmission through the cervical and upper thoracic regions of the vertebral column in man. *Journal of Anatomy* 148: 245.

———. 1999. Mechanism of change in the orientation of the articular process of the zygapophyseal joint at the thoracolumbar junction. *Journal of Anatomy* 195 (2): 199-209.

Patel, Biren A, and Roshna E Wunderlich. 2010. Dynamic pressure patterns in the hands of olive baboons (Papio anubis) during terrestrial locomotion: implications for cercopithecoid primate hand morphology. *The Anatomical Record* 293 (4): 710-718

Panjabi, Manohar M, Takeori Oda, Joseph J Crisco, Jiri Dvorak, and Dieter Grob. 1993. Posture affects motion coupling patterns of the upper cervical spine. *Journal of Orthopaedic Research* 11 (4): 525-536.

Paradis, Emmanuel. 2005. Statistical analysis of diversification with species traits. *Evolution* 59 (1): 1-12.

Pedley, Timothy J. 1977. *Scale Effects in Animal Locomotion: Based on the Proceedings of An International Symposium Held at Cambridge University, September, 1975.* Academic Press.

Penning, L. 1968. *Functional Pathology of the Cervical Spine.* Excerpta medica foundation.

Penning, L and J T Wilmink. 1987. Rotation of the cervical spine: A CT study in normal subjects. *Spine* 12 (8): 732-738.

Perneger, Thomas V. 1998. What's wrong with bonferroni adjustments. *BMJ: British Medical Journal* 316 (7139): 1236.

Preuschoft, H. 1978. Recent results concerning the biomechanics of man's acquisition of bipedality. *Recent Advances in Primatology* 3: 435-458.

Preuschoft, H, S Hayama, and M M Günther. 1988. Curvature of the lumbar spine as a consequence of mechanical necessities in japanese macaques trained for bipedalism. *Folia Primatologica* 50 (1-2): 42-58.

Reynolds, Thomas R. 1985. Stresses on the limbs of quadrupedal primates. *American Journal of Physical Anthropology* 67 (4): 351-362.

Rice, William R. 1989. Analyzing tables of statistical tests. *Evolution* 43 (1): 223-225.

Robinson, John Talbot. 1972. *Early Hominid Posture and Locomotion.* University of Chicago Press Chicago.

Rose, M D. 1975. Functional proportions of primate lumbar vertebral bodies. *Journal of Human Evolution* 4 (1): 21-38.

Ross, C F, C A Lockwood, J G Fleagle, and W L Jungers. 2002. Adaptation and behavior in the pirmate fossil record. *Reconstructing behavior in the primate fossil record*. New York: Kluwer Academic. 1-39.

Rudwick, Martin John Spencer. 1964. The inference of function from structure in fossils. *The British Journal for the Philosophy of Science* 15 (57): 27-40.

Ruff, Christopher B, and Alan Walker. 1993. Body size and body shape. *The Nariokotome Homo erectus skeleton*. Harvard University Press 234-265.

Ruff, Christopher B. 2000. Body size, body shape, and long bone strength in modern humans. *Journal of Human Evolution* 38 (2): 269-290.

Russo, Gabrielle A. 2010. Prezygapophyseal articular facet shape in the catarrhine thoracolumbar vertebral column. *American Journal of Physical Anthropology* 142 (4): 600-612.

Russo, Gabrielle A., and E. Christopher Kirk. 2013. Foramen magnum position in bipedal mammals. *Journal of Human Evolution*. In press.

Schultz, Adolph H. 1930. The skeleton of the trunk and limbs of higher primates. *Human Biology* 2 (3): 303-438.

———. 1937. Proportions, variability and asymmetries of the long bones of the limbs and the clavicles in man and apes. *Human Biology* 9 (3): 281-328.

———. 1942. Conditions for balancing the head in primates. *American Journal of Physical Anthropology* 29 (4): 483-497.

———. 1960. *Vertebral Column and Thorax*. Karger Publishers.

———. 1968. The recent hominoid primates. *Perspectives on human evolution* 1: 122-195.

———. 1969. *The life of primates*. London: Weidenfeld & Nicolson.

Senut, Brigitte, Masato Nakatsukasa, Yutaka Kunimatsu, Yoshihiko Nakano, Tomo Takano, Hiroshi Tsujikawa, Daisuke Shimizu, Miyuki Kagaya, and Hidemi Ishida. 2004. Preliminary analysis of nacholapithecus scapula and clavicle from nachola, kenya. *Primates* 45 (2): 97-104.

Shapiro, L. 1993. Functional morphology of the vertebral column in primates. *Postcranial Adaptation in Nonhuman Primates* 121-149.

———. 1995. Functional morphology of indrid lumbar vertebrae. *American Journal of Physical Anthropology* 98 (3): 323-342.

———. 2007. Morphological and functional differentiation in the lumbar spine of lorisids and galagids. *American Journal of Primatology* 69: 86-102.

Shapiro, Liza J, Cornelia VM Seiffert, Laurie R Godfrey, William L Jungers, Elywn L Simons, and Gisèle Randria. 2005. Morphometric analysis of lumbar vertebrae in extinct malagasy strepsirrhines. *American Journal of Physical Anthropology* 128 (4): 823-839.

Shapiro, Liza J and Cornelia VM Simons. 2002. Functional aspects of strepsirrhine lumbar vertebral bodies and spinous processes. *Journal of Human Evolution* 42 (6): 753-783.

Shea, Brian T, Steven R Leigh, and Colin P Groves. 1993. Multivariate craniometric variation in chimpanzees. *Species, Species Concepts, and Primate Evolution* 265-296.

Schmitt, Daniel. 2011. Translating Primate Locomotor Biomechanical Variables from the Laboratory to the Field. *Primate Locomotion* 7-27 Springer:New York.

Schoonaert, Kirsten, Kristiaan D'Août, and Peter Aerts. 2006. A dynamic force analysis system for climbing of large primates. *Folia Primatologica* 77 (3): 246-254.

Singh, S. 1965. Variations of the superior articular facets of atlas vertebrae. *Journal of Anatomy* 99 (3): 565.

Slijper, E.1946. Comparative biologic-anatomical investigations on the vertebral column and spinal musculature of mammals.*Verh K Ned Akad Wet* 42:1–128.

Smith, Richard J. 2009. Use and misuse of the reduced major axis for line-fitting. *American Journal of Physical Anthropology* 140 (3): 476-486.

Smith, Richard J., and James M. Cheverud. 2002. Scaling of sexual dimorphism in body mass: a phylogenetic analysis of Rensch's rule in primates. *International Journal of Primatology* 23 (5): 1095-1135.

Smith, Richard J and William L. Jungers. 1997. Body mass in comparative primatology. *Journal of Human Evolution* 32 (6): 523-559.

Sokal, R R and F J Rohlf. 1995. *Biometry* New York. NY: WH Freeman & Co.

Spencer, Mark A. 2003. Tooth-root form and function in platyrrhine seed-eaters. *American Journal of Physical Anthropology* 122 (4): 325-335.

Stern Jr, Jack T and Randall L Susman. 1983. The locomotor anatomy of australopithecus afarensis. *American Journal of Physical Anthropology* 60 (3): 279-317.

Strait, D S and Ross C F. 1999. Kinematic data on primate head and neck posture: implications for the evolution of basicranial flexion and an evaluation of registration planes used in paleoanthropology. *American Journal of Physical Anthropology* 108: 205-222.

Susman, Randall L, J T Stern Jr, and William L Jungers. 1984. Arboreality and bipedality in the hadar hominids. *Folia Primatologica* 43 (2-3): 113-156.

Susman, R L. 1993. Hominid postcranial remains from Swartkrans. In (C. K. Brain, Ed.) *A Cave's Chronicle of Early Man*, 117–136. Pretoria: South Africa.

Susman, Randall L, Darryl de Ruiter, and C K Brain. 2001. Recently identified postcranial remains of paranthropus and early homo from swartkrans cave, south africa. *Journal of Human Evolution* 41 (6): 607-629.

Swindler, Daris Ray and Charles D Wood. 1982. *An Atlas of Primate Gross Anatomy: Baboon, Chimpanzee, and Man.* RE Krieger Publishing Company.

Tabachnick, Barbara G, Linda S Fidell, and Steven J Osterlind. 2001. Using multivariate statistics. Harper & Row, New York.

Tocheri, Matthew W, Caley M Orr, Susan G Larson, Thomas Sutikna, E Wahyu Saptomo, Rokus Awe Due, Tony Djubiantono, Michael J Morwood, and William L Jungers. 2007. The primitive wrist of homo floresiensis and its implications for hominin evolution. *Science* 317 (5845): 1743-1745.

Toerien, M J. 1961. The length and inclination of the primate cervical spinous processes. *Transactions of the Royal Society of South Africa* 36 (2): 95-105.

Togasaki, Daniel M, Albert Hsu, Meghana Samant, Bijan Farzan, Louis E DeLanney, J. William Langston, Donato A. Di Monte, and Maryka Quik. The Webcam system: a simple, automated, computer-based video system for quantitative measurement of movement in nonhuman primates. *Journal of neuroscience methods* 145 (1): 159-166.

Tominaga, Teiji, Curtis A Dickman, Volker K H Sonntag, and Stephen Coons. 1995. Comparative anatomy of the baboon and the human cervical spine. *Spine* 20 (2): 131-137.

Tondury, G. 1959. La colonne cervicale, son developpement et ses modifications durant la vie. *Acta Orthop. Belg* 25: 602-26.

Trinkaus, Erik. 1983. Neandertal postcrania and the adaptive shift to modern humans. *The Mousterian Legacy: Human Biocultural Change in the Upper Pleistocene* 164: 165-200.

Tuttle, Russell H. 1969. Knuckle-walking and the problem of human origins. *Science* 166 (3908): 953-961.

Voisin, Jean-Luc. 2006. Clavicle, a neglected bone: Morphology and relation to arm movements and shoulder architecture in primates. *The Anatomical Record Part A: Discoveries in Molecular, Cellular, and Evolutionary Biology* 288 (9): 944-953.

Voisin, J L and A Balzeau. 2004. Internal structures of the clavicle. Method and preliminary results on pan, gorilla and homo. *Bull Mém Soc Anthrop* 16: 5-16.

Vrba, E S. 1979. A new study of the scapula of australopithecus africanus from sterkfontein. *American Journal of Physical Anthropology* 51 (1): 117-129.

Ward, Carol V. 1991. *Functional anatomy of the lower back and pelvis of the miocene hominoid proconsul nyanzae from mfangano island, kenya*. PhD Dissertation. Johns Hopkins University.

———. 1993. Torso morphology and locomotion in proconsul nyanzae. *American Journal of Physical Anthropology* 92 (3): 291-328.

Ward, Carol V, William H Kimbel, Elizabeth H Harmon, and Donald C Johanson. 2012. New postcranial fossils of Australopithecus afarensis from Hadar, Ethiopia (1990–2007). *Journal of human evolution* 63 (1): 1-51.

Walker, Alan, and Richard Erskine Leakey. 1993. eds. *The Nariokotome Homo erectus skeleton*. Harvard University Press.

Walter, Robert C. 1994. Age of Lucy and the First Family: Single-crystal 40Ar/39Ar dating of the Denen Dora and lower Kada Hadar members of the Hadar Formation, Ethiopia. *Geology* 22 (1): 6-10.

Warton, David I, Ian J Wright, Daniel S Falster, and Mark Westoby. 2006. Bivariate line-fitting methods for allometry. *Biological Reviews* 81 (2): 259-291.

Womack, Wesley, P. Devin Leahy, Vikas V. Patel, and Christian M. Puttlitz. 2011. Finite element modeling of kinematic and load transmission alterations due to cervical intervertebral disc replacement. *Spine* 36 (17): 1126-1133.

Wood, B A. 1991. *Koobi Fora Research Project IV: Hominid Cranial Remains From Koobi Fora*. Oxford, UK.

White, Augustus A and Manohar M Panjabi. 1990. *Clinical Biomechanics of the Spine.* Lippincott Philadelphia.

Whyne, C M, S S Hu, S Klisch, and J C Lotz. 1998. Effect of the pedicle and posterior arch on vertebral body strength predictions in finite element modeling. *Spine* 23: 899-907.

Yeager, C P. 1990. Proboscis monkey (*Nasalis larvatus*) social organization: group structure. *Am. J. Primatol* 20: 95-106.

Yoganandan, Narayan, Dennis J Maiman, Frank Pintar, Gautam Ray, Joel B Myklebust, Anthony Sances Jr, and Sanford J Larson. 1988. Microtrauma in the lumbar spine: A cause of low back pain. *Neurosurgery* 23 (2): 162-168.

Yoganandan, Narayan, Srirangam Kumaresan, and Frank A Pintar. 2001. Biomechanics of the cervical spine part 2. Cervical spine soft tissue responses and biomechanical modeling. *Clinical Biomechanics* 16 (1): 1-27.

Young, Nathan M. 2008. A comparison of the ontogeny of shape variation in the anthropoid scapula: Functional and phylogenetic signal. *American Journal of Physical Anthropology* 136 (3): 247-264.

Zomlefer, M R, J Provencher, G Blanchette, and S Rossignol. 1984. Electromyographic study of lumbar back muscles during locomotion in acute high decerebrate and in low spinal cats. *Brain Research* 290 (2): 249-260.

APPENDIX A

EXTANT OSTEOLOGICAL SAMPLE FOR COMPARATIVE MORPHOMETRICS

Species	Wild	Zoo	Unk*	Total N	Body mass (kg)	Body mass source
Alouatta caraya. n=2						
male	1			1	6.42	Smith and Jungers, 1997
female	1			1	4.33	Smith and Jungers, 1997
unknown sex						
Alouatta guariba. n=2						
male						
female	2			2	4.55	Smith and Jungers, 1997
unknown sex						
Alouatta palliata. n=16						
male	9			9	7.15	Smith and Jungers, 1997
female	4		1	5	5.35	Smith and Jungers, 1997
unknown sex	2			2		
Alouatta seniculus. n=1						
male	1			1	6.69	Smith and Jungers, 1997
female						
unknown sex						
Ateles fusiceps, n=13						
male	9			9	8.89	Smith and Jungers, 1997
female	4			4	9.16	Smith and Jungers, 1997
unknown sex						
Ateles geoffroyi, n=7						
male			1	1	7.78	Smith and Jungers, 1997
female	2	2		4	7.29	Smith and Jungers, 1997
unknown sex	1	1		2	7.54	
Avahi laniger, n=8						
male	3			3	1.03	Smith and Jungers, 1997
female	1			1	1.32	Smith and Jungers, 1997
unknown sex	4			4	1.18	
Cebus apella, n=19						
male	11		1	12	3.65	Smith and Jungers, 1997
female	4	3		7	2.52	Smith and Jungers, 1997
unknown sex						
Cercocebus torquatus, n=7						
male	2	1		3	9.47	Smith and Jungers, 1997
female	3			3	5.5	Smith and Jungers, 1997
unknown sex			1	1	7.49	
Cercopithecus mitis, n=21						
male	11			11	5.85	Smith and Cheverud, 2002
female	10			10	3.93	Smith and Cheverud, 2002
unknown sex						
Chlorocebus aethiops, n=14						
male	3	4	1	8	4.26	Smith and Cheverud, 2002
female	1	5		6	2.98	Smith and Cheverud, 2002
unknown sex						
Chlorocebus pygerythrus, n=14						
male	1	1		8	4.26	Smith and Cheverud, 2002
female	2			6	2.98	Smith and Cheverud, 2002
unknown sex						
Colobus guereza, n=21						
male	12			12	9.89	Smith and Cheverud, 2002
female	7			7	7.9	Smith and Cheverud, 2002
unknown sex	2			2	8.9	
Erythrocebus patas, n=8						
male	3	2		5	12.4	Smith and Jungers, 1997
female	1	2		3	6.5	Smith and Jungers, 1997
unknown sex						
Gorilla beringei, n=13						
male	8			8	162.5	Smith and Cheverud, 2002
female	5			5	97.5	Smith and Cheverud, 2002
unknown sex						

Gorilla g. gorilla, n=10						
male	5			5	169.3	Smith and Cheverud, 2002
female	5			5	75.7	Smith and Cheverud, 2002
unknown sex						
Hapalemur griseus, n=8						
male	1			1	0.987	Smith and Cheverud, 2002
female	6	1		7	0.903	Smith and Cheverud, 2002
unknown sex						
Homo sapiens, n=20						
male	10			10	60.2	Smith and Cheverud, 2002
female	10			10	53.6	Smith and Cheverud, 2002
unknown sex						
Hylobates agilis, n=1						
male						
female			1	1	5.82	Smith and Jungers, 1997
unknown sex						
Hylobates albibarbis, n=4						
male	2			2	5.7	Smith and Jungers, 1997
female	2			2	5.3	Smith and Jungers, 1997
unknown sex						
Hylobates klossii, n=2						
male	1			1	5.67	Smith and Jungers, 1997
female	1			1	5.92	Smith and Jungers, 1997
unknown sex						
Hylobates lar, n=3						
male	1			1	5.67	Smith and Jungers, 1997
female	1			1	5.92	Smith and Jungers, 1997
unknown sex	1			1	5.62	
Hylobates moloch, n=2						
male	1			1	6.58	Smith and Jungers, 1997
female		1		1	6.03	Smith and Jungers, 1997
unknown sex						
Hylobates muelleri, n=5						
male	2			2	5.71	Smith and Jungers, 1997
female	3			3	5.35	Smith and Jungers, 1997
unknown sex						
Indri indri, n=9						
male	1	1		2	5.83	Smith and Jungers, 1997
female	1			1	6.84	Smith and Jungers, 1997
unknown sex	6			6	6.33	
Lemur catta, n=13						
male	5		2	7	2.21	Smith and Jungers, 1997
female		4		4	2.21	Smith and Jungers, 1997
unknown sex	2			2	2.21	
Lepilemur mustelinus, n=18						
male	4			4	0.78	Smith and Jungers, 1997
female	9			9	0.78	Smith and Jungers, 1997
unknown sex						
Macaca fuscata, n=5						
male	2	1		3	11	Smith and Jungers, 1997
female	2			2	8.03	Smith and Jungers, 1997
unknown sex						
Macaca nemestrina, n=8						
male	4	2	1	7	11.2	Smith and Jungers, 1997
female	1			1	6.5	Smith and Jungers, 1997
unknown sex						
Macaca nigra, n=4						
male			2	2	9.89	Smith and Jungers, 1997
female			1	1	5.47	Smith and Jungers, 1997
unknown sex			1	1	7.68	
Macaca tonkeana, n=3						
male		3		3	14.9	Smith and Jungers, 1997
female						
unknown sex						
Mandrillus sphinx, n=13						

male	7	3	1	11	31.6	Smith and Jungers, 1997
female	2			2	12.9	Smith and Jungers, 1997
unknown sex						
Miopithecus talapoin, n=9						
male	1			1	1.38	Smith and Cheverud, 2002
female	2	3	1	6	1.12	Smith and Cheverud, 2002
unknown sex	1	1		2	1.25	
Nasalis larvatus, n=19						
male	15		1	16	20.4	Smith and Jungers, 1997
female	3			3	9.82	Smith and Jungers, 1997
unknown sex						
Nomascus concolor, n=2						
male			1	1	7.62	Smith and Jungers, 1997
female	1			1	7.79	Smith and Jungers, 1997
unknown sex						
Nomascus leucogenys, n=3						
male						
female		1		1	7.32	Smith and Jungers, 1997
unknown sex	1		1	2	7.37	
Pan t. troglodytes, n=21						
male	9		1	10	59.7	Smith and Cheverud, 2002
female	9			9	45.8	Smith and Cheverud, 2002
unknown sex			1	1	52.8	
Papio anubis, n=21						
male	8		1	9	25.1	Smith and Jungers, 1997
female	7			7	13.3	Smith and Jungers, 1997
unknown sex	5			5	19.2	
Pithecia pithecia, n=19						
male	13			13	1.94	Smith and Jungers, 1997
female	3		1	4	1.58	Smith and Jungers, 1997
unknown sex	1		1	2		
Pithecia irrorato, n=1						
male	1			1	2.25	Smith and Jungers, 1997
female						
unknown sex						
Pongo pygmaeus, n=22						
male	9	1		10	78.3	Smith and Cheverud, 2002
female	8	1	2	11	35.8	Smith and Cheverud, 2002
unknown sex			1	1	57.1	
Propithecus diadema, n=4						
male						
female	2			2	6.26	Smith and Jungers, 1997
unknown sex	2			2	6.1	
Propithecus verrauxi, n=15						
male	4	1		5	3.25	Smith and Jungers, 1997
female	6			6	2.95	Smith and Jungers, 1997
unknown sex	4			4	3.1	
Pygathrix nemaeus, n=6						
male	4			4	11	Smith and Cheverud, 2002
female	1	1		2	8.44	Smith and Cheverud, 2002
unknown sex						
Rhinopithecus roxellana, n=4						
male						
female	4			4	11.6	Smith and Cheverud, 2002
unknown sex						
Semopithecus entellus, n=6						
male	2	1		3	11.4	Smith and Cheverud, 2002
female		3		3	6.91	Smith and Cheverud, 2002
unknown sex						
Symphalangus syndactylus n=6						
male	1			1		
female	4		1	5		
unknown sex						
Tarsius bancanus, n=3						
male			1	1	0.128	Smith and Jungers, 1997

female			2	2	0.117	Smith and Jungers, 1997
unknown sex						
Tarsius syrichta, n=13						
male	1	8		9	0.134	Smith and Jungers, 1997
female						
unknown sex	1	3		4	0.128	
Theropithecus gelada, n=8						
male	1	1	2	4	19	Smith and Jungers, 1997
female	2	1	1	4	11.7	Smith and Jungers, 1997
unknown sex						
Varecia v. varigata, n=13						
male		3		3	3.47	Smith and Cheverud, 2002
female	2	5		7	3.51	Smith and Cheverud, 2002
unknown sex	1	1	1	3	3.49	
Total sample size	367	72	34	483		

APPENDIX B

SUMMARY STATISTIC TABLE OF EXTANT FEMALE VERTEBRAL METRICS

TABLE X. Summary statistics for vertebral metrics in females

C1		GM	VBVL	VBDL	VB ECC	UNC	SPL	ATPL	PTPL	PCSA	LCSA	SCSA	TPAA	TPPA	AFA
Alouatta caraya	n	1					1		1	1	1			1	
	mean	26.91					1.66		30.56	21.53	10.28			76.61	
	sd	-					-		-	-	-			-	
Alouatta guariba	n	2					0		1	1	1			1	
	mean	27.59					-		28.17	24.32	4.94			76.11	
	sd	0.4					-		-	-	-			-	
Alouatta palliata	n	4					4		4	4	4			4	
	mean	28.42					1.82		31.07	21.43	8.78			75.13	
	sd	0.96					1		3.09	6.38	2.28			2.69	
Alouatta seniculus	n														
	mean														
	sd														
Ateles fusciceps	n	2					2		2	2	2			5	
	mean	32.40					2.21		37.18	17.19	12.39			70.96	
	sd	0.98					0.01		0.78	1.39	0.42			2.75	
Ateles geoffroyi	n	4					4		4	3	4			2	
	mean	30.89					1.80		34.37	15.10	11.97			69.18	
	sd	1.28					0.33		2.59	5.24	5.51			3.56	
Avahi laniger	n	1					1		1	1	1			1	
	mean	15.44					0.85		22.18	3.50	2.14			72.81	
	sd	-					-		-	-	-			-	
Cebus apella	n	12					12		12	12	12			8	
	mean	26.42					1.08		25.63	11.09	4.41			67.78	
	sd	1.1					0.31		1.57	2.71	0.98			3.59	
Cercocebus torquatus	n	2					2		2	2	2			3	
	mean	30.11					1.77		29.60	13.43	6.07			65.45	
	sd	2.2					0.34		3.58	2.38	1.04			5.13	
Cercopithecus mitis	n	7					7		6	7	7			10	
	mean	28.30					1.02		30.46	12.27	5.75			63.65	
	sd	3.07					0.13		1.85	2.27	2.11			6.42	
Chlorocebus aethiops	n	3					3		3	3	3			4	
	mean	26.28					1.58		30.46	15.59	4.83			70.09	
	sd	1.79					0.27		0.57	4.76	0.98			0.96	
Chlorocebus pygerythrus	n	2					2		2	2	2			2	
	mean	28.26					1.39		30.30	11.90	5.54			69.43	
	sd	0.09					0.08		0.04	2.74	0.03			1.83	
Colobus guereza	n	4					4		4	4	4			6	
	mean	32.86					1.34		36.91	22.82	4.74			73.89	

	sd	1.45	0.45	2.54	5.05	2.13	4.80
Erythrocebus patas	n	2	2	2	2	2	2
	mean	31.89	1.76	33.08	16.54	6.45	65.28
	sd	0.94	0.30	0.23	0.2	1.78	2.04
Gorilla beringei	n	3	3	3	3	3	5
	mean	64.93	8.76	74.55	144.36	49.94	72.84
	sd	0.64	1.43	3.35	16.41	3.50	4.16
Gorilla g. gorilla	n	3	3	3	3	3	3
	mean	62.62	4.41	67.23	89.13	33.54	69.30
	sd	2.87	1.47	4.6	22.80	8.30	6.74
Hapalemur griseus	n	6	7	7	7	7	8
	mean	18.84	1.06	21.66	3.01	3.87	66.04
	sd	0.32	0.21	0.89	0.54	0.94	6.19
Homo sapiens	n	9	9	8	9	9	10
	mean	62.16	5.99	66.63	54.49	28.08	58.20
	sd	1.97	1.31	3.22	11.54	9.50	4.20
Hylobates agilis	n						
	mean						
	sd						
Hylobates klossii	n	1	1	1	1	1	1
	mean	30.04	1.17	31.64	11.36	3.11	66.90
	sd	-	-	-	-	-	-
Hylobates lar	n	1	1	1	1	1	1
	mean	33.32	3.75	34.70	14.49	3.80	62.84
	sd	-	-	-	-	-	-
Hylobates muelleri	n	4	3	2	3	3	5
	mean	31.61	2.55	37.75	10.34	7.76	64.88
	sd	0.81	0.62	0.71	0.62	0.96	7.70
Indri indri	n	4	4	4	4	4	1
	mean	27.68	3.42	36.89	14.99	17.94	68.69
	sd	0.87	2.32	2.55	2.54	4.43	-
Lemur catta	n	4	4	4	4	4	4
	mean	22.04	1.61	28.24	5.00	7.76	65.96
	sd	0.18	0.42	1.06	1.07	1.62	2.11
Lepilemur mustelinus	n	12	12	12	12	12	14
	mean	14.99	0.90	17.69	3.24	3.54	66.14
	sd	1.13	0.14	0.97	0.53	0.91	5.07
Macaca fuscata	n	2	2	2	2	2	2
	mean	33.74	1.77	31.12	32.22	9.16	66.14
	sd	2.69	0.12	0.81	2.63	3.12	3.97
Macaca nemestrina	n	1	1	1	1	1	1
	mean	35.18	1.54	33.18	26.94	4.54	74.24
	sd	-	-	-	-	-	-

Macaca nigra	n	1	1	1	1	1	1
	mean	32.62	1.82	31.61	32.50	6.45	72.37
	sd	-	-	-	-	-	-
Macaca tonkeana	n						
	mean						
	sd						
Mandrillus sphinx	n	2	2	2	2	2	2
	mean	39.58	2.00	40.84	32.82	9.87	69.79
	sd	0.16	0.71	1.9	3.75	2.11	5.98
Miopithecus talapoin	n	4	3	3	4	4	6
	mean	21.50	0.67	19.28	5.97	1.37	62.33
	sd	1.69	0.10	0.57	1.43	0.34	5.58
Nasalis larvatus	n	3	3	3	3	3	3
	mean	32.06	1.05	35.70	33.00	7.34	66.76
	sd	1.96	0.52	2.11	15.86	0.24	3.79
Nomascus concolor	n	1	1	1	1	1	1
	mean	33.83	2.70	39.92	22.47	13.01	61.08
	sd	-	-	-	-	-	-
Nomascus leucogenys	n	1	1	1	1	1	1
	mean	34.46	1.65	40.88	14.66	7.76	68.31
	sd	-	-	-	-	-	-
Pan t. troglodytes	n	8	6	6	6	6	7
	mean	54.37	5.24	60.12	46.17	24.75	67.63
	sd	3.45	2.12	1.85	9.86	5.72	3.42
Papio anubis	n	6	5	6	6	6	6
	mean	43.27	3.00	48.09	40.65	16.08	69.88
	sd	1.92	0.78	3.34	10.53	5.32	3.60
Pithecia irrorata	n						
	mean						
	sd						
Pithecia pithecia	n	3	3	3	3	3	4
	mean	20.98	1.38	22.67	8.94	5.49	70.07
	sd	0.64	0.32	0.86	2.03	1.08	4.47
Pongo pygmaeus	n	9	9	9	9	9	9
	mean	56.19	4.31	57.64	59.59	31.86	70.70
	sd	3.11	1.62	3.75	21.16	12.91	6.70
Propithecus diadema	n	3	3	3	2	2	1
	mean	25.76	1.80	32.22	9.23	8.71	72.36
	sd	2.24	0.56	6.68	6.38	3.28	-
Propithecus verreauxi	n	4	4	4	3	4	5
	mean	22.51	2.17	31.21	8.81	11.79	66.62

	sd	6.91	0.74	1.35	0.93	2.82		3.26	
Pygathrix nemaeus	n	2	2	2	2	2		2	
	mean	30.34	2.29	30.69	14.76	11.54		64.08	
	sd	2.71	1.18	2.5	7.53	5.16		3.83	
Rhinopithecus roxellana	n	3	3	3	3	3		3	
	mean	37.84	1.67	33.92	16.9	5.78		71.43	
	sd	3.73	0.59	0.49	3.79	2.50		2.31	
Semnopithecus entellus	n	2	2	2	2	2		2	
	mean	28.61	1.36	30.45	18.54	6.02		71.16	
	sd	0.02	0.16	0.07	4.42	1.62		6.41	
Symphalangus syndactylus	n	3	3	3	3	3		3	
	mean	38.28	2.61	43.83	18.92	17.08		69.46	
	sd	0.14	0.53	3.58	1.89	4.77		6.74	
Tarsius bancanus	n	2	2	2	0	2		2	
	mean	12.73	0.80	12.95	-	9.07		71.15	
	sd	0.09	0.02	0.04	-	2.56		13.13	
Tarsius syrichta	n								
	mean								
	sd								
Theropithecus gelada	n	2	2	2	2	2		3	
	mean	39.68	1.77	40.89	31.46	10.47		75.37	
	sd	0.31	0.47	0.01	3.76	7.18		3.00	
Varecia v. variegata	n	4	4	4	4	4		5	
	mean	26.09	1.81	32.83	11.31	13.29		65.94	
	sd	0.31	0.21	1.2	6.82	6.13		4.13	

C2		**GM**	**VBVL**	**VBDL**	**VB ECC**	**UNC**	**SPL**	**ATPL**	**PTPL**	**PCSA**	**LCSA**	**SCSA**	**TPAA**	**TPPA**	**AFA**
Alouatta caraya	n	1		0	1		1	1	1	1	1	1		1	
	mean	24.79		-	12.08		25.71	14.47	10.58	34.52				45.58	
	sd	-		-	-		-	-	-	-				-	
Alouatta guariba	n	2		2	2		1	2	2	2	2	2		2	
	mean	26.78		0.88	9.21		21.04	6.52	7.95	25.95				52.15	
	sd	0.74		0.01	0.01		-	2.08	1.98	1.76				5.78	
Alouatta palliata	n	4		4	4		4	4	4	4	4	4		4	
	mean	25.99		1.06	9.06		24.24	8.91	9.49	30.68				59.25	
	sd	0.77		0.07	2.12		1.83	2.81	3.50	10.95				2.36	
Alouatta seniculus	n														
	mean														
	sd														
Ateles	n	3		3	3		3	3	3	3	3	3		5	

fusciceps									
	mean	28.77	0.80	11.95	25.96	16.42	13.79	29.99	62.27
	sd	0.85	0.08	1.32	0.06	2.18	2.61	3.74	5.31
Ateles geoffroyi	n	3	3	3	3	3	3	3	2
	mean	27.99	1.05	10.97	24.05	10.44	11.21	25.44	62.34
	sd	0.38	0.13	1.82	1.15	2.28	3.08	3.50	3.94
Avahi laniger	n	1	1	1	1	1	1	1	1
	mean	15.32	1.1	4.41	12.39	3.75	2.97	7.99	49.24
	sd	-	-	-	-	-	-	-	-
Cebus apella	n	5	4	5	5	4	5	5	7
	mean	24.53	0.74	6.09	19.54	5.16	4.69	13.41	65.09
	sd	0.8	0.08	0.53	1.11	1.36	0.91	2.55	25.33
Cercocebus torquatus	n	2	2	2	1	2	2	2	3
	mean	28.09	0.96	7.17	20.89	6.75	7.42	12.81	55.08
	sd	1.92	0.17	1.82	-	4.14	2.85	1.27	10.10
Cercopithecus mitis	n	8	8	8	7	8	8	8	9
	mean	25.42	0.85	6.35	22.59	8.59	6.50	18.05	50.69
	sd	3.63	0.06	1.21	1.77	2.47	2.88	2.56	3.72
Chlorocebus aethiops	n	3	3	3	3	3	3	3	5
	mean	24.34	0.95	6.73	19.37	9.22	5.87	15.02	48.05
	sd	1.49	0.15	0.42	1.35	1.65	0.91	2.66	2.90
Chlorocebus pygerythrus	n	2	2	2	2	2	2	2	2
	mean	26.13	0.97	6.85	18.34	9.96	5.74	11.89	46.48
	sd	0.08	0.06	0.24	0.47	2.12	1.27	5.18	2.25
Colobus guereza	n	4	4	4	4	4	4	4	5
	mean	30.06	0.91	9.36	25.09	10.61	10.30	19.33	50.39
	sd	1.27	0.22	1.48	2.22	3.18	2.72	9.76	5.42
Erythrocebus patas	n	2	2	2	2	2	2	2	3
	mean	29.52	1.10	9.63	22.79	12.02	10.87	16.45	52.17
	sd	0.71	0.18	0.8	1.73	5.28	2.45	1.32	3.82
Gorilla beringei	n	3	3	3	3	3	3	3	5
	mean	59.89	0.84	25.74	52.48	75.40	77.14	116.13	50.90
	sd	1.82	0.13	2.87	2.02	4.26	17.03	47.08	2.56
Gorilla g. gorilla	n	5	5	5	5	5	5	5	5
	mean	57.88	0.97	20.17	50.25	43.19	44.59	65.40	49.39
	sd	2.1	0.18	2.06	2.02	2.91	7.71	19.58	3.37
Hapalemur griseus	n	7	8	8	7	7	8	7	8
	mean	17.32	0.84	4.75	12.29	4.31	3.41	8.57	56.99
	sd	0.38	0.19	0.75	0.50	0.28	0.59	1.25	2.16
Homo sapiens	n	9	9	9	8	9	9	9	10
	mean	58.06	0.83	14.30	47.22	40.83	43.22	148.14	56.58
	sd	1.9	0.07	1.67	2.21	18.04	14.49	31.30	4.75
Hylobates	n	1	1	1	1	1	1	1	1

agilis										
	mean	30.23		1.08	10.23	27.00	6.63	14.76	21.25	53.75
	sd	-		-	-	-	-	-	-	-
Hylobates klossii	n	1		1	1	1	1	1	1	1
	mean	28.09		0.99	6.05	17.92	8.05	3.46	17.17	47.47
	sd	-		-	-	-	-	-	-	-
Hylobates lar	n	1		1	1	1	1	1	1	1
	mean	30.86		0.91	8.17	24.39	14.17	7.01	28.49	50.28
	sd	-		-	-	-	-	-	-	-
Hylobates muelleri	n	4		4	4	2	4	4	4	4
	mean	29.21		0.99	7.10	21.43	14.54	7.74	18.97	47.69
	sd	1.10		0.08	0.72	0.20	3.41	1.69	4.66	2.68
Indri indri	n	1		1	1	1	1	1	1	1
	mean	25.04		1.16	9.73	21.89	18.61	22.08	24.73	61.60
	sd	-		-	-	-	-	-	-	-
Lemur catta	n	4		3	4	4	3	4	3	4
	mean	20.62		0.75	5.62	15.97	9.71	8.47	17.20	57.58
	sd	0.32		0.12	0.25	0.73	0.60	3.27	2.72	4.50
Lepilemur mustelinus	n	12		8	12	12	9	12	12	14
	mean	13.59		0.98	3.79	10.20	2.81	2.47	6.21	53.48
	sd	1.00		0.12	0.37	0.68	0.52	0.59	1.78	4.88
Macaca fuscata	n	2		2	2	2	2	2	2	2
	mean	31.72		1.08	9.39	22.63	16.30	12.95	17.48	47.41
	sd	3.61		0.28	0.52	2.04	0.22	0.10	7.90	0.21
Macaca nemestrina	n	1		1	1	1	1	1	1	1
	mean	32.86		1.04	9.76	24.29	13.99	12.67	15.70	56.88
	sd	-		-	-	-	-	-	-	-
Macaca nigra	n	1		1	1	1	0	1	1	1
	mean	30.95		1.21	9.29	21.18	-	9.60	10.53	46.43
	sd	-		-	-	-	-	-	-	-
Macaca tonkeana	n									
	mean									
	sd									
Mandrillus sphinx	n	2		2	2	2	2	2	2	2
	mean	36.61		1.21	11.8	27.82	14.78	9.97	19.93	51.88
	sd	0.08		0.17	1.63	0.58	1.69	1.41	8.73	2.92
Miopithecus talapoin	n	4		4	4	4	4	4	4	6
	mean	19.63		0.93	3.04	12.86	2.77	2.38	4.44	49.08
	sd	0.21		0.07	0.4	0.31	0.54	0.51	1.03	7.14
Nasalis larvatus	n	3		2	3	3	2	3	3	3
	mean	31.09		1.1	8.19	21.82	13.89	11.50	15.29	46.45
	sd	3.64		0.12	1.18	2.84	3.46	0.50	1.27	3.89
Nomascus concolor	n	1		1	1	1	1	1	1	1

	mean	30.93	0.76	8.88	26.41	17.39	13.41	42.30	48.99
	sd	-	-	-	-	-	-	-	-
Nomascus leucogenys	n	1	1	1	1	1	1	1	1
	mean	32.53	0.67	10.26	24.36	12.31	11.85	17.25	47.25
	sd	-	-	-	-	-	-	-	-
Pan t. troglodytes	n	9	9	9	9	9	9	9	8
	mean	50.56	0.87	15.01	40.34	39.63	35.91	70.44	52.38
	sd	2.04	0.14	1.93	2.91	9.32	6.32	31.24	5.77
Papio anubis	n	6	6	6	6	6	6	6	6
	mean	38.85	1.11	14.04	30.84	19.24	17.33	30.28	49.97
	sd	2	0.12	1.04	2.76	6.13	3.37	4.43	5.02
Pithecia irrorata	n								
	mean								
	sd								
Pithecia pithecia	n	4	3	4	4	2	4	4	4
	mean	19.15	0.78	4.88	17.57	7.21	4.13	8.90	49.51
	sd	0.57	0.1	1.56	0.66	3.24	0.85	4.44	8.21
Pongo pygmaeus	n	9	8	9	7	9	9	9	9
	mean	51.86	0.89	24.19	45.18	53.54	31.39	64.86	53.59
	sd	3.15	0.14	4.08	4.37	13.18	9.55	23.67	3.99
Propithecus diadema	n	2	2	2	2	2	2	2	1
	mean	24.24	1.00	6.78	19.45	11.81	8.27	16.86	51.83
	sd	2.53	0.22	1.86	4.59	6.40	1.24	8.78	-
Propithecus verreauxi	n	4	5	6	6	5	6	6	6
	mean	23.34	1.09	6.96	16.87	7.67	5.60	19.79	52.16
	sd	1.72	0.11	0.79	1.30	3.65	1.89	2.37	5.46
Pygathrix nemaeus	n	2	2	2	2	2	2	2	2
	mean	27.41	1.08	8.18	18.44	8.98	6.64	19.32	46.85
	sd	3.37	0.05	0.04	0.68	3.37	1.42	2.33	7.78
Rhinopithecus roxellana	n	4	4	4	4	4	4	4	4
	mean	33.30	0.97	9.66	23.76	15.52	11.95	13.00	50.26
	sd	1.19	0.07	0.34	1.26	1.27	3.47	3.59	3.36
Semnopithecus entellus	n	3	1	3	3	1	3	3	3
	mean	29.58	1.4	8.75	24.15	17.84	12.56	19.72	55.12
	sd	4.54	-	1.04	3.53	-	4.08	8.13	1.51
Symphalangus syndactylus	n	5	4	5	5	5	5	5	5
	mean	34.07	0.78	9.31	28.79	15.34	16.01	32.79	58.57
	sd	0.75	0.10	1.97	2.99	5.54	9.13	9.56	7.30
Tarsius bancanus	n	4	4	4	4	0	4	4	2
	mean	11.73	1.34	2.06	7.99	-	0.91	3.05	78.37
	sd	0.4	0.13	0.08	0.10	-	0.05	0.70	26.65

Tarsius syrichta	n													
	mean													
	sd													
Theropithecus gelada	n	1		1		1		1	1	1	1	2		
	mean	36.35		1.37		11.54		28.71	18.65	16.25	27.48	45.17		
	sd	-		-		-		-	-	-	-	1.40		
Varecia v. variegata	n	6		4		6		6	4	6	6	7		
	mean	23.73		0.85		7.65		18.10	12.76	11.31	26.49	55.73		
	sd	0.66		0.05		0.37		1.37	2.24	5.08	9.36	5.71		

C3		GM	VBVL	VBDL	VB ECC	UNC	SPL	ATPL	PTPL	PCSA	LCSA	SCSA	TPAA	TPPA	AFA
Alouatta caraya	n	1	1	1	0	1	0		1	1	0	0		0	0
	mean	26.91	4.33	6.71	-	0.78	-		9.75	27.55	-	-		-	-
	sd	-	-	-	-	-	-		-	-	-	-		-	-
Alouatta guariba	n	2	2	2	2	2	2		1	2	2	2		2	2
	mean	25.99	5.82	5.96	0.65	3.66	8.58		23.00	7.46	8.58	4.26		63.94	150.90
	sd	0.40	0.89	0.36	0.02	0.26	0.64		-	5.33	4.52	0.75		1.98	7.97
Alouatta palliata	n	4	4	4	4	4	4		4	4	4	3		4	4
	mean	25.81	7.56	6.07	0.76	2.74	8.40		25.37	5.31	10.47	4.41		53.87	149.87
	sd	1.22	0.88	0.84	0.05	0.85	0.49		1.76	1.76	1.80	2.22		4.56	9.72
Alouatta seniculus	n														
	mean														
	sd														
Ateles fusciceps	n	3	3	3	3	3	3		3	3	3	3		6	6
	mean	28.43	9.21	7.84	0.72	2.21	7.89		22.80	6.88	10.89	4.89		64.42	139.78
	sd	0.72	0.38	0.52	0.06	0.45	0.55		1.81	0.87	3.93	1.82		4.19	9.05
Ateles geoffroyi	n	4	4	4	4	4	4		4	4	4	4		2	2
	mean	27.06	8.94	8.35	0.82	3.18	9.44		25.38	10.48	13.15	8.80		64.12	140.44
	sd	0.70	0.63	0.39	0.08	0.53	0.40		1.28	3.09	4.47	3.47		1.16	1.33
Avahi laniger	n	1	1	1	1	1	1		1	1	1	1		0	1
	mean	15.25	6.86	6.07	0.70	1.15	3.09		10.50	1.88	1.52	0.48		-	119.17
	sd	-	-	-	-	-	-		-	-	-	-		-	-
Cebus apella	n	5	5	5	5	5	5		4	5	5	5		7	7
	mean	23.38	4.95	4.69	0.71	1.78	4.58		17.77	4.77	3.81	1.94		61.34	138.03
	sd	1.03	0.70	0.42	0.01	0.45	0.89		0.49	0.77	1.31	0.64		2.10	7.58
Cercocebus torquatus	n	3	2	2	3	2	3		2	3	3	3		3	3
	mean	26.51	5.83	6.58	0.71	2.22	5.58		19.41	5.00	7.97	5.10		62.04	132.91
	sd	2.04	0.01	0.64	0.18	0.62	1.86		1.32	1.55	0.88	1.68		2.74	6.47
Cercopithecus mitis	n	8	7	7	7	7	7		6	7	7	7		10	10
	mean	24.58	6.02	5.86	0.73	2.89	4.39		24.05	5.07	4.85	3.19		60.46	130.06
	sd	3.61	0.79	0.59	0.05	0.47	0.78		1.82	1.52	3.24	1.09		3.36	5.80

Chlorocebus aethiops	n	3	3	3	3	3	3	3	3	3	3	4	4
	mean	23.68	7.22	6.28	0.81	1.90	5.46	19.64	4.52	6.04	5.85	60.62	130.91
	sd	1.16	0.69	0.48	0.20	0.62	0.62	0.82	1.02	1.62	0.76	2.39	7.24
Chlorocebus pygerythrus	n	2	2	2	2	2	2	2	2	2	2	2	2
	mean	25.41	6.63	6.07	0.66	2.14	5.97	20.63	5.15	4.64	6.22	55.66	132.64
	sd	0.53	1.07	0.86	0.23	0.33	0.98	2.45	0.21	2.28	6.50	3.52	8.35
Colobus guereza	n	4	4	4	4	4	4	4	4	4	4	6	5
	mean	29.69	7.4	7.25	0.73	2.58	6.64	25.20	10.61	7.7	3.15	55.48	131.39
	sd	1.68	0.62	1.03	0.13	0.49	1.75	2.57	4.04	1.38	0.85	4.56	5.30
Erythrocebus patas	n	2	2	2	2	2	2	2	2	2	2	3	3
	mean	28.7	7.96	8.04	1.10	3.08	6.75	24.23	6.09	9.86	3.92	59.66	126.65
	sd	1.15	0.46	0.16	0.22	0.90	1.48	1.87	2.29	1.39	0.11	7.81	15.61
Gorilla beringei	n	3	3	3	3	3	3	3	3	3	3	4	4
	mean	57.91	14.34	14.92	0.97	4.56	44.90	54.28	47.59	76.23	46.21	58.50	129.57
	sd	1.53	1.24	0.80	0.07	1.30	7.69	3.98	2.30	8.36	14.80	4.24	10.04
Gorilla g. gorilla	n	5	5	5	5	5	5	4	5	5	5	5	5
	mean	55.75	12.06	12.67	1.01	3.67	40.46	48.99	43.04	30.83	34.41	49.41	137.01
	sd	1.7	1.17	2.04	0.09	1.57	12.59	3.47	7.94	7.81	14.47	2.42	13.61
Hapalemur griseus	n	6	7	6	6	6	6	6	6	6	7	7	7
	mean	16.8	4.69	4.75	0.68	0.72	2.15	11.21	1.69	2.63	1.50	59.60	130.24
	sd	0.56	0.45	0.28	0.08	0.18	0.52	0.48	0.38	0.53	0.75	2.90	8.06
Homo sapiens	n	9	9	9	9	9	9	8	9	9	9	10	10
	mean	56.09	11.36	11.57	0.74	2.54	12.64	46.10	25.77	23.90	42.71	51.99	134.99
	sd	1.7	1.29	0.92	0.04	1.03	1.00	2.22	5.82	4.88	10.70	2.53	12.65
Hylobates agilis	n	1	1	1	1	1	1	1	1	1	1	1	0
	mean	29.27	7.87	7.77	0.96	3.63	7.12	23.13	7.99	12.11	8.68	53.62	-
	sd	-	-	-	-	-	-	-	-	-	-	-	-
Hylobates klossii	n												
	mean												
	sd												
Hylobates lar	n	1	1	1	0	1	1	1	1	1	1	1	1
	mean	29.92	7.47	7.01	-	2.83	5.11	21.07	11.22	4.58	5.33	50.22	119.32
	sd	-	-	-	-	-	-	-	-	-	-	-	-
Hylobates muelleri	n	1	1	1	1	1	1	1	1	1	1	2	1
	mean	27.93	7.80	7.32	0.82	0.07	4.93	19.65	5.28	3.73	4.71	52.07	146.30
	sd	-	-	-	-	-	-	-	-	-	-	2.18	-
Indri indri	n	1	1	1	1	1	1	1	1	1	1		1
	mean	25.25	16.70	14.6	0.71	1.10	11.54	21.99	10.04	11.49	5.98		123.16
	sd	-	-	-	-	-	-	-	-	-	-		-
Lemur catta	n	3	3	3	3	3	3	3	3	3	3	3	3
	mean	20.19	8.35	8.19	0.68	1.43	4.94	15.93	5.87	6.32	3.19	62.75	135.66
	sd	0.4	0.45	0.09	0.05	0.66	0.36	0.48	1.08	2.00	0.54	3.53	5.70
Lepilemur	n	8	8	4	8	2	8	8	6	8	7	8	9

mustelinus														
	mean	14.12	5.11	4.42	0.64	0.35	1.65	9.83	1.48	1.40	1.32	51.31	129.25
	sd	1.57	0.64	0.25	0.07	0.25	0.4	0.81	0.32	0.5	0.45	4.25	8.59
Macaca fuscata	n	2	2	2	2	2	2	2	2	2	2	2	2
	mean	30.71	7.44	7.35	0.93	2.70	7.04	23.82	10.32	9.73	5.12	60.29	136.92
	sd	2.2	0.32	0.79	0.23	0.29	1.34	1.97	0.08	0.41	1.25	0.40	13.04
Macaca nemestrina	n	1	1	1	1	1	1	1	1	1	1	1	1
	mean	31.62	6.33	6.4	0.81	2.44	9.14	24.98	9.22	7.04	2.94	61.26	122.52
	sd	-	-	-	-	-	-	-	-	-	-	-	-
Macaca nigra	n												
	mean												
	sd												
Macaca tonkeana	n												
	mean												
	sd												
Mandrillus sphinx	n	2	2	2	2	2	2	2	2	2	2	2	2
	mean	36.08	7.88	9.12	0.79	3.21	10.38	28.30	11.56	11.79	4.91	55.52	139.80
	sd	1.05	0.82	0.01	0.06	0.12	0.2	1.73	3.37	2.11	2.24	0.58	0.96
Miopithecus talapoin	n	4	4	3	4	3	4	4	3	4	2	6	6
	mean	19.50	3.94	3.89	0.72	1.15	2.02	12.69	1.15	1.34	0.50	50.90	129.43
	sd	0.22	0.19	0.28	0.09	0.49	0.34	0.21	0.14	0.21	0.15	2.03	7.50
Nasalis larvatus	n	1	1	1	1	1	1	1	1	1	1	2	2
	mean	26.59	7.77	8.02	1.04	3.29	8.60	22.26	5.28	11.39	6.31	56.06	143.61
	sd	-	-	-	-	-	-	-	-	-	-	8.88	3.01
Nomascus concolor	n	1	1	1	1	1	1	1	1	1	1	1	1
	mean	29.70	8.63	7.79	0.80	2.08	8.23	23.58	13.44	14.13	8.4	58.48	143.45
	sd	-	-	-	-	-	-	-	-	-	-	-	-
Nomascus leucogenys	n	1	1	1	1	1	1	1	1	1	1	1	1
	mean	31.74	7.09	7.17	0.74	3.12	8.77	22.00	9.09	6.28	4.59	51.04	135.04
	sd	-	-	-	-	-	-	-	-	-	-	-	-
Pan t. troglodytes	n	9	9	9	9	9	9	9	9	9	9	9	9
	mean	49.78	11.07	11.23	0.84	3.91	20.79	39.27	24.46	18.48	14.06	54.42	133.66
	sd	2.41	0.47	0.74	0.07	0.90	2.65	2.07	5.30	9.83	4.23	3.58	8.41
Papio anubis	n	7	7	7	7	7	7	7	7	7	7	6	6
	mean	38.28	10.25	10.24	0.89	4.73	11.59	32.77	16.95	16.46	10.43	61.88	133.49
	sd	1.95	1.79	1.52	0.10	0.55	1.37	4.41	3.13	3.77	4.44	2.26	8.35
Pithecia irrorata	n												
	mean												
	sd												
Pithecia pithecia	n	2	2	2	2	2	2	2	2	2	2	1	2
	mean	18.73	4.72	4.62	0.71	2.07	5.33	16.04	2.54	3.61	2.36	57.50	136.49
	sd	0.99	0.25	0.41	0.02	0.08	1.47	2.11	1.04	0.84	0.90	-	8.97

Pongo pygmaeus	n	9	9	9	9	9	9		9	9	9	9		9	9
	mean	50.75	11.23	11.35	0.92	4.40	30.21		43.53	37.25	20.85	24.63		54.43	124.64
	sd	2.94	2.14	1.68	0.17	1.74	5.52		4.53	13.59	8.82	11.11		3.19	14.52
Propithecus diadema	n	2	2	2	2	2	2		2	2	2	2		1	1
	mean	23.90	9.37	9.50	0.57	0.79	3.94		17.64	7.23	5.63	2.83		53.42	137.72
	sd	2.26	3.56	2.25	0.2	0.83	1.85		4.58	4.08	1.18	1.72		-	-
Propithecus verreauxi	n	4	6	4	5	4	6		6	4	6	6		6	5
	mean	22.76	8.98	8.65	0.74	1.96	5.01		15.57	5.02	4.50	3.49		55.78	133.98
	sd	1.3	0.29	0.42	0.18	0.51	0.69		1.36	0.69	1.19	0.69		4.34	3.06
Pygathrix nemaeus	n	2	2	2	2	2	2		2	2	2	2		1	2
	mean	27.21	8.55	8.16	0.75	1.95	6.85		18.43	7.35	6.32	6.02		51.27	135.57
	sd	3.09	0.53	1.12	0.15	0.39	1.5		2.14	1.85	1.18	1.96		-	3.65
Rhinopithecus roxellana	n	4	4	4	4	4	4		4	4	4	4		4	4
	mean	32.03	6.76	7.37	0.96	2.87	8.63		23.70	9.03	11.67	3.87		58.30	129.13
	sd	0.81	0.35	0.66	0.09	0.63	1.95		1.13	1.15	4.54	1.95		5.22	16.20
Semnopithecus entellus	n	1	1	1	1	1	1		1	1	1	1		1	1
	mean	27.21	7.69	8.09	0.65	1.41	7.50		20.58	8.29	7.04	4.14		56.03	123.54
	sd	-	-	-	-	-	-		-	-	-	-		-	-
Symphalangus syndactylus	n	3	3	3	3	2	3		3	3	3	3		3	3
	mean	33.49	8.56	8.26	0.88	3.42	8.29		26.50	9.16	16.35	7.26		54.26	130.04
	sd	1.21	1.03	0.71	0.10	1.79	1.06		3.16	0.74	7.44	0.61		5.17	14.62
Tarsius bancanus	n	4	4	4	4	4	2		4	0	4	0		2	2
	mean	11.91	3.29	2.33	1.09	0.17	0.32		7.75	-	0.43	-		56.76	105.15
	sd	0.14	0.42	0.05	0.11	0.06	0.00		0.02	-	0.14	-		5.06	7.61
Tarsius syrichta	n														
	mean														
	sd														
Theropithecus gelada	n	2	2	2	2	2	2		1	2	2	2		3	3
	mean	34.63	9.88	9.75	0.94	3.07	8.77		29.42	11.16	15.00	6.50		62.71	135.85
	sd	1.86	0.9	0.01	0.07	0.31	0.13		-	3.36	2.86	1.01		3.39	8.82
Varecia v. variegata	n	4	4	4	4	4	4		4	4	4	4		3	5
	mean	22.89	9.75	9.89	0.62	1.33	7.80		19.41	8.30	9.20	4.09		68.80	137.35
	sd	0.34	0.37	0.22	0.04	0.6	0.85		1.45	3.37	2.59	1.58		4.72	4.92

C4		**GM**	**VBVL**	**VBDL**	**VB ECC**	**UNC**	**SPL**	**ATPL**	**PTPL**	**PCSA**	**LCSA**	**SCSA**	**TPAA**	**TPPA**	**AFA**
Alouatta caraya	n	1	1	1	1	1	1	0	1	1	1	1	1	1	1
	mean	24.61	7.54	6.61	0.58	2.82	12.69	-	29.43	9.71	6.99	5.58	41.84	60.80	139.47
	sd	-	-	-	-	-	-	-	-	-	-	-	-	-	-
Alouatta guariba	n	2	2	2	2	2	2	1	2	2	2	2	0	2	2

	mean	25.58	6.21	6.17	0.63	2.91	9.87	22.98	24.87	6.55	5.19	4.96	-	63.31	140.25
	sd	0.18	0.57	0.38	0.01	0.03	1.68	-	2.67	3.97	0.12	1.20	-	9.85	2.73
Alouatta palliata	n	4	4	4	4	4	4	4	4	4	4	4	4	4	4
	mean	25.98	6.70	5.86	0.77	2.62	9.43	27.31	27.07	6.73	10.38	4.07	52.69	65.45	151.85
	sd	0.88	0.73	0.64	0.10	0.20	0.75	2.83	2.27	1.71	2.47	1.54	3.31	3.83	12.36
Alouatta seniculus	n														
	mean														
	sd														
Ateles fusciceps	n	3	3	3	3	3	3	3	3	3	3	3	6	6	6
	mean	28.78	8.73	7.89	0.71	3.52	9.25	23.80	27.12	12.84	14.36	6.66	37.26	63.66	138.59
	sd	1.21	0.35	0.29	0.06	0.75	1.63	3.46	0.37	2.16	1.28	1.3	4.32	4.84	7.71
Ateles geoffroyi	n	4	4	4	4	4	4	3	4	4	4	4	2	2	2
	mean	27.05	8.67	8.01	0.80	3.33	9.01	22.61	25.20	7.58	11.20	4.57	39.12	64.40	139.61
	sd	0.96	0.50	0.30	0.08	0.42	0.49	3.68	1.87	3.41	0.93	0.33	4.07	5.50	1.19
Avahi laniger	n	1	1	1	1	0	1	0	1	1	1	1	1	1	1
	mean	15.37	6.83	6.61	0.57	-	2.88	-	10.46	1.39	2.09	0.87	20.56	43.54	133.42
	sd	-	-	-	-	-	-	-	-	-	-	-	-	-	-
Cebus apella	n	6	6	6	6	6	6	4	6	6	6	6	8	8	8
	mean	23.72	4.70	4.60	0.67	2.19	5.72	15.26	18.06	3.56	4.23	1.83	35.03	63.84	131.53
	sd	1.12	0.50	0.43	0.02	0.40	0.98	0.63	0.67	1	1.45	0.61	8.43	4.17	10.34
Cercocebus torquatus	n	3	3	3	3	3	3	2	3	3	3	3	4	4	4
	mean	26.86	5.83	6.42	0.81	2.16	6.36	18.09	21.23	4.52	6.89	3.19	44.93	60.36	135.16
	sd	1.76	0.39	0.84	0.13	0.58	1.70	0.86	1.90	1.45	1.76	1.08	3.57	2.24	9.36
Cercopithecus mitis	n	8	8	8	8	8	8	6	7	9	9	9	9	9	9
	mean	24.82	5.87	5.50	0.78	2.74	4.95	18.27	23.8	4.62	3.94	2.53	34.05	56.46	133.21
	sd	3.67	0.85	0.48	0.11	0.49	0.94	2.48	1.94	1.95	1.97	1.56	3.88	2.67	7.40
Chlorocebus aethiops	n	4	4	4	4	4	4	3	4	4	4	4	5	5	5
	mean	23.91	6.33	5.63	0.64	2.36	6.51	15.22	19.77	3.83	5.16	2.79	36.14	56.27	122.09
	sd	1.09	1.12	0.65	0.05	0.30	1.4	0.48	0.67	0.5	0.91	1.37	3.28	3.59	12.43
Chlorocebus pygerythrus	n	1	1	1	1	1	1	0	1	2	2	2	0	1	1
	mean	25.71	6.47	5.66	0.48	1.5	5.74	-	18.9	2.48	3.53	0.76	-	50.53	137.92
	sd	-	-	-	-	-	-	-	-	3.51	5.00	1.07	-	-	-
Colobus guereza	n	4	4	4	4	4	4	4	4	5	5	5	6	6	6
	mean	30.05	7.46	7.25	0.78	2.64	6.19	23.57	26.26	7.83	5.98	2.33	37.52	51.15	136.21
	sd	1.50	1.19	0.73	0.03	0.33	2.23	2.33	2.62	5.43	3.54	1.95	3.33	2.06	12.12
Erythrocebus patas	n	2	2	2	2	2	2	2	2	2	2	2	3	3	3
	mean	29.34	7.58	7.96	0.83	2.43	8.55	20.18	24.81	6.05	8.88	3.34	36.75	60.74	135.81
	sd	0.64	0.13	0.58	0.04	0.36	1.12	0.81	0.65	0.36	1.14	1.36	2.15	3.70	1.62
Gorilla beringei	n	3	3	3	3	3	3	1	2	3	3	3	3	4	4
	mean	57.25	14.12	13.37	0.96	7.03	57.31	38.29	56.10	48.77	72.58	47.6	34.04	60.38	147.30
	sd	0.71	0.99	0.32	0.08	0.81	7.75	-	1.71	6.34	11.82	14.26	1.86	4.60	7.99
Gorilla g.	n	5	5	5	5	5	5	4	3	5	5	5	5	5	5

gorilla															
	mean	55.83	11.39	12.66	0.94	4.46	50.33	32.43	52.47	45.99	42.71	39.49	26.91	48.51	141.52
	sd	1.79	1.52	1.44	0.05	1.74	6.39	4.85	3.66	4.78	13.07	10.30	2.56	4.85	15.20
Hapalemur griseus	n	6	7	5	6	5	6	4	6	7	7	7	7	7	7
	mean	16.75	4.37	4.31	0.65	0.98	2.46	9.52	11.56	1.16	2.32	0.56	33.09	57.00	133.91
	sd	0.42	0.22	0.28	0.08	0.29	0.78	0.49	0.48	0.87	1.16	0.38	2.72	3.51	8.66
Homo sapiens	n	9	9	9	9	9	9	7	7	9	9	9	10	10	9
	mean	55.67	10.45	11.15	0.77	3.95	12.35	38.67	47.58	26.23	17.39	41.72	36.16	53.00	137.37
	sd	1.35	0.91	0.79	0.05	0.84	1.92	1.46	2.63	5.80	6.00	14.72	3.40	2.29	8.63
Hylobates agilis	n	1	1	1	1	1	1	0	1	1	1	1	1	1	1
	mean	29.61	6.94	7.33	0.83	3.42	8.34	-	24.01	4.51	10.78	9.59	32.24	58.18	149.39
	sd	-	-	-	-	-	-	-	-	-	-	-	-	-	-
Hylobates klossii	n														
	mean														
	sd														
Hylobates lar	n	1	1	1	1	1	1	0	1	1	1	1	1	1	1
	mean	30.07	7.18	6.36	1.10	2.67	6.43	-	21.02	9.28	3.68	5.38	29.45	46.74	124.18
	sd	-	-	-	-	-	-	-	-	-	-	-	-	-	-
Hylobates muelleri	n	1	1	1	1	1	1	1	1	3	3	3	1	1	1
	mean	27.6	7.23	7.32	0.8	1.25	5.86	15.43	19.50	1.95	1.61	1.63	31.44	53.88	146.20
	sd	-	-	-	-	-	-	-	-	3.38	2.79	2.82	-	-	-
Indri indri	n	1	1	1	1	1	1	0	1	1	1	1	0	0	1
	mean	25.25	14.36	15.37	0.58	0.92	12.36	-	21.17	9.73	17.46	6.32	-	-	121.75
	sd	-	-	-	-	-	-	-	-	-	-	-	-	-	-
Lemur catta	n	3	3	2	3	2	3	0	3	3	3	3	1	3	3
	mean	20.31	7.32	7.39	0.56	1.66	4.68	-	16.10	4.10	4.16	5.27	19.98	57.72	137.35
	sd	0.64	0.25	0.66	0.13	0.66	0.35	-	0.76	3.60	0.97	1.79	-	5.10	6.68
Lepilemur mustelinus	n	9	9	4	9	3	9	5	9	9	9	9	3	9	9
	mean	13.93	4.42	3.82	0.71	0.64	1.53	8.81	9.90	0.66	1.33	1.07	32.26	49.40	125.62
	sd	1.51	0.55	0.45	0.13	0.24	0.34	0.50	0.90	0.68	0.39	0.69	4.99	4.98	6.13
Macaca fuscata	n	2	2	2	2	2	2	0	2	2	2	2	2	2	2
	mean	30.60	7.82	7.75	0.94	2.58	7.40	-	23.67	9.01	9.67	4.47	36.53	61.26	131.77
	sd	2.32	0.99	0.91	0.31	0.05	1.03	-	0.18	1.80	2.33	1.63	8.85	5.40	0.81
Macaca nemestrina	n	1	1	1	1	1	1	0	1	1	1	1	1	1	1
	mean	31.93	7.1	7.26	0.90	2.74	9.00	-	24.60	5.68	9.47	3.46	36.01	59.72	134.61
	sd	-	-	-	-	-	-	-	-	-	-	-	-	-	-
Macaca nigra	n														
	mean														
	sd														
Macaca tonkeana	n														
	mean														
	sd														
Mandrillus sphinx	n	2	2	2	2	2	2	2	2	2	2	2	2	2	2
	mean	35.91	8.31	9.38	0.79	2.94	10.61	23.76	27.72	9.81	12.87	2.88	33.59	57.84	151.87

	sd	1	0.49	1.20	0.08	0.51	0.37	0.61	0.24	0.62	1.78	1.34	7.14	0.73	2.44
Miopithecus talapoin	n	4	4	4	4	4	4	4	4	4	4	4	6	6	6
	mean	19.52	3.31	3.45	0.77	1.25	2.43	11.21	13.03	1.26	1.51	0.24	31.71	50.95	135.52
	sd	0.44	0.13	0.35	0.05	0.33	0.78	0.39	0.27	0.55	0.35	0.30	3.90	2.57	8.09
Nasalis larvatus	n	2	2	2	2	2	2	2	2	2	2	2	2	2	2
	mean	27.26	6.78	8.24	1.05	4.31	8.50	18.83	23.64	8.61	12.11	1.92	31.60	55.68	135.77
	sd	0.90	0.21	0.58	0.16	0.57	1.16	2.28	0.07	4.52	4.21	1.12	3.59	1.73	9.24
Nomascus concolor	n	1	1	1	1	1	1	0	1	1	1	1	0	1	1
	mean	30.42	7.73	7.31	0.83	2.27	8.4	-	24.27	8.18	12.45	7.82	-	51.60	148.34
	sd	-	-	-	-	-	-	-	-	-	-	-	-	-	-
Nomascus leucogenys	n	1	1	1	1	1	1	0	1	1	1	1	0	1	1
	mean	32.14	7.3	7.33	0.77	3.08	6.92	-	21.93	8.38	4.96	6.36	-	47.32	116.82
	sd	-	-	-	-	-	-	-	-	-	-	-	-	-	-
Pan t. troglodytes	n	9	9	9	9	9	9	9	9	9	9	9	9	9	9
	mean	49.35	10.68	10.90	0.84	4.24	24.45	30.65	39.57	25.73	19.67	17.20	32.81	54.70	138.84
	sd	2.17	0.6	0.67	0.12	1.21	2.52	2.51	1.91	5.34	7.52	4.86	2.50	2.76	5.07
Papio anubis	n	7	7	7	7	7	7	7	6	7	7	7	7	7	6
	mean	38.31	9.25	9.63	0.82	4.06	12.18	25.58	35.56	14.89	17.24	7.27	42.22	62.17	132.69
	sd	1.91	1.14	1.13	0.14	0.81	1.13	3.23	4.81	3.48	3.04	3.38	8.10	4.74	7.63
Pithecia irrorata	n														
	mean														
	sd														
Pithecia pithecia	n	3	3	2	3	2	3	2	3	3	3	3	3	3	3
	mean	18.72	5.36	4.87	0.67	1.78	5.44	14.49	16.12	2.62	3.12	1.58	38.74	58.34	106.90
	sd	0.56	0.47	0.13	0.14	0.42	1.07	2.02	1.58	2.27	0.33	0.93	3.35	4.86	53.86
Pongo pygmaeus	n	9	9	9	9	9	9	9	8	10	10	10	9	9	9
	mean	50.65	10.34	11.05	0.83	3.98	33.94	33.79	45.36	33.57	22.93	22.62	33.68	57.10	137.51
	sd	2.87	1.85	1.92	0.18	1.88	3.74	3.68	5.08	17.48	12.90	9.94	2.89	3.25	9.53
Propithecus diadema	n	2	2	2	2	2	2	1	2	2	2	2	1	1	1
	mean	23.66	9.71	9.34	0.59	1.50	4.40	16.62	17.73	7.97	5.09	2.47	35.02	61.82	131.37
	sd	2.03	0.99	1.49	0.07	0.24	2.69	-	4.21	1.05	0.19	0.46	-	-	-
Propithecus verreauxi	n	4	6	4	6	4	6	0	6	6	6	6	4	6	6
	mean	23.06	8.16	8.33	0.75	1.75	4.07	-	16.03	4.37	3.58	3.98	42.35	54.29	132.02
	sd	1.38	0.69	0.19	0.16	0.81	1.18	-	1.09	2.51	2.02	0.58	0.70	7.70	5.62
Pygathrix nemaeus	n	2	2	2	2	2	2	1	2	2	2	2	2	2	2
	mean	27.21	7.88	7.94	0.96	2.50	5.82	13.28	18.50	6.38	6.98	6.80	37.37	55.94	130.22
	sd	2.8	1.51	0.76	0.01	0.21	0.95	-	2.42	1.21	1.30	2.58	6.11	2.15	9.22
Rhinopithecus roxellana	n	4	4	3	4	3	4	3	3	4	4	4	3	4	3
	mean	32.08	6.64	6.97	0.88	3.31	9.53	21.17	23.91	8.90	10.47	1.94	40.50	56.92	129.99
	sd	1.11	0.97	0.86	0.03	1.05	2.55	1.47	1.68	2.29	1.62	1.34	3.77	4.51	8.08
Semnopithecus	n	2	2	2	2	2	2	2	2	2	2	2	2	2	2

entellus															
	mean	27.12	6.45	7.09	0.62	2.48	6.49	17.85	21.66	6.39	8.64	1.98	42.87	62.51	105.65
	sd	0.73	0.71	0.59	0.1	0	1.73	1	0.11	1.62	1.54	1.24	7.67	1.19	3.89
Symphalangus syndactylus	n	4	4	3	4	3	4	0	4	4	4	4	1	4	4
	mean	34.00	9.05	8.23	0.78	3.23	9.19	-	24.93	8.27	11.96	6.44	42.74	55.85	139.77
	sd	0.68	0.86	0.54	0.09	0.63	1.68	-	1.89	0.96	6.29	1.35	-	2.63	10.46
Tarsius bancanus	n	2	2	2	1	1	2	1	2	0	2	0	2	2	2
	mean	11.79	2.92	2.15	0.83	0.5	0.55	6.01	7.58	-	0.67	-	34.03	45.25	117.68
	sd	0.05	0.21	0.30	-	-	0.13	-	0.09	-	0.31	-	4.65	4.47	60.53
Tarsius syrichta	n														
	mean														
	sd														
Theropithecus gelada	n	1	1	1	1	1	1	1	1	1	1	1	3	3	3
	mean	33.05	9.01	9.04	0.75	3.80	9.48	26.12	31.46	9.44	11.78	5.82	43.98	64.81	133.43
	sd	-	-	-	-	-	-	-	-	-	-	-	5.92	0.25	6.07
Varecia v. variegata	n	4	4	4	4	3	4	1	4	4	4	4	6	6	6
	mean	22.81	9.33	9.50	0.66	2.02	7.36	15.82	19.62	7.47	8.97	4.10	42.16	65.54	141.35
	sd	0.42	0.85	0.22	0.08	0.50	0.34	-	1.15	3.53	3.2	2.72	10.98	1.83	6.84

C5		**GM**	**VBVL**	**VBDL**	**VB ECC**	**UNC**	**SPL**	**ATPL**	**PTPL**	**PCSA**	**LCSA**	**SCSA**	**TPAA**	**TPPA**	**AFA**
Alouatta caraya	n	1	1	1	1	1	1	0	1	1	1	1	1	1	1
	mean	24.19	8.05	7.77	0.68	2.40	15.28	-	29.31	11.34	10.93	5.88	39.22	63.73	156.47
	sd	-	-	-	-	-	-	-	-	-	-	-	-	-	-
Alouatta guariba	n	2	2	2	2	2	2	0	1	2	2	2	1	2	2
	mean	26.10	6.43	6.52	0.52	2.88	11.59	-	24.90	4.43	6.27	4.44	39.41	63.88	134.24
	sd	1.22	0.45	0.22	0.02	0.15	2.88	-	-	1.48	0.09	0.88	-	14.87	0.30
Alouatta palliata	n	4	4	4	4	4	4	4	4	4	4	4	4	4	4
	mean	25.73	6.07	6.08	0.75	2.97	11.35	25.31	27.98	5.72	10.34	5.12	47.00	63.34	144.98
	sd	0.83	0.82	0.93	0.05	0.56	0.94	3.45	1.53	1.18	3	1.66	9.94	9.48	3.89
Alouatta seniculus	n														
	mean														
	sd														
Ateles fusciceps	n	3	3	3	3	3	3	3	3	3	3	3	6	6	6
	mean	28.45	7.89	7.96	0.64	3.87	11.34	23.25	28.27	10.85	18.45	5.82	42.39	71.21	136.09
	sd	1.26	0.67	0.57	0.09	0.37	3.15	1.99	2.02	2.85	2.48	1.94	8.90	5.91	8.62
Ateles geoffroyi	n	4	4	4	4	4	4	4	4	4	4	4	2	2	2
	mean	27.27	7.66	8.27	0.68	3.65	12.55	21.82	25.89	6.79	11.65	5.38	38.13	66.57	143.12
	sd	1.06	0.89	0.4	0.06	0.62	1.81	2.30	1.77	0.67	2.51	1.11	4.64	5.19	6.16
Avahi laniger	n	1	1	1	1	1	1	1	1	1	1	1	1	1	1
	mean	15.44	6.65	5.97	0.5	0.33	4.09	9.04	11.37	1.78	1.90	1.24	35.78	49.93	131.44
	sd	-	-	-	-	-	-	-	-	-	-	-	-	-	-

Cebus apella	n	6	6	6	6	6	6	6	6	6	6	6	7	8	8
	mean	23.67	4.87	4.78	0.63	1.80	6.58	14.76	19.61	3.46	3.82	1.37	35.92	65.18	129.88
	sd	0.90	0.59	0.48	0.04	0.78	1.32	1.15	1.15	0.71	0.40	0.52	3.26	5.65	10.37
Cercocebus torquatus	n	3	3	3	3	3	3	3	2	3	3	3	4	4	4
	mean	26.81	5.74	6.21	0.76	2.08	6.97	16.20	22.41	3.73	6.98	2.89	37.75	62.78	131.92
	sd	1.90	1.01	0.84	0.08	0.20	1.70	1.31	0.02	0.86	1.17	1.77	7.97	1.47	5.28
Cercopithecus mitis	n	6	6	6	6	6	6	6	5	7	7	7	7	7	8
	mean	24.87	5.48	5.40	0.81	2.57	4.3	16.91	25.00	5.05	4.12	2.01	34.78	60.12	134.00
	sd	3.67	0.71	0.66	0.10	0.36	0.61	1.85	3.20	2.84	2.40	1.35	1.62	2.97	7.02
Chlorocebus aethiops	n	4	4	4	4	4	4	4	4	4	4	4	6	6	6
	mean	24.06	5.76	5.81	0.62	2.33	7.64	15.45	21.48	3.25	4.45	2.97	33.61	61.53	134.28
	sd	1.11	0.43	0.50	0.08	0.50	1.66	0.49	1.59	0.36	0.86	0.80	2.61	2.48	9.46
Chlorocebus pygerythrus	n	1	1	1	1	1	1	1	1	1	1	1	1	1	1
	mean	25.56	6.68	5.87	0.65	1.32	5.07	16.77	21.46	3.62	5.53	7.75	40.14	60.35	135.66
	sd	-	-	-	-	-	-	-	-	-	-	-	-	-	-
Colobus guereza	n	3	3	3	3	3	3	3	3	3	3	3	4	4	5
	mean	30.02	7.10	6.99	0.65	2.62	7.24	22.25	28.75	7.47	6.62	2.15	35.16	54.45	140.52
	sd	1.78	0.96	0.91	0.10	0.23	2.06	1.22	3.26	3.22	0.48	0.86	2.11	3.00	11.38
Erythrocebus patas	n	2	2	2	2	2	2	2	2	2	2	2	3	3	3
	mean	29.41	7.14	7.60	0.76	2.11	9.86	19.27	27.48	5.35	8.14	2.49	30.40	60.64	134.03
	sd	0.78	1.47	0.72	0.07	0.12	0.84	1.22	0.94	0.54	0.25	0.03	0.89	6.13	8.29
Gorilla beringei	n	3	2	2	3	2	3	3	3	3	3	3	5	5	5
	mean	57.43	13.92	13.50	0.82	6.74	61.59	37.81	53.54	47.04	78.71	60.42	35.18	63.78	136.67
	sd	1.06	0.76	0.56	0.05	0.25	5.34	1.07	2.34	4.61	17.2	8.57	4.26	3.70	9.99
Gorilla g. gorilla	n	5	5	5	5	5	5	4	5	5	5	5	5	5	5
	mean	55.63	11.45	12.94	0.84	4.84	56.13	33.41	52.86	41.51	64.52	61.81	28.61	54.81	139.83
	sd	1.29	1.22	0.83	0.12	1.72	5.72	1.17	4.58	6.61	14.46	10.64	2.22	3.46	8.82
Hapalemur griseus	n	5	5	5	6	5	5	6	6	7	7	7	6	6	6
	mean	16.79	3.87	4.20	0.65	0.81	2.91	10.25	12.06	1.17	2.17	0.57	43.81	57.86	127.81
	sd	0.63	0.22	0.26	0.12	0.27	0.49	0.45	0.58	0.87	1.19	0.40	4.60	2.59	6.99
Homo sapiens	n	9	9	9	9	9	9	9	9	9	9	9	10	10	10
	mean	55.63	11.10	11.73	0.73	3.02	14.10	38.65	49.35	28.94	16.87	35.65	33.24	52.63	130.98
	sd	1.02	1.11	0.84	0.07	0.73	2.06	1.24	2.71	7.31	3.23	11.60	3.11	2.69	8.19
Hylobates agilis	n	1	1	1	1	1	1	1	1	1	1	1	1	1	1
	mean	29.86	6.67	7.31	0.85	3.02	8.92	16.70	22.95	7.71	10.89	6.11	31.99	58.73	146.88
	sd	-	-	-	-	-	-	-	-	-	-	-	-	-	-
Hylobates klossii	n														
	mean														
	sd														
Hylobates lar	n	1	1	1	1	1	1	1	1	1	1	1	1	1	1
	mean	30.47	7.48	6.83	0.97	2.58	8.01	16.06	20.55	9.43	5.37	4.79	28.23	47.20	149.68
	sd	-	-	-	-	-	-	-	-	-	-	-	-	-	-

Hylobates muelleri	n	3	3	1	3	3	3	2	2	1	1	1	2	2	2
	mean	29.15	6.66	7.45	0.87	2.09	6.47	15.48	20.68	5.15	5.13	4.59	30.37	48.91	148.05
	sd	1.47	0.65	-	0.14	0.99	1.32	0.20	0.88	-	-	-	5.92	5.33	0.37
Indri indri	n	1	1	1	1	1	1	0	1	1	1	1	0	1	1
	mean	25.05	14.05	14.06	0.59	0.62	13.79	-	20.05	11.39	22.45	8.27	-	57.52	125.80
	sd	-	-	-	-	-	-	-	-	-	-	-	-	-	-
Lemur catta	n	3	3	2	3	2	3	3	3	2	3	3	3	3	3
	mean	20.12	7.27	7.21	0.56	2.46	4.33	14.39	16.61	4.24	4.91	2.54	43.93	62.23	138.26
	sd	0.40	0.20	0.40	0.04	0.51	0.79	0.69	1.42	0.07	1.13	1.15	9.38	1.36	4.56
Lepilemur mustelinus	n	8	8	3	8	2	8	8	8	8	8	8	7	9	9
	mean	13.42	4.05	3.96	0.65	0.12	1.49	8.81	10.42	0.37	1.22	1.36	37.93	47.53	122.56
	sd	0.35	0.48	0.34	0.14	0.07	0.36	0.49	0.69	0.52	0.35	0.40	4.93	9.29	13.54
Macaca fuscata	n	2	2	2	2	2	2	2	2	2	2	2	2	2	2
	mean	31.22	6.97	6.94	0.78	2.41	6.80	19.12	26.66	7.76	9.82	3.67	39.80	62.56	151.20
	sd	2.42	0.18	0.46	0.03	0.31	0.83	1.49	1.17	0.97	0.87	0.55	13.15	4.62	0.59
Macaca nemestrina	n	1	1	1	1	1	1	1	1	1	1	1	1	1	1
	mean	32.52	6.21	6.12	0.72	2.02	9.31	19.17	26.35	7.20	5.04	3.41	34.18	62.02	143.37
	sd	-	-	-	-	-	-	-	-	-	-	-	-	-	-
Macaca nigra	n	1	1	1	1	1	1	1	1	1	1	1	1	1	1
	mean	30.44	7.69	7.58	0.63	2.00	9.16	19.57	26.04	7.84	4.69	2.44	35.88	62.89	147.98
	sd	-	-	-	-	-	-	-	-	-	-	-	-	-	-
Macaca tonkeana	n														
	mean														
	sd														
Mandrillus sphinx	n	2	2	2	2	2	2	2	2	2	2	2	2	2	2
	mean	35.70	7.21	8.76	0.71	2.93	11.79	22.37	31.66	10.13	12.19	3.43	40.79	61.55	148.00
	sd	0.75	0.31	0.64	0.06	0.16	0.25	2.04	2.54	1.36	1.00	0.55	4.06	2.56	11.19
Miopithecus talapoin	n	5	5	4	5	4	5	5	5	5	5	5	7	7	7
	mean	19.27	3.66	3.95	0.72	1.16	3.21	10.60	14.55	0.92	1.50	0.74	28.54	55.74	137.12
	sd	0.36	0.32	0.36	0.06	0.22	0.46	0.58	0.65	0.73	0.41	0.20	2.35	4.42	9.12
Nasalis larvatus	n	3	3	2	3	2	3	3	2	3	3	3	2	2	2
	mean	28.43	7.53	8.18	1.00	4.34	6.77	17.68	23.20	5.75	11.06	2.06	32.98	60.13	148.03
	sd	1.73	0.78	0.29	0.14	0.46	3.24	1.61	0.78	5.30	3.08	0.56	0.55	2.04	0.06
Nomascus concolor	n	1	1	1	1	1	1	0	1	1	1	1	1	1	1
	mean	29.73	6.82	7.29	0.80	2.50	10.45	-	21.11	8.78	10.53	9.54	35.47	55.53	142.04
	sd	-	-	-	-	-	-	-	-	-	-	-	-	-	-
Nomascus leucogenys	n	1	1	1	1	1	1	0	1	1	1	1	0	1	1
	mean	31.64	6.96	7.15	0.64	2.60	9.23	-	19.09	6.23	8.25	7.08	-	60.39	133.18
	sd	-	-	-	-	-	-	-	-	-	-	-	-	-	-
Pan t. troglodytes	n	9	9	9	9	9	9	9	9	9	9	9	9	9	9
	mean	49.12	10.74	11.37	0.75	4.17	26.65	30.85	41.48	28.07	21.57	19.20	34.16	56.75	139.64
	sd	2.2	0.93	0.47	0.08	0.72	2.21	1.74	1.44	5.79	6.83	6.07	3.03	3.02	6.28

Papio anubis	n	7	7	7	7	7	7	6	6	7	7	7	6	7	7
	mean	38.50	8.80	9.55	0.80	3.84	12.49	24.57	38.98	14.07	16.95	7.32	37.44	63.30	128.20
	sd	1.74	1.90	1.02	0.05	0.62	3.22	2.57	5.22	3.45	2.24	3.04	6.39	5.16	7.05
Pithecia irrorata	n														
	mean														
	sd														
Pithecia pithecia	n	3	3	3	3	3	3	3	3	3	3	3	3	3	3
	mean	18.75	4.95	4.95	0.68	1.92	7.37	13.94	16.95	2.98	3.82	1.68	40.05	55.05	141.94
	sd	0.64	0.31	0.47	0.12	0.26	1.80	1.01	1.97	0.32	0.24	0.51	7.67	4.78	8.41
Pongo pygmaeus	n	9	9	9	9	9	9	9	9	10	10	10	9	9	9
	mean	50.49	10.75	11.92	0.68	3.72	37.23	34.10	48.19	32.21	27.31	27.42	33.47	59.73	137.03
	sd	2.36	1.81	1.39	0.12	2.29	4.18	3.95	4.55	14.87	13.08	13.21	2.53	5.88	5.14
Propithecus diadema	n	2	2	2	2	2	2	1	2	2	2	2	1	1	1
	mean	22.89	8.94	9.12	0.49	1.16	5.01	16.36	18.32	5.99	5.29	3.55	33.14	54.61	132.21
	sd	1.10	1.90	1.46	0.08	0.04	2.35	-	4.39	2	1.05	0.23	-	-	-
Propithecus verreauxi	n	4	6	4	5	4	6	6	6	6	6	6	5	6	6
	mean	22.72	8.30	8.56	0.64	1.62	5.08	14.75	16.65	2.68	3.84	4.19	44.01	59.26	132.19
	sd	1.26	1.16	0.55	0.18	0.70	0.9	1.15	1.18	2.11	1.99	1.58	5.20	6.37	5.17
Pygathrix nemaeus	n	2	2	2	2	2	2	2	2	2	2	2	2	2	2
	mean	27.37	8.40	8.56	0.57	1.45	6.97	16.27	18.35	6.12	6.28	4.21	35.83	54.95	130.57
	sd	3.54	1.56	1.03	0.06	0.22	1.79	1.61	2.51	3.70	1.30	0.60	8.04	1.56	0.37
Rhinopithecus roxellana	n	2	2	2	2	2	2	2	2	2	2	2	2	2	2
	mean	32.31	6.08	8.15	0.80	3.50	11.37	21.46	24.77	8.00	10.64	3.43	39.48	62.40	130.63
	sd	0.75	0.11	0.50	0.00	0.27	0.18	1.97	0.04	2.52	3.61	0.93	8.39	3.43	3.81
Semnopithecus entellus	n	2	2	0	2	0	2	2	2	0	2	2	2	2	2
	mean	26.89	6.06	-	0.77	-	6.86	15.93	22.68	-	8.18	1.47	51.21	64.59	139.54
	sd	0.62	0.13	-	0.03	-	1.46	2.30	0.55	-	0.94	0.33	22.76	3.83	0.04
Symphalangus syndactylus	n	4	4	3	4	2	4	3	4	4	4	4	4	4	4
	mean	34.04	9.08	8.88	0.66	1.82	10.33	21.63	24.48	7.98	11.40	6.25	36.46	52.96	140.49
	sd	0.80	1.39	1.11	0.10	1.60	1.26	2.59	2.35	1.94	3.84	1.70	7.00	10.67	6.44
Tarsius bancanus	n	2	2	2	2	1	2	2	2	0	2	0	2	2	2
	mean	11.69	2.59	2.10	1.09	0.68	0.90	6.09	7.89	-	0.51	-	28.27	46.09	86.62
	sd	0.58	0.25	0.13	0.22	-	0.04	0.17	0.05	-	0.26	-	0.06	2.93	12.62
Tarsius syrichta	n														
	mean														
	sd														
Theropithecus gelada	n	2	2	2	2	2	2	2	2	2	2	2	3	3	3
	mean	34.78	8.53	8.82	0.78	3.29	10.84	24.48	34.57	13.64	14.26	5.02	35.39	68.17	137.67
	sd	1.94	1.53	0.45	0.05	0.68	1.20	0.94	1.51	0.60	2.22	0.60	1.66	2.52	5.09
Varecia v. variegata	n	6	6	4	6	5	6	6	6	5	6	6	7	7	7

	mean	22.75	8.48	9.28	0.54	1.49	7.35	17.60	19.58	8.36	7.69	2.37	57.09	65.35	135.55
	sd	0.60	0.65	0.35	0.09	0.84	0.52	1.60	1.50	2.00	1.88	1.07	4.12	3.17	3.14

C6		GM	VBVL	VBDL	VB ECC	UNC	SPL	ATPL	PTPL	PCSA	LCSA	SCSA	TPAA	TPPA	AFA
Alouatta caraya	n	1	1	1	1	1	1	1	1	1	1	1	1	1	1
	mean	24.31	7.66	7.23	0.51	3	15.60	20.37	32.58	11.74	10.68	8.72	42.65	65.34	161.22
	sd	-	-	-	-	-	-	-	-	-	-	-	-	-	-
Alouatta guariba	n	2	2	2	2	2	2	1	0	2	2	2	1	2	2
	mean	25.63	7.21	7.05	0.52	1.81	14.08	14.89	-	5.50	8.37	6.57	34.24	65.60	139.72
	sd	0.12	1.1	0.89	0.10	0.02	2.74	-	-	0.50	3.42	0.59	-	15.61	4.10
Alouatta palliata	n	4	4	4	4	4	4	4	4	4	4	4	4	4	4
	mean	25.64	6.12	6.35	0.72	2.58	13.95	17.77	28.99	6.08	10.82	6.01	40.71	63.79	147.95
	sd	0.84	0.78	0.89	0.05	0.54	1.38	1.85	1.54	1.10	2.48	2.30	5.80	4.97	7.61
Alouatta seniculus	n														
	mean														
	sd														
Ateles fusciceps	n	3	3	3	3	3	3	3	3	3	3	3	6	6	6
	mean	28.54	8.31	8.78	0.51	2.98	16.88	25.31	32.85	11.26	16.28	11.14	44.77	68.95	139.33
	sd	1.43	0.21	0.83	0.03	0.83	5.24	1.45	1.76	1.75	2.41	4.37	6.04	3.76	5.98
Ateles geoffroyi	n	3	3	3	3	3	3	3	3	3	3	3	1	1	1
	mean	27.43	8.55	9.20	0.53	3.27	17.34	22.50	29.03	7.62	16.11	7.66	33.63	63.67	155.55
	sd	1.04	1.03	0.45	0.10	0.48	1.07	2.06	1.31	0.58	3.45	1.39	-	-	-
Avahi laniger	n	1	1	1	1	1	1	1	1	1	1	1	1	1	1
	mean	15.5	5.89	5.77	0.45	0.25	6.19	7.56	12.77	1.51	3.70	2.01	38.11	42.66	125.80
	sd	-	-	-	-	-	-	-	-	-	-	-	-	-	-
Cebus apella	n	6	6	6	6	6	6	6	6	6	6	6	8	8	8
	mean	23.45	4.87	4.89	0.54	1.56	8.23	16.75	21.24	3.41	4.51	2.04	42.09	62.47	136.87
	sd	0.90	0.48	0.27	0.03	0.15	1.26	1.33	1.04	1.06	0.98	0.41	9.23	4.22	8.45
Cercocebus torquatus	n	3	3	3	3	3	3	3	3	3	3	3	4	4	4
	mean	26.6	5.83	5.89	0.63	1.96	7.79	18.49	24.91	4.55	6.99	2.16	42.82	62.03	127.35
	sd	2.10	0.49	0.45	0.03	0.22	2.44	0.51	1.34	1.82	1.98	0.83	5.20	3.47	11.41
Cercopithecus mitis	n	5	5	5	5	5	5	5	5	5	5	5	10	10	10
	mean	27.52	5.88	5.90	0.60	2.50	5.38	20.51	28.67	6.19	6.00	2.33	33.51	60.38	140.65
	sd	0.93	0.58	0.65	0.15	0.36	0.64	2.17	2.84	2.14	1.89	0.87	1.70	3.57	6.84
Chlorocebus aethiops	n	4	4	4	4	4	4	4	4	4	4	4	6	6	6
	mean	24.00	6.21	6.09	0.61	2.07	8.77	17.49	25.09	4.10	4.86	2.62	33.39	59.99	140.21
	sd	1.40	0.58	0.52	0.04	0.37	1.09	0.92	1.53	1.73	0.96	0.70	2.62	2.93	8.08
Chlorocebus pygerythrus	n	2	2	2	2	2	2	2	2	2	2	2	2	2	2
	mean	25.71	5.95	5.99	0.59	2.21	6.50	17.66	24.67	3.69	4.12	4.08	29.95	54.08	142.55
	sd	0.35	0.06	0.40	0.06	0.06	0.83	1.51	0.16	0.13	0.50	3.39	5.78	2.09	7.76
Colobus guereza	n	4	4	4	4	4	4	4	4	4	4	4	7	7	7

	mean	30.26	7.38	7.62	0.55	2.63	8.21	20.96	29.77	9.47	7.18	2.44	33.71	54.42	143.45
	sd	1.44	1.06	1.13	0.08	0.38	1.74	1.46	3.60	1.67	1.74	0.68	5.96	4.48	11.59
Erythrocebus patas	n	2	2	2	2	2	2	2	2	2	2	2	2	3	3
	mean	29.22	6.20	7.58	0.79	2.25	11.15	22.05	31.59	5.33	8.68	2.33	39.25	61.06	135.74
	sd	0.62	0.77	0.9	0.04	0.17	1.63	0.39	1.17	1.06	0.60	0.25	9.82	4.43	14.36
Gorilla beringei	n	3	2	2	3	2	3	2	3	3	3	3	4	3	3
	mean	57.83	15.00	14.00	0.69	6.54	58.04	49.13	50.74	49.24	97.88	72.57	35.87	64.44	130.50
	sd	1.44	1.00	1.39	0.07	0.52	6.17	2.43	0.50	9.34	26.16	21.32	2.86	1.40	17.34
Gorilla g. gorilla	n	5	5	5	5	5	5	4	5	5	5	5	5	5	5
	mean	55.56	11.79	14.05	0.71	4.95	55.34	43.03	54.36	38.01	80.39	66.49	34.32	60.76	140.81
	sd	1.55	1.81	1.24	0.02	2.01	3.53	5.60	5.44	8.21	19.13	11.97	2.77	3.75	8.94
Hapalemur griseus	n	5	6	5	6	4	6	6	5	5	6	6	6	6	6
	mean	16.86	4	4.16	0.56	0.90	4.02	9.37	13.12	1.69	2.83	0.66	43.14	54.95	133.67
	sd	0.32	0.55	0.17	0.08	0.60	0.87	0.46	0.76	0.47	0.85	0.21	5.54	3.18	4.40
Homo sapiens	n	9	9	9	9	9	9	7	6	9	9	9	10	10	9
	mean	55.27	11.32	12.05	0.70	2.78	21.71	41.91	54.06	27.61	26.00	27.65	37.58	57.65	141.03
	sd	1.07	1.12	0.93	0.05	0.70	4.42	2.59	5.04	5.98	6.87	10.12	2.94	3.17	13.17
Hylobates agilis	n	1	1	1	1	1	1	1	1	1	1	1	1	1	1
	mean	29.58	6.75	7.99	0.82	1.79	9.95	20.98	23.38	6.53	11.19	5.66	35.50	65.73	150.98
	sd	-	-	-	-	-	-	-	-				-	-	-
Hylobates klossii	n														
	mean														
	sd														
Hylobates lar	n	1	1	1	1	1	1	1	1	1	1	1	1	1	1
	mean	30.25	7.27	7.46	0.86	3.00	9.53	18.61	20.34	8.51	5.81	4.28	35.23	50.43	150.45
	sd	-	-	-	-	-	-	-	-	-	-	-	-	-	-
Hylobates muelleri	n	1	1	0	1	1	1	1	1	1	1	1	1	1	1
	mean	27.50	7.68	-	0.66	0.64	7.14	20.01	21.02	7.55	7.13	4.39	39.01	63.53	145.18
	sd	-	-	-	-	-	-	-	-	-	-	-	-	-	-
Indri indri	n	1	1	1	1	1	1	1	1	1	1	1	1	1	1
	mean	25.52	12.25	13.41	0.48	2.11	14.88	15.90	22.95	16.28	25.19	10.61	51.23	54.28	128.49
	sd	-	-	-	-	-	-	-	-	-	-	-	-	-	-
Lemur catta	n	3	3	2	3	3	3	3	3	3	3	3	3	3	3
	mean	19.98	6.58	7.46	0.61	1.64	5.08	13.08	17.34	4.39	4.78	2.17	50.27	58.15	141.07
	sd	0.46	0.61	0.47	0.11	0.13	1.48	0.46	1.32	0.94	1.90	0.60	6.30	5.19	8.88
Lepilemur mustelinus	n	6	6	3	6	2	6	6	6	3	6	5	7	7	6
	mean	13.07	3.98	3.68	0.59	0.53	1.45	8.05	11.11	0.94	1.43	1.15	49.95	47.83	122.92
	sd	0.41	0.44	0.33	0.15	0.35	0.34	0.39	0.49	0.17	0.41	0.23	3.26	4.10	7.56
Macaca fuscata	n	2	2	2	2	2	2	2	2	2	2	2	2	2	2
	mean	31.36	6.25	6.93	0.66	2.55	7.51	21.75	29.94	8.93	7.23	4.77	40.43	61.32	145.44
	sd	2.69	0.73	0.58	0.07	0.63	1.05	2.97	1.35	2.32	0.99	2.73	3.82	2.73	1.03
Macaca nemestrina	n	1	1	1	1	1	1	1	1	1	1	1	1	1	1
	mean	32.53	6.31	6.21	0.72	1.69	9.56	23.05	31.40	5.24	5.12	2.07	35.42	60.22	139.24

	sd	-	-	-	-	-	-	-	-	-	-	-	-	-	-	
Macaca nigra	n	1	1	0	1	0	1	1	1	0	1	1	1	1	1	
	mean	29.43	6.55	-	0.52	-	7.80	23.06	29.34	-	5.28	2.76	38.37	61.90	152.98	
	sd	-	-	-	-	-	-	-	-	-	-	-	-	-	-	
Macaca tonkeana	n															
	mean															
	sd															
Mandrillus sphinx	n	2	2	2	2	2	2	2	2	2	2	2	2	2	2	
	mean	35.89	7.80	9.07	0.65	2.84	11.70	22.77	33.94	12.91	11.07	4.63	47.94	56.67	148.61	
	sd	0.52	0.01	0.47	0.08	0.12	1.03	0.93	1.82	1.11	1.84	0.12	4.55	8.53	4.80	
Miopithecus talapoin	n	4	4	4	4	4	4	4	4	3	3	3	6	6	6	
	mean	19.48	3.64	3.87	0.70	1.00	3.99	11.13	16.16	1.32	1.29	0.66	31.29	50.40	135.90	
	sd	0.39	0.32	0.13	0.11	0.28	0.41	1.38	0.41	0.33	0.20	0.11	5.78	4.38	10.80	
Nasalis larvatus	n	2	2	2	2	2	2	2	2	2	2	2	2	2	2	
	mean	27.93	7.08	8.41	0.82	3.49	10.05	20.77	25.88	10.32	9.26	2.83	31.81	58.04	141.91	
	sd	1.47	0.23	0.13	0.03	0.17	0.31	1.29	0.23	1.09	3.23	0.15	2.81	3.12	10.76	
Nomascus concolor	n	1	1	1	1	1	1	1	1	1	1	1	1	1	1	
	mean	30.31	5.90	7.89	0.88	3.31	10.82	24.27	21.49	8.43	12.08	7.40	43.92	56.25	152.82	
	sd	-	-	-	-	-	-	-	-	-	-	-	-	-	-	
Nomascus leucogenys	n	1	1	1	1	1	1	0	1	1	1	1	1	1	1	
	mean	31.52	6.75	8	0.67	2.92	9.34	-	22.16	15.75	8.34	4.64	42.47	51.53	135.44	
	sd	-	-	-	-	-	-	-	-	-	-	-	-	-	-	
Pan t. troglodytes	n	9	9	9	9	9	9	9	9	9	9	9	9	9	9	
	mean	48.72	10.81	11.32	0.59	5.07	29.41	34.48	43.80	33.28	30.49	28.67	32.50	58.77	145.93	
	sd	2.01	1.23	0.76	0.05	1.11	2.39	3.63	2.60	9.39	7.90	5.39	4.03	3.26	6.83	
Papio anubis	n	7	7	7	7	7	7	4	5	7	7	7	7	7	7	
	mean	38.5	8.81	9.66	0.69	3.24	13.40	27.87	43.97	15.35	18.67	7.90	38.73	58.60	136.08	
	sd	1.86	2.23	1.17	0.05	0.59	2.80	1.70	4.52	5.33	3.02	1.56	13.32	3.95	7.76	
Pithecia irrorata	n															
	mean															
	sd															
Pithecia pithecia	n	3	3	3	3	3	3	3	3	3	3	3	3	3	3	
	mean	18.54	5.17	5.29	0.66	1.42	8.25	13.79	17.91	2.77	4.39	1.82	42.06	58.66	138.26	
	sd	1.05	0.27	0.74	0.08	0.54	1.75	2.63	2.61	0.52	1.25	0.62	13.04	4.31	5.08	
Pongo pygmaeus	n	10	10	10	10	9	10	10	10	10	10	10	9	10	10	
	mean	50.74	11.15	12.23	0.60	3.57	37.86	34.22	47.60	41.01	41.54	37.89	32.18	58.36	143.05	
	sd	2.52	1.67	1.56	0.12	2.04	3.08	3.53	4.86	10.89	9.72	9.92	3.28	3.38	6.49	
Propithecus diadema	n	1	1	1	1	1	1	1	1	1	1	1	1	1	1	
	mean	25.23	9.82	10.05	0.59	1.38	14.15	17.35	23.52	8.61	8.65	7.61	46.80	57.89	136.26	
	sd	-	-	-	-	-	-	-	-	-	-	-	-	-	-	
Propithecus verreauxi	n	4	6	4	6	4	6	5	6	4	6	6	6	6	6	

	mean	23.16	7.86	8.50	0.58	1.37	10.01	13.28	18.13	6.60	5.78	6.43	49.54	55.33	135.30
	sd	1.18	0.67	0.18	0.12	0.73	0.79	1.09	1.56	1.26	0.89	1.46	3.28	5.01	4.09
Pygathrix nemaeus	n	2	2	2	2	2	2	2	2	2	2	2	2	2	2
	mean	27.62	8.27	8.65	0.55	1.12	9.41	15.84	20.04	5.65	8.12	6.64	40.95	55.40	135.20
	sd	3.13	0.38	0.03	0.09	0.42	0.54	2.62	2.85	0.17	1.25	0.67	11.41	3.51	1.13
Rhinopithecus roxellana	n	3	3	2	3	2	3	3	3	2	3	3	3	3	3
	mean	31.88	6.76	7.82	0.66	2.77	11.10	23.96	28.06	9.89	10.17	3.61	37.84	58.14	131.20
	sd	0.63	0.39	0.68	0.04	0.96	1.40	0.94	1.77	2.18	3.69	0.64	4.66	2.77	10.14
Semnopithecus entellus	n														
	mean														
	sd														
Symphalangus syndactylus	n	4	4	4	4	4	4	4	4	4	4	4	4	4	4
	mean	33.76	8.57	9.16	0.56	2.86	11.15	21.40	24.99	8.85	10.98	6.38	41.59	61.27	140.88
	sd	1.10	1.46	1.73	0.06	0.05	1.81	2.15	3.68	1.91	4.18	2.12	5.94	9.27	11.75
Tarsius bancanus	n	2	2	2	1	2	2	2	2	0	2	0	2	2	2
	mean	11.74	2.02	1.92	0.62	0.44	0.97	5.82	8.98	-	0.72	-	29.14	50.06	99.10
	sd	0.14	0.26	0.13	-	0.34	0.10	0.31	0.18	-	0.29	-	3.29	7.17	12.39
Tarsius syrichta	n														
	mean														
	sd														
Theropithecus gelada	n	3	3	3	3	3	3	3	3	3	3	3	4	4	4
	mean	34.91	8.02	9.84	0.88	3.71	9.84	24.56	38.58	12.04	12.98	5.11	40.20	67.72	140.61
	sd	1.39	0.17	0.51	0.31	1.01	3.38	0.85	1.54	5.08	2.22	1.45	8.11	4.91	5.70
Varecia v. variegata	n	5	5	5	5	5	5	5	5	5	5	5	6	6	6
	mean	22.66	8.00	9.09	0.51	1.92	7.53	16.97	21.39	7.55	9.64	2.84	52.49	60.21	138.94
	sd	0.86	0.74	0.69	0.02	0.38	0.99	1.74	1.23	2.89	2.48	1.08	5.57	4.01	4.29

C7		**GM**	**VBVL**	**VBDL**	**VB ECC**	**UNC**	**SPL**	**ATPL**	**PTPL**	**PCSA**	**LCSA**	**SCSA**	**TPAA**	**TPPA**	**AFA**
Alouatta caraya	n	1	1	1	1	1	1		1	1	1	1		1	1
	mean	24.52	7.77	7.48	0.43	3.12	18.87		36.84	27.69	14.92	10.99		59.30	146.81
	sd	-	-	-	-	-	-		-	-	-	-		-	-
Alouatta guariba	n	2	2	2	2	2	2		1	2	2	2		2	2
	mean	25.33	6.89	7.09	0.42	2.12	16.63		27.98	10.10	11.37	11.33		60.39	144.44
	sd	0.54	0.92	0.37	0.09	0.17	0.61		-	1.72	0.73	2.47		4.04	4.36
Alouatta palliata	n	4	4	4	4	4	4		4	4	4	4		4	4
	mean	25.48	6.43	6.61	0.47	2.10	16.53		32.12	10.78	13.69	8.24		66.41	146.37
	sd	0.97	0.48	0.40	0.05	0.34	1.09		2.97	2.67	2.18	1.09		2.27	7.34
Alouatta seniculus	n														
	mean														

	sd													
Ateles fusciceps	n	3	3	3	3	3	3	3	3	3	3	6	6	
	mean	28.4	8.56	9.49	0.39	3.73	19.62	36.26	18.72	27.02	17.16	70.61	145.99	
	sd	1.13	0.64	0.32	0.09	0.88	2.36	1.60	5.53	7.13	3.39	2.76	14.14	
Ateles geoffroyi	n	4	3	3	3	3	3	3	3	3	3	2	2	
	mean	26.68	8.61	9.38	0.40	3.48	18.31	30.82	17.90	19.68	13.97	65.78	154.17	
	sd	1.06	0.21	0.47	0.08	0.44	1.26	3.04	1.44	3.68	2.76	2.29	4.27	
Avahi laniger	n	1	1	1	1	1	1	1	1	1	1	1	1	
	mean	15.44	5.25	4.99	0.47	1.13	6.53	14.34	4.15	3.05	2.62	41.45	136.45	
	sd	-	-	-	-	-	-	-	-	-	-	-	-	
Cebus apella	n	6	6	6	6	5	6	6	6	6	6	8	8	
	mean	23.56	5.45	5.42	0.32	1.11	12.25	23.87	5.05	5.51	3.48	61.86	132.07	
	sd	1	0.34	0.49	0.03	0.27	1.15	1.12	0.33	2.12	0.80	5.95	8.84	
Cercocebus torquatus	n	3	3	3	3	3	3	3	3	3	3	3	3	
	mean	27.62	5.63	5.69	0.53	1.96	9.4	28.15	7.31	6.67	2.54	59.21	143.02	
	sd	2.06	0.25	0.48	0.12	0.15	2.03	1.08	1.24	1.29	0.40	3.76	5.69	
Cercopithecus mitis	n	8	8	8	8	8	8	8	8	8	8	10	10	
	mean	25.11	5.49	5.98	0.54	2.21	7.79	30.29	9.74	5.25	2.36	58.79	142.20	
	sd	3.57	0.52	0.44	0.04	0.35	1.84	2.14	2.64	1.82	0.68	5.82	8.29	
Chlorocebus aethiops	n	4	4	4	4	4	4	4	4	4	4	6	6	
	mean	24.14	5.85	6.13	0.54	2.09	9.84	27.68	7.65	4.73	3.23	56.43	145.24	
	sd	1.40	0.68	0.63	0.09	0.42	1.33	1.34	1.74	1.17	1.34	4.54	4.35	
Chlorocebus pygerythrus	n	2	2	2	2	2	2	2	2	2	2	2	2	
	mean	25.46	6.18	6.12	0.50	1.62	8.84	27.73	7.88	4.84	3.53	57.12	143.25	
	sd	0.24	0.37	0.18	0.04	0.62	0.62	0.25	1.94	0.03	0.50	3.31	5.53	
Colobus guereza	n	2	2	2	2	2	2	2	2	2	2	4	4	
	mean	30.26	7.31	7.57	0.51	3.04	11.95	33.14	13.73	8.58	4.97	56.44	155.44	
	sd	0.53	0.81	0.66	0	0.17	0.87	1.27	2.63	1.71	0.05	6.82	7.38	
Erythrocebus patas	n	2	2	2	2	2	2	2	2	2	2	2	3	
	mean	29.35	6.23	7.11	0.59	2.06	12.11	33.56	13.12	8.87	3.25	54.15	139.18	
	sd	0.30	0.32	0.69	0.01	0.52	1.73	0.81	1.38	0.91	0.69	4.09	17.21	
Gorilla beringei	n	3	3	3	3	3	3	3	3	3	3	4	4	
	mean	58.25	13.27	14.98	0.56	5.73	52.87	60.07	59.57	111.36	67.23	75.94	148.26	
	sd	0.92	1.99	1.02	0.03	0.51	5.99	4.25	5.98	27.23	11.55	5.95	12.75	
Gorilla g. gorilla	n	5	5	5	5	5	5	5	5	5	5	5	5	
	mean	54.57	12.69	14.73	0.62	4.71	51.78	60.79	47.70	86.37	73.96	70.90	154.05	
	sd	1.23	1.06	1.04	0.11	2.26	3.44	6.01	7.73	6.78	17.98	1.67	6.18	
Hapalemur griseus	n	5	5	5	5	5	5	5	7	7	7	6	6	
	mean	18.76	3.58	4.09	0.39	0.56	6.39	15.3	2.16	2	0.67	53.20	135.02	
	sd	4.40	0.28	0.25	0.05	0.52	1.10	0.79	1.55	1.57	0.47	3.00	18.27	
Homo sapiens	n	9	9	9	9	9	9	8	9	9	9	10	10	
	mean	54.66	12.90	13.4	0.60	2.48	26.68	61.18	39.91	53.73	39.15	67.56	155.45	

	sd	1.24	0.99	0.59	0.03	0.80	3.10	3.77	9.63	14.91	7.19	2.49	16.19
Hylobates agilis	n	1	1	1	1	1	1	1	1	1	1	1	1
	mean	29.72	6.32	7.06	0.65	2.82	14.66	32.23	10.76	21.13	14.36	75.47	164.26
	sd	-	-	-	-	-	-	-	-	-	-	-	-
Hylobates klossii	n												
	mean												
	sd												
Hylobates lar	n	1	1	1	1	1	1	1	1	1	1	1	1
	mean	29.75	7.14	7.37	0.67	2.10	11.66	28.09	12.23	14.09	13.6	70.02	161.20
	sd	-	-	-	-	-	-	-	-	-	-	-	-
Hylobates muelleri	n												
	mean												
	sd												
Indri indri	n	1	1	1	1	1	1	1	1	1	1	0	1
	mean	24.49	10.73	12.95	0.43	0.73	15.76	27.22	28.22	29.12	12.98	-	141.59
	sd	-	-	-	-	-	-	-	-	-	-	-	-
Lemur catta	n	4	4	3	4	3	4	4	3	4	4	4	4
	mean	20.29	6.54	6.84	0.42	1.36	6.53	21.14	8.48	5.72	2.75	60.47	143.00
	sd	0.50	0.67	0.56	0.02	0.55	1.21	0.79	1.47	2.26	0.79	3.97	0.40
Lepilemur mustelinus	n	6	6	4	6	3	6	6	4	6	6	7	6
	mean	15.01	3.43	3.47	0.45	0.26	1.95	13.37	2.13	1.13	0.92	51.82	128.35
	sd	3.11	0.48	0.57	0.04	0.30	0.51	0.82	0.36	0.31	0.58	3.52	9.45
Macaca fuscata	n	2	2	2	2	2	2	2	2	2	2	2	2
	mean	31.18	6.35	6.71	0.58	2.53	9.75	35.41	15.25	7.87	6.92	62.27	150.74
	sd	2.29	0.33	0.86	0.06	0.33	0.19	2.21	1.47	0.33	1.58	1.87	14.22
Macaca nemestrina	n	1	1	1	1	1	1	1	1	1	1	1	1
	mean	32.59	6.40	7.01	0.56	0.08	11.14	36.76	10.83	6.17	4.09	64.31	141.48
	sd	-	-	-	-	-	-	-	-	-	-	-	-
Macaca nigra	n												
	mean												
	sd												
Macaca tonkeana	n												
	mean												
	sd												
Mandrillus sphinx	n	2	2	2	2	2	2	2	2	2	2	2	2
	mean	37.17	7.75	9.13	0.56	2.51	16.08	40.68	17.35	12.45	7.42	59.22	145.57
	sd	0.54	0.4	0.64	0.05	0.56	0.18	0.21	7.83	0.07	2.36	5.10	10.90
Miopithecus talapoin	n	5	5	5	5	5	5	4	5	5	5	7	7
	mean	19.43	3.63	3.87	0.63	1.05	4.17	18.04	2.24	1.56	1.41	50.03	140.17
	sd	0.49	0.19	0.27	0.07	0.19	0.37	1.32	0.31	0.51	0.25	5.07	10.63
Nasalis larvatus	n	2	2	2	2	2	2	2	2	2	2	2	2
	mean	27.92	7.24	8.92	0.73	3.61	13.41	29.41	14.30	12.50	6.72	53.50	152.57
	sd	1.14	0.18	0.33	0.08	0.17	0.15	0.50	3.53	2.20	1.38	3.03	0.05

Nomascus concolor	n	1	1	1	1	1	1	1	1	1	1	1	1
	mean	28.82	5.82	6.98	0.67	3.08	13.12	30.12	14.87	16.26	8.37	78.87	125.94
	sd	-	-	-	-	-	-	-	-	-	-	-	-
Nomascus leucogenys	n	1	1	1	1	1	1	1	1	1	1	1	1
	mean	31.04	6.58	7.57	0.64	2.80	14.2	27.37	11.87	12.23	7.33	62.96	154.34
	sd	-	-	-	-	-	-	-	-	-	-	-	-
Pan t. troglodytes	n	8	8	8	8	8	8	8	9	9	9	8	8
	mean	47.79	10.45	11.65	0.50	5.35	30.71	53.64	30.30	39.16	34.03	65.42	149.30
	sd	1.32	0.98	0.75	0.05	1.00	2.30	3.24	13.85	16.47	13.59	3.09	12.26
Papio anubis	n	6	6	6	6	6	6	5	7	7	7	6	6
	mean	38.65	8.53	9.84	0.63	3.04	16.32	49.21	19.68	16.79	8.09	57.21	132.77
	sd	1.97	1.84	1.35	0.12	0.41	3.11	3.66	10.40	7.56	4.17	3.71	6.02
Pithecia irrorata	n												
	mean												
	sd												
Pithecia pithecia	n	3	3	2	3	2	3	3	4	4	4	3	3
	mean	18.06	4.19	4.99	0.45	1.93	9.41	19.93	2.71	3.32	1.54	67.13	142.59
	sd	0.86	0.78	0.53	0.07	0.63	1.08	1.65	3.26	2.29	1.03	1.30	4.72
Pongo pygmaeus	n	9	9	9	9	9	5	9	10	10	10	9	9
	mean	52.24	11.62	12.87	0.53	4.08	34.80	51.58	40.80	57.86	44.64	70.42	157.52
	sd	4.31	1.88	1.81	0.05	1.93	3.27	3.88	18.45	27.43	20.93	6.55	7.62
Propithecus diadema	n	2	2	2	2	2	2	2	2	2	2	1	1
	mean	23.42	6.46	7.94	0.45	1.83	12.38	22.78	11.84	9.62	6.46	62.29	141.97
	sd	2.25	2.51	1.70	0.02	0.32	5.39	6.55	1.41	2.67	3.07	-	-
Propithecus verreauxi	n	3	5	4	5	4	5	5	6	6	6	5	5
	mean	22.37	7.20	8.11	0.56	1.38	10.78	20.84	6.24	5.83	4.82	52.34	138.14
	sd	1.78	0.80	0.44	0.14	0.44	0.63	1.66	4.88	3.06	2.49	4.88	6.35
Pygathrix nemaeus	n	2	2	2	2	2	2	2	2	2	2	2	2
	mean	27.18	8.04	8.25	0.53	1.19	10.78	23.44	8.16	9.38	8.37	51.96	138.91
	sd	3.100	0.11	0.00	0.10	0.12	0.10	3.18	1.58	2.99	3.25	3.29	9.31
Rhinopithecus roxellana	n	2	2	1	2	2	2	2	3	3	3	2	2
	mean	31.87	6.86	8.4	0.54	2.69	9.38	31.56	9.69	6.17	2.97	58.44	139.25
	sd	1.23	0.86	-	0.01	0.07	0.90	1.58	8.47	5.99	2.94	4.53	0.71
Semnopithecus entellus	n	2	2	0	2	0	2	2	0	2	2	2	2
	mean	26.58	6.45	-	0.50	-	9.37	26.05	-	8.64	3.18	62.61	133.91
	sd	0.34	0.44	-	0.00	-	0.51	0.29	-	1.62	0.43	13.13	10.38
Symphalangus syndactylus	n	5	5	4	5	4	5	3	5	5	5	5	5
	mean	33.33	8.47	9.37	0.51	2.56	14.18	31.06	21.71	14.22	11.45	64.81	159.91
	sd	1.00	1.26	0.80	0.04	1.26	1.68	3.33	5.11	2.86	3.34	3.88	8.47
Tarsius bancanus	n	3	3	3	3	3	3	3	0	3	0	2	2

	mean	11.71	1.93	1.97	0.87	0.16	1.23	9.90	-	0.29	-	56.83	107.70
	sd	0.46	0.35	0.06	0.08	0.08	0.08	0.41	-	0.27	-	11.49	9.27
Tarsius syrichta	n												
	mean												
	sd												
Theropithecus gelada	n	3	3	3	3	3	3	3	3	3	3	4	4
	mean	35.59	7.25	10.25	0.75	3.61	12.22	41.96	15.04	12.24	4.32	60.56	143.92
	sd	1.34	0.97	0.92	0.27	0.98	2.47	3.93	4.46	1.74	1.17	4.13	5.01
Varecia v. variegata	n	5	5	5	5	5	5	5	6	6	6	6	6
	mean	22.63	8.37	8.98	0.36	1.23	9.67	23.86	11.64	8.49	3.12	58.30	148.60
	sd	0.74	0.76	0.63	0.03	0.48	0.64	0.82	5.94	4.54	1.67	2.86	2.93

Abbreviations are as follows: sd = standard deviation; GM = geometric mean; VBVL = vertebral body ventral length; VBDL = vertebral body dorsal length; VB ECC = vertebral body eccentricity; UNC = uncinate process height; SPL = spinous process length; ATPL anterior transverse process length; PTPL = posterior transverse process length; PCSA = pedicle cross-sectional area; LCSA = lamina cross-sectional area; SCSA = spinous process cross-sectional area; TPAA = transverse process angle – anterior tubercle; TPPA = transverse process angle – posterior tubercle; AFA – superior article facet angle.

APPENDIX C

SUMMARY STATISTIC TABLE OF EXTANT MALE VERTEBRAL METRICS

Summary statistics for vertebral metrics in males

C1		GM	VBVL	VBDL	VB ECC	UNC	SPL	ATPL	PTPL	PCSA	LCSA	SCSA	TPAA	TPPA	AFA
Alouatta caraya	n	1					1		1	1	1			1	
	mean	30.99					2.29		40.36	31.47	16.18			89.73	
	sd	-					-		-	-	-			-	
Alouatta guariba	n														
	mean														
	sd														
Alouatta palliata	n	8					7		7	7	7			6	
	mean	30.54					3.08		37.98	28.16	14.09			85.80	
	sd	1.14					0.59		2.11	5.51	3.29			1.56	
Alouatta seniculus	n	1					1		1	1	1			1	
	mean	32.97					2.95		40.47	32.61	21.56			80.05	
	sd	-					-		-	-	-			-	
Ateles fusciceps	n	8					7		7	8	8			9	
	mean	32.08					2.35		37.83	16.11	15.29			71.25	
	sd	1.08					0.45		2.71	4.85	6.90			3.73	
Ateles geoffroyi	n	1					1		1	1	1			1	
	mean	31.61					2.53		35.49	21.47	15.42			72.36	
	sd	-					-		-	-	-			-	
Avahi laniger	n	3					3		3	3	3			3	
	mean	16.82					1.14		22.08	4.12	5.08			62.08	
	sd	0.84					0.18		0.46	1.06	2.33			1.55	
Cebus apella	n	8					8		7	8	8			6	
	mean	28.08					1.44		29.06	16.63	5.89			76.89	
	sd	0.89					0.19		2.19	3.17	0.94			6.77	
Cercocebus torquatus	n	3					2		2	3	3			3	
	mean	35.59					1.95		43.01	36.74	12.38			74.56	
	sd	2.1					0.04		0.91	3.65	2.44			6.72	
Cercopithecus mitis	n	4					4		4	4	4			8	
	mean	31.96					1.49		36.84	16.98	7.66			72.89	
	sd	1.05					0.26		0.91	2.86	1.81			4.35	
Chlorocebus aethiops	n	8					6		6	6	6			8	
	mean	30.25					1.32		32.31	17.14	5.52			71.72	
	sd	0.89					0.33		1.87	5.62	2.59			4.36	
Chlorocebus pygerythrus	n	2					2		2	2	2			2	
	mean	31.54					1.80		35.20	14.10	8.29			71.14	
	sd	1.70					0.49		2.96	2.78	2.60			1.81	
Colobus guereza	n	9					8		9	9	9			10	

	mean	33.36	1.82	38.03	20.98	7.81	74.72
	sd	0.53	0.35	2.70	7.47	1.61	4.62
Erythrocebus patas	n	3	3	3	3	3	4
	mean	36.10	2.4	45.85	29.21	8.83	70.83
	sd	0.74	1.00	1.16	8.15	3.91	3.18
Gorilla beringei	n	3	3	3	3	3	4
	mean	73.48	8.60	85.41	169.21	70.90	70.50
	sd	0.67	1.75	4.94	53.22	19.76	5.75
Gorilla g. gorilla	n	4	4	4	3	4	6
	mean	71.69	9.78	77.02	124.32	58.33	72.98
	sd	4.32	5.10	9.70	7.78	10.74	7.26
Hapalemur griseus	n						1
	mean						62.43
	sd						-
Homo sapiens	n	11	11	11	11	11	10
	mean	65.56	6.68	74.11	70.54	34.22	58.83
	sd	3.71	0.98	5.00	22.05	10.95	4.37
Hylobates agilis	n						
	mean						
	sd						
Hylobates klossii	n	1	1	1	1	1	1
	mean	34.87	1.68	33.67	13.07	7.68	61.48
	sd	-	-	-	-	-	-
Hylobates lar	n	1	1	1	1	1	0
	mean	34.33	2.65	42.60	18.28	18.54	-
	sd	-	-	-	-	-	-
Hylobates muelleri	n	3	3	3	3	3	3
	mean	33.58	1.71	35.43	12.44	5.14	64.96
	sd	0.84	0.58	0.96	1.87	1.39	0.30
Indri indri	n	5	5	5	5	5	2
	mean	13.24	1.83	36.78	11.44	17.49	63.07
	sd	0.60	0.36	1.86	1.51	4.75	7.53
Lemur catta	n	6	5	5	5	5	7
	mean	22.19	1.45	27.78	5.28	5.87	65.15
	sd	0.74	0.18	1.74	1.60	0.66	2.68
Lepilemur mustelinus	n	4	3	4	4	4	4
	mean	15.55	0.92	18.68	3.11	3.75	60.95
	sd	1.69	0.18	3.22	0.30	0.68	2.08
Macaca fuscata	n	3	3	3	3	3	3
	mean	36.99	2.04	36.99	54.93	11.11	71.79
	sd	1.25	0.64	1.06	14.67	4.46	2.04
Macaca nemestrina	n	6	6	6	6	6	7
	mean	38.75	2.07	40.43	36.32	11.79	73.97

	sd	1.00	0.29	2.42	9.66	2.80	6.69
Macaca nigra	n	2	1	1	2	2	1
	mean	42.4	1.58	36.05	66.38	9.12	74.82
	sd	7.89	-	-	12.17	3.22	-
Macaca tonkeana	n	2	2	2	2	2	2
	mean	36.17	2.10	36.73	54.90	6.01	74.31
	sd	0.33	0.49	0.96	1.69	1.22	4.19
Mandrillus sphinx	n	9	9	9	9	9	11
	mean	47.40	4.19	56.57	67.63	23.46	75.09
	sd	3.14	1.31	6.10	19.6	6.49	4.70
Miopithecus talapoin	n	1	1	1	1	1	1
	mean	22.87	0.86	23.72	6.59	2.50	60.07
	sd	-	-	-	-	-	-
Nasalis larvatus	n	15	13	13	14	14	15
	mean	35.09	1.40	39.73	35.03	8.93	70.28
	sd	2.61	0.32	2.60	9.50	3.83	4.83
Nomascus concolor	n	1	1	1	1	1	1
	mean	34.96	2.96	36.74	9.64	9.56	70.10
	sd	-	-	-	-	-	-
Nomascus leucogenys	n						
	mean						
	sd						
Pan t. troglodytes	n	8	8	8	8	8	11
	mean	56.45	4.31	61.20	50.72	28.00	66.79
	sd	1.00	1.01	3.41	10.62	5.46	4.17
Papio anubis	n	9	9	9	9	9	9
	mean	47.43	3.23	56.39	56.52	19.79	71.67
	sd	2.28	0.72	3.58	9.41	4.01	2.52
Pithecia irrorata	n	1	1	1	1	1	1
	mean	23.08	1.89	29.66	22.99	11.91	78.61
	sd	-	-	-	-	-	-
Pithecia pithecia	n	11	11	11	11	11	11
	mean	22.38	1.44	25.44	10.17	7.60	73.77
	sd	0.87	0.27	1.86	3.02	3.03	5.10
Pongo pygmaeus	n	9	9	8	9	8	5
	mean	64.23	6.62	69.55	92.89	55.77	78.27
	sd	6.65	1.34	4.20	26.70	13.36	8.13
Propithecus diadema	n						
	mean						
	sd						
Propithecus verreauxi	n	3	4	4	3	4	3

	mean	25.79			1.87		30.14	10.05	8.72			60.89	
	sd	1.17			0.39		2.14	1.82	0.47			4.41	
Pygathrix nemaeus	n	4			4		4	4	4			4	
	mean	34.73			1.74		36.11	36.74	7.56			68.72	
	sd	1.06			0.31		2.51	11.53	0.75			2.10	
Rhinopithecus roxellana	n												
	mean												
	sd												
Semnopithecus entellus	n	1			1		1	1	1			2	
	mean	42.74			1.57		44.6	34.52	7.26			69.80	
	sd	-			-		-	-	-			5.53	
Symphalangus syndactylus	n	1			1		1	1	1			1	
	mean	39.21			2.94		40.47	36	20.22			65.48	
	sd	-			-		-	-	-			-	
Tarsius bancanus	n	1			1		1	0	1			1	
	mean	13.19			0.67		14.12	-	0.89			74.97	
	sd	-			-		-	-	-			-	
Tarsius syrichta	n	5			5		5	3	4			8	
	mean	12.09			0.62		13.23	1.93	1.00			72.63	
	sd	0.31			0.12		0.43	0.42	0.28			5.99	
Theropithecus gelada	n	1			1		1	1	1			4	
	mean	42.13			1.69		46.57	56.18	6.02			74.32	
	sd	-			-		-	-	-			6.51	
Varecia v. variegata	n	1			1		1	1	1			1	
	mean	25.66			1.38		33.29	9.18	9.29			60.00	
	sd	-			-		-	-	-			-	

C2		GM	VBVL	VBDL	VB ECC	UNC	SPL	ATPL	PTPL	PCSA	LCSA	SCSA	TPAA	TPPA	AFA
Alouatta caraya	n	1			1		1		1	1	1	1		1	
	mean	29.12			1.01		15.53		34.98	13.18	21.14	63.56		64.85	
	sd	-			-		-		-	-	-	-		-	
Alouatta guariba	n														
	mean														
	sd														
Alouatta palliata	n	8			8		8		7	8	8	7		6	
	mean	28.75			1.05		13.09		32.19	15.65	17.58	48.35		64.12	
	sd	0.63			0.16		1.38		2.24	6.21	3.88	17.06		14.53	
Alouatta seniculus	n	1			1		1		1	1	1	1		1	
	mean	29.60			0.93		19.4		36.67	14.49	30.9	37.36		69.83	
	sd	-			-		-		-	-	-	-		-	

Ateles fusciceps	n	8	8	8	8	8	8	8	9
	mean	28.85	0.81	10.92	25.81	11.98	13.24	24.66	60.33
	sd	0.79	0.11	1.64	2.42	2.79	3	7.63	6.50
Ateles geoffroyi	n	1	1	1	1	1	1	1	1
	mean	27.61	0.92	11.09	23.93	10.34	14.86	34.31	58.79
	sd	-	-	-	-	-	-	-	-
Avahi laniger	n	2	2	2	2	2	2	2	1
	mean	18.53	1.23	3.99	11.82	5.29	3.22	5.72	52.52
	sd	4.23	0.06	0.83	0.82	0.89	0.26	2.45	-
Cebus apella	n	12	12	11	12	12	12	12	9
	mean	25.89	0.79	7.88	22.36	8.51	6.75	14.12	63.02
	sd	2.49	0.09	0.90	1.77	1.22	2.76	5.48	5.76
Cercocebus torquatus	n	2	1	2	2	2	2	2	2
	mean	34.09	1.28	11.17	28.26	23.85	17.77	35.64	48.99
	sd	1.86	-	0.61	2.60	0.91	3.56	6.81	1.23
Cercopithecus mitis	n	5	5	5	5	5	5	5	10
	mean	29.72	1.01	9.14	28.48	12.66	11.17	16.56	55.20
	sd	1.32	0.10	1.80	0.98	3.23	4.14	1.53	3.31
Chlorocebus aethiops	n	7	7	7	7	8	8	8	7
	mean	27.99	1.05	8.54	22.97	12.33	6.44	15.67	49.85
	sd	0.73	0.09	1.17	1.74	7.08	4.02	7.98	4.13
Chlorocebus pygerythrus	n	2	2	2	2	2	2	2	2
	mean	28.89	1.09	7.77	24.82	10.71	8.17	24.13	45.50
	sd	0.92	0.02	0.04	1.81	2.43	1.10	9.63	0.57
Colobus guereza	n	12	11	12	12	12	12	12	12
	mean	30.60	0.97	11.81	26.80	12.49	13.13	22.11	55.62
	sd	0.75	0.10	1.46	1.82	2.82	3.36	5.54	7.18
Erythrocebus patas	n	3	3	3	3	3	3	3	4
	mean	32.74	1.20	14.26	30.13	17.26	14.75	20.71	53.58
	sd	1.51	0.19	1.19	2.02	9.29	7.92	12.49	5.72
Gorilla beringei	n	4	4	4	4	4	4	4	5
	mean	66.36	1.18	36.19	63.96	107.91	95.26	271.10	51.53
	sd	1.45	0.07	4.84	3.43	18.98	26.58	111.79	2.97
Gorilla g. gorilla	n	4	4	4	4	4	4	4	6
	mean	65.61	1.09	27.67	63.91	86.03	79.69	148.63	52.60
	sd	3.08	0.24	5.90	3.36	30.39	14.41	71.52	2.70
Hapalemur griseus	n	0	0	0	0	0	0	0	1
	mean	-	-	-	-	-	-	-	56.22
	sd	-	-	-	-	-	-	-	-
Homo sapiens	n	11	11	11	10	11	11	11	10
	mean	60.86	0.83	16.27	53.17	70.50	55.09	128.72	56.74
	sd	3.38	0.10	2.52	3.52	21.26	15.19	98.07	3.31

Hylobates agilis	n								
	mean								
	sd								
Hylobates klossii	n	1	1	1	1	0	1	1	1
	mean	30.66	0.84	7.20	18.67	-	7.07	27.14	43.15
	sd	-	-	-	-	-	-	-	-
Hylobates lar	n	1	1	1	1	1	1	1	0
	mean	32.1	1.05	8.89	23.01	25.23	16.99	48.70	-
	sd	-	-	-	-	-	-	-	-
Hylobates muelleri	n	4	4	4	4	4	4	4	4
	mean	31.06	1.03	6.92	22.91	10.57	7.19	18.19	46.77
	sd	0.87	0.06	0.23	0.93	0.71	1.20	6.89	2.08
Indri indri	n	0	2	2	2	2	2	2	2
	mean	-	0.74	10.26	20.22	14.48	14.39	26.90	48.96
	sd	-	0.12	1.44	2.42	9.60	1.98	5.42	7.87
Lemur catta	n	7	7	7	6	7	7	7	6
	mean	20.45	0.83	5.48	15.23	6.60	5.92	11.52	47.62
	sd	0.91	0.09	0.60	0.86	1.91	1.75	6.24	11.95
Lepilemur mustelinus	n	4	4	4	4	4	4	4	4
	mean	14.01	1.06	3.79	10.69	3.35	2.26	6.38	51.06
	sd	1.50	0.21	0.82	1.02	0.71	0.49	0.99	8.52
Macaca fuscata	n	3	3	3	3	3	3	2	3
	mean	34.41	1.30	11.46	27.37	14.59	12.24	22.72	69.06
	sd	1.04	0.20	0.66	1.14	5.31	2.19	6.78	24.90
Macaca nemestrina	n	5	5	5	4	5	5	5	6
	mean	35.74	1.07	13.67	28.94	15.72	20.33	25.91	64.31
	sd	0.91	0.18	2.61	1.64	3.72	8.50	8.26	25.09
Macaca nigra	n	2	2	2	2	2	2	2	1
	mean	35.54	1.21	13.98	27.34	19.08	18.22	21.99	45.42
	sd	1.88	0.26	3.32	1.94	0.68	0.81	8.41	-
Macaca tonkeana	n	3	3	3	3	3	3	3	3
	mean	33.79	1.03	11.49	25.49	12.79	13.25	17.23	50.51
	sd	1.02	0.1	1.18	1.2	0.25	2.68	4.83	1.57
Mandrillus sphinx	n	9	9	9	9	9	9	9	11
	mean	43.29	1.08	18.86	38.92	35.59	39.97	53.69	58.39
	sd	2.84	0.17	3.21	5.1	12.39	14.39	16.31	11.74
Miopithecus talapoin	n	1		1	1		1	1	1
	mean	21.27		4.97	15.13		3.59	7.43	50.36
	sd	-		-	-		-	-	-
Nasalis larvatus	n	16	15	15	13	16	16	16	13
	mean	33.75	1.12	10.55	25.10	15.26	13.23	19.84	49.54
	sd	3.11	0.09	1.58	2.83	3.39	3.32	5.77	6.29
Nomascus	n	1	1	1	1	1	1	1	1

concolor									
	mean	31.75	0.98	9.67	25.38	17.99	10.40	16.92	47.03
	sd	-	-	-	-	-	-	-	-
Nomascus leucogenys	n								
	mean								
	sd								
Pan t. troglodytes	n	9	8	9	9	9	9	9	12
	mean	52.69	0.86	15.70	42.66	49.77	39.99	89.20	51.93
	sd	1.52	0.12	2.61	2.17	9.34	10.78	20.38	4.03
Papio anubis	n	9	9	9	9	9	9	9	9
	mean	43.40	1.17	16.77	37.22	27.32	23.41	40.63	50.16
	sd	1.98	0.09	3.46	2.81	7.53	8.21	12.06	3.23
Pithecia irrorata	n	1	1	1	1	1	1	1	1
	mean	21.51	1.10	7.47	22.50	11.29	9.74	22.52	68.57
	sd	-	-	-	-	-	-	-	-
Pithecia pithecia	n	13	10	13	13	10	13	13	11
	mean	20.65	0.86	6.34	19.44	5.85	5.64	14.69	62.30
	sd	0.61	0.15	0.75	1.11	1.78	2.93	5.84	8.25
Pongo pygmaeus	n	9	9	9	9	9	9	9	4
	mean	57.76	1.00	37.83	55.35	92.97	68.10	120.02	56.16
	sd	6.26	0.11	7.87	4.10	11.81	22.56	44.17	6.50
Propithecus diadema	n								
	mean								
	sd								
Propithecus verreauxi	n	4	3	4	5	4	4	5	4
	mean	22.99	1.04	6.70	17.30	9.50	7.58	14.68	48.23
	sd	1.09	0.18	0.95	2.04	1.88	0.86	3.96	3.38
Pygathrix nemaeus	n	4	3	4	3	4	4	4	4
	mean	32.63	1.00	11.04	23.84	16.63	10.04	14.23	52.87
	sd	0.98	0.12	0.96	1.65	4.01	2.01	3.93	4.01
Rhinopithecus roxellana	n								
	mean								
	sd								
Semnopithecus entellus	n	2	2	2	1	2	2	2	3
	mean	37.37	1.13	13.46	32.23	18.30	12.55	33.98	59.87
	sd	2.51	0.2	2.81	-	0.26	3.27	7.25	5.27
Symphalangus syndactylus	n	1	1	1	0	0	1	1	0
	mean	39.54	0.76	8.90	-	-	22.77	72.79	-
	sd	-	-	-	-	-	-	-	-
Tarsius bancanus	n	1	1	1	1	0	1	1	1
	mean	12.12	1.46	2.53	8.37	-	0.70	3.82	57.74

	sd	-		-		-	-	-	-	-	-			
Tarsius syrichta	n	8		8		8	9	6	8	9	9			
	mean	11.20		1.00		2.10	7.68	1.02	1.03	3.71	55.61			
	sd	0.32		0.09		0.15	0.46	0.06	0.23	0.71	5.41			
Theropithecus gelada	n	1		1		1	1	1	1	1	2			
	mean	39.15		1.06		12.96	32.57	24.98	17.24	36.58	54.63			
	sd	-		-		-	-	-	-	-	4.81			
Varecia v. variegata	n	2		1		2	2	2	2	2	2			
	mean	23.79		0.75		8.26	19.12	14.58	11.05	25.87	59.10			
	sd	0.28		-		1	0.42	2.90	2.54	0.65	2.88			

C3		GM	VBVL	VBDL	VB ECC	UNC	SPL	ATPL	PTPL	PCSA	LCSA	SCSA	TPAA	TPPA	AFA
Alouatta caraya	n	1	1	1	1	1	1		1	1	1	1		1	1
	mean	28.73	11.24	10.68	0.83	2.87	16.27		34.41	21.44	17.02	7.50		84.10	145.38
	sd	-	-	-	-	-	-		-	-	-	-		-	-
Alouatta guariba	n														
	mean														
	sd														
Alouatta palliata	n	8	8	8	8	8	8		7	8	8	8		5	5
	mean	28.28	9.77	7.06	0.74	2.12	12.30		32.52	10.38	15.65	9.00		62.23	144.49
	sd	0.74	1.33	0.59	0.12	1.12	2.09		1.66	2.60	3.13	1.26		7.13	5.95
Alouatta seniculus	n	1	1	1	1	1	1		1	1	1	1		1	1
	mean	27.64	10.05	9.83	0.78	3.61	18.98		41.71	22.42	25.63	5.35		76.57	152.11
	sd	-	-	-	-	-	-		-	-	-	-		-	-
Ateles fusciceps	n	8	8	7	8	7	8		8	7	8	8		8	8
	mean	28.27	8.79	8.50	0.67	3.71	9.96		26.45	10.71	13.73	5.76		61.78	138.97
	sd	1.14	0.65	0.98	0.08	0.64	0.82		2.00	3.39	4.07	1.97		3.91	7.41
Ateles geoffroyi	n	1	1	1	1	1	1		1	1	1	1		1	1
	mean	27.56	8.48	8.41	0.7	3.50	10.56		26.46	9.44	9.73	5.52		63.18	121.80
	sd	-	-	-	-	-	-		-	-	-	-		-	-
Avahi laniger	n	2	2	2	2	2	2		2	2	2	1		3	2
	mean	15.7	5.93	5.88	0.66	0.74	1.46		10.50	2.20	2.25	0.72		47.14	131.54
	sd	0.16	0.13	0.30	0.11	0.12	0.47		0.13	0.62	0.06	-		3.94	0.18
Cebus apella	n	12	12	12	12	12	12		11	12	12	12		10	10
	mean	24.83	5.65	5.67	0.76	2.47	6.49		21.68	5.75	6.14	2.54		70.55	133.43
	sd	0.78	0.66	0.42	0.10	0.57	1.37		1.33	1.83	1.56	0.83		3.70	6.92
Cercocebus torquatus	n	1	1	1	1	1	1		1	1	1	1		1	1
	mean	33.18	8.56	8.84	1.00	3.05	9.25		31.47	19.94	14.85	7.39		67.99	145.01
	sd	-	-	-	-	-	-		-	-	-	-		-	-
Cercopithecus mitis	n	5	5	5	5	5	5		5	5	5	5		10	7

	mean	29.28	8.01	7.65	0.90	3.45	7.46	30.16	8.76	7.96	3.79	64.76	134.32
	sd	1.25	0.56	0.56	0.20	0.65	0.82	2.72	2.18	3.09	1.03	3.90	5.97
Chlorocebus aethiops	n	8	8	8	8	8	8	8	8	8	8	8	10
	mean	27.62	7.65	6.88	0.83	2.35	7.03	23.73	6.98	6.93	4.80	54.42	132.79
	sd	0.82	1.22	0.93	0.07	0.47	1.80	3.12	2.16	1.20	1.89	9.29	8.64
Chlorocebus pygerythrus	n	2	2	2	2	2	2	2	2	2	2	2	2
	mean	28.27	6.98	6.75	0.97	3.06	5.68	27.05	5.90	6.25	6.93	58.28	126.02
	sd	0.80	0.55	0.71	0.05	0.67	1.20	0.95	1.73	2.16	0.07	1.00	10.80
Colobus guereza	n	11	11	11	11	11	11	10	11	11	11	12	12
	mean	30.11	8.12	7.69	0.80	3.04	7.23	27.31	10.73	11.58	4.65	59.83	131.17
	sd	0.63	0.75	0.75	0.06	0.70	1.02	1.68	2.26	1.97	1.25	7.84	11.13
Erythrocebus patas	n	3	3	3	3	3	3	3	3	3	3	4	4
	mean	33.12	11.91	12.14	1.00	3.40	10.53	31.46	9.25	18.93	7.22	63.17	137.49
	sd	0.52	0.55	0.66	0.09	0.47	1.84	1.34	2.75	3.70	2.43	3.31	4.42
Gorilla beringei	n	4	4	4	4	4	4	4	4	4	4	4	3
	mean	65.49	17.86	17.80	1.16	7.21	75.30	63.75	91.68	97.75	68.78	56.27	126.11
	sd	1.45	1.09	1.45	0.10	1.56	5.45	5.87	12.76	17.83	10.85	4.02	18.27
Gorilla g. gorilla	n	4	4	4	4	4	4	4	4	4	4	7	7
	mean	64.95	16.10	15.23	1.16	5.42	57.90	62.32	73.37	51.29	47.35	54.35	133.55
	sd	3.62	1.00	1.28	0.10	1.90	13.73	2.97	24.98	20.45	17.11	3.83	4.29
Hapalemur griseus	n	0	0	0	0	0	0	0	0	0	0	1	1
	mean	-	-	-	-	-	-	-	-	-	-	62.55	138.69
	sd	-	-	-	-	-	-	-	-	-	-	-	-
Homo sapiens	n	11	11	11	11	11	11	10	11	11	11	10	10
	mean	57.75	12.19	12.65	0.74	3.28	14.28	50.37	31.52	28.72	50.98	53.40	114.69
	sd	3.29	1.33	1.26	0.10	1.54	2.02	3.71	5.64	11.31	13.26	3.29	29.72
Hylobates agilis	n												
	mean												
	sd												
Hylobates klossii	n												
	mean												
	sd												
Hylobates lar	n	1	1	1	1	1	1	1	1	1	1	0	0
	mean	31.96	8.73	7.15	1.05	2.95	5.31	24.34	13.44	7.47	13.77	-	-
	sd	-	-	-	-	-	-	-	-	-	-	-	-
Hylobates muelleri	n												
	mean												
	sd												
Indri indri	n	0	2	2	2	2	2	2	2	2	2	2	2
	mean	-	15.21	14.12	0.61	0.70	11.75	19.95	9.80	13.31	4.88	76.50	129.57
	sd	-	0.73	0.36	0.07	0.98	0.66	2.04	2.98	0.44	1.18	26.91	4.43
Lemur catta	n	6	6	6	6	5	6	6	6	6	6	6	6
	mean	20.23	7.45	7.53	0.61	1.3	4.17	15.38	4.49	4.61	2.41	59.13	135.77

	sd	0.67	0.84	0.69	0.07	0.32	0.74	0.86	3.3	1.18	1.33	3.28	7.63
Lepilemur mustelinus	n	4	4	3	4	2	4	4	4	4	4	4	4
	mean	13.76	5.36	4.88	0.68	0.54	1.54	10.48	1.15	1.67	0.97	49.49	131.42
	sd	1.11	0.83	0.47	0.05	0.42	0.25	1.49	0.89	0.56	0.71	4.73	4.67
Macaca fuscata	n	3	3	3	3	3	3	3	3	3	3	3	3
	mean	33.73	8.14	8.67	0.9	3.25	7.54	29.66	21.88	10.09	6.57	57.49	116.99
	sd	0.85	1.22	1.32	0.07	0.66	0.90	1.45	12.52	3.76	2.17	3.46	37.37
Macaca nemestrina	n	6	6	6	6	5	6	5	6	6	6	7	7
	mean	34.79	8.76	9.59	0.84	2.63	10.10	30.75	13.98	15.06	5.76	66.62	139.43
	sd	0.63	0.88	0.74	0.11	0.58	1.18	1.74	4.23	5.55	2.23	8.82	10.76
Macaca nigra	n	2	2	1	2	1	2	2	2	2	2	1	1
	mean	34.94	10.57	9.89	0.87	0.86	9.91	30.52	4.87	13.15	7.32	64.07	145.54
	sd	1.40	0.83	-	0.18	-	1.32	3.03	6.89	1.37	0.01	-	-
Macaca tonkeana	n	3	3	3	3	3	3	2	3	3	3	3	2
	mean	32.88	7.47	7.69	0.98	2.74	9.64	27.60	9.66	11.71	4.37	60.64	140.17
	sd	1.58	1.69	1.41	0.11	0.66	3.20	4.56	2.70	0.68	0.18	8.15	1.81
Mandrillus sphinx	n	9	9	9	9	9	9	8	9	9	9	11	11
	mean	42.53	12.57	12.59	0.90	4.38	15.87	39.58	24.88	29.26	10.61	60.41	136.63
	sd	3.09	2.51	2.63	0.15	1.21	3.53	5.02	9.24	8.62	4.15	6.04	5.70
Miopithecus talapoin	n												
	mean												
	sd												
Nasalis larvatus	n	16	16	14	15	15	16	11	16	16	16	13	14
	mean	31.35	8.76	8.81	0.99	3.03	7.56	25.00	10.13	13.20	4.30	58.64	139.22
	sd	1.72	1.01	0.96	0.08	0.64	2.20	2.56	3.99	2.98	1.38	4.94	9.19
Nomascus concolor	n	1	1	1	1	1	1	1	1	1	1	1	1
	mean	30.68	8.16	7.07	0.93	2.86	7.37	22.46	6.58	5.99	6.87	54.67	137.27
	sd	-	-	-	-	-	-	-	-	-	-	-	-
Nomascus leucogenys	n												
	mean												
	sd												
Pan t. troglodytes	n	9	9	9	9	8	9	9	9	9	9	11	11
	mean	52.26	11.66	11.43	0.92	4.16	22.88	40.90	28.87	21.43	17.42	53.98	133.56
	sd	1.43	0.50	0.67	0.09	0.63	7.29	2.25	6.59	6.74	6.90	3.19	5.60
Papio anubis	n	9	9	9	9	9	9	9	9	9	9	9	9
	mean	42.01	12.81	12.39	0.94	4.65	14.89	40.87	25.27	25.18	12.91	67.55	131.13
	sd	1.67	1.79	1.04	0.10	0.81	1.97	2.31	6.92	7.44	2.52	2.09	9.02
Pithecia irrorata	n	1	1	1	1	1	1	1	1	1	1	1	1
	mean	21.11	6.81	6.91	0.72	1.81	8.92	21.81	5.37	5.93	2.38	66.94	141.96
	sd	-	-	-	-	-	-	-	-	-	-	-	-
Pithecia pithecia	n	12	12	10	12	10	12	11	10	12	12	14	13

	mean	20.20	6.00	5.60	0.73	2.00	6.78	18.88	4.74	4.46	2.06	63.54	133.40	
	sd	0.53	0.62	0.67	0.16	0.36	1.24	1.20	1.38	2.09	1.41	7.06	8.38	
Pongo pygmaeus	n	9	9	9	9	9	9	9	9	9	9	9	9	
	mean	56.98	13.95	14.30	0.97	6.12	43.54	54.97	64.15	46.92	51.09	63.17	135.53	
	sd	4.79	1.10	1.43	0.06	1.69	8.71	3.38	12.32	19.25	13.08	9.18	8.48	
Propithecus diadema	n													
	mean													
	sd													
Propithecus verreauxi	n	3	5	3	3	3	3	5	3	3	3	3	3	
	mean	23.01	9.52	8.60	0.70	1.07	4.87	15.78	6.04	5.48	3.22	54.11	130.27	
	sd	1.59	0.32	0.75	0.09	0.69	1.3	1.76	2.83	0.75	1.25	8.84	4.68	
Pygathrix nemaeus	n	3	3	3	3	3	3	3	3	3	3	3	3	
	mean	32.25	8.53	8.68	0.84	2.69	6.34	20.40	13.70	8.11	7.36	59.08	138.17	
	sd	0.05	1.02	0.61	0.22	1.06	0.97	9.21	3.45	1.78	3.23	5.58	14.78	
Rhinopithecus roxellana	n													
	mean													
	sd													
Semnopithecus entellus	n	2	2	2	2	2	2	1	2	2	2	3	3	
	mean	35.97	10.38	10.02	0.90	2.74	8.82	32.13	11.53	14.74	6.34	65.20	119.26	
	sd	2.57	0.64	0.52	0.03	2.26	2.92	-	3.69	2.48	1.22	3.53	11.82	
Symphalangus syndactylus	n	1	1	1	1	1	1	0	1	1	1	1	1	
	mean	34.53	8.35	8.64	0.81	3.29	5.47	-	17.07	10.14	18.99	45.38	139.85	
	sd	-	-	-	-	-	-	-	-	-	-	-	-	
Tarsius bancanus	n	1	1	1	1	1	1	1	0	1	0	1	1	
	mean	11.88	3.24	2.56	0.89	0.17	0.51	7.92	-	0.51	-	52.11	142.23	
	sd	-	-	-	-	-	-	-	-	-	-	-	-	
Tarsius syrichta	n	10	11	10	10	8	10	11	11	11	0	8	9	
	mean	10.79	2.59	2.35	0.93	0.20	0.34	7.61	0.48	0.35	-	50.72	132.55	
	sd	0.41	0.27	0.08	0.06	0.10	0.07	0.19	0.31	0.13	-	3.22	12.70	
Theropithecus gelada	n	2	2	2	2	2	2	2	2	2	2	3	3	
	mean	33.8	8.78	9.54	0.88	4.78	10.57	32.78	13.67	17.74	8.6	70.45	128.30	
	sd	5.76	3.03	1.17	0.03	1.62	0.95	0.21	2.34	2.02	3.63	7.08	5.24	
Varecia v. variegata	n	1	1	1	1	1	1	1	1	1	1	1	1	
	mean	22.69	10.28	9.95	0.75	0.8	7.65	18.72	9.37	6.21	2.95	63.46	138.27	
	sd	-	-	-	-	-	-	-	-	-	-	-	-	

C4		GM	VBVL	VBDL	VB ECC	UNC	SPL	ATPL	PTPL	PCSA	LCSA	SCSA	TPAA	TPPA	AFA
Alouatta caraya	n	1	1	1	1	0	1	1	1	1	1	1	1	1	1
	mean	28.34	10.17	9.79	0.74	-	17.91	39.27	33.44	20.65	23.17	5.75	65.26	85.43	144.77
	sd	-	-	-	-	-	-	-	-	-	-	-	-	-	-

Alouatta guariba	n														
	mean														
	sd														
Alouatta palliata	n	9	9	9	9	9	9	9	9	9	9	9	7	7	7
	mean	28.32	7.51	7.13	0.81	2.86	14.03	33.58	34.45	10.21	14.56	6.85	56.88	71.77	139.65
	sd	1.24	0.81	0.51	0.09	0.65	1.93	4.59	2.86	3.93	2.66	1.92	2.48	2.43	5.15
Alouatta seniculus	n	1	1	1	1	1	1	1	1	1	1	1	1	1	0
	mean	28.83	9.06	10.24	0.65	3.25	18.39	42.99	38.94	19.02	17.28	3.25	66.43	79.50	-
	sd	-	-	-	-	-	-	-	-	-	-	-	-	-	-
Ateles fusciceps	n	7	7	7	7	7	7	7	7	7	7	7	8	8	8
	mean	28.32	8.60	8.76	0.63	3.17	9.24	23.75	26.82	8.22	12.75	4.62	44.27	66.70	136.34
	sd	0.84	0.84	0.47	0.07	0.56	1.65	1.76	1.77	2.39	5.51	1.01	7.63	4.21	10.30
Ateles geoffroyi	n	1	1	1	1	1	1		1	1	1	1	1	1	1
	mean	27.92	8.22	8.23	0.61	3.92	8.78		25.67	10.39	12.9	10.81	30.66	62.64	139.25
	sd	-	-	-	-	-	-		-	-	-	-	-	-	-
Avahi laniger	n	3	3	3	3	3	3	1	3	3	3	3	1	3	3
	mean	15.62	5.97	5.60	0.60	0.50	2.45	9.54	10.71	2.07	2.62	1.70	24.36	49.50	131.47
	sd	0.63	0.50	0.23	0.07	0.24	0.72	-	0.38	0.30	0.53	0.91	-	8.27	2.41
Cebus apella	n	12	12	12	12	12	12	10	12	12	12	12	10	10	10
	mean	24.74	5.40	5.46	0.75	2.22	6.56	18.47	21.33	5.81	5.39	2.19	41.34	71.18	133.50
	sd	0.75	0.42	0.42	0.10	0.70	1.21	1.62	1.59	1.98	1.11	0.77	6.73	2.58	5.20
Cercocebus torquatus	n	1	1	1	1	2	1	1	1	1	1	1	1	1	1
	mean	32.73	8.15	9.73	0.99	3.28	9.4	26.76	29.36	17.02	18.60	6.21	54.67	66.98	132.08
	sd	-	-	-	-	1.33	-	-	-	-	-	-	-	-	-
Cercopithecus mitis	n	5	5	5	5	4	5	5	5	5	5	5	11	11	11
	mean	29.09	7.41	7.04	0.87	3.49	6.93	21.62	30.73	8.92	7.53	3.53	38.57	62.66	135.41
	sd	1.12	0.80	0.79	0.22	0.53	1.72	2.07	2.52	2.88	3.00	1.00	2.74	2.56	8.13
Chlorocebus aethiops	n	8	8	8	8	8	8	7	8	8	8	8	7	8	8
	mean	27.51	7.18	6.44	0.75	2.54	7.22	19.59	24.25	6.83	7.25	3.78	40.84	60.50	138.42
	sd	0.64	1.03	0.62	0.08	0.48	1.09	2.04	2.60	2.24	1.84	1.58	2.99	6.31	7.77
Chlorocebus pygerythrus	n	2	2	2	2	2	2	2	2	2	2	2	2	2	2
	mean	28.42	6.66	6.53	0.91	3.14	7.03	20.63	28.53	5.13	6.68	4.36	40.06	61.64	127.89
	sd	1.16	0.60	0.19	0.07	0.45	2.40	0.93	1.92	1.37	2.29	1.49	1.39	2.58	11.34
Colobus guereza	n	11	11	11	11	11	11	10	11	11	11	11	11	12	12
	mean	30.18	6.94	7.01	0.73	2.88	7.56	25.43	28.14	10.29	9.73	5.17	40.05	58.38	134.82
	sd	0.86	0.89	0.81	0.05	0.47	1.64	2.10	1.93	3.27	2.32	1.94	8.20	5.87	16.70
Erythrocebus patas	n	4	4	4	4	4	4	4	4	4	4	4	5	5	5
	mean	32.99	10.53	10.60	0.92	3.77	11.25	24.88	35.72	9.42	12.95	5.10	37.58	64.74	139.66
	sd	0.63	0.76	0.65	0.08	0.28	3.63	2.11	3.93	4.47	2.5	2.14	4.15	3.37	8.73
Gorilla beringei	n	4	4	4	4	5	4	2	3	4	4	4	4	4	4
	mean	64.65	17.80	16.61	0.99	7.11	84.79	39.28	66.75	90.17	100.32	78.14	30.14	59.37	135.15

	sd	2.05	0.96	0.64	0.04	2.67	2.70	1.10	2.23	16.56	18.79	22.26	4.55	2.93	13.51
Gorilla g. gorilla	n	4	4	4	4	3	4	4	4	4	4	4	6	7	7
	mean	64.27	15.53	15.52	1.08	5.79	81.49	43.70	65.53	81.17	73.89	89.34	31.60	52.37	136.53
	sd	3.05	1.12	1.46	0.09	1.28	9.33	2.23	2.60	13.68	12.67	18.72	2.01	9.87	25.25
Hapalemur griseus	n														
	mean														
	sd														
Homo sapiens	n	11	11	11	11	11	11	10	9	11	11	11	10	10	10
	mean	57.65	11.31	12.43	0.76	4.03	13.80	42.07	51.72	31.14	21.34	54.67	34.66	52.77	114.29
	sd	3.25	1.10	1.55	0.07	1.75	3.14	1.93	5.21	7.05	7.78	25.49	3.96	3.74	18.10
Hylobates agilis	n														
	mean														
	sd														
Hylobates klossii	n														
	mean														
	sd														
Hylobates lar	n	1	1	1	1	1	1	0	1	1	1	1	0	0	0
	mean	31.97	8.19	8.19	0.85	2.27	8.78	-	25.37	13.34	9.06	8.41	-	-	-
	sd	-	-	-	-	-	-	-	-	-	-	-	-	-	-
Hylobates muelleri	n	3	3	1	3	3	3	2	3	3	3	3	3	3	3
	mean	29.60	6.93	8.03	0.88	2.29	5.79	15.12	21.81	8.01	4.04	3.79	29.01	50.64	140.02
	sd	0.26	0.74	-	0.07	0.74	0.22	1.29	0.73	1.56	0.58	1.59	6.73	6.85	5.39
Indri indri	n	0	1	1	1	1	1	0	1	1	1	1	0	1	1
	mean	-	13.19	13.13	0.60	3.35	13.92	-	20.62	10.97	14.92	5.56	-	53.77	120.15
	sd	-	-	-	-	-	-	-	-	-	-	-	-	-	-
Lemur catta	n	7	7	7	7	6	7	3	7	7	7	7	2	7	7
	mean	19.79	6.81	6.95	0.61	1.40	4.13	12.04	15.58	4.68	3.88	2.68	34.39	59.96	140.32
	sd	0.63	0.96	0.71	0.05	0.66	1.27	2.70	0.88	1.63	0.61	1.28	1.28	6.21	4.11
Lepilemur mustelinus	n	3	3	2	3	2	3	1	3	3	3	3	1	3	3
	mean	13.86	4.92	4.82	0.58	0.85	1.43	8.57	10.66	1.17	1.65	0.88	31.84	49.59	131.66
	sd	1.46	0.97	1.36	0.15	0.63	0.01	-	1.52	1.11	0.18	0.76	-	7.48	12.90
Macaca fuscata	n	3	3	3	3	3	3	2	3	3	3	3	2	3	3
	mean	33.64	7.05	8.19	0.92	2.23	8.11	24.90	32.17	12.45	10.07	5.73	29.70	60.30	139.05
	sd	1.4	1.33	0.97	0.18	1.71	2.26	1.85	2.31	2.58	1.33	2.45	11.84	6.15	9.63
Macaca nemestrina	n	6	6	6	6	6	5	2	3	6	6	6	2	5	7
	mean	34.75	7.60	7.95	0.81	3.48	9.72	28.27	32.33	14.55	11.80	5.00	38.03	57.97	141.12
	sd	0.78	0.88	1.17	0.15	1.22	0.82	0.88	1.16	5.10	4.71	0.95	16.77	8.16	3.79
Macaca nigra	n	1	1	0	0	1	1	1	1	0	1	0	0	0	0
	mean	35.97	7.67	-	-	4.08	11.26	27.81	34.36	-	9.13	-	-	-	-
	sd	-	-	-	-	-	-	-	-	-	-	-	-	-	-
Macaca tonkeana	n	3	3	3	3	2	3	3	2	3	3	3	1	1	2
	mean	33.72	6.28	6.79	0.83	2.82	9.09	23.90	28.32	8.56	8.21	3.88	44.47	64.39	145.52
	sd	0.32	0.23	0.87	0.24	0.10	3.16	1.61	1.97	1.45	1.82	0.67	-	-	0.14

Mandrillus sphinx	n	9	9	9	9	9	9	8	8	9	9	9	11	11	11
	mean	42.61	11.09	11.35	0.89	4.06	17.21	31.68	41.33	25.73	30.34	8.72	44.52	57.80	137.18
	sd	3.10	2.07	2.11	0.17	0.92	3.67	5.85	6.38	10.36	12.52	3.16	17.30	8.93	8.93
Miopithecus talapoin	n	1	1	0	1	1	1	1	1	0	1	1	1	1	1
	mean	20.70	3.80	-	0.85	3.47	3.89	13.40	15.44	-	2.33	0.73	38.11	59.10	131.81
	sd	-	-	-	-	-	-	-	-	-	-	-	-	-	-
Nasalis larvatus	n	14	14	11	14	12	14	11	11	14	14	14	9	9	13
	mean	31.32	8.02	8.81	0.92	3.07	7.39	21.58	25.14	10.57	12.59	5.18	36.50	61.66	142.97
	sd	1.76	0.66	0.61	0.09	1.13	2.13	2.72	2.82	4.29	4.06	2.06	4.99	4.54	5.91
Nomascus concolor	n	1	1	1	1	1	1	1	1	1	1	1	1	1	1
	mean	30.62	7.90	8.16	0.86	1.16	6.94	16.21	22	6.12	6.57	6.88	32.85	50.55	141.34
	sd	-	-	-	-	-	-	-	-	-	-	-	-	-	-
Nomascus leucogenys	n														
	mean														
	sd														
Pan t. troglodytes	n	8	8	8	8	8	8	6	8	8	8	8	10	10	10
	mean	52.61	11.28	11.08	0.84	3.93	25.02	32.62	42.97	29.88	22.59	16.64	35.76	58.04	131.33
	sd	1.79	0.85	0.49	0.06	0.64	3.25	3.28	3.36	7.44	7.37	3.68	8.35	7.63	10.34
Papio anubis	n	9	9	9	9	9	9	9	8	9	9	9	9	9	9
	mean	42.99	12.1	12.01	0.87	4.28	14.66	32.83	42.41	25.18	26.3	11.4	49.93	68.10	132.88
	sd	1.53	1.05	1.02	0.06	1.32	2.01	3.12	2.54	6.52	6.44	3.24	6.12	2.55	9.86
Pithecia irrorata	n	1	1	1	1	1	1	1	1	1	1	1	1	1	1
	mean	20.10	5.93	6.39	0.71	4.12	10.92	18.96	21.21	4.38	7.86	2.58	50.22	77.38	139.88
	sd	-	-	-	-	-	-	-	-	-	-	-	-	-	-
Pithecia pithecia	n	11	11	10	11	10	11	10	9	11	11	11	9	9	11
	mean	20.34	5.13	5.32	0.69	2.51	7.38	16.72	18.35	3.39	5.15	1.72	44.34	67.13	134.22
	sd	0.59	0.73	0.69	0.14	0.55	1.72	1.88	1.76	1.51	2.66	0.69	5.95	6.58	7.75
Pongo pygmaeus	n	9	8	8	8	8	8	8	8	8	8	8	9	9	9
	mean	58.00	13.53	14.36	0.82	5.63	50.87	43.01	55.6	58.09	53.96	52.54	36.73	65.18	135.94
	sd	3.42	0.98	1.61	0.09	1.7	4.59	2.68	3.15	14.36	20.69	14.92	3.99	5.85	10.96
Propithecus diadema	n														
	mean														
	sd														
Propithecus verreauxi	n	3	5	3	3	3	3	1	5	3	3	5	3	3	3
	mean	22.78	8.89	8.52	0.65	1.26	4.87	14.88	16.03	5.55	5.06	3.15	40.44	56.47	133.14
	sd	1.14	0.42	0.64	0.03	0.57	0.56	-	1.75	2.70	0.94	0.81	7.10	6.42	3.09
Pygathrix nemaeus	n	4	4	4	4	3	4	3	4	3	4	4	3	4	4
	mean	31.74	8.24	8.46	0.84	2.50	8.02	20.57	25.42	10.01	8.18	4.34	36.02	59.16	137.28
	sd	0.88	1.00	0.78	0.10	0.31	0.79	0.93	2.84	2.27	1.12	1.27	4.00	4.24	6.52
Rhinopithecus roxellana	n														

	mean														
	sd														
Semnopithecus entellus	n	2	2	2	2	2	2	1	1	2	2	2	2	3	3
	mean	36.23	8.51	9.35	0.93	3.16	8.56	27.90	34.4	13.90	13.91	9.16	38.98	63.87	120.79
	sd	2.64	0.96	0.21	0.03	0.40	2.90	-	-	1.52	1.25	1.60	1.34	0.57	12.96
Symphalangus syndactylus	n	1	1	1	1	1	1	0	0	1	1	1	0	1	1
	mean	35.00	8.91	8.87	0.79	1.72	6.52	-	-	11.66	14.48	16.10	-	55.83	130.46
	sd	-	-	-	-	-	-	-	-	-	-	-	-	-	-
Tarsius bancanus	n	1	1	1	1	0	1	0	1	0	1	0	1	1	1
	mean	12.03	2.89	2.24	0.50	-	0.65	-	8.09	-	0.41	-	34.96	47.82	93.04
	sd	-	-	-	-	-	-	-	-	-	-	-	-	-	-
Tarsius syrichta	n	5	6	5	4	2	5	3	6	6	6	0	5	9	9
	mean	10.80	2.25	2.11	0.82	0.67	0.39	5.98	7.61	0.43	0.34	-	29.06	42.98	124.82
	sd	0.49	0.23	0.06	0.05	0.05	0.11	0.95	0.15	0.35	0.17	-	7.71	4.24	19.53
Theropithecus gelada	n	1	1	1	1	0	1	1	1	1	1	1	3	3	3
	mean	37.89	8.09	8.76	0.77	-	12.47	29.25	36.27	11.06	18.55	14.60	38.65	62.24	137.53
	sd	-	-	-	-	-	-	-	-	-	-	-	1.97	11.10	4.26
Varecia v. variegata	n	1	1	1	1	1	1	0	1	1	1	1	1	1	1
	mean	23.09	10.16	8.57	0.63	0.28	7.85	-	17.77	6.31	6.18	3.35	37.03	56.35	131.78
	sd	-	-	-	-	-	-	-	-	-	-	-	-	-	-

C5		GM	VBVL	VBDL	VB ECC	UNC	SPL	ATPL	PTPL	PCSA	LCSA	SCSA	TPAA	TPPA	AFA
Alouatta caraya	n	1	1	1	1	1	1	1	1	1	1	0	1	1	1
	mean	28.34	10.22	10.11	0.73	3.63	20.47	28.16	36.67	18.61	24.68	-	50.22	83.84	148.76
	sd	-	-	-	-	-	-	-	-	-	-	-	-	-	-
Alouatta guariba	n														
	mean														
	sd														
Alouatta palliata	n	9	9	9	9	9	9	9	9	9	9	9	7	7	7
	mean	28.33	7.60	7.09	0.80	2.75	14.76	32.31	34.91	9.18	14.96	7.37	49.48	73.14	144.08
	sd	1.19	0.83	0.36	0.11	0.51	1.81	3.52	2.51	3.26	2.86	2.14	7.52	2.98	8.78
Alouatta seniculus	n	1	1	1	1	1	1	1	1	1	1	1	1	1	1
	mean	29.05	8.45	10.47	0.55	3.91	20.19	37.34	38.91	19.03	19.60	4.89	53.36	80.55	148.86
	sd	-	-	-	-	-	-	-	-	-	-	-	-	-	-
Ateles fusciceps	n	7	7	7	7	7	7	7	7	7	7	7	7	7	7
	mean	28.61	7.58	8.84	0.59	3.45	13.59	23.47	28.9	9.11	14.41	6.42	43.90	70.45	139.41
	sd	0.93	0.65	0.48	0.07	0.57	4.17	1.67	1.16	1.85	5.27	2.29	5.51	4.08	4.12
Ateles geoffroyi	n	1	1	1	1	1	1	1	1	1	1	1	1	1	1
	mean	27.81	7.53	8.01	0.57	4.03	9.92	21.71	25.7	8.17	15.42	7.14	39.53	67.31	144.08
	sd	-	-	-	-	-	-	-	-	-	-	-	-	-	-

Avahi laniger	n	3	3	3	3	3	3	3	3	3	3	3	2	2	3
	mean	15.46	5.49	5.52	0.56	1.09	3.72	8.45	11.38	1.73	2.15	1.65	26.66	49.37	128.37
	sd	0.31	0.44	0.31	0.08	0.12	0.09	0.39	0.27	0.37	0.51	0.58	8.60	11.45	5.33
Cebus apella	n	12	12	12	12	12	12	12	12	12	12	12	9	10	10
	mean	24.78	5.04	5.57	0.72	2.43	7.55	17.85	22.41	5.02	5.30	2.40	42.72	74.60	136.24
	sd	0.68	0.32	0.46	0.12	0.41	1.63	1.99	1.14	1.62	1.22	0.76	3.54	5.13	7.97
Cercocebus torquatus	n	3	3	3	3	3	3	2	3	3	3	3	2	3	3
	mean	32.76	7.85	8.99	0.83	3.28	9.96	20.54	31.95	13.65	14.64	6.10	30.22	61.61	128.51
	sd	1.55	0.51	0.45	0.02	0.03	1.34	0.64	3.60	3.37	4.82	2.92	3.95	7.31	7.70
Cercopithecus mitis	n	5	5	5	5	5	5	5	5	5	5	5	11	11	11
	mean	29.43	7.26	7.49	0.81	2.89	7.99	21.17	32.29	9.11	7.61	3.18	36.69	64.64	141.94
	sd	1.12	0.89	0.58	0.14	0.62	2.01	2.12	1.77	2.38	3.45	1.03	2.88	2.68	5.93
Chlorocebus aethiops	n	8	8	8	8	8	8	7	8	8	8	8	8	8	8
	mean	27.53	6.81	6.36	0.76	2.73	8.56	19.47	26.11	5.54	6.34	3.51	34.80	60.50	134.78
	sd	0.60	0.57	0.67	0.17	0.76	2.36	1.97	3.63	1.45	1.50	1.43	3.04	4.06	5.62
Chlorocebus pygerythrus	n	2	2	2	2	2	2	2	2	2	2	2	2	2	2
	mean	28.61	7.04	7.12	0.90	3.02	6.61	20.54	28.15	6.03	6.84	5.88	38.42	62.58	131.02
	sd	1.39	0.16	0.16	0.07	0.37	1.94	0.24	4.07	3.25	1.08	0.15	0.78	1.40	12.45
Colobus guereza	n	11	11	11	11	11	11	11	11	12	12	12	12	12	12
	mean	30.30	6.73	6.90	0.69	2.89	7.36	24.10	30.14	9.21	8.17	3.57	39.00	61.44	132.84
	sd	0.64	0.65	0.62	0.06	0.35	1.20	1.81	1.34	4.11	3.16	1.73	3.56	3.02	8.42
Erythrocebus patas	n	4	4	4	4	4	4	4	4	4	4	4	5	5	5
	mean	32.90	9.92	10.14	0.94	3.87	12.57	25.21	36.89	10.86	14.61	4.58	34.63	63.95	138.72
	sd	0.56	0.46	1.03	0.24	0.43	1.62	2.67	2.92	4.70	3.83	1.22	2.51	1.64	5.29
Gorilla beringei	n	4	3	4	4	3	4	4	3	4	4	4	4	4	5
	mean	64.88	17.87	16.55	0.82	7.67	86.41	40.55	65.63	82.03	116.04	81.65	33.69	61.36	142.62
	sd	2.04	0.67	1.42	0.11	0.99	4.30	4.93	0.78	19.55	17.73	16.51	3.64	4.01	13.73
Gorilla g. gorilla	n	4	4	3	4	4	4	4	4	4	4	4	7	7	7
	mean	64.97	16.19	16.74	0.82	4.21	85.33	43.38	68.08	76.05	95.81	92.85	32.14	57.23	141.09
	sd	2.94	2.53	1.33	0.10	2.97	6.6	2.03	3.48	13.59	24.24	21.36	1.33	3.82	15.54
Hapalemur griseus	n														
	mean														
	sd														
Homo sapiens	n	11	11	11	11	11	10	9	9	11	11	10	10	10	10
	mean	57.9	10.99	12.52	0.73	3.99	15.40	42.77	54.28	29.18	17.46	49.60	34.27	53.51	135.83
	sd	3.10	1.61	1.10	0.07	1.44	3.67	1.70	4.26	6.38	3.73	14.73	3.26	2.37	5.20
Hylobates agilis	n														
	mean														
	sd														
Hylobates klossii	n	1	1	0	1	1	1	0	1	1	1	1	1	1	1
	mean	31.02	7.41	-	0.82	1.53	7.54	-	19.92	0	5.29	5.08	25.78	48.91	149.50
	sd	-	-	-	-	-	-	-	-	-	-	-	-	-	-

Hylobates lar	n	1	1	1	1	1	1	0	1	1	1	1	0	0	0
	mean	32.34	8.66	7.83	0.86	3.06	8.02	-	24.80	10.15	10.99	8.12	-	-	-
	sd	-	-	-	-	-	-	-	-	-	-	-	-	-	-
Hylobates muelleri	n	1	1	0	1	1	1	1	1	0	1	1	1	1	1
	mean	29.80	6.79	-	0.66	0.41	7.71	15.96	22.98	-	4.60	3.58	30.15	58.15	155.14
	sd	-	-	-	-	-	-	-	-	-	-	-	-	-	-
Indri indri	n	0	1	1	1	1	1	0	1	1	1	1	0	1	1
	mean	-	15.37	12.98	0.83	0.66	14.41	-	20.22	14.18	16.88	6.52	-	54.82	122.95
	sd	-	-	-	-	-	-	-	-	-	-	-	-	-	-
Lemur catta	n	6	6	6	6	6	6	6	6	6	6	6	6	6	6
	mean	20.13	5.94	7.01	0.58	1.39	4.17	12.74	16.04	3.98	4.93	1.92	42.30	55.94	135.49
	sd	0.57	0.89	1.18	0.06	0.46	0.83	2.30	0.76	0.71	1.18	0.73	7.15	4.41	8.60
Lepilemur mustelinus	n	3	3	2	3	2	3	3	3	3	3	3	3	3	3
	mean	14.1	4.45	4.37	0.71	0.36	1.30	9.26	11.11	0.89	1.14	1.08	32.02	48.26	138.19
	sd	1.20	0.84	1.29	0.12	0.12	0.12	1.12	1.31	0.92	0.37	1.13	12.71	6.79	6.20
Macaca fuscata	n	3	3	3	3	3	3	3	3	3	3	3	3	3	3
	mean	33.94	7.62	7.77	0.84	3.31	9.34	23.42	33.11	12.83	10.08	4.89	32.97	61.23	146.54
	sd	0.91	1.35	1.32	0.08	0.29	0.64	3.21	0.65	5.25	3.65	2.45	2.27	7.54	3.95
Macaca nemestrina	n	6	6	6	6	6	6	6	5	6	6	6	5	6	7
	mean	34.71	7.69	8.10	0.73	3.08	10.43	24.93	33.91	13.03	11.31	4.8	43.42	64.75	140.92
	sd	0.33	0.87	0.56	0.10	1.02	1.24	1.96	2.69	3.43	4.50	0.93	6.52	12.01	7.32
Macaca nigra	n														
	mean														
	sd														
Macaca tonkeana	n	3	3	3	3	3	3	3	3	3	3	3	3	3	3
	mean	33.74	5.79	6.75	0.92	3.11	9.96	21.96	31.49	7.20	7.22	4.36	37.06	64.19	141.71
	sd	0.66	0.99	0.43	0.05	0.62	3.75	1.32	2.81	1.74	0.18	1.24	4.11	3.29	2.71
Mandrillus sphinx	n	9	9	9	9	9	9	9	9	9	9	9	11	11	11
	mean	42.76	10.30	11.45	0.85	3.69	19.28	30.03	44.32	22.98	29.64	7.96	34.74	60.77	136.83
	sd	3.05	1.56	2.02	0.18	1.02	4.14	6.28	6.38	6.67	11.02	1.97	7.15	3.97	5.53
Miopithecus talapoin	n														
	mean														
	sd														
Nasalis larvatus	n	15	15	13	15	14	15	12	11	15	15	15	12	12	13
	mean	31.82	7.51	9.07	0.89	3.44	8.97	21.39	25.61	10.22	11.72	4.13	34.11	59.26	140.53
	sd	1.68	1.03	0.84	0.10	1.20	2.72	2.16	2.72	2.87	3.03	1.27	2.73	5.11	2.93
Nomascus concolor	n	1	1	1	1	1	1	1	1	1	1	1	1	1	1
	mean	31.11	7.94	7.47	0.72	2.52	8.35	14.69	20.35	6.22	8.60	7.76	30.91	48.53	144.05
	sd	-	-	-	-	-	-	-	-	-	-	-	-	-	-
Nomascus leucogenys	n														
	mean														
	sd														
Pan t.	n	8	8	8	8	8	8	8	8	8	8	8	10	11	11

troglodytes															
	mean	52.11	11.58	11.69	0.78	4.30	27.69	33.10	44.55	28.67	26.81	24.75	34.97	59.10	142.63
	sd	1.85	1.04	0.55	0.08	0.60	2.74	3.81	2.98	6.26	6.94	8.04	3.43	4.01	7.08
Papio anubis	n	9	9	9	9	9	9	9	9	9	9	9	9	9	9
	mean	43.09	10.97	11.60	0.85	4.18	17.07	32.25	47.80	24.21	25.79	8.86	45.83	66.43	133.07
	sd	1.34	1.15	0.80	0.05	0.85	2.13	1.62	3.04	5.80	6.02	3.40	6.41	3.63	6.62
Pithecia irrorata	n	1	1	1	1	1	1	1	1	1	1	1	1	1	1
	mean	20.35	5.56	5.92	0.68	2.55	8.54	21.24	23.40	6.05	6.74	3.02	47.05	64.48	146.22
	sd	-	-	-	-	-	-	-	-	-	-	-	-	-	-
Pithecia pithecia	n	10	10	10	10	10	10	10	9	10	10	10	10	10	11
	mean	20.30	5.34	5.33	0.65	2.15	8.18	16.91	19.40	3.17	5.65	1.56	44.64	68.38	133.83
	sd	0.63	0.92	0.65	0.11	0.54	2.02	1.83	1.90	0.73	2.51	0.56	3.85	4.49	11.20
Pongo pygmaeus	n	8	8	8	8	8	8	8	8	8	8	8	9	9	9
	mean	58.41	13.47	14.86	0.70	5.92	54.27	42.96	58.72	60.21	65.04	59.08	36.16	66.39	136.34
	sd	3.13	1.25	1.04	0.11	1.64	4.42	3.49	5.12	17.79	20.00	7.30	4.63	9.37	13.45
Propithecus diadema	n														
	mean														
	sd														
Propithecus verreauxi	n	3	5	3	4	3	4	5	5	5	5	5	3	3	3
	mean	22.70	8.29	8.61	0.67	1.15	6.50	14.67	16.99	2.88	4.34	5.02	39.90	55.63	133.19
	sd	1.24	0.80	0.77	0.12	0.54	2.33	0.99	0.99	2.78	2.84	2.15	7.89	6.96	1.20
Pygathrix nemaeus	n	4	4	4	4	4	4	4	4	4	4	4	4	4	4
	mean	31.83	8.13	8.70	0.90	2.12	9.11	20.14	25.39	10.67	7.50	4.11	39.46	60.18	143.52
	sd	1.20	1.28	1.05	0.05	0.12	1.09	2.54	2.78	1.27	0.61	0.86	4.80	3.37	3.42
Rhinopithecus roxellana	n														
	mean														
	sd														
Semnopithecus entellus	n	2	2	2	2	2	2	1	1	2	2	2	2	2	3
	mean	35.46	8.97	9.24	0.88	3.10	8.97	27.28	36.81	11.93	12.38	7.90	37.60	60.74	128.88
	sd	3.07	0.17	0.82	0.07	0.71	5.29	-	-	4.33	2.70	0.75	5.33	3.52	5.87
Symphalangus syndactylus	n	1	1	1	1	1	0	0	1	1	1	1	0	1	1
	mean	35.16	7.88	9.07	0.74	3.77	-	-	25.07	10.73	12.24	8.20	-	59.63	145.46
	sd	-	-	-	-	-	-	-	-	-	-	-	-	-	-
Tarsius bancanus	n	1	1	1	1	1	1	1	1	0	1	0	1	1	1
	mean	12.07	2.63	2.33	0.92	0.10	0.79	6.42	8.47	-	0.27	-	32.96	49.83	82.28
	sd	-	-	-	-	-	-	-	-	-	-	-	-	-	-
Tarsius syrichta	n	5	5	5	5	3	5	6	5	6	6	0	9	9	9
	mean	10.78	2.13	2.00	0.82	0.34	0.47	6.29	8.47	0.61	0.40	-	27.64	47.80	120.31
	sd	0.53	0.25	0.17	0.04	0.26	0.12	0.46	0.47	0.49	0.21	-	3.81	4.87	20.88
Theropithecus gelada	n	2	2	2	2	2	2	1	2	2	2	2	4	4	4
	mean	33.92	8.34	9.50	0.97	4.95	11.00	28.92	34.33	14.08	15.32	7.85	32.62	64.48	135.64
	sd	5.62	0.19	0.42	0.02	0.33	4.79	-	8.16	2.14	1.03	2.41	9.63	10.16	5.62
Varecia v. variegata	n	2	2	1	2	1	2	2	1	2	2	2	2	2	2

	mean	22.85	8.84	9.55	0.55	0.78	7.53	18.05	20.21	2.99	6.73	2.38	56.70	66.66	135.94
	sd	0.29	0.01	-	0.03	-	0.21	0.95	-	4.23	0.26	0.94	2.79	1.05	0.84

C6		GM	VBVL	VBDL	VB ECC	UNC	SPL	ATPL	PTPL	PCSA	LCSA	SCSA	TPAA	TPPA	AFA
Alouatta caraya	n	1	1	1	1	1	1	1	1	1	1	1	1	1	1
	mean	28.59	9.89	10.45	0.60	2.94	24.22	28.64	38.34	15.76	20.63	10.93	48.10	77.45	159.52
	sd	-	-	-	-	-	-	-	-	-	-	-	-	-	-
Alouatta guariba	n														
	mean														
	sd														
Alouatta palliata	n	9	9	9	9	9	9	9	9	9	9	9	7	7	7
	mean	28.27	6.97	7.17	0.80	2.88	17.14	23.86	35.45	9.68	14.46	8.87	41.26	67.17	148.51
	sd	1.15	0.61	0.42	0.12	0.71	1.93	2.90	2.70	2.39	3.02	2.10	5.23	2.50	6.61
Alouatta seniculus	n	1	1	1	1	1	1	1	1	1	1	1	1	1	1
	mean	29.08	8.59	10.12	0.53	3.02	23.10	25.19	42.31	15.15	16.18	8.89	46.80	80.02	139.76
	sd	-	-	-	-	-	-	-	-	-	-	-	-	-	-
Ateles fusciceps	n	7	7	7	7	7	7	7	7	7	7	7	8	8	8
	mean	28.28	8.79	9.18	0.47	3.16	20.53	24.16	33.01	10.05	16.68	10.26	43.60	66.46	147.77
	sd	0.93	0.69	0.59	0.05	0.52	1.31	3.75	1.84	3.20	3.98	1.52	5.39	5.24	7.53
Ateles geoffroyi	n	1	1	1	1	1	1	1	1	1	1	1	1	1	1
	mean	28.13	8.71	8.69	0.54	4.31	17.74	22.07	31.29	7.50	19.99	13.75	41.19	65.24	149.67
	sd	-	-	-	-	-	-	-	-	-	-	-	-	-	-
Avahi laniger	n	3	3	3	3	2	3	3	3	3	3	3	3	3	3
	mean	15.55	5.32	5.26	0.55	1.07	5.93	7.61	12.12	2.24	2.40	2.17	40.21	46.67	121.67
	sd	0.43	0.61	0.32	0.06	0.58	0.27	0.87	0.47	0.62	0.58	0.36	4.40	6.90	5.35
Cebus apella	n	12	12	12	12	12	12	12	12	12	12	12	9	10	10
	mean	24.50	5.60	5.75	0.58	1.86	9.91	20.29	25.54	4.96	6.04	2.21	54.59	70.09	136.04
	sd	0.78	0.50	0.43	0.09	0.28	1.65	1.87	1.43	1.06	1.44	0.80	10.63	8.34	8.44
Cercocebus torquatus	n	3	3	3	3	3	3	3	2	3	3	3	3	3	3
	mean	32.70	8.42	8.93	0.84	2.94	11.56	25.88	34.67	13.74	14.19	3.77	55.29	63.01	137.18
	sd	1.27	1.35	0.36	0.07	0.41	2.32	0.84	2.17	0.28	3.46	0.45	3.99	4.36	5.25
Cercopithecus mitis	n	5	5	5	5	5	5	5	5	5	5	5	10	11	10
	mean	29.35	6.86	7.50	0.70	2.67	9.89	24.90	36.00	8.06	8.48	2.25	40.83	65.57	127.72
	sd	1.08	0.42	0.68	0.10	0.74	1.36	3.25	0.97	2.38	4.52	0.53	8.53	3.97	3.40
Chlorocebus aethiops	n	8	8	8	8	8	8	7	8	8	8	8	8	8	10
	mean	27.50	7.06	6.76	0.69	2.39	9.56	21.55	29.95	6.78	5.69	3.54	34.59	60.35	140.86
	sd	0.62	0.89	0.68	0.11	0.62	1.98	1.74	2.63	3.52	1.61	1.56	2.87	7.91	3.77
Chlorocebus pygerythrus	n	2	2	2	2	2	1	2	2	2	2	1	2	2	2
	mean	28.31	6.40	6.99	0.75	2.69	6.95	16.71	34.51	5.52	4.40	2.34	36.60	62.99	128.82
	sd	0.97	0.50	0.33	0.00	0.06	-	6.68	1.34	1.88	0.81	-	3.35	0.81	9.33
Colobus guereza	n	10	10	10	10	10	10	9	8	10	10	10	11	11	11
	mean	30.80	6.86	7.48	0.56	2.78	7.78	25.8	33.06	12.24	9.06	3.69	37.60	57.28	136.42
	sd	0.71	0.78	0.59	0.09	0.55	2.10	2.70	1.68	3.18	2.02	1.65	5.45	4.15	6.36
Erythrocebus patas	n	4	4	4	4	4	4	4	4	4	4	4	5	5	5
	mean	33.06	9.79	10.61	0.78	3.46	14.29	29.13	43.44	9.78	14.44	4.68	46.13	60.06	142.56
	sd	0.90	1.04	0.96	0.11	0.49	3.21	2.18	2.92	3.97	6.41	1.02	14.91	6.45	3.47
Gorilla beringei	n	3	3	3	3	3	2	3	2	3	3	3	4	4	5

	mean	65.65	16.44	16.60	0.66	9.40	84.62	62.57	59.83	87.20	149.03	115.34	37.88	66.22	150.36
	sd	1.68	1.84	0.87	0.07	2.05	2.21	0.86	1.31	32.83	34.54	29.69	5.95	7.32	5.99
Gorilla g. gorilla	n	4	4	3	4	4	4	3	4	4	3	4	6	6	5
	mean	64.68	16.09	17.42	0.63	5.72	79.62	52.61	68.00	68.24	145.67	119.48	33.54	62.37	144.47
	sd	2.26	2.01	2.82	0.06	0.88	7.85	5.93	3.36	21.61	55.02	31.62	4.77	6.26	15.41
Hapalemur griseus	n	0	0	0	0	0	0	0	0	0	0	0	1	1	1
	mean	-	-	-	-	-	-	-	-	-	-	-	41.22	58.61	146.53
	sd	-	-	-	-	-	-	-	-	-	-	-	-	-	-
Homo sapiens	n	11	11	11	11	11	11	9	8	11	11	11	9	10	10
	mean	57.30	11.56	12.45	0.70	4.15	23.19	46.36	57.95	37.48	35.80	31.51	37.30	57.02	110.44
	sd	3.31	1.37	1.07	0.10	0.90	4.93	2.57	4.77	9.03	13.19	9.30	3.59	4.37	18.91
Hylobates agilis	n														
	mean														
	sd														
Hylobates klossii	n	1	1	0	1	1	1	1	0	0	1	1	0	0	0
	mean	28.29	6.83	-	0.85	0.53	8.82	16.88	-	-	5.55	3.93	-	-	-
	sd	-	-	-	-	-	-	-	-	-	-	-	-	-	-
Hylobates lar	n	1	1	1	1	1	1	0	1	1	1	1	0	0	0
	mean	31.69	6.41	8.17	0.60	4.99	10.37	-	21.19	9.76	14.82	5.62	-	-	-
	sd	-	-	-	-	-	-	-	-	-	-	-	-	-	-
Hylobates muelleri	n	1	1	0	1	1	1	1	1	1	1	1	1	1	1
	mean	29.44	6.28	-	0.73	2.91	8.05	18.34	19.04	8.73	6.84	4.08	36.94	56.10	145.43
	sd	-	-	-	-	-	-	-	-	-	-	-	-	-	-
Indri indri	n	0	1	1	1	1	1	1	1	1	1	1	1	1	1
	mean	-	10.27	12.20	0.69	2.69	15.69	15.35	21.96	11.01	17.64	9.12	42.40	49.16	125.82
	sd	-	-	-	-	-	-	-	-	-	-	-	-	-	-
Lemur catta	n	6	6	6	6	6	6	6	6	6	6	6	6	6	6
	mean	20.24	6.62	6.88	0.56	1.74	5.87	12.98	17.64	3.36	4.82	1.80	47.62	54.95	133.88
	sd	0.48	0.84	0.43	0.04	0.38	1.15	0.59	0.65	0.64	0.90	0.62	5.29	7.68	2.45
Lepilemur mustelinus	n	3	3	3	3	3	3	3	3	3	3	2	3	3	3
	mean	13.77	4.43	4.42	0.58	0.11	1.29	7.85	11.23	1.29	2.00	0.73	45.20	46.15	126.38
	sd	1.54	0.67	0.76	0.06	0.03	0.19	1.08	1.81	0.83	0.61	0.04	9.31	6.89	2.42
Macaca fuscata	n	3	3	3	3	3	3	3	3	3	3	3	3	3	3
	mean	33.85	7.25	8.31	0.67	2.66	11.92	28.93	37.14	10.07	9.89	3.28	40.92	62.50	147.38
	sd	1.03	0.88	0.81	0.11	0.56	1.38	0.69	0.89	3.39	2.56	0.23	8.11	2.44	5.69
Macaca nemestrina	n	6	6	6	6	6	6	5	4	6	6	6	5	6	7
	mean	35.02	7.00	7.79	0.63	3.12	11.15	29.20	39.93	12.8	10.57	5.03	44.91	64.32	132.52
	sd	0.28	0.51	0.88	0.07	0.81	2.13	2.12	2.47	3.35	3.04	2.70	6.56	6.57	5.56
Macaca nigra	n	1	1	1	1	1	1	1	1	1	1	1	0	0	0
	mean	37.64	6.71	7.86	0.99	3.21	13.72	24.7	39.28	10.93	10.63	5.67	-	-	-
	sd	-	-	-	-	-	-	-	-	-	-	-	-	-	-
Macaca tonkeana	n	3	3	3	3	3	3	3	2	3	3	3	3	3	3
	mean	33.79	6.24	7.08	0.67	2.78	10.57	25.26	33.70	7.04	6.50	3.69	42.04	62.80	145.43
	sd	0.86	0.33	0.47	0.03	0.15	3.83	1.93	1.79	1.14	1.28	0.62	0.79	2.36	4.80
Mandrillus sphinx	n	9	9	9	9	9	9	9	9	9	9	9	11	11	11
	mean	43.17	9.58	11.54	0.75	4.16	21.11	33.19	49.23	23.51	29.91	8.00	46.83	57.43	139.24
	sd	3.08	1.87	1.93	0.14	0.75	3.60	5.21	6.63	7.48	11.86	2.10	6.13	5.62	8.51
Miopithecus talapoin	n	1	1	0	1	0	1	1	1	0	1	1	1	1	1
	mean	20.81	4.27	-	0.78	-	3.64	12.82	18.79	-	3.03	1.67	36.59	55.56	136.82
	sd	-	-	-	-	-	-	-	-	-	-	-	-	-	-

Nasalis larvatus	n	15	15	14	15	14	15	12	10	15	15	15	13	13	14
	mean	31.76	8.01	9.12	0.73	3.09	9.49	25.16	28.38	13.46	10.25	5.42	38.13	54.92	145.76
	sd	1.83	0.98	1.09	0.07	0.85	3.03	2.51	3.03	3.62	1.86	3.32	5.79	4.59	6.33
Nomascus concolor	n	1	1	1	1	1	1	0	1	1	1	1	1	1	1
	mean	31.63	7.97	8.17	0.52	3.52	8.83	-	22.45	7.62	7.88	6.83	31.97	42.55	144.76
	sd	-	-	-	-	-	-	-	-	-	-	-	-	-	-
Nomascus leucogenys	n														
	mean														
	sd														
Pan t. troglodytes	n	8	9	9	9	9	9	9	9	9	9	9	10	10	10
	mean	51.62	11.37	11.96	0.62	4.82	30.82	35.09	45.29	34.36	35.12	36.88	33.77	57.31	147.51
	sd	2.10	1.27	0.81	0.05	0.95	3.67	4.06	3.42	8.05	8.27	4.10	4.22	3.75	6.92
Papio anubis	n	9	9	9	9	9	9	9	9	9	9	9	9	9	9
	mean	43.05	10.85	11.86	0.7	3.97	18.18	34.44	52.01	23.23	25.30	9.51	42.00	63.21	135.62
	sd	1.52	0.99	1.02	0.06	1.07	3.82	2.78	2.41	4.03	6.60	2.76	5.95	4.40	10.80
Pithecia irrorata	n	1	1	1	1	1	1	1	1	1	1	1	1	1	1
	mean	20.58	5.65	6.26	0.72	2.90	12.59	17.62	23.97	4.15	9.56	2.25	54.69	70.96	150.64
	sd	-	-	-	-	-	-	-	-	-	-	-	-	-	-
Pithecia pithecia	n	10	10	10	10	10	10	10	9	10	10	10	10	10	11
	mean	20.13	5.41	5.63	0.61	1.99	9.44	16.82	20.76	3.85	6.52	1.90	51.22	68.40	140.59
	sd	0.64	0.80	0.71	0.15	0.31	1.99	2.17	2.17	1.08	4.17	0.65	5.71	4.47	7.63
Pongo pygmaeus	n	8	8	8	8	8	7	7	8	8	8	8	8	8	7
	mean	58.90	13.85	15.13	0.62	4.74	55.94	42.60	61.12	63.85	84.40	67.70	36.61	65.56	136.10
	sd	4.20	1.77	1.28	0.08	1.64	2.97	3.64	6.84	26.98	26.74	13.67	8.17	9.57	11.40
Propithecus diadema	n														
	mean														
	sd														
Propithecus verreauxi	n	4	5	4	4	4	4	5	5	4	4	5	4	4	4
	mean	22.50	7.87	8.19	0.48	1.85	9.71	12.91	18.07	6.07	5.76	5.69	46.71	53.40	132.03
	sd	0.89	0.83	0.41	0.03	0.32	0.58	1.03	1.05	0.40	0.87	1.20	10.34	4.78	4.02
Pygathrix nemaeus	n	4	4	4	4	4	4	3	3	4	4	4	4	4	4
	mean	31.85	8.16	8.45	0.82	2.16	9.68	22.99	28.80	9.96	8.27	5.00	41.44	59.42	143.47
	sd	0.99	1.24	0.90	0.06	0.56	0.52	4.02	1.13	1.36	0.90	2.99	4.71	1.74	2.45
Rhinopithecus roxellana	n														
	mean														
	sd														
Semnopithecus entellus	n	2	2	2	2	2	2	2	1	2	2	2	3	2	3
	mean	35.69	8.30	9.39	0.65	2.77	9.80	27.73	40.00	12.33	12.36	7.18	35.84	61.49	131.26
	sd	2.74	0.61	1	0.01	0.22	2.64	2.67	-	7.26	0.42	0.19	2.54	0.92	5.17
Symphalangus syndactylus	n	1	1	1	1	1	1	1	0	1	1	1	1	1	1
	mean	34.85	8.11	9.50	0.58	3.17	10.22	24.73	-	12.15	12.62	7.01	41.77	53.57	144.46
	sd	-	-	-	-	-	-	-	-	-	-	-	-	-	-
Tarsius bancanus	n	1	1	1	1	1	1	1	1	0	1	0	1	1	1
	mean	11.87	2.29	2.05	0.69	0.23	1.19	6.19	9.50	-	0.36	-	30.83	54.37	86.94
	sd	-	-	-	-	-	-	-	-	-	-	-	-	-	-
Tarsius syrichta	n	5	6	5	6	4	5	6	6	4	6	1	9	9	9

	mean	10.79	2.00	1.82	0.68	0.37	0.68	6.34	9.22	0.89	0.43	0.99	32.95	55.66	124.63
	sd	0.46	0.18	0.06	0.09	0.21	0.17	0.46	0.33	0.25	0.16	-	4.20	8.46	20.39
Theropithecus gelada	n	2	1	1	2	1	2	2	1	1	2	2	3	3	2
	mean	35.23	5.44	8.55	0.81	5.18	11.93	26.54	45.11	20.21	15.6	6.41	38.70	60.65	102.77
	sd	5.88	-	-	0.12	-	5.99	0.06	-	-	0.06	0.44	6.95	9.17	36.81
Varecia v. variegata	n	1	1	1	1	1	1	1	1	1	1	1	1	1	1
	mean	23.15	9.59	9.14	0.47	0.66	5.99	16.45	20.19	9.12	7.85	2.79	55.44	53.03	140.09
	sd	-	-	-	-	-	-	-	-	-	-	-	-	-	-

C7		GM	VBVL	VBDL	VB ECC	UNC	SPL	ATPL	PTPL	PCSA	LCSA	SCSA	TPAA	TPPA	AFA
Alouatta caraya	n	1	1	1	1	1	1		1	1	1	1		1	1
	mean	28.27	8.28	9.84	0.50	3.81	26.00		45.62	31.05	26.73	21.53		57.16	152.49
	sd	-	-	-	-	-	-		-	-	-	-		-	-
Alouatta guariba	n														
	mean														
	sd														
Alouatta palliata	n	9	9	9	9	9	9		9	9	9	9		7	7
	mean	28.09	7.51	7.44	0.58	2.70	20.03		36.64	15.26	16.64	12.53		65.43	146.48
	sd	1.25	0.83	0.44	0.08	0.81	1.20		2.96	2.73	3.11	3.05		4.70	10.57
Alouatta seniculus	n	1	1	1	1	1	1		1	1	1	1		0	1
	mean	29.11	8.74	10.12	0.47	3.40	26.01		42.48	18.59	31.88	12.01		-	144.31
	sd	-	-	-	-	-	-		-	-	-	-		-	-
Ateles fusciceps	n	7	7	7	7	7	7		7	7	7	7		8	8
	mean	27.74	8.24	9.26	0.33	3.42	20.61		37.24	21.75	25.37	17.97		67.51	157.30
	sd	0.90	0.63	0.55	0.03	0.87	1.65		1.69	4.64	5.98	3.07		6.12	12.19
Ateles geoffroyi	n	1	1	1	1	1	1		1	1	1	1		1	1
	mean	27.62	8.51	8.48	0.39	3.35	18.09		34.04	17.05	22.92	16.21		62.71	159.49
	sd	-	-	-	-	-	-		-	-	-	-		-	-
Avahi laniger	n	3	3	3	3	2	3		3	3	3	3		3	3
	mean	15.26	4.57	5.05	0.45	0.80	6.58		15.95	4.55	3.42	2.52		59.56	137.99
	sd	0.52	0.54	0.61	0.05	0.22	0.57		1.40	1.2	0.36	0.24		2.11	4.28
Cebus apella	n	12	12	12	12	12	12		12	12	12	12		9	10
	mean	24.34	5.74	5.98	0.39	1.50	14.28		27.98	7.91	7.51	3.92		69.12	145.59
	sd	0.95	0.50	0.65	0.07	0.69	2.19		1.46	2.16	1.77	1.12		4.24	4.66
Cercocebus torquatus	n	3	3	3	3	3	3		3	3	3	3		3	3
	mean	33.13	7.7	8.77	0.71	3.03	14.29		40.36	20.76	15.80	4.57		60.45	134.07
	sd	2.12	0.78	0.62	0.04	0.76	0.91		2.68	11.89	4.33	0.57		4.51	10.62
Cercopithecus mitis	n	5	5	5	5	5	5		5	5	5	5		10	11
	mean	29.78	6.94	7.51	0.60	2.20	10.94		39.45	14.92	8.85	3.78		62.83	144.22
	sd	1.09	0.61	0.77	0.05	0.10	1.65		0.73	5.000	2.84	1.14		5.29	6.05
Chlorocebus aethiops	n	7	7	7	7	7	7		7	8	8	8		7	7
	mean	27.78	6.98	7.33	0.61	2.58	12.23		32.95	10.02	6.06	3.61		56.90	143.07
	sd	0.74	0.97	0.39	0.08	0.52	1.57		3.12	4.96	2.96	1.88		6.78	8.88
Chlorocebus pygerythrus	n	2	2	2	2	2	2		2	2	2	2		2	2
	mean	28.15	7.09	7.30	0.60	2.00	11.20		37.43	16.59	5.63	4.60		62.32	148.89
	sd	1.36	0.36	0.06	0.03	0.75	1.94		1.63	4.09	0.16	0.23		4.24	8.30
Colobus guereza	n	10	10	10	10	10	10		8	11	11	11		10	9

	mean	30.90	7.28	7.73	0.48	2.74	11.38	37.95	15.71	9.32	4.04	58.43	147.10
	sd	0.61	1.12	0.99	0.04	0.81	1.82	1.90	6.33	4.18	1.94	3.16	10.76
Erythrocebus patas	n	4	4	4	4	4	4	4	4	4	4	5	5
	mean	33.39	8.98	10.23	0.75	3.59	17.16	45.54	21.59	13.52	6.64	59.22	140.64
	sd	0.71	0.45	0.53	0.12	0.61	3.54	4.24	9.55	3.89	1.66	8.25	11.63
Gorilla beringei	n	3	3	3	3	3	3	3	3	3	3	4	5
	mean	66.11	15.47	17.99	0.62	8.85	68.14	79.00	77.44	179.64	108.75	75.89	151.89
	sd	2.24	2.61	1.72	0.04	1.31	4.80	11.17	24.63	26.86	7.75	2.16	11.28
Gorilla g. gorilla	n	3	4	4	4	4	4	4	4	4	4	6	6
	mean	66.11	13.55	17.29	0.54	7.42	72.50	74.45	81.01	155.99	113.52	75.85	144.28
	sd	2.24	0.81	1.68	0.04	1.36	7.39	5.43	26.02	35.68	21.07	7.65	8.48
Hapalemur griseus	n											1	1
	mean											57.09	132.52
	sd											-	-
Homo sapiens	n	10	10	10	10	10	10	9	10	10	10	9	9
	mean	56.51	13.57	14.31	0.60	3.63	29.75	66.36	46.76	68.26	52.27	65.64	101.12
	sd	3.22	0.95	0.78	0.06	1.00	1.72	4.77	12.76	18.19	14.44	4.72	9.17
Hylobates agilis	n												
	mean												
	sd												
Hylobates klossii	n												
	mean												
	sd												
Hylobates lar	n	1	1	1	1	1	1	1	1	1	1	0	0
	mean	31.38	7.30	7.98	0.62	4.38	14.02	30.61	19.18	14.39	11.78	-	-
	sd	-	-	-	-	-	-	-	-	-	-	-	-
Hylobates muelleri	n												
	mean												
	sd												
Indri indri	n	0	1	1	1	1	1	1	1	1	1	1	1
	mean	-	11.13	10.98	0.69	2.46	16.09	24.05	11.28	15.78	12.09	52.04	125.81
	sd	-	-	-	-	-	-	-	-	-	-	-	-
Lemur catta	n	6	5	5	5	5	5	5	5	5	5	6	6
	mean	20.29	5.80	6.52	0.42	1.50	7.46	20.81	8.03	4.42	2.18	56.11	143.80
	sd	0.63	1.07	0.76	0.07	0.57	0.46	0.69	2.31	0.59	0.82	3.18	3.22
Lepilemur mustelinus	n	2	2	1	2	1	2	2	1	2	2	2	2
	mean	13.50	3.70	3.87	0.50	0.34	1.57	13.38	2.72	1.06	0.42	53.77	125.58
	sd	0.35	0.09	-	0.00	-	1.14	1.25	-	0.24	0.60	1.48	0.46
Macaca fuscata	n	3	3	3	3	3	3	3	3	3	3	3	3
	mean	34.16	7.03	7.51	0.73	2.61	13.10	42.99	16.71	9.67	3.84	62.17	150.83
	sd	1.33	0.86	0.99	0.11	0.71	1.19	2.55	3.26	2.36	1.01	1.93	1.52
Macaca nemestrina	n	6	6	6	6	6	6	4	6	6	6	6	6
	mean	35.18	6.80	7.52	0.61	2.95	13.33	43.40	20.85	12.89	6.21	67.10	144.83
	sd	0.63	0.53	0.88	0.04	0.28	2.75	4.01	6.97	3.75	1.14	4.70	6.54
Macaca nigra	n	1	1	1	1	1	1	1	1	1	1	0	0
	mean	37.51	5.72	8.25	0.79	3.37	15.84	41.26	24.14	13.43	2.23	-	-
	sd	-	-	-	-	-	-	-	-	-	-	-	-
Macaca tonkeana	n	3	3	3	3	3	3	3	3	3	3	3	3
	mean	33.09	5.37	7.01	0.60	2.61	14.08	39.69	16.46	7.57	3.90	61.45	144.00
	sd	0.33	0.64	0.97	0.09	1.01	2.33	2.97	2.20	2.69	1.26	3.11	3.81

Mandrillus sphinx	n	9	9	9	9	9	9	9	9	9	9	10	11	
	mean	43.39	8.95	10.93	0.71	3.75	25.35	55.23	44.18	31.96	10.94	61.38	143.16	
	sd	3.07	1.62	1.98	0.10	1.22	3.97	8.18	18.65	12.01	4.58	5.21	8.62	
Miopithecus talapoin	n													
	mean													
	sd													
Nasalis larvatus	n	12	10	9	10	8	9	7	9	10	10	9	12	
	mean	31.54	7.94	9.07	0.65	3.10	14.75	33.92	19.25	17.11	14.84	54.66	151.52	
	sd	1.87	0.94	0.78	0.08	0.53	3	1.89	6.54	3.13	6.52	5.06	6.38	
Nomascus concolor	n	1	1	1	1	1	1	1	1	1	1	1	1	
	mean	30.62	7.26	8.49	0.51	2.98	14.99	29.86	13.84	10.44	9.69	71.28	152.05	
	sd	-	-	-	-	-	-	-	-	-	-	-	-	
Nomascus leucogenys	n													
	mean													
	sd													
Pan t. troglodytes	n	8	8	8	8	8	8	8	8	8	8	11	11	
	mean	50.81	10.67	12.59	0.51	6.23	31.81	55.44	38.36	53.02	49.31	67.14	146.67	
	sd	2.36	0.72	1.08	0.07	1.14	3.86	2.94	10.07	13.51	10.52	5.44	8.80	
Papio anubis	n	8	8	8	8	8	8	8	9	9	9	8	8	
	mean	43.34	10.09	12.00	0.69	3.41	19.6	58.48	31.99	24.04	10.51	60.96	138.99	
	sd	1.70	0.67	1.17	0.05	0.49	5.03	4.07	15.15	10.54	6.29	4.85	9.25	
Pithecia irrorata	n	1	1	1	1	1	1	1	1	1	1	1	1	
	mean	20.80	5.68	5.42	0.46	2.59	12.97	25.59	6.59	10.57	3.25	68.92	142.80	
	sd	-	-	-	-	-	-	-	-	-	-	-	-	
Pithecia pithecia	n	11	11	11	11	11	11	11	12	12	12	8	12	
	mean	20.13	5.13	5.79	0.42	1.78	11.45	22.43	5.42	7.21	2.68	63.74	133.22	
	sd	0.62	0.82	0.94	0.11	0.58	2.05	2.04	2.88	4.14	1.30	3.28	16.12	
Pongo pygmaeus	n	8	8	8	8	8	8	8	8	8	8	8	8	
	mean	64.15	13.98	16.04	0.57	6.09	54.17	62.97	65.62	103.50	85.38	72.03	145.54	
	sd	5.04	1.71	1.29	0.08	2.46	4.28	5.25	19.23	27.48	11.87	6.87	10.12	
Propithecus diadema	n													
	mean													
	sd													
Propithecus verreauxi	n	4	5	4	4	4	4	5	4	4	4	4	4	
	mean	22.33	7.37	8.14	0.48	1.02	10.62	20.60	22.33	10.62	10.81	48.06	137.44	
	sd	1.01	0.65	0.49	0.06	0.27	0.59	2.01	1.01	0.59	1.52	7.93	5.31	
Pygathrix nemaeus	n	3	3	3	3	3	3	3	3	3	3	3	3	
	mean	31.17	8.55	8.10	0.67	1.6	13.21	31.96	31.17	13.21	16.32	58.82	145.68	
	sd	0.68	0.84	0.82	0.02	0.62	0.77	3.24	0.68	0.77	8.64	5.84	18.11	
Rhinopithecus roxellana	n													
	mean													
	sd													
Semnopithecus entellus	n	2	2	2	2	2	2	1	2	2	2	3	3	
	mean	36.57	7.92	9.80	0.57	2.33	11.72	43.67	24.13	12.83	8.95	60.04	124.88	
	sd	3.04	0.16	0.74	0.05	0.86	2.11	-	1.30	3.91	4.67	4.00	8.27	
Symphalangus	n	1	1	1	1	1	0	1	1	1	1	1	1	

syndactylus														
	mean	34.24	7.59	10.10	0.45	3.90	-	32.79	37.11	14.57	3.83		77.84	142.27
	sd	-	-	-	-	-	-	-	-	-	-		-	-
Tarsius bancanus	n	1	1	1	1	1	1	1	0	1	0		1	1
	mean	12.34	1.94	2.02	0.62	0.35	1.4	10.08	-	0.40	-		55.39	111.41
	sd	-	-	-	-	-	-	-	-	-	-		-	-
Tarsius syrichta	n	5	5	5	5	4	5	5	4	5	2		9	9
	mean	10.80	1.99	1.88	0.59	0.11	0.79	10.06	0.86	0.38	0.58		57.68	110.59
	sd	0.67	0.21	0.05	0.13	0.15	0.21	0.43	0.24	0.03	0.13		4.19	15.20
Theropithecus gelada	n	2	1	1	2	1	2	1	2	2	2		3	3
	mean	35.09	5.94	8.68	0.75	3.62	15.43	48.33	23.45	15.82	9.09		69.14	140.39
	sd	4.85	-	-	0.10	-	3.13	-	4.25	0.04	2.87		7.45	8.94
Varecia v. variegata	n	2	2	2	2	2	2	2	2	2	2		2	2
	mean	22.36	8.75	9.33	0.34	1.28	7.46	23.58	16.37	9.70	4.61		55.35	146.31
	sd	0.17	0.83	0.30	0.04	0.69	3.53	0.22	2.31	0.69	2.74		3.10	3.23

Abbreviations are as follows: sd = standard deviation; GM = geometric mean; VBVL = vertebral body ventral length; VBDL = vertebral body dorsal length; VB ECC = vertebral body eccentricity; UNC = uncinate process height; SPL = spinous process length; ATPL anterior transverse process length; PTPL = posterior transverse process length; PCSA = pedicle cross-sectional area; LCSA = lamina cross-sectional area; SCSA = spinous process cross-sectional area; TPAA = transverse process angle – anterior tubercle; TPPA = transverse process angle – posterior tubercle; AFA – superior article facet angle.